MASTERARBEIT | MASTER'S THESIS

Titel | Title

Phenotypic Plasticity in Cancer-Associated Fibroblasts and its Functional Impact on Colorectal Cancer

verfasst von | submitted by

Elisa Ebner BSc.

angestrebter akademischer Grad | in partial fulfilment of the requirements for the degree of

Master of Science (MSc)

Wien | Vienna, 2025

Studienkennzahl lt. Studienblatt | Degree programme code as it appears on the student record sheet:	UA 066 865
Studienrichtung lt. Studienblatt | Degree programme as it appears on the student record sheet:	Masterstudium Molecular Biology
Betreut von | Supervisor:	Mag. Dr. Helmut Dolznig

Abstract
The tumour microenvironment (TME) plays a critical role in cancer progression, metastasis, and therapeutic resistance. Among its components, cancer-associated fibroblasts (CAF) represent the predominant cell type and are key mediators of extracellular matrix (ECM) remodelling, cytokine secretion, and modulation of immune responses. While CAFs are a crucial part of the TME, understanding their biology is challenging due to their heterogeneity, diverse origins, and the current lack of reliable, standardised markers.
This in vitro study investigates the influence of cytokines within the TME on the expression of phenotypic markers of colorectal cancer (CRC). CAF were treated with fibrosis-associated cytokines (IL-4, IL-13), inflammatory cytokines (IL-1β and TNF-α), and TGF-β1, either alone or in combination. The expression of most widely used colorectal CAF markers—alpha-smooth muscle actin (α-SMA) and fibroblast activation protein (FAP)—was quantified using immunofluorescence staining assessed by In-Cell Western and confocal imaging. CRC-CAF expressed basal α-SMA levels. IL-4 and IL-13 treatment independently upregulated α-SMA in a TGF-β1-receptor (ALK5)-independent manner, though less potently than TGF-β1. IL-1β and TNF-α did not downregulate basal α-SMA levels. FAP was significantly upregulated by TGF-β1 treatment. FAP expression was not induced by IL-4 alone but was significantly upregulated when combined with TGF-β1. IL-1β and TNF-α moderately upregulated FAP. All four cytokines (IL-4 + TGF-β1 + IL-1β + TNF-α) upregulated α-SMA and FAP the most significantly. Cytokine treatment also modulated expression of additional CAF markers, including PD-L2, IL-1R1, and podoplanin (PDPN), highlighting the phenotypic plasticity of CAFs. To assess functional consequences, conditioned media (CM) from cytokine-pretreated CAFs was applied to patient-derived colorectal cancer organoids (PDOs). IL-1β + TNF-α-treated CAF-CM significantly increased the viability (measured by Cell Titer-Glo 3D) of PDOs, with the most substantial pro-tumourigenic effects observed following treatment with the combination of all four cytokines. Additionally, a matched PDO-CAF co-culture system was established using a transwell-based organoid-organotypic assay (OOTA). Cytokine treatment induced distinct morphological changes in organoids. Confocal imaging revealed cytokine-specific effects on proliferation (Ki-67), apoptosis (cleaved caspase-3), and mesenchymal markers (α-SMA and FAP). IL-1β + TNF-α promoted both proliferation and apoptosis, whereas IL-4 + TGF-β1 reduced proliferation. Contrary to previous results in 2D, α-SMA was upregulated the most with IL-4 + TGF-β1 in the OOTA. Maximum FAP expression occurred, like in 2D culture, with the combination of all four cytokines.
These findings underscore the dynamic regulation of CAF phenotypes by TME cytokines and their functional impact on tumour cell behaviour. Improved characterisation of CAF subsets is essential, given their correlation with patient prognosis and growing interest as therapeutic targets in colorectal cancer. Further studies are warranted to elucidate their prognostic value and potential for clinical intervention.

Abstrakt
Die Tumormikroumgebung (TMU) spielt eine entscheidende Rolle bei der Progression, Metastasierung und Therapieresistenz bei Krebs. Tumor-assoziierte Fibroblasten (TAFs) stellen den vorherrschenden Zelltyp dar und sind zentrale Vermittler der Remodellierung der extrazellulären Matrix (ECM), der Zytokinsekretion sowie der Modulation immunologischer Reaktionen. Trotz ihrer zentralen Funktion ist die TAF-Biologie komplex, da TAF hochgradig heterogen sind, von unterschiedlichen Zelltypen abstammen und bislang keine standardisierten Marker zur zuverlässigen Identifikation aufweisen.
Diese In-vitro-Studie untersucht, wie Zytokine der TMU die Expression phänotypischer Marker von aus kolorektalem Karzinom abgeleiteten TAFs beeinflussen. Hierzu wurden TAFs mit Fibrose-assoziierten Zytokinen (IL-4, IL-13), entzündlichen Zytokinen (IL-1β und TNF-α) sowie TGF-β1, einzeln oder in Kombination, behandelt. Die Expression der am häufigsten verwendeten TAF-Marker im kolorektalen Karzinom – alpha-smooth muscle Aktin (α-SMA) und Fibroblasten aktivierendes Protein (FAP) – wurde mittels Immunfluoreszenz-Färbemethoden quantifiziert durch In-Cell-Western-Assays und konfokaler Mikroskopie. TAF exprimierten unbehandelt ein Grundlevel von α-SMA. IL-4 und IL-13 induzierten eine erhöhte Expression von α-SMA, unabhängig vom TGF-β1-Rezeptor (ALK5), jedoch weniger stark als TGF-β1. IL-1β und TNF-α beeinflussten α-SMA nicht. FAP wurde durch TGF-β1 hochreguliert. IL-4 allein induzierte FAP nicht, jedoch signifikant in Kombination mit TGF-β1. IL-1β und TNF-α beeinflussten FAP moderat. Darüber hinaus veränderten die Zytokine die Expression weiterer TAF-Marker wie PD-L2, IL-1R1 und Podoplanin (PDPN), was die Eigenschaft der phänotypischen Plastizität von TAFs hervorhebt. Organoide von Patienten mit kolorektalem Karzinom wurden in konditionierten Medien (KM) von Zytokin vorbehandelten TAFs kultiviert. Der ATP-Gehalt der Organoide wurde mit Cell Titer-Glo 3D auf Basis eines Luciferase-Assays gemessen. Das KM von mit IL-1β + TNF-α vorbehandelten TAFs erhöhte signifikant den zellulären Gehalt von ATP, jedoch wurden die stärksten protumorigen Effekte nach Behandlung mit der Kombination IL-4 + IL-1β + TNF-α + TGF-β1 beobachtet. Darüber hinaus wurde ein auf einem Transwell-basiertes Co-Kultursystem (organoid-organotypic assay, OOTA) aus Patienten-Organoiden und TAFs desselben Patienten etabliert. Die Zytokinvorbehandlung führte zu deutlichen morphologischen Veränderungen in den Organoiden. Konfokale Bildgebung zeigte zytokin-spezifische Effekte auf Proliferation (Ki-67), Apoptose (gespaltene Caspase-3) sowie auf mesenchymale Marker (α-SMA und FAP). IL-1β + TNF-α förderten sowohl Proliferation als auch Apoptose, während IL-4 + TGF-β1 die Proliferation reduzierten. Im Gegensatz zum vorigen Experiment bewirkte IL-4 + TGF-β1 die stärkste α-SMA-Induktion. Die maximale FAP-Expression wurde, wie zuvor in 2D-Kultur, bei der Kombination aller vier Zytokine beobachtet.
Diese Ergebnisse verdeutlichen die dynamische Regulation von TAF-Phänotypen durch Zytokine der TMU und deren funktionellen Einfluss auf das Verhalten von Tumorzellen. Eine verbesserte Charakterisierung von TAF-Subtypen ist essenziell, da ihre Präsenz mit der

Prognose der Patienten korreliert und sie zunehmend als therapeutische Zielstrukturen im kolorektalen Karzinom untersucht werden. Weitere Studien sind erforderlich, um ihren prognostischen Wert und ihr Potenzial für klinische Interventionen zu klären.

Table of contents

Abbreviations 1

List of figures 5
List of tables 8

1. Introduction 9

1.1 Colorectal Cancer 9

1.1.1 Pathogenesis and Disease Progression 9
1.1.2 Risk Factors of Colorectal Cancer 11
1.1.3 Classification and Treatment of Colorectal Cancer 11

1.2 The Tumour Microenvironment 15
1.3 Cancer-associated Fibroblast (CAF) 17

1.3.1 Fibroblasts and Myofibroblasts during Wound Healing 17
1.3.2 Cancer-associated fibroblast (CAF): Definition and Marker 19
1.3.3 Origin of CAFs 20
1.3.4 CAF activation 21
1.3.5 CAF heterogeneity and subtypes 22
1.3.6 CAF function 26
1.3.7 CAF therapy 26

1.4 CAF markers 28

1.4.1 Alpha-smooth muscle actin 28
1.4.2 Fibroblast activation protein 31
1.4.3 IL1R1 32
1.4.4 Podoplanin 32
1.4.5 Programmed cell death ligand 2 33

1.5 Aim of the thesis 34

2. Methods 35

2.1 Material 35

2.1.1 Consumables 35
2.1.2 Reagents 36
2.1.3 Media formulations 38
2.1.4 Buffers and Supplements 38
2.1.5 Antibodies, IgG and dies 39
2.1.6 Treatments 41
2.1.7 Devices and software 41

2.2. Cell culture 41
2.2.1 Passaging of CAFs 42
2.2.2 Passaging of organoids 42
2.2.3 Thawing and freezing of CAFs 42
2.2.4 Thawing and freezing of organoids 43
2.2.5 Starvation 43
2.2.6 Seeding of cells 43
2.3 In-Cell Western Assay 44
2.4 Immunofluorescence (IF) staining for confocal microscopy 45
2.5 CellTiter-Glo 3D Viability assay of organoids in CAF-conditioned media 47
2.6 Organoid Organotypic Transwell Assay (OOTA) 47
2.7 Statistics 50
3. Results 52
3.1 The effect of IL-4, TGF-β1 and IFN-γ treatment on α-SMA expression in CAF 6388/19 52
3.2 The effect of IL-4, IL-13, TGF-β1 and TGF-β signalling inhibition (A 83-01) on α-SMA expression in CAF 6388/19 56
3.3 Determining the effect of IL-4, IL-13, TGF-β1 and TGF-β1 signalling inhibition (A 83-01) on α-SMA expression in CAF 6388/19 using immunofluorescence staining for confocal microscopy 60
3.4 The influence of IL-4, TGF-β1, IL-1β+ TNF-α and treatment combinations on CAF BGM2008 expression of α-SMA, FAP, IL-1-R1, PDPLN and PD-L2. 64
3.5 The influence of IL-4, TGF-β1, IL-1β+ TNF-α and treatment combinations on CAF BGM2008 expression of α-SMA and FAP using immunofluorescence staining for confocal microscopy 70
3.6 The influence of IL-4, TGF-β1, IL-1β+ TNF-α treated CAF 6388/19 conditioned media and its effect on BGM2008 CRC organoid growth using Cell-Titer-Glo 3D assay 74
3.7 The influence of IL-4, TGF-β1, IL-1β + TNF-α and combinations of these treatments on CAF BGM2008 conditioned media and its effect on patient-matched CRC organoid viability using Cell Titer Glo 3D assay. 79
3.8 OOTA co-culture of pretreated BGM2008 CAF with patient- matched CRC-Organoids 84
4.Discussion 97
4.1 Cytokine regulation of colonic CAF marker expression 100
4.1.1 IL-4, IL-13, TGF-β1, IFN-γ, IL-1β and TNF-α differentially influence α-SMA expression 100
4.1.2 IL-4, TGF-β1, IL-1β and TNF-α differentially influence FAP expression 108
4.1.3 IL-4, TGF-β1, IL-1β and TNF-α Differentially Regulate CAF Markers: IL-1R1,

PDPN, and PD-L2 109
4.2 Impact of cytokine-pretreated CAF conditioned media on colorectal cancer organoid growth 112
4.3 Cytokine effect in CAF-PDO co-culture (OOTA) 116
5. Conclusion 122
6. Literature 123
6. Appendix 159

Abbreviations

Abbreviation	Meaning	Abbreviation	Meaning
α-SMA	Alpha-Smooth Muscle Actin	**5-FU**	5-Fluorouracil
ACTA2	Actin Alpha 2, Smooth Muscle Actin gene	**AFM**	Atomic Force Microscopy
AKT	Protein Kinase B	**ALDH**	Aldehyde Dehydrogenase
ALK	Anaplastic Lymphoma Kinase	**ANXA1+**	Annexin A1 Positive
APC	Adenomatous Polyposis Coli	**ATRA**	All-trans-retinoic acid
ATP	Adenosine Triphosphate	**apCAF**	Antigen-Presenting Cancer-Associated Fibroblast
BMSC	Bone Marrow-Derived Mesenchymal Stromal Cell	**BMP**	Bone Morphogenetic Protein
CAF(s)	Cancer-Associated Fibroblast(s)	**CAR-T**	Chimeric Antigen Receptor T-cell
CBC	Crypt Base Columnar Stem Cell	**CD**	Cluster of Differentiation
CD3+ or 8+	Cluster of Differentiation 3 or 8 Positive T Cells	**CDH**	Cadherin
cCAF	Cycling Cancer-Associated Fibroblast	**CM**	Conditioned Media
COL1A	Collagen Type I Alpha	**COX**	Cyclooxygenase
CRIS	Colorectal Intrinsic Subtypes	**CRISPRi**	CRISPR Interference
CSC	Cancer Stem Cell	**CXCL**	C-X-C Motif Chemokine Ligand
CXCR	C-X-C motif chemokine receptor	**DCN**	Decorin
dCAF	Developing Cancer-Associated Fibroblast	**dMMR**	Deficient Mismatch Repair
ECM	Extracellular Matrix	**ED-A FN**	Extra Domain A Fibronectin
EGFR	Epidermal Growth Factor Receptor	**ELISA**	Enzyme-Linked Immunosorbent Assay

EMT	Epithelial-Mesenchymal Transition	**EndMT**	Endothelial-to-mesenchymal transition
EGM-2MV	Endothelial Growth Media	**ENAS**	Organoid media (EGF, Noggin, and R-spondin (or Wnt3a))
FAK	Focal Adhesion Kinase	**FAP**	Fibroblast Activation Protein / Familial Adenomatous Polyposis
FBS	Fetal Bovine Serum	**FSP (S100A4)**	Fibroblast-Specific Protein
FDA	Food and Drug Administration	**FGF**	Fibroblast Growth Factor
rhFGF-B	Recombinant Human Fibroblast Growth Factor B	**GPX**	Glutathione Peroxidase
GMC-SF	Glial-Mesenchymal Cancer Stem Fibroblast	**GREM**	Gremlin (BMP inhibitor)
Hh	Hedgehog (signalling pathway)	**HIF**	Hypoxia-Inducible Factor
HSF	Heat Shock Factor Protein	**iCAF**	Inflammatory Cancer-Associated Fibroblast
iCMS	Intrinsic Consensus Molecular Subtype	**IFN-γ**	Interferon-Gamma
ifnCAF	Interferon-Response Cancer-Associated Fibroblast	**IGF**	Insulin-like Growth Factor
IL	Interleukin	**IL1R1**	Interleukin 1 Receptor Type 1
INFG	Interferon-Gamma (alternative abbreviation)	**ISC**	Intestinal Stem Cell
IMF	Intrinsic-MSI Fibrosis System	**IRAK**	Interleukin-1 Receptor-Associated Kinase
IgG	Immunoglobulin G	**ICW**	In-Cell Western
JAK	Janus Kinase	**Ki-67**	Proliferation Marker
KRAS	Kirsten Rat Sarcoma Viral Oncogene Homolog	**LGR**	Leucine-rich Repeat-containing G-protein Coupled Receptor
LIF	Leukaemia Inhibitory Factor	**LUM**	Lumican

MAF	Metastasis-Associated Fibroblast	**MAPK**	Mitogen-Activated Protein Kinase
MASSPEC	Mass Spectrometry	**mCAF**	Matrix Cancer-Associated Fibroblast
mTOR	Mechanistic Target of Rapamycin	**myCAF**	Myofibroblastic Cancer-Associated Fibroblast
MDSCs	Myeloid-Derived Suppressor Cells	**meCAF**	Metabolic Cancer-Associated Fibroblast
mesCAF	Mesothelial Cancer-Associated Fibroblast	**MHC**	Major Histocompatibility Complex
MFAP	Microfibril-Associated Protein	**MLH1-s**	Silencing of MLH1 Protein Expression by Promoter Hypermethylation
MMP	Matrix Metalloproteinase	**MSC(s)**	Mesenchymal Stem Cell(s)
MSI	Microsatellite Instability	**MSS**	Microsatellite Stability
MYC	MYC Proto-Oncogene	**NaOH**	Sodium Hydroxide
NF-κB	Nuclear Factor Kappa-Beta	**NG**	Neural/Glial Antigen
NOTCH	Neurogenic Locus Notch Homolog	**NRAS**	Neuroblastoma RAS Viral Oncogene Homolog
Omin	Organoid Minimal Media	**OOTA**	Organoid organotypic Transwell assay
pCAF	Proliferative Cancer-Associated Fibroblast	**PD-1/2**	Programmed Cell Death Protein 1/2
PDAC	Pancreatic Ductal Adenocarcinoma	**PDGFR α/β**	Platelet-Derived Growth Factor Receptor Alpha/Beta
PDPLN	Podoplanin	**PDL**	Programmed Death Ligand
PI3K	Phosphoinositide 3-Kinase	**PDTO**	Patient-Derived Tumour Organoid
PBS	Phosphate-Buffered Saline	**qPCR**	Quantitative Polymerase Chain Reaction
Rho/Rock	Rho-Associated Protein Kinase / ROCK Pathway	**RT**	Room Temperature
ROS	Reactive Oxygen Species	**sc-RNA-seq**	Single-Cell RNA Sequencing
SNAIL	Zinc Finger Transcription Factor SNAIL	**SMAD**	SMAD Family of Proteins

Src	Proto-Oncogene Tyrosine-Protein Kinase Src	**STAT**	Signal Transducer and Activator of Transcription
TAM	Tumour-Associated Macrophage	**TAK**	Transforming Growth Factor Beta-Activated Kinase
TAZ	Transcriptional Co-Activator with PDZ-Binding Motif	**TGF-β**	Transforming Growth Factor Beta
TGFBR	Transforming Growth Factor Beta Receptor	**TE**	Trypsin-EDTA
Th2	T Helper 2 Cell	**TIL**	Tumour-Infiltrating Lymphocyte
TME	Tumour Microenvironment	**TNF-α**	Tumour Necrosis Factor Alpha
TNFR	Tumour Necrosis Factor Receptor	**TNFSF4 (OX40L)**	Tumour Necrosis Factor Superfamily Member 4
TNM	Tumour-Node-Metastasis	**TP53**	Tumour Protein p53
TRAF	TNF Receptor-Associated Factor	**uPAR**	Urokinase-Type Plasminogen Activator Receptor
VEGF	Vascular Endothelial Growth Factor	**VIM**	Vimentin
WNT	Wingless/Integrated Signalling Pathway	**Wnt/β-catenin**	Wnt Signalling Pathway Involving Beta-Catenin
YAP	Yes-Associated Protein		

List of figures

Introduction:

Figure 1: **Colorectal cancer disease progression** with time-dependent cancer hallmarks and occurring mutations (J. Li et al., 2021)
No changes, Li J, Ma X, Chakravarti D, Shalapour S, DePinho RA. Genetic and biological hallmarks of colorectal cancer. Genes Dev. 2021 Jun;35(11-12):787-820. doi: 10.1101/gad.348226.120. PMID: 34074695; PMCID: PMC8168558.
Open Access - Creative Commons CC BY-NC 4.0
https://pubmed.ncbi.nlm.nih.gov/34074695/#&gid=article-figures&pid=figure-1-uid-0 (27.02.2025)

Figure 2: **Colorectal cancer classification systems overview** (Dunne & Arends, 2024)
No changes, Dunne PD, Arends MJ. Molecular pathological classification of colorectal cancer-an update. Virchows Arch. 2024 Feb;484(2):273-285. doi: 10.1007/s00428-024-03746-3. Epub 2024 Feb 6. Erratum in: Virchows Arch. 2024 Feb;484(2):287. doi: 10.1007/s00428-024-03773-0. PMID: 38319359; PMCID: PMC10948573.
Open Access - Creative Commons CC BY 4.0
https://pubmed.ncbi.nlm.nih.gov/38319359/#&gid=article-figures&pid=fig-1-uid-0 (27.02.2025)

Figure 3: **Phases of tissue repair and myofibroblast activation** (Younesi et al., 2024)
No changes, Younesi FS, Miller AE, Barker TH, Rossi FMV, Hinz B. Fibroblast and myofibroblast activation in normal tissue repair and fibrosis. Nat Rev Mol Cell Biol. 2024 Aug;25(8):617-638. doi: 10.1038/s41580-024-00716-0. Epub 2024 Apr 8. Erratum in: Nat Rev Mol Cell Biol. 2024 Aug;25(8):671. doi: 10.1038/s41580-024-00744-w. PMID: 38589640.
https://www.nature.com/articles/s41580-024-00716-0/figures/1 (27.02.2025) Permission ordered over https://marketplace.copyright.com, profile name Elisa Ebner, Licence ID: 1582766-1. Order number 1582766. Permission is also granted according to this webpage: https://www.nature.com/nature-portfolio/reprints-and-permissions/permissions-requests (27.02.2025)

Figure 4: **Cancer associated fibroblasts (CAF)** (based on Pancreatic ductal adenocarcinoma (PDAC) (A) CAF differentiate from various cell types. (B) CAF characterisation: ECM depletion and stiffness, secretome, metabolism and markers (C) CAF subsets and their spatial location (D) CAF subsets: iCAF, myCAF and apCAF (Papait et al., 2022)
No changes, Papait A, Romoli J, Stefani FR, Chiodelli P, Montresor MC, Agoni L, Silini AR, Parolini O. Fight the Cancer, Hit the CAF! Cancers (Basel). 2022 Jul 22;14(15):3570. doi:

10.3390/cancers14153570. PMID: 35892828; PMCID: PMC9330284.
Open Access - Creative Commons CC BY 4.0
https://pubmed.ncbi.nlm.nih.gov/35892828/#&gid=article-figures&pid=figure-1-uid-0
(27.02.2025)

Figure 5: **Myofibroblast activation states as a continuum.** (Hinz & Lagares, Myofibroblasts - Methods in Molecular Biology 2299, Springer 2021). Chapter 3: Myofibroblast Markers and Microscopy Detection Methods in Cell Culture and Histology Fereshteh S. Younesi, Dong Ok Son, Joao Firmino, and Boris Hinz
ISSN 1064-3745 Methods in Molecular Biology ISBN 978-1-0716-1381-8 Matrix and Mechanobiology Program Massachusetts General Hospital Charlestown, MA, USA Laboratory of Tissue Regeneration Fibrosis and Tumour Microenvironment Massachusetts General Hospital Harvard Medical School Boston, MA, USA ISSN 1940-6029 (electronic) ISBN 978-1-0716-1382-5 (eBook) https://doi.org/10.1007/978-1-0716-1382-5 ©Springer Science+Business Media, LLC, part of Springer Nature 2021
Permission ordered over https://marketplace.copyright.com, profile name Elisa Ebner, Licence ID: 1582766-1. Order number 1620737 (16.06.2025)

All copyright issues checked with: https://marketplace.copyright.com/ (16.06.2025)

Methods:

Figure 6: **Visual representation of α-SMA positive area measurements using ImageJ software** (Picture taken by Elisa Ebner)

Figure 7: **Visual representation of organoid size measurements using ImageJ software** (Picture taken by Elisa Ebner)

Results:

Figure 8: **In-Cell Western (ICW) assay of CAF 6388/19 shows upregulation of α-SMA upon IL-4 and TGF-β1 treatment.**

Figure 9: **In-Cell Western (ICW) assay shows the effect of IL-4, IL-13, TGF-β1 and A 83-01 (TGF-β1 signalling inhibition) on α-SMA expression in CAF 6388/19.**

Figure 10: **Confocal microscopy shows the effect of IL-4, IL-13, TGF-β1 and A 83-01 (TGF-β1 signalling inhibition) on α-SMA expression in CAF 6388/19.**

Figure 11: **In-Cell Western (ICW) assay measuring CAF BGM2008 marker regulation**

(α-SMA, FAP, IL-1R1, PDPLN and PD-L2) upon treatment of 2ng/ml of IL-4, TGFβ-1, IL-1β+ TNF-α and different combinations (as indicated).

Figure 12: **Confocal microscopy shows the effect of IL-4, TGF-β1 and IL-1β +TNF-α treatment on α-SMA and FAP expression in CAF BGM2008.**

Figure 13: **The influence of cytokine pre-treated CAF conditioned media on CRC BGM2008 organoid viability using Cell Titer Glo 3D assay.**

Figure 14: **The influence of IL-4, TGF-β1, IL-1β+ TNF-α and combinations of these treatments on CAF BGM2008 conditioned media and their effect on patient-matched organoid viability using Cell Titer Glo 3D assay.**

Figure 15: **CAF-BGM2008 (p12) and CRC organoid BGM2008 (p19) co-culture (OOTA) with different cytokine treatment conditions**

Figure 16: **Confocal images of CAF BGM2008 (p12) and CRC organoid BGM2008 (p19) co-culture (OOTA) showing Ki-67 and Cleaved Caspase 3 (CC3) staining**

Figure 17: **Confocal images of CAF BGM2008 (p12) and CRC organoid BGM2008 (p19) co-culture (OOTA) showing CAF upregulation of α-SMA and FAP**

Figure 18: **Simplified overview of cytokine signalling (IL-4 and IL-13, TGF-β, IFN-γ and IL-1β + TNF-α) and its impact on CAF phenotypes.** TGF-β is associated with α-SMA expression and a myCAF phenotype, whereas treatment with IL-1β + TNF-α leads to an iCAF phenotype (by Elisa Ebner)

All results figures are generated with GraphPad Prism 10, PowerPoint and/or pictures taken by Elisa Ebner at the Medical University of Vienna

Appendix:

Figure 19: **Confocal images of CAF 6388/19 (p11) showing upregulation of α-SMA with treatment of 2ng/ml of IL-4, TGFβ-1, IL-13 and 1μM A 83-01 in different combinations (as indicated) for 48 hours**. (n=15) Nuclei stained by DAPI (blue), Vimentin (red), α-SMA (green).

Figure 20: **Confocal images of CAF BGM2008 (p7) showing upregulation of α-SMA with treatment of 2ng/ml of IL-4, TGFβ-1, IL-1β + TNF-α different combinations (as indicated) for 48 hours**. (n=6) Nuclei stained by DAPI (blue), Vimentin (red), α-SMA

(green).

Figure 21: **Microscope images of OOTA (CAF-BGM2008 (p12)) and CRC organoid co-culture) showing organoids with treatment of 2ng/ml of IL-4, TGFβ-1, IL-1β + TNF-α different combinations (as indicated) for 5 days. (A)** seeding of 5 randomly chosen OOTA **(B)** n=3 pictures per condition analysed **(C**) area analysed with ImageJ, n=3 pictures per condition

Figure 22: **Confocal images of OOTA (CAF-BGM2008 (p12) and CRC organoid BGM2008 (not visible) co-culture) showing upregulation of α-SMA with treatment of 2ng/ml of IL-4, TGFβ-1, IL-1β + TNF-α different combinations (as indicated) for 48 hours.** (n=6) Nuclei stained by DAPI (blue), Vimentin (red), α-SMA (green).

Figure 23: **Confocal images of OOTA (CAF-BGM2008 (p12) and CRC organoid BGM2008 co-culture) showing upregulation of FAP with treatment of 2ng/ml of IL-4, TGFβ-1, IL-1β + TNF-α different combinations (as indicated) for 48 hours.** (n=6) Nuclei stained by DAPI (blue), FAP (yellow). Vimentin not depicted for clarity.

List of tables

Table 1: 2.1.1 Consumables……35
Table 2: 2.1.2 Reagents……36
Table 3: 2.1.3 Media formulations……38
Table 4: 2.1.4 Buffers and Supplements……38
Table 5: 2.1.5 Antibodies, IgG and dye……39
Table 6: 2.1.6 Treatments……41
Table 7: 2.1.7 Devices and Software……41
Table 8: 4. Discussion: Summary of combined 2D and 3D assessment of CAF phenotypes and organoid growth/viability (BGM2008) ……...99

1. Introduction

1.1 Colorectal Cancer

Colorectal cancer (CRC) is a malignant neoplasm originating from uncontrolled cell growth in the colon or rectum (Nikiteas et al., 2016). CRC is a major health burden, with significant morbidity and mortality rates despite advances in diagnosis and treatment. Colorectal cancer ranks as the third most prevalent malignancy, accounting for 10% of all cancer cases (Mármol et al., 2017; Sung et al., 2021; Alrushaid et al., 2023). As for mortality, CRC is the second leading cause of cancer-related deaths, and the number of cases is likely to rise in the coming decades (Hossain et al., 2022; Marcellinaro et al., 2024). Factors contributing to this trend may include the shift in age distribution, the adoption of a western lifestyle in developing countries, including obesity and physical inactivity (M. Arnold et al., 2017;Kasi et al., 2019;Russo et al., 2019;Akimoto et al., 2021).

1.1.1 Pathogenesis and Disease Progression

The colorectal epithelium undergoes continuous regeneration, with cells proliferating at the base of the crypts and differentiating as they migrate towards the lumen (L. H. Nguyen et al., 2020). Gradients of signalling molecules regulate colon tissue architecture, particularly components of the Wnt pathway, which play a crucial role in stem cell compartmentalisation and differentiation dynamics (Cernat et al., 2014; Reynolds et al., 2014). Wnt ligands are produced by both epithelial and stromal cells, contributing to colonic healing and regeneration (Das et al., 2022). Disruptions in this process, including alterations in cellular proliferation and apoptosis, can lead to the formation of adenomas (Marcellinaro et al., 2024). Initially, the disease presents as abnormal growths or polyps in the inner lining of the colon or rectum. Over time, these polyps can progress to cancer (see Figure 1). This follows the well-established adenoma-carcinoma sequence, which involves the acquisition of distinct genetic mutations during progression (see Figure 1) (Marcellinaro et al., 2024). Approximately 80% of CRC cases are sporadic, originating from random somatic mutations (Hossain et al., 2022). The Wnt/β-catenin pathway, TGF-β (SMAD), NF-κB, PI3K/Akt, KRAS, BRAF, TP53, Delta/Notch, JAK/STAT, Hippo/YAP/TAZ and MYC pathways are typical mutational hits in CRC (Muzny et al., 2012; Dobre et al., 2021; Sakai et al., 2018; Pandurangan et al., 2018; Brown & Ried, 2022). Already in 1990, it was evident that the stepwise accumulation of mutations in the combination of APC-KRAS-TP53 and SMAD4 is prevalent in most colorectal cancer cases (see Figure 1) (Fearon & Vogelstein, 1990). This was validated by stepwise introducing these mutations in normal human intestinal stem cells (ISCs) in organoid cultures, leading to full blown carcinomas in mouse xenografts and substantiating the role of cancer stem cells in the process (Drost et al., 2015). Furthermore, epigenetic alterations, e.g. aberrant DNA methylation, drive CRC development (Raskov et al., 2020).

The universal hallmarks of cancer are also true for colorectal cancer. The core pan-cancer hallmarks consist of evading growth suppressors, avoiding immune destruction, enabling replicative immortality (e.g. through telomere dysfunction or telomerase reactivation), tumour-promoting inflammation, activating invasion and metastasis, inducing vasculature, genome instability and mutation, resisting cell death, deregulating cellular energetics, and sustaining proliferative signalling (Hanahan & Weinberg, 2011). Additional enabling factors were added, such as non-mutational epigenetic reprogramming, polymorphic microbes, senescent cells and phenotypic plasticity (Hanahan, 2022). These hallmarks influence colorectal cancer at specific stages, as can be seen in Figure 1 (J. Li et al., 2021). However, in recent years, it has become evident that some of these hallmarks not only apply to cancer cells but to a complex system of various cells that contribute to them, called the tumour microenvironment (TME) (de Visser & Joyce, 2023). The importance of the TME is exemplified in the Immunoscore as a prognostic tool that evaluates the density and distribution of immune cells (mainly CD3+ T lymphocytes and CD8+ cytotoxic T cells) within the tumour centre and invasive margin. A higher Immunoscore, indicating stronger immune infiltration, is linked to a better prognosis and survival. It provides additional information beyond traditional staging systems to assess cancer prognosis and guide treatment decisions (G. Sun et al., 2019).

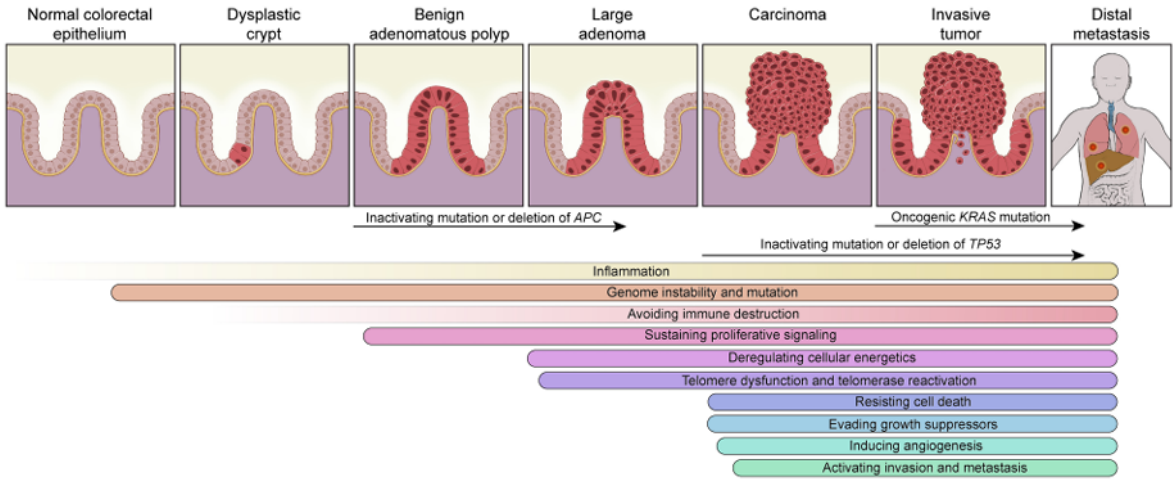


Figure 1: **Colorectal cancer disease progression** *with time-dependent cancer hallmarks and occurring mutations (J. Li et al., 2021)*

1.1.2 Risk Factors of Colorectal Cancer

Genetic predispositions significantly increase susceptibility to colorectal cancer. Familial adenomatous polyposis (FAP) is a hereditary condition resulting from mutations in the APC gene, leading to excessive polyp formation in the colon. Individuals with FAP are at a heightened risk for colorectal cancer. Chronic inflammation also serves as a notable risk factor, as it consists of a constant cycle of injury and repair (T. Hirano et al., 2020; Percario et al., 2021; Zhao et al., 2021). Conditions such as inflammatory bowel disease (IBD), including ulcerative colitis and Crohn's disease, are associated with a 15–20% probability of developing colorectal cancer over 30 years (Rizzo et al., 2011; Long et al., 2017; Alrushaid et al., 2023). Inflammatory processes involve complex interactions between immune cells, cytokines, and pro-inflammatory mediators, which can promote tumour initiation, progression, and metastasis (Terzić et al., 2010; Janakiram & Rao, 2014). Furthermore, gut microbiota contributes to CRC development through complex interactions (Grivennikov et al., 2012; Shah & Itzkowitz, 2022).Colorectal cancer in later stages evades the immune system's attacks through numerous anti-inflammatory mechanisms (Burgos-Molina et al., 2024).

Lifestyle choices play a crucial role in cancer risk. Diets high in red and processed meats, low in dietary fibre, and deficient in fruits and vegetables are associated with an elevated risk (Tuan & Chen, 2016). Additionally, lack of exercise, obesity and polymorphisms in insulin and obesity-related genes have been linked as contributing factors (Tavirani et al., 2013). Moreover, tobacco usage and excessive alcohol consumption are significant risk factors for colorectal cancer (Alaryani & Alrdahe, 2022;Ismail & Shatat, 2024). Incidence rates of colon cancer increase steeply after the age of 50, classifying it as an age-related disease in concordance with most cancers (Song et al., 2020; Friedenreich et al., 2021).

1.1.3 Classification and Treatment of Colorectal Cancer

CRC is classified by stages, ranging from 0 (carcinoma in situ) to stage IV, where distant metastasis occurs. Several methods of tumour staging exist, with the tumour-node-metastasis (TNM) staging being the most significant to date (Arena & Bilchik, 2013). These stagings, based on histopathological features, are crucial for treatment decisions and prognosis (Yantiss, 2017).

Early stages of CRC are curable with surgery and adjuvant therapy, which comprises chemotherapy and/or radiotherapy. First-line therapy is often 5-FU (fluorouracil) in combination with oxaliplatin (FOLFOX) (Hossain et al., 2022). Late-stage metastatic colon cancer is challenging to treat; the 5-year survival of patients is low (~15%) but has seen slight improvement in the last decade (Gallicchio et al., 2022). Late-stage and recurrent colorectal cancer requires targeted therapy, which may include cetuximab, an anti-EGFR (epidermal growth factor receptor) agent, and bevacizumab, an anti-VEGF (vascular

endothelial growth factor) agent, both of which are anti-angiogenesis agents (Xie et al., 2020). However, most patients do not benefit from targeted therapy and drug resistance often leads to the recurrence of the cancer (Groenendijk & Bernards, 2014). Intratumour genetic heterogeneity contributes to treatment failures as resistant subclones may be selected for during therapy. Improved genomic analyses and clinical data collection are crucial for addressing tumour diversity and identifying new therapeutic targets (Mroz & Rocco, 2017).

Colorectal cancer is a heterogeneous disease with diverse molecular alterations and clinical outcomes. Molecular subtypes based on genetic and epigenetic biomarkers can help predict treatment response and prognosis (see Figure 2) (Müller et al., 2016). The Cancer Genome Atlas Project classifications of 2012 have identified two primary mechanisms of genomic instability: chromosomal instability (CIN) and microsatellite instability (MSI). The majority, 84%, of CRCs are CIN, non-hypermutated, microsatellite-stable (MSS) cancers, characterised by high DNA somatic copy number alterations (SCNA), and harbour mutations in APC, TP53, KRAS, SMAD4, and PIK3CA. About 16 % of CRCs display hypermutations with either microsatellite instability (MSI) due to defective mismatch repair (dMMR) (~13 %) or ultra mutations with DNA polymerase proofreading problems (~3%) (see Figure 2) (Muzny et al., 2012;Müller et al., 2016).

In 2015, a consortium of scientists unified bulk RNA expression data of CRC into four consensus molecular subtypes (CMS): CMS1 (hypermutated, CIN low, microsatellite instability, strong immune activation/evasion, hypermethylated, BRAF mutation, RTK/MAPK activation, JAK/STAT signalling high, 14%), CMS2 (canonical, epithelial, WNT and MYC signalling activation, 37%), CMS3 (epithelial, metabolic dysregulation, KRAS mutation, RTK/MAPK activation), CMS4 (mesenchymal, TGF-β activation, stromal invasion and angiogenesis, matrix remodelling, EMT high) and a unclassified mixed group (13%) (see Figure 2) (Guinney et al., 2015, Müller et al., 2016).

Several molecular subtyping studies identified fibroblast infiltration and CAF-related genes as indicative of disease relapse (Dunne & Arends, 2024).

In 2016, the Colorectal Intrinsic Subtypes (CRIS) classification limited the TME impact by expression profiling of patient-derived xenograft models (PDX) and dividing them into five subtypes. CRIS-A hallmarks are MSI, KRAS mutations and increased mucous production. CRIS-B has been shown to increase TGF-β pathway activation in conjunction with EMT. CRIS-C depends on EGFR signalling with sensitivity to EGFR inhibitors. In CRIS-D, the WNT pathway is active with IGF-2 gene overexpression or amplification. CRIS-E consists of a Paneth cell-like phenotype with TP53 mutations (see Figure 2) (Isella et al., 2017).

In 2002, the single-cell intrinsic consensus molecular subtype (iCMS) classification of colorectal cancer (CRC) was published, serving as an update to the CMS system. The division of the groups is based on short copy number alterations (SCNA), with iCMS2 defined as SCNA-high and iCMS3 as SCNA-low. Almost all MSI tumours are categorized in iCMS3, grouped with high mutation frequency, CIMP, right-sidedness, and mucinous

tumours. CMS4 is divided into iCMS2 (better prognosis) and iCMS3 (worse prognosis). CMS1 tumours are mainly characterized as iCMS3. Interestingly, iCMS3 tumours are associated with mutations in BRAF, KRAS, and PIK3CA, whereas iCMS2 tumours exhibit mutations in APC and TP53. A novel intrinsic-MSI fibrosis (IMF) system considers the iCMS classification, microsatellite instability, and CAF-related fibrosis grading (see Figure 2) (Joanito et al., 2022).

The COLON MAP study found that classical adenomas most likely arise from APC mutations in the crypt LGR5+ stem cell base, leading to MSS tumours. In contrast, serrated polyps acquired BRAF mutations and are MSI-high. (see Figure 2B; Chen et al., 2021).

A classification based on pathway rather than gene mutation analysis results in three pathway-derived subtypes (PDS): PDS1 (26%), PDS2 (31%), and PDS3 (30%), as well as a heterogeneous residual group of 13% of CRC. Epithelial-rich CMS2 is split into two subtypes, PDS1 and PDS3. The inflammatory/stromal CMS1/CMS4 subtypes are added within a single subtype, PDS2. Stroma-related epithelial-to-mesenchymal transition (EMT), TGF-β pathway activation, and interferon responses are key regulators in PDS2 (see Figure 2) (Malla et al., 2024; Dunne & Arends, 2024).

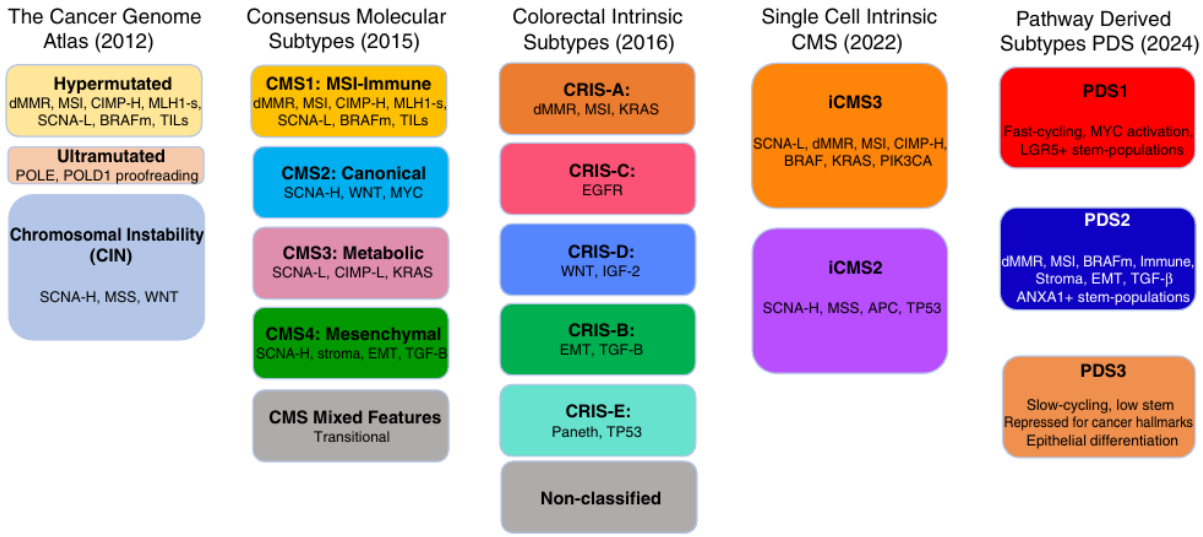


***Figure 2*: Colorectal cancer classification systems overview.** *Abbreviations: dMMR, deficient mismatch repair; MSI, microsatellite instability; MSS, microsatellite stability; CIMP, CpG island methylator phenotype (-H, high or -L, low); SCNA, somatic copy number alteration (-H, high or -L, low); MLH1-s, silencing of MLH1 protein expression by promoter hypermethylation; BRAFm, BRAF mutation; TILs, tumour infiltrating lymphocytes; EMT, epithelial-mesenchymal transition; CBC, LGR5+ crypt base columnar stem cell; RSC, ANXA1+ regenerative stem cell; SMI, Stem Maturation Index* (Dunne & Arends, 2024)

Immunotherapy has emerged as a promising treatment for colorectal cancer, particularly for patients with mismatch repair-deficient and microsatellite instability-high (dMMR/MSI-H) tumours (Golshani & Zhang, 2020; Fan et al., 2021; Ganesh, 2022). Immune checkpoint inhibitors targeting PD-1, such as pembrolizumab and nivolumab, have shown efficacy in this subset of patients, leading to FDA approval for metastatic CRC treatment (Boland & Ma, 2017;H. Hirano et al., 2021). However, most CRC patients are not MSI-H, necessitating the exploration of additional biomarkers and strategies to expand immunotherapy benefits (Hou et al., 2022).

1.2 The Tumour Microenvironment

Cancer originates from mutations that accumulate in cancer cells, but both disease advancement and treatment responses are heavily influenced by non-mutated cells within the tumour's surrounding microenvironment (Sahai et al., 2020). Emerging evidence highlights the crucial contribution of the tumour microenvironment (TME) to tumour progression, metastasis and therapeutic response (Zhang et al., 2022).

The TME is a complex system comprising various cell types, including epithelial, endothelial, stromal, and immune cells. Stromal cells constitute a heterogeneous, organ-specific group that is essential for connective tissue homeostasis. Members of this group are, for example, fibroblasts, pericytes and adipocytes (Manetti, 2021). Additionally, extracellular matrix components, metabolic substrates and signalling molecules are of importance in the TME (Gallo et al., 2021; J. Li et al., 2022). The TME is a challenge to decode due to its high structural and functional complexity (Belhabib et al., 2021). Importantly, the primary cell type of the TME is the cancer-associated fibroblast (CAF), which plays a central role in shaping it (LeBleu & Kalluri, 2018;Q. Zhang et al., 2023). Secreted factors, including cytokines, chemokines, and growth factors, mediate the complex interactions between CAFs and other components of the TME (K. Wright et al., 2023). Depending on the context, the crosstalk of cells in the TME can both favour and hinder tumour progression (Zafari et al., 2022).

The host response to cancer cells results in a fibrosis-like mechanism known as the desmoplastic reaction. This is characterised by dense extracellular matrix and fibrous stroma, which plays a significant role in cancer progression, including colorectal cancers (H. Sato et al., 2023; Ueno et al., 2021). In numerous epithelial tumours, such as pancreatic, lung, breast, and colorectal cancers, the stroma can make up as much as 90% of the tumour mass (D'Arcangelo et al., 2020).

The immune system plays a crucial role in colorectal cancer (CRC) development, progression, and treatment outcomes (Formica et al., 2014; IJsselsteijn et al., 2019). Cancer elicits a host response, which leads immune cells (like T-cells and neutrophils) to eliminate it. Still, cancer evolves strategies to escape the immune system's destruction (Dunn et al., 2004). Tumours can adopt various immune evasion strategies, like inducing immunosuppressive environments, ultimately undermining the immune system's ability to mount an effective response (Kather & Halama, 2019; Guo et al., 2020). The immune response dynamics in CRC are further complicated by phenomena such as immune exhaustion, wherein prolonged exposure to tumour antigens diminishes the functionality of T-cells. This condition presents significant challenges in treatment, particularly with the advent of immune checkpoint inhibitors, which are designed to reinvigorate exhausted T-cells and enhance anti-tumour activity (Wozniakova et al., 2022; Cornista et al., 2023).

While inflammation is essential for tissue repair, it can also influence these processes to promote tumourigenesis (Hanahan & Weinberg, 2011). At the tumour initiation stage, chronic inflammation is present, which can be caused by disruption of tissue homeostasis, like in an aberrant wound healing process (West et al., 2015). This may be caused by

environmental factors, e.g. smoking and can lead to oxidative stres by ROS, leading to DNA damage and epigenetic changes (Schmitt & Greten, 2021). In later stages, inflammation is heightened due to cancer cell-derived factors. Hypoxia and activated oncogenes further drive transcription and secretion of pro-inflammatory cytokines, chemokines and growth factors from cancer cells (Schmitt & Greten, 2021). Tumour-induced inflammation plays a crucial role in determining the outcome of cancer (West et al., 2015).

However, tumour cells can evade immune surveillance by altering cytokine profiles or reprogramming immune cells to create an immunosuppressive TME and CAFs play a central role in managing this process (Y. Zhang et al., 2020).

Metastasis, the spread of cancer cells to distant organs, is the primary cause of cancer-related deaths (Steeg, 2016;Fares et al., 2020). This complex process involves multiple steps, including invasion, intravasation, extravasation, and colonisation (Valastyan & Weinberg, 2011). Key hallmarks of metastasis include motility, invasion, modulation of the microenvironment, cellular plasticity, and colonisation ability (Welch & Hurst, 2019). Metastatic cells interact with the TME, evade immune surveillance, and adapt to new sites (Obenauf & Massagué, 2015). The epithelial-to-mesenchymal transition (EMT) is a defining mechanism of this process (Chaffer & Weinberg, 2011). Additionally, CAFs play a vital role in tumour metastasis across various cancer types (Asif et al., 2021).

1.3 Cancer-associated Fibroblast (CAF)

1.3.1 Fibroblasts and Myofibroblasts during Wound Healing

Fibroblasts are cells of primarily mesenchymal origin, which play a crucial role in maintaining and repairing connective tissue, hence producing tissue-specific extracellular matrix (ECM) (Sahai et al., 2020; Plikus et al., 2021). The ECM is a dynamic network of macromolecules, such as collagens, fibronectins, laminins, elastins, proteoglycans, and integrins; which provide structural support and biochemical cues to cells (Yue, 2014; Theocharis et al., 2016). Fibroblasts are present in nearly all organs and normal tissues, playing a key role in tissue homeostasis, inflammation and fibrosis during wound healing (Glabman et al., 2022). Usually, fibroblasts are in a resting state and only become activated upon damage, triggering a wound healing response (Figure 3) (Kalluri, 2016).
After epithelial damage and blood coagulation, an inflammatory phase begins, during which immune system cells are recruited and cytokines are produced, resulting in the formation of granulation tissue (Figure 3). Following this, the growth phase starts with neovascularisation, the recruitment of repair macrophages and fibroblasts migrating to the wound area and starting to proliferate (Rodrigues et al., 2019; Younesi et al., 2024). Meanwhile, tissue-resident fibroblasts also undergo phenotypic and functional changes, acquiring a transient active phenotype. In this state, fibroblasts are referred to as (proto-)myofibroblasts (Kalluri, 2016). First (proto-)myofibroblasts begin to produce collagen and form contractile actomyosin stress fibres, which facilitate wound closure and maintain mechanical organ integrity. Later, myofibroblasts fully mature, adopting a highly contractile phenotype characterised by the expression of α-smooth muscle actin (α-SMA) and its localisation in stress fibres (Figure 3). A network is established between microfilament bundles and ECM proteins, supporting cellular contractility and enabling myofibroblasts to maintain their surrounding microenvironment. This leads also to an increase in the production of ECM components (Fotsitzoudis et al., 2022). Myofibroblasts create the mechanical conditions that promote and sustain their contractile phenotype through a positive feedback loop (Calvo et al., 2013; Younesi et al., 2024). However, the balance of myofibroblast activity is critical; excessive activation can lead to fibrosis and scarring, while insufficient activation can impair wound healing (Figure 3) (Sarrazy et al., 2011; Hinz & Lagares, 2021). Additionally, fibroblasts during wound healing express specific markers, among them fibroblast activation protein (FAP), a membrane-bound protein, and vimentin, part of the cytoskeleton (Puré & Blomberg, 2018; Younesi et al., 2024).
In the final maturation phase of wound healing, the overall number of fibroblastic cells and vessels is reduced by programmed cell death (see Figure 3) (Hinz, 2016).
During fibrosis, the activation of fibroblasts into myofibroblasts is persistent, and hence different from acute wound healing (Kalluri, 2016). However, the TME shares remarkable similarities with a chronic wound-healing process, often described as "wounds that do not

heal" (Rybinski et al., 2014; Foster et al., 2018). The constantly active fibroblast state is maintained partially by epigenetic remodelling in the activated fibroblasts, which increases anti-apoptotic pathways and triggers increased proliferation (Kalluri, 2016). Importantly, fibroblasts not only produce the ECM and contract it, but also promote angiogenesis, influence epithelial stem cells, and impact the immune system by secreting chemokines and cytokines. This means fibroblasts maintain a highly diverse crosstalk with a plethora of different cells (Kendall & Feghali-Bostwick, 2014; Sahai et al., 2020, Plikus et al., 2021). Thus, fibroblasts are involved in various physiological and pathological processes, including ageing, cancer, and inflammation (Boraldi et al., 2024).
The challenge in defining fibroblasts primarily arises from the absence of specific markers that are not found in other cell types. Fibroblasts are typically characterised by their morphology, location within tissues, and the lack of markers linked to different other cell lineages (Sahai et al., 2020).

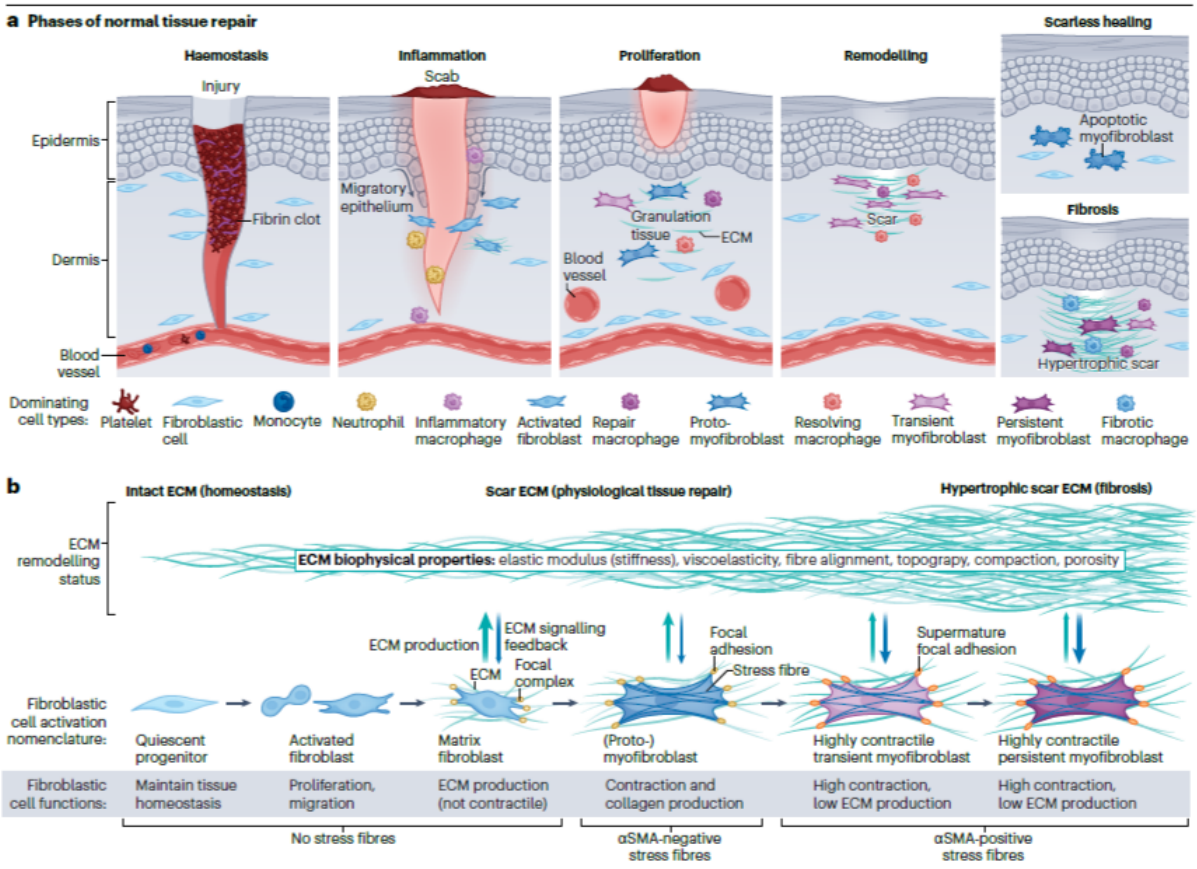


Figure 3: Phases of tissue repair and myofibroblast activation *(Younesi et al., 2024)*

1.3.2 Cancer-associated fibroblast (CAF): Definition and Marker

In the context of cancer, the active phenotype of fibroblasts found in the TME is called cancer-associated fibroblast (CAF) (Madar et al., 2013; Czekay et al., 2022). CAFs still share many characteristics with the fibroblasts mentioned above. However, compared to normal fibroblasts, CAFs exhibit increased proliferation, migration, secretion, and a distinct morphology, as well as a higher metabolism, accompanied by aberrant ECM production (see Figure 4). CAFs are typically larger than inactive fibroblasts, with a spindle shape, dented nuclei, and branching cytoplasm (Glabman et al., 2022). Additionally, CAFs are more vulnerable to epigenetic modifications (Chhabra & Weeraratna, 2023). It has been shown that CAFs impact various cancer hallmarks such as tumourigenesis, proliferation, angiogenesis, EMT, migration, invasion, metastasis, stemness, immunity and therapy resistance (Tommelein et al., 2015;L. Deng et al., 2021; Hanahan, 2022). Additionally, CAFs are implicated in tumour-promoting inflammation and fibrosis (Glabman et al., 2022). CAFs play a crucial role in regulating key mechanisms involved in cancer progression and metastasis, as well as in influencing treatment response by promoting cancer cell survival and aggressiveness (Linares et al., 2021).

Interestingly, genetic alterations like mutations seen in cancer cells are seldom detected in CAFs (Liao et al., 2019). Multiple signalling mechanisms are involved in the transformation of resting fibroblasts into CAF and many need to be discovered. The known pathways include the activation of the Hippo pathway, loss of p53, and activation of heat shock factor protein 1 (HSF-1), driven by inflammation and alterations in the structure and composition of the ECM (Glabman et al., 2022). Additionally, other well-known signalling pathways abundant in cancer, including the transforming growth factor-β (TGF-β), Hedgehog (Hh), Notch, Wnt, nuclear factor kappa-B (NF-κB), Janus kinase (JAK)/signal transducer and activator of transcription (STAT), mitogen-activated protein kinase (MAPK), and phosphoinositide 3-kinase (PI3K)/AKT pathways, as well as transcription factors, including hypoxia-inducible factor (HIF), Snail, and Twist moderate the generation, activation, heterogeneity, metabolic features and cancer-promoting phenotype of CAFs (Z. Fang et al., 2023a). Thus, the exact definition of CAFs and which markers they harbour, is a highly debated and evolving topic (Nurmik et al., 2020a)

A 2020 consensus statement of experts in the field defined CAF as “cells negative for epithelial, endothelial, and leukocyte markers with an elongated morphology and lacking the mutations found within cancer cells” (Sahai et al., 2020). Additionally, mesenchymal markers verify the cells’ identity as fibroblasts. However, this may not be sufficient to exclude cell types like pericytes and adipocytes (Sahai et al., 2020). Mesenchymal stem cells (MSCs) express a similar but less complex set of surface markers and can differentiate into osteoblasts, chondrocytes, and adipocytes. Transdifferentiation from non-fibroblast lineages can occur through epithelial-to-mesenchymal transition (EMT) and endothelial-to-mesenchymal transition (EndMT) (Glabman et al., 2022).

Activated CAF markers comprise but are not limited to: α-smooth muscle actin (α-SMA; Gene name: ACTA2), fibroblast activation protein (FAP), microfibril-associated protein 5 (MFAP5), Tenascin-C (TNC). Whereas fibroblast (not CAF-specific) markers include fibroblast-specific protein 1 (FSP1, also known as S100A4), platelet-derived growth factor receptor α/β (PDGFR α/β), Periostin (POSTN), and Vimentin (VIM). These markers have also been used to delineate various sub-populations of CAFs (Nurmik et al., 2020). Since the phenotypes of CAFs vary across different tumours, studies on CAFs require the use of multiple biomarkers to classify these cells precisely (Glabman et al., 2022).
The collagen subtype COL11A1 has been proposed as a pan-cancer-specific biomarker for activated CAFs (Jia et al., 2016). Additionally, ECM proteins often secreted by CAF are tenascin-C, periostin (POSTN), fibronectin, and neural/glial antigen 2 (NG2) chondroitin sulphate proteoglycan (Glabman et al., 2022).
Identifying a universal marker for activated fibroblasts is challenging due to their high heterogeneity. Several biomarkers have been identified to detect CAFs; however, none are specific to fibroblasts. The available markers typically indicate a change in functional state and often delineate CAF into specific subtypes (Yang et al., 2023; Zhao et al., 2023; Allen, 2024; Nurmik et al., 2020; Glabman et al., 2022).

1.3.3 Origin of CAFs

CAFs originate from several precursor cells, including normal fibroblasts, stellate cells, mesenchymal stem cells (MSCs), adipocytes, epithelial cells, endothelial cells, pericytes, stellate cells, cancer stem cells, and monocytes (see Figure 4) (Nair et al., 2017; Lavie et al., 2022; Glabman et al., 2022).Some of these are recruited from distant sites, like the bone marrow, while others differentiate from tissue-resident cells. Normal fibroblasts, particularly tissue-resident fibroblasts, are the most common source of CAFs (Xiang et al., 2022). However, circulating fibrocytes can also invade the TME. Some CAFs are thought to evolve from epithelial or endothelial cells that have undergone trans differentiation (via epithelial or endothelial mesenchymal transition (EMT/EndMT) (Fotsitzoudis et al., 2022). The exact origin of CAFs and the mechanism of how they are activated are still debated (Sahai et al., 2020).
CAFs gradually change with progressing cancer, a process termed stromatogenesis (Sahai et al., 2020; Chhabra & Weeraratna, 2023). While predominantly tumour-promoting, some CAF subsets may restrain tumour growth functions, particularly in the early stages of cancer development (Biffi & Tuveson, 2021; Abudukelimu et al., 2024). Normal fibroblasts exert a tumour-suppressive effect, but when they turn into CAFs, they tend to promote tumour growth (Sahai et al., 2020). The transition from fibroblasts to CAFs is mainly irreversible, yet the CAF phenotype remains flexible within or across different tumour types (Glabman et al., 2022). An alternative hypothesis has been proposed, suggesting that CAFs represent a cell state driven by autocrine and paracrine signalling, rather than a distinct cell type (Kalluri, 2016).

1.3.4 CAF activation

Activation is a term that is not well-defined and can mean any increased or novel characteristic or function of CAFs. This can refer to various changes, such as cell contraction, migration, proliferation, cytokine secretion, and ECM remodelling (see Figure 4) (Hinz, 2016). The most widely agreed-upon activated CAF phenotype is characterised by high ECM production and remodelling, with high α-SMA and FAP expression (Nurmik et al., 2020; Sahai et al., 2020). However, the expression of these markers is highly dynamic, vary between subpopulations and tumours and do not represent all CAF-associated functions (Nurmik et al., 2020). Additionally, to their contractile capabilities, CAFs display an increase in the secretion of many factors (Belhabib et al., 2021). Furthermore, increased proliferation can be detected, as they become more metabolically active and exhibit enhanced migration capabilities (see Figure 4) (Kalluri, 2016).

The activation of fibroblasts into CAFs is believed to be mainly driven by cancer cell-derived factors (Yang et al., 2023). However, other cell types (e.g. macrophages) might also be involved in CAF activation. CAF and macrophages have been described as having a reciprocal relationship (Comito et al., 2014). The impact of growth factors, cytokines, and paracrine interactions mainly drives the activation of CAFs (Avagliano et al., 2018). Moreover, Notch signalling via direct contact and several nuclear receptors may play a part in CAF activation (Liao et al., 2019). Additionally, many contributing factors influence CAF generation, such as inflammation, ECM stiffness and metabolic reprogramming (Calvo et al., 2013;Avagliano et al., 2018; Sahai et al., 2020).

Signals leading to CAF activation can be grouped into several mechanisms, including tumour growth factor β (TGF-β) signalling, inflammatory signalling (IL-1, IL-6, and TNF), direct cell-cell contact, extracellular matrix stiffness, DNA damage, physiological stress, and receptor tyrosine ligands (Sahai, 2020).

The most established route for activating CAFs is the tumour growth factor-β (TGF-β) pathway (Hanley et al., 2014; Shi et al., 2020; Chandra Jena et al., 2021). TGF-β family ligands activate the SMAD signalling, which, in combination with serum response factor (SRF), upregulate α-SMA expression and the contractile cytoskeleton (Hawinkels et al., 2014; Sahai et al., 2020). Lysophosphatidic acid produced by cancer cells works in synergy with TGF-β to promote the activation and enhance the contractility of CAFs (Sahai et al., 2020).

Furthermore, direct contact between cancer cells and CAF can lead to activation, which promotes tumour growth and metastasis (Sahai et al., 2020). Essential proteins and receptors activated by direct contact are: cadherins, integrins, fibronectin, ephrin-receptors and Notch (Yamaguchi & Sakai, 2015; Labernadie et al., 2017; Strell et al., 2019; Kakarla et al., 2022; Dhungel & Dragoi, 2024). Additionally, hetero-cellular gap junction communication exists, working unidirectionally from CAF to cancer (M. Luo et al., 2018).

Various cytokines and growth factors, such as epidermal growth factor (EGF), fibroblast

growth factor (FGF) and platelet-derived growth factor (PDGF), have been shown to promote the differentiation of various cell types into CAFs. These growth factors activate receptor tyrosine kinases (Sahai et al., 2020; Glabman et al., 2022; Yang et al., 2023).
IL-1 from innate immune cells activates NF-κB in CAFs, leading to IL-6 production through the JAK1-STAT3 pathway and promoting CAF differentiation (Erez et al., 2010; Sanz-Moreno et al., 2011). Furthermore, the signalling of JAK1–STAT3 leads to increased Rho-dependent actomyosin contractility (Sanz-Moreno et al., 2011a). Additionally, modifications in histone acetylation in response to STAT3 further drive the activation of CAF through an epigenetic switch (Albrengues et al., 2015).
The stiffness of the ECM can affect CAF function via YAP/TAZ, involving yet again the upregulation of SMAD, leading to increased α-SMA transcription and thus creating a feedback loop (Calvo et al., 2013).
Cellular stress activates CAFs, such as misfolded protein response, reactive oxygen species (ROS), hypoxia or DNA breaks (Scherz-Shouval et al., 2014; Costa et al., 2014; Arcucci et al., 2016; Glabman et al., 2022).
Furthermore, cancer therapies modulate CAF behaviour, which might influence therapy resistance (Sahai 2020). All the above-described mechanisms can lead to senescence in fibroblasts, where they don't proliferate but secrete inflammatory cytokines, a state also termed senescence-associated secretory phenotype (SASP) (Takasugi et al., 2022).
Overall, the exact origin of CAFs and activation mechanisms within the TME are versatile but still not fully understood. Future studies utilizing lineage tracing for the cell of origin will be crucial for gaining deeper insights into CAF origins and their evolution during tumourigenesis (Glabman et al., 2022).

1.3.5 CAF heterogeneity and subtypes

As already outlined above, the functions of CAFs are manifold and highly diverse (Ganguly et al., 2020; Louault et al., 2020).Fibroblasts in healthy tissues are already very heterogeneous, and their diversity even increases when they turn into CAFs (Shaw & Rognoni, 2020). This means CAFs within a distinct tumour show high heterogeneity, but this diversity furthermore increases when accounting for different cancer types (K. Wright et al., 2023).
Further, CAF heterogeneity can be modulated by several tumour cell-derived growth factors and chemokines, including epidermal growth factor (EGF), platelet-derived growth factor (PDGF), fibroblast growth factor (FGF), interleukin-6 (IL-6), tumour necrosis factor α (TNF-α) and interleukin 1β (IL-1β) (Yang et al., 2023).
In 2017, Öhlund et al. categorized CAFs of pancreatic ductal adenocarcinoma (PDAC) in a co-culture experiment, which simulated the desmoplastic reaction observed in patients (Öhlund et al., 2017; Fiorini et al., 2020). Two distinct setups resulted in two different subtypes: myofibroblastic CAFs (myCAFs), characterized by high α-SMA and low IL-6 expression, and inflammatory CAFs (iCAFs), characterized by low α-SMA and high IL-6

expression (see Figure 4). MyCAFs, activated by direct contact with cancer cells, are located adjacent to the tumour cells. In contrast, iCAFs are induced by cancer cell-derived or immune cells-derived factors like IL-1α and TNF-α and are situated more distantly from tumour cells (see Figure 4). Functionally, iCAFs promote tumour progression by secreting inflammatory cytokines and growth factors that enhance cancer cell proliferation, metastasis, and chemoresistance. In contrast, myCAFs exhibit a dual role, inhibiting or promoting tumour growth depending on the tumour stage and the surrounding TME (Öhlund et al., 2017). These two opposing subtypes have been frequently identified in different cancers (Sahai et al., 2020). But whether these subtypes are specific for pancreatic cancer only has yet to be determined.

Furthermore, subpopulations are interchangeable, depending on culture conditions (Elyada et al., 2019). The functional specialization of CAF might be transient, as it has been shown that TGF-β transforms fibroblasts into myCAFs, which in turn simultaneously inhibit their transformation into iCAFs by downregulating IL1R1 expression, a key factor for NF-κB signalling and the subsequent production of IL-6 (Biffi et al., 2019). The myofibroblast state is dependent on a variety of extracellular cues; therefore, it can be reasoned that if these cues change, the myofibroblast changes as well, making it highly adaptable (Avery et al., 2018; Malik et al., 2019). Hence, the system is highly dynamic with changes in dominant subpopulations and their connected functions, leading to different patient prognoses in different cancers (Asif et al., 2021). Some functions are subset-specific (myCAF/iCAF) or marker-specific (FAP). Myofibroblastic CAF (myCAF) play a crucial role in cancer progression by promoting ECM production and remodelling, supporting cell-ECM interactions, and playing a role in regulating adaptive immune responses (Özdemir et al., 2014). iCAFs are typically defined by their secretory and pro-inflammatory phenotype (Glabman et al., 2022). However, these two subtypes may represent the extremes of a functional spectrum influenced by IL-1-R1 expression, which is regulated by the balance between TGF-β signaling (promoting myCAFs) and IL-1/JAK/STAT signalling (promoting iCAFs) activation (Biffi et al., 2019).

CAFs can also be classified based on their location, such as within the primary tumour, circulating in the bloodstream or at metastatic sites (MAFs) (Glabman et al., 2022). Adding to the complexity, the temporal evolution of CAFs during tumour progression makes it challenging to isolate the specific impact of their spatial distribution (Kalluri, 2016; D'Arcangelo et al., 2020).

Further research investigating single-cell RNA sequencing and bulk sequencing of PDAC revealed a new subtype named antigen-presenting CAFs (apCAFs). These apCAFs are characterized by the expression of primary histocompatibility complex class II molecules (MHC II) (see Figure 4) (Elyada et al., 2019; Yang et al., 2023; Papait et al., 2022).

A variety of rarely occurring CAFs have been described across different cancers using single-cell RNA sequencing: proliferative CAFs (pCAFs) or cycling CAFs (cCAFs), developing CAFs (dCAFs), interferon-response CAFs (ifnCAFs), matrix CAFs (mCAFs),

metabolic CAFs (meCAFs), mesothelial CAFs (mesCAFs), EMT-like CAFs, epithelial to mesenchymal transition-like CAFs, tumour-like CAFs (tCAFs), reticular-like CAFs (rCAFs) and vascular CAFs (vCAFs) (Glabman et al., 2022; Kazakova et al., 2024). Recent scRNA-sequencing transcriptome data of several cancers suggest that there are between 3 and 4 major subsets of fibroblasts (H. Luo et al., 2022; C. Ma et al., 2023; B. Chen et al., 2023). However some of these subsets may share overlapping characteristics and exhibit context-dependent or tumour-dependent variability (Glabman et al., 2022).

Specific mutations, such as those in KRAS and p53, can affect CAF characteristics. Pancreatic ductal adenocarcinoma (PDAC) shows that p53 mutations increase tumour necrosis factor (TNF) secretion and enhance ECM remodelling. Although these studies are limited by not factoring in the non-genetic effect of the TME (Tape et al., 2016; Vennin et al., 2019; Sahai et al., 2020). PDAC and breast cancer, both of which are frequently characterised by a dense desmoplastic stroma, the classification of subtypes is more precisely defined (Lunardi et al., 2014; Wang, 2015; Elyada et al., 2019; Bartoschek et al., 2018;Sebastian et al., 2020;Di Maggio & El-Shakankery, 2020). However, in CRC, no clear subtypes have been established yet, with several papers proposing different subtypes. Two distinct single-cell transcriptomic profiles for colorectal cancer-associated fibroblasts (CAFs) have been identified by Li et al. CAF-A cells have been associated with the expression of matrix metalloproteinase 2 (MMP2), decorin (DCN), and collagen type 1 alpha 2 (COL1A2). In contrast, CAF-B cells harbour myofibroblast markers such as ACTA2 (α-SMA), TAGLN, and PDGFA. CAF-A are associated with ECM remodelling, whereas CAF-B are proposed as activated myofibroblasts (H. Li et al., 2017). Zhang et al found two subsets of CAF in CRC: ACTA2+ myofibroblasts and FAP+ CAF, with different subsets of tumour-associated macrophages (TAM) interacting with them (L. Zhang et al., 2020). Additionally, CAFs have been grouped by a separate study, which identified podoplanin (PDPN), α-SMA, and S100A4 (FSP), each associated with distinct prognostic outcomes. The high expression of the marker PDPN+ led to a better prognosis, whereas the combination of the absence of PDPN with high α-SMA or S100A4 showed a poor prognosis (Choi et al., 2013).

Another single-cell sequencing and transcriptomics study identified CRC-CAF based on four different marker expressions (ACTA2, FAP, PDGFRB, and NOTCH3). This group identified four high-risk marker expressions (TCF7L1, FLNA, GPX3, and MMP11) associated with ECM remodelling, PI3K signalling, and focal adhesion pathways. They also associated the identified genes with predictions in response to PDL-1 immunotherapy (Zhao & Chen, 2022). In future studies, the use of single-cell sequencing and other novel techniques to identify fibroblast subsets holds promise for providing greater clarity on this specific topic (Lavie et al., 2022).

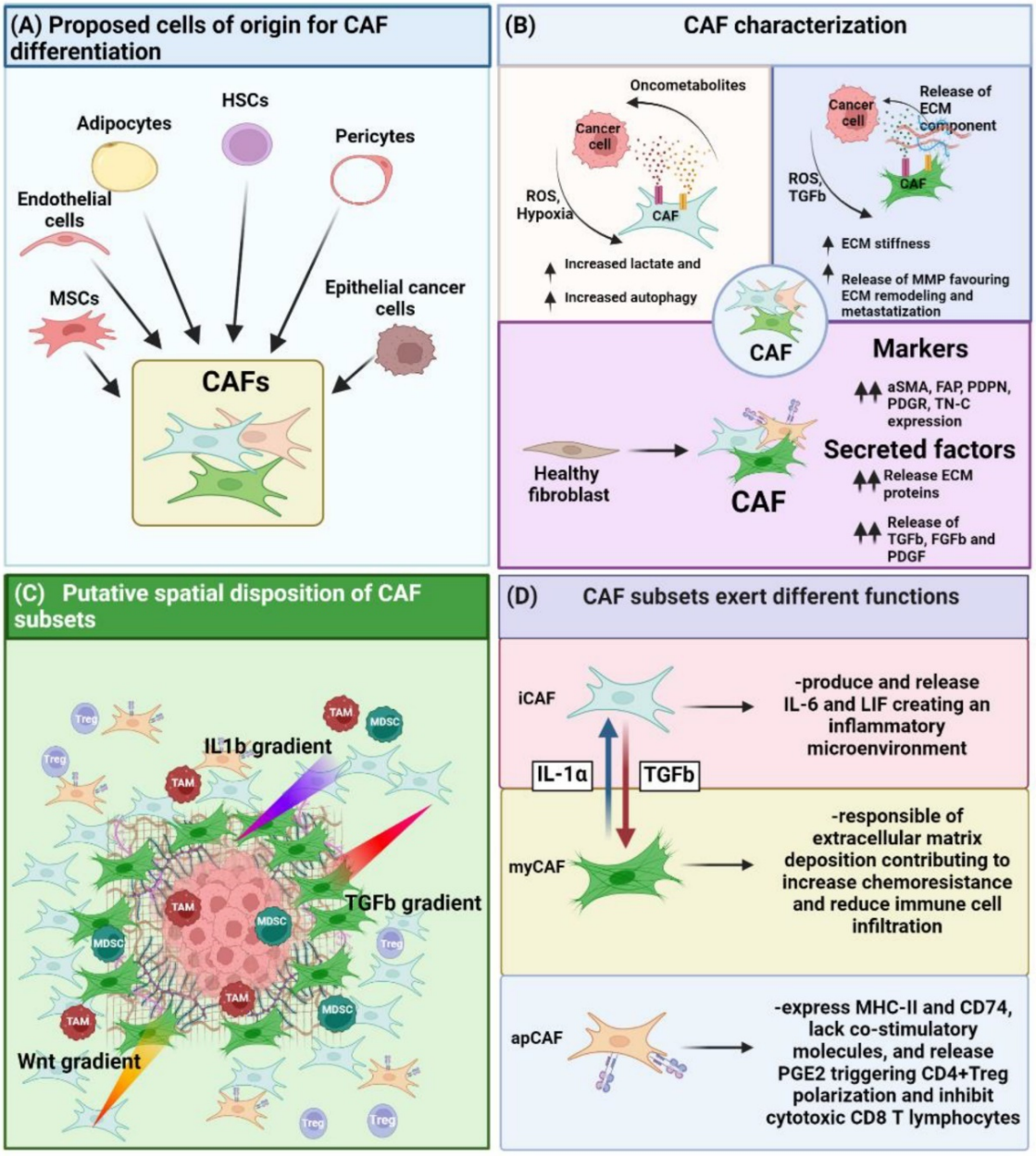


Figure 4: **Cancer associated fibroblasts (CAFs)** (based on Pancreatic ductal adenocarcinoma (PDAC) **(A)** CAFs can be derived from various cell types. **(B)** CAF characterisation: ECM depletion and stiffness, secretome, metabolism and markers **(C)** CAF subsets and their spatial location **(D)** CAF subsets: iCAF, myCAF and apCAF (Papait et al., 2022)

1.3.6 CAF function

CAFs provide the nurturing "soil" where cancer "seeds" thrive and proliferate (Chhabra & Weeraratna, 2023). However, the cancer “seed” shapes the CAF “soil” according to its needs (Belhabib et al., 2021). CAF play an essential role in tumour progression by influencing multiple cancer hallmarks, including cancer growth, angiogenesis, metastasis, immune evasion and therapy resistance (Tommelein et al., 2015;Deng et al., 2021;Asif et al., 2021; Czekay et al., 2022; Glabman et al., 2022). The main CAF functions that support cancer are CAF-directed extracellular matrix remodelling, secretion of factors, metabolism and direction of the immune system (Deng et al., 2021;Glabman et al., 2022).

CAFs support tumour growth by secretion of growth factors (Linares et al., 2021;Biffi & Tuveson, 2021)and metabolic reprogramming (Z. Li et al., 2021).

CAFs produce and remodel the extracellular matrix, which increases fibrosis and stiffness, thereby facilitating proliferation, invasion, EMT, and metastasis. Additionally, this forms a physical barrier that prevents immune and drug penetration (Winkler et al., 2020;Asif et al., 2021).

CAFs promote tumour invasion and metastasis mainly by secretion of pro-metastasis factors and remodelling the ECM (Erdogan & Webb, 2017; Asif et al., 2021).

CAF induce Angiogenesis: Promoting blood vessel formation to nourish the tumour (Z. Zhang et al., 2025)

CAFs modulate the immune system: They contribute to chronic inflammation that promotes tumour progression and create an immunosuppressive microenvironment that helps tumour cells evade immune detection (Monteran & Erez, 2019; Mhaidly & Mechta-Grigoriou, 2021)

CAFs contribute to therapy resistance: playing a role in resistance to cancer therapies, including chemotherapy and immunotherapy (Y. Chen et al., 2021)

1.3.7 CAF therapy

Recent research has identified IL-1 and TGF-β as key cytokines secreted by tumours that drive the heterogeneity of CAFs. TGF-β signalling suppresses IL-1 receptor 1 (IL-1R1) expression, inhibits IL-1 responses, and promotes the differentiation of fibroblasts into myofibroblast CAFs. In contrast, IL-1 signalling activates the JAK/STAT pathway, leading to the development of inflammatory CAFs (Yoshida, 2020). This dynamic has led to the concept of a "stromal switch," where tumour-promoting CAFs could potentially be reprogrammed into tumour-suppressing CAFs (D. Yang et al., 2023). Small-molecule inhibitors targeting TGF-β signalling have shown promise in modulating CAF activity and suppressing tumour progression (Z. Fang et al., 2023; Yoshida, 2020).

CAFs and their secretome are emerging as valuable targets for cancer diagnosis, prognosis, and therapy. Several cytokines within the CAF secretome are being explored as potential biomarkers in clinical settings (Linares et al., 2021). For instance, chemotherapy has been

shown to increase the representation of stromal cells in residual tumours, and CAFs can support tumour regrowth after DNA damage through the secretion of WNT-16B (Y. Sun et al., 2012). Epigenetic alterations, such as DNA methylation changes, are also recognised as key determinants of CAF phenotype and are being investigated in clinical trials (Linares et al., 2021)

Therapeutic strategies targeting CAFs include those aimed at directly depleting CAFs, reducing their tumour-promoting functions, or reprogramming them to a quiescent state. Chemotherapy strategies focus on reverting activated cancer-associated fibroblasts (CAF) to a quiescent state using agents like all-trans-retinoic acid (ATRA) or minnelide, which disrupts TGF-β signalling. The angiotensin receptor II antagonist losartan has also been shown to reduce CAF activation, decrease desmoplasia, and improve drug delivery and immunotherapy efficacy, with ongoing trials investigating its use in pancreatic cancer (Glabman et al., 2022).

Recent research also targets immunosuppressive CAF functions by inhibiting key signalling pathways such as IL-6, LIF, TGF-β, and the CXCL12/CXCR4 axis, which plays a role in cancer progression and immunosuppression. CXCR4 inhibitors, such as plerixafor, have been shown to reduce fibrosis, normalise vasculature, and enhance the efficacy of checkpoint inhibitors (Glabman et al., 2022). Additionally, targeting CAF-derived proteins through secretome analysis holds potential for identifying new therapeutic targets and prognostic markers (De Boeck et al., 2013).

Despite preclinical promise, targeting CAFs in human clinical trials has faced challenges. Trials aimed at targeting CAFs in melanoma, breast cancer, pancreatic cancer, and colorectal cancer have been unsuccessful so far (Glabman et al., 2022). The complexity of CAF biology, including their diverse origins and functional plasticity, complicates the development of effective therapies (Yoshida, 2020; L. Deng et al., 2021;Chhabra & Weeraratna, 2023). Further research is needed to understand CAF heterogeneity better and develop more effective CAF-directed treatments (Abudukelimu et al., 2024). Additionally, the modulation of CAFs, rather than their complete ablation, is emerging as a more viable strategy (Sahai et al., 2020). Challenges in targeting CAFs include their heterogeneity, plasticity, lack of specific markers, and issues with current animal models (Glabman et al., 2022).

1.4 CAF markers

1.4.1 Alpha-smooth muscle actin

Alpha-smooth muscle actin (α-SMA), also known as smooth muscle aortic alpha-actin (ACTA2), is a member of the actin protein family, a conserved group essential for cell motility, structure, and integrity. α-SMA plays a crucial role in wound healing and the activation of myofibroblasts. α-SMA integrates into stress fibres, thus contributes to the contractility of myofibroblasts, which are involved in tissue remodelling (Nurmik et al., 2020). Myofibroblast activation is a continuum (see Figure 5): initially, fibroblasts transition to a proto-myofibroblast state, which is migratory and ECM-producing, and eventually into a fully activated myofibroblast, marked by the high *de novo* synthesis of α-SMA (see Figure 5). These myfibroblasts then contract the ECM through α-SMA integration into stress fibres, making them a key component in wound healing and fibrosis (Hinz & Lagares, 2021).
Signalling pathways such as TGF-β, Wnt/β-catenin, and Hedgehog are known to drive myofibroblast differentiation and α-SMA expression (C. Han et al., 2020).Given the significantly higher number of myofibroblasts in the TME, α-SMA has become a significant indicator protein for CAFs and is widely recognised as a CAF marker across various tumour types, including breast (Muchlińska et al., 2022), pancreatic (Geng et al., 2021), cholangiocarcinoma (Sirica & Gores, 2014) and non-small cell lung cancers (Irvine et al., 2021). α-SMA expression may promote tumour progression through ECM remodelling and thus is a widely used indicator of cancer prognosis (Nurmik et al., 2020; C. Han et al., 2020). However, like other CAF markers, α-SMA expression varies across CAF subtypes, highlighting CAF heterogeneity and underscoring that its expression is not specific to CAFs alone, as smooth muscle cells and pericytes also express α-SMA (Nurmik et al., 2020; Kalluri, 2016). Consequently, α-SMA is often used in combination with other markers to characterise CAF populations more precisely (D. Yang et al., 2023).The molecular mechanisms that regulate α-SMA expression in CAFs remain incompletely understood, particularly in response to microenvironmental cues and therapeutic interventions (Nurmik et al., 2020).
We have only partial insights into the impact of α-SMA on cancer growth and progression. For example, in luminal breast cancer, α-SMA^{+} CAFs promote tumour growth by secreting osteopontin, which increases Ki-67 expression, a marker of proliferation, in adjacent tumour cells (Muchlińska et al., 2022). α-SMA+ CAFs also enhance angiogenesis, correlate with lymph node metastasis, and increase cancer stem cell (CSC) frequency (Cao et al., 2025). Other possible effects of α-SMA reported in studies include IL–6–mediated chemoresistance (Quante et al., 2011; Mellone et al., 2016; McAndrews et al., 2022). BMP-4 signalling that modulates cancer stemness (Quante et al., 2011; McAndrews et al., 2021) and autophagy-dependent regulatory T cell synapse formation, which promotes immune evasion (Varveri et al., 2024). Conversely, in colorectal and pancreatic cancers, depletion of α-SMA+ CAFs

is associated with greater invasiveness, metastasis, and reduced survival, indicating that, in these settings, these cells restrain tumour progression (Özdemir et al., 2014; McAndrews et al., 2021; McAndrews et al., 2022). Additionally, α-SMA$^+$ CAFs may secrete a range of cytokines and chemokines, such as M-CSF, IL-6, IL-8, IL-10, TGF-β, CCL-2, and CXCL12, which additionally induce macrophage differentiation and M2 polarisation, which contributes to immunosuppressive TME (Mace et al., 2013; Nagarsheth et al., 2017).

Despite its importance, α-SMA's specificity and prognostic value are context-dependent. Its expression varies by cancer type and CAF source (Micalet et al., 2024; Kumar et al., 2023). Quantitative assessments range from as low as 0.35% to nearly 50% α-SMA-positive areas in tumour stroma (Tsujino et al., 2007;Ikuta et al., 2018; Zhu et al., 2012).

Some CRC studies link higher α-SMA expression with poor prognosis, while others find no strong statistical associations (Hawinkels et al., 2014; Sculthorpe et al., 2024; Sinn et al., 2014; K.-H. Sun et al., 2016). A study shows that α-SMA-positive CAF suppress CSCs and limits tumour progression (McAndrews et al., 2021).The pro-tumour effect of α-SMA may be particularly observable in mismatch repair–proficient CRCs (Sculthorpe et al., 2024). Neoadjuvant therapy in CRC is linked to increased α-SMA/epithelial area ratio, which correlates with poor recurrence-free survival (Verset et al., 2015). In addition, studies report that TGF-β/Smad activation induces α-SMA and upregulates matrix metalloproteinase, which drives key processes such as EMT, invasion, and chemoresistance in CRC (Hawinkels et al., 2014). Thus, in CRC, α-SMA$^+$ CAFs display complex, sometimes opposing functions. These findings indicate that α-SMA expression defines a heterogeneous fibroblast population with context-dependent effects on cancer progression.

Therapeutic strategies targeting α-SMA$^+$ CAFs are being explored, though outcomes have been mixed (Özdemir et al., 2014; Sculthorpe et al., 2024). Nonetheless, α-SMA remains an essential marker of CAF activation, providing a useful tool for the functional assessment of the TME. Combination therapies involving CAF-targeted agents, chemotherapy, and immunotherapy are under investigation, with bispecific antibodies offering one promising approach (Kalluri, 2016; Cao et al., 2025; D. Yang et al., 2023).

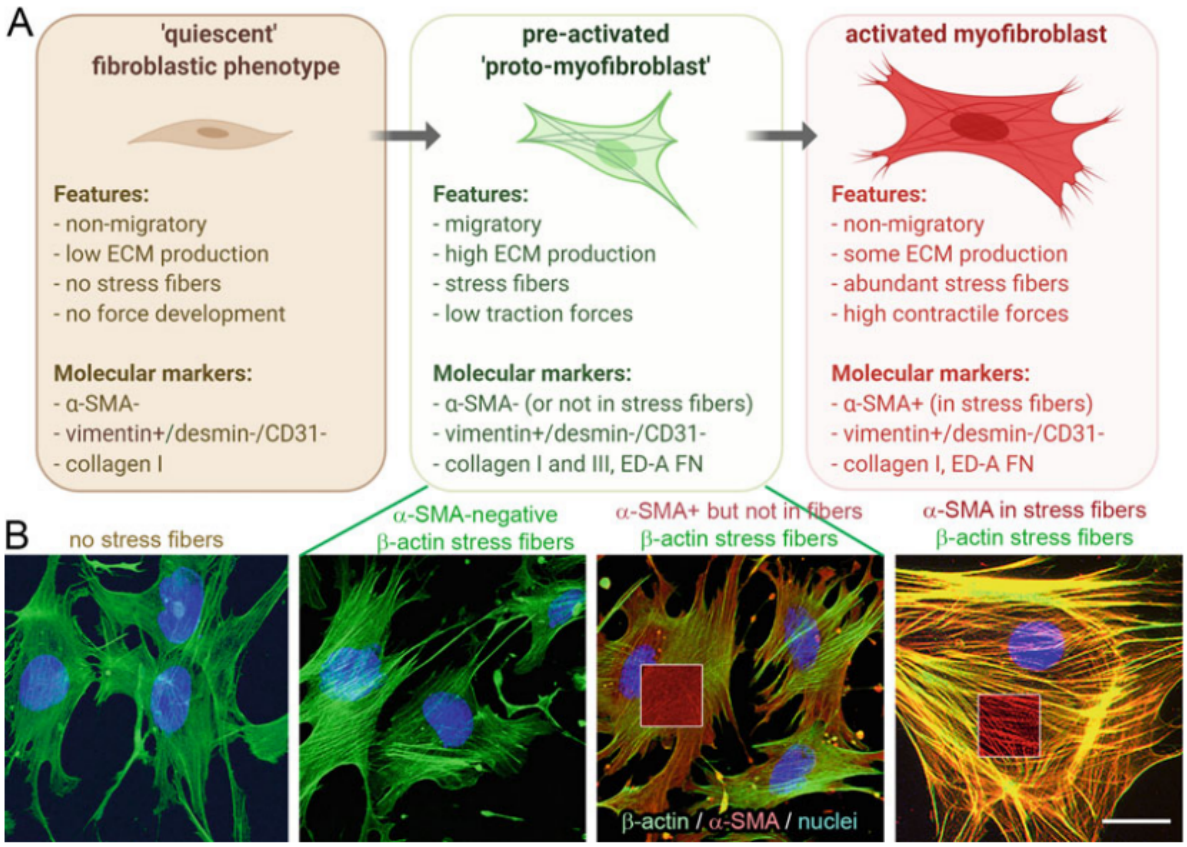


Figure 5: **Myofibroblast activation states as a continuum.** (Hinz & Lagares, Myofibroblasts - Methods in Molecular Biology 2299, Springer 2021).

1.4.2 Fibroblast activation protein

Fibroblast activation protein alpha (FAP) is a membrane-bound serine protease belonging to the dipeptidyl peptidase (DPP) family, which is predominantly expressed in CAFs during wound healing and in fibrotic and inflammatory conditions such as arthritis or cirrhosis (Fitzgerald & Weiner, 2020; Busek et al., 2018; Cao et al., 2025). While its expression is minimal in healthy adult tissues, FAP is significantly upregulated in over 90% of epithelial cancers in the stroma, including colorectal, breast, pancreatic, and lung cancers, especially at the invasive fronts of tumours, where it correlates with poor prognosis, therapy resistance and more aggressive cancer subtypes (Coto-Llerena et al., 2020; Kalaei et al., 2023; Cao et al., 2025).

Functionally, FAP acts as a dual-specific protease, exhibiting both dipeptidyl peptidase and endopeptidase activity. It cleaves ECM components, such as collagen I and III and fibronectin, thereby remodelling the TME to promote angiogenesis, invasion, EMT and immunosuppression. FAP is activated by cytokines such as TGF-β, IL-1β, and TNF-α, and activates downstream pathways including PI3K/AKT, SHH, and STAT3, probably independently of its enzymatic activity (Fitzgerald & Weiner, 2020; Xin et al., 2021). Furthermore, it was shown that FAP-positive CAFs produce ECM that facilitates cancer migration (Z. Cao et al., 2025). Moreover, FAP's interactions with integrins and matrix metalloproteinases further facilitate tumour cell migration and immune evasion. FAP^+ CAFs contribute significantly to the immunosuppressive nature of the TME and thus enhance the resistance to immune checkpoint blockade. FAP^+ CAFs secrete immunomodulatory chemokines such as CXCL12 and CCL2, excluding cytotoxic T-cells and recruiting myeloid-derived suppressor cells (MDSCs), thus enhancing immune evasion (D. T. Fearon, 2014; Feig et al., 2013; Cao et al., 2025). In a transgenic mouse model, eliminating FAP-expressing cells triggered rapid hypoxic necrosis, driven by IFN-γ and TNF-α, both linked to $CD8^+$ T-cell-mediated tumour cell destruction (Kraman et al., 2010; Z. Cao et al., 2025). Genetic deletion and pharmacologic inhibition of FAP inhibited tumour growth in a mouse model of CRC (Santos et al., 2009). Furthermore, FAP silencing in CAFs impaired tumour-promoting functions in preclinical studies (Cao et al., 2025).

FAP is widely considered as one of the most viable CAF markers for potential clinical application, and several therapeutic approaches have been developed, including monoclonal antibodies (e.g., Sibrotuzumab), small molecule inhibitors (e.g. Talabostat), radiotherapy-conjugates, CAR-T cells, and FAP-targeted vaccines (Busek et al., 2018; Xin et al., 2021). However, clinical trials of Talabostat and Sibrotuzumab in colorectal cancer failed to demonstrate efficacy in Phase II, highlighting the limitations of targeting FAP in isolation (Nurmik et al., 2020).

Emerging data from single cell sequencing studies, show that FAP expression is restricted to specific CAF subpopulations, while other fibroblasts within the TME do not express FAP at all (H. Li et al., 2017 ; Nurmik et al., 2020). In CRC specifically, FAP is mainly expressed

in stromal cells and less frequently in epithelial cancer cells and is linked to deeper invasion, lymph node metastasis, poor survival, and resistance to PD-L1 immune checkpoint blockade (Henry et al., 2007; Henriksson et al., 2011; Qi et al., 2022). Hence, FAP expression is believed to be a key factor in the shift from a tumour-resistant to a tumour-permissive microenvironment (Barrett & Puré, 2020).

1.4.3 IL1R1

Interleukin-1 (IL-1) signalling has emerged as a critical driver of CAF activation and immune modulation within the TME. Activation of the JAK/STAT pathway by IL-1 signalling promotes the differentiation of fibroblasts into inflammatory CAFs, which secrete tumour-promoting cytokines and express immune-inhibitory markers, thereby contributing to an immunosuppressive TME, supporting tumour growth and dampening effective immune responses (Gelfo et al., 2018).
IL-1 receptor type 1 (IL-1R1) has been identified as a marker of a CAF subset with potent immunosuppressive and tumour-supportive functions. IL-1α/β stimulation of IL-1R1$^+$ CAFs generates fibroblasts capable of suppressing T-cell activity and inhibiting macrophage function while simultaneously promoting tumour progression (Koncina et al., 2023). Notably, IL-1R1 activation has been linked to fibroblast senescence, enhanced migration, angiogenesis, and resistance to therapy through downstream pathways, including JAK/STAT and PI3K/AKT (Díaz-Maroto et al., 2021; Díaz-Maroto et al., 2019; Ma et al., 2021;Nicolas et al., 2022). Clinical relevance is underscored by the observation that high IL-1R1 expression correlates with poor prognosis and resistance to targeted therapies, including cetuximab, particularly in KRAS-mutant CRC (Gelfo et al., 2018). Recent findings suggest that IL-1 receptor antagonists can enhance chemosensitivity to fluorouracil by dampening inflammatory signalling via NF-κB, offering a potential strategy for overcoming resistance in CRC patients (Yan et al., 2020). Furthermore, targeting both IL-1R1$^+$ CAFs and immune checkpoints, such as PD-L2, is being explored as a promising approach to disrupt the immunosuppressive TME and improve immunotherapy efficacy (Gorchs et al., 2019; K. C. Y. Huang et al., 2020).

1.4.4 Podoplanin

Podoplanin (PDPN) is a transmembrane glycoprotein widely expressed in CAFs, as well as in various lymph vessels, tumour cells, epithelial cells, and inflammatory macrophages (Pula et al., 2013; Nurmik et al., 2020). While not fibroblast-specific, PDPN is markedly upregulated in CAFs compared to normal fibroblasts and plays a pivotal role in cancer progression, inflammation, and tissue remodelling (Quintanilla et al., 2019). Its expression has been associated with both tumour-promoting and context-dependent prognostic roles across cancer types, highlighting its complex and dualistic function in the TME (Choi et al.,

2013; Suzuki et al., 2022; Nurmik et al., 2020).
Mechanistically, PDPN contributes to tumour progression by enhancing cell motility, migration, and invasion, mainly through activation of the Rho/ROCK signalling pathway in CAF and cancer cells, which facilitates ECM remodelling and invasion in both *in vitro* and *in vivo* models (Wright et al., 2023; Quintanilla et al., 2019). PDPN-expressing CAFs influence overall and disease-free survival, underlining their relevance in clinical prognosis (Pula et al., 2013; Quintanilla et al., 2019). Despite its expression in multiple cell types, recent studies emphasise PDPN's utility in identifying pro-tumourigenic fibroblast subpopulations, which are often correlated with worse clinical outcomes in various tumours (Nurmik et al., 2020). This makes PDPN a valuable, albeit not exclusive, marker for interrogating fibroblast heterogeneity within the TME.
In CRC, PDPN serves as a marker of distinct CAF subpopulations, with PDPN-positive CAFs located near tumour tissue considered to be a significant prognostic factor (Oleynikova et al., 2023). Interestingly, some studies report a correlation between PDPN expression and favourable prognosis in CRC (Choi et al., 2013), in contrast to findings in other cancers where PDPN expression is linked to poor outcomes (Suchanski et al., 2017; Hu et al., 2018).

1.4.5 Programmed cell death ligand 2

CAFs contribute to immune evasion, and Programmed cell death ligand 2 (PD-L2), a ligand for the PD-1 immune checkpoint, plays a significant role in various cancers (Y. Wang et al., 2023). PD-L2 is expressed at higher levels in CAFs compared to normal fibroblasts, promoting immune evasion by inhibiting T-cell proliferation and contributing to an immunosuppressive environment (Gorchs et al., 2019). In CRC, PD-L2 expression correlates with tumour progression, with elevated PD-L2 levels in some studies linked to favourable survival outcomes (K. C. Y. Huang et al., 2020a). However, PD-L2's role remains controversial, as it has been associated with both tumour promotion and immune response modulation (Rozali et al., 2012; Pyo et al., 2019). PD-L2 may promote tumour growth by inhibiting T-cell activity, particularly in CRC, where high PD-L2 expression correlates with poorer prognosis in some cases (H. Yang et al., 2019). In line, PD-L2$^+$ CAFs influence the function of tumour-infiltrating lymphocytes (TILs), leading to a more immunosuppressive TME (Lv et al., 2023). However, PD-L2 overexpression can also be associated with improved survival rates in advanced stages of CRC (Huang et al., 2020).
Recently it has been shown that PD-L2 functions as an independent immune checkpoint in CRC, distinct from PD-L1, and offers a complementary therapeutic strategy to PD-1/PD-L1 blockade (L. Zhu et al., 2024). Hence, targeting both PD-L1 and PD-L2 could enhance immunotherapy effectiveness in cancers like CRC, potentially improving patient outcomes (Passardi et al., 2019; Gorchs et al., 2019).

1.5 Aim of the thesis

This thesis aims to investigate CAF subtypes derived from human colon cancer *in vitro.* First, we wanted to know how cytokines of the TME modulate the expression of the myofibroblast CAF marker α-SMA. A particular focus is placed on the dependency of such activation on canonical TGF-β receptor signalling, and the potential for synergistic effects between the cytokines IL-4, IL-13, IFN-γ, and TGF-β1. Additionally, this research wishes to evaluate how external factors, such as culture conditions or the presence of pathway inhibitors (e.g., A-83-01), modulate CAF responses to cytokine stimulation. Two methods, In-Cell western and confocal imaging, should be utilised to characterise the dynamic changes in the expression of α-SMA, following treatment with the abovementioned cytokines and inhibitors. We then planned to additionally test the influence of inflammatory cytokines, IL-1β and TNF-α, and assessed the impact on further CAF markers, such as FAP, PD-L2, PDPN, and IL-1R1.
Secondly, we wanted to know how the defined cytokine environments (IL-4, TGF-β1, IL-1β and TNF-α) shape the tumour-modulatory functions of CAFs. For this, we planned to use conditioned media from CAF to explore the effects of cytokine-pretreated CAFs on the viability of patient-isolated colorectal cancer organoids. To test organoid viability, we wanted to implement the CellTiter-Glo 3D assay, which measures luminescence as a quantity of ATP content. Furthermore, we wanted to test how cytokine-treated CAFs influence the viability, morphology, and proliferative behaviour of matched patient-derived colorectal cancer organoids in a three-dimensional co-culture system. We intended to use an organotypic trans-well assay (OOTA), a co-culture assay where cytokine pre-treated CAFs are distributed in a collagen gel with organoids in Matrigel on top. Moreover, we wanted to evaluate proliferation and apoptosis of organoids by staining for Ki-67 and Caspase-3, respectively. Further, we thought to stain the OOTA CAFs for markers α-SMA and FAP and quantify the staining using confocal microscopy.
The thesis ultimately seeks to contribute to a deeper understanding of stromal plasticity in the TME, with implications for therapeutic targeting of tumour-stroma crosstalk in colorectal cancer. Through the examination of CAF phenotype regulation, α-SMA, FAP and other markers expression in CAFs, we aim to uncover novel insights into the molecular mechanisms driving CAF activation within the TME. Understanding these cytokine pathways in CAFs holds promise for developing novel precision medicine strategies. Understanding the interplay between cytokine signalling and marker expression in CAFs is essential for clarifying the pathogenesis of fibrotic diseases and the interplay between tumour cells and the stromal microenvironment in colorectal cancer.

2. Methods

2.1 Material

2.1.1 Consumables

Table 1

Product	Company	Product#
Cell counting chamber slides	Invitrogen by Thermo Fisher ScientificTM, Waltham, MA, USA	C10314 or C10283
Cell strainer (70 µm)	Corning Incorporated, New York, USA	352350
Cryo Tubes (2 ml)	VWR International, Radnor, Pennsylvania, USA	10018-754
CytoOne Multiwell plates (TC-treated)	Starlab international GmbH, Hamburg, Germany	CC7682-7506 (6-well), CC7682-7512 (12-well), CC7682-7596 (96-well)
CytoOne Tissue Culture Dishes (TC-treated)	Starlab international GmbH, Hamburg, Germany	CC7682-3394 (100 mm) CC7682-3359 (60 mm)
Eppendorf Tube	Eppendorf AG, Hamburg Germany	0030121023 (0.5 ml) 0030120086 (1.5 ml)
Falcon Tube	Sarstedt AG & Co. KG, Nümbrecht, Germany	62.554.502 (15 ml) 62.548.004 (50 ml)
Filtropor S plus 0.2 µm	Sarstedt AG & Co. KG, Nümbrecht, Germany	83.1826.102 (0.2 µm)
Pipette Filter tips	Sarstedt AG & Co. KG, Nümbrecht, Germany	70.1130.210 (10 µl) 70.3030.255 (100 µl) 70.3031.255 (200 µl) 70.3060.255 (1000 µl)
Polyester mesh (mesh size: 100 µm; fiber diameter: 77 µm)	Bückmann GmbH & Co, Mönchengladbach, Germany	20000194
Polystyrene Round-Bottom Tube 5 ml (FACS tube)	Corning Incorporated, New York, USA	353054
Serological pipette	Sarstedt AG & Co. KG, Nümbrecht, Germany	86.1253.001 (5 ml) 86.1254.001 (10 ml)

		86.1685.001 (25 ml) 86.1256.001 (50 ml)
Syringe (10 ml)	B. Braun Austria GmbH, Maria Enzersdorf, Austria	4606108V
Millicell Cell culture Inserts 0,4 µm, 30 mm (Transwell)	Sigma-Aldrich/Millipore	PICM0RG50

2.1.2 Reagents

Table 2

Product	**Company**	**Product#**
Collagen Type I Rat Tail (3.52 mg/ml)	Corning Incorporated, New York, USA	354236
Dimethyl sulfoxide (DMSO)	Sigma-Aldrich, St. Louis, MO, USA	D4540-500ML
Dulbecco's Modified Eagle Medium (DMEM)	Gibco, Thermo Fisher Scientific™, Waltham, MA, USA	21969-035
Dulbecco's Modified Eagle Medium (DMEM) advanced F12	Gibco, Thermo Fisher Scientific™, Waltham, MA, USA	21969-035
Dulbecco's Phosphate-Buffered Saline (1x PBS), (10x PBS)	Gibco, Thermo Fisher Scientific™, Waltham, MA, USA	14190-094, 14200-067
Endothelial Cell Growth Medium MV2 (EGM)	PromoCell GmbH, Heidelberg, Germany	C-22022
Ethanol 70%	VWR International, Radnor, Pennsylvania, USA	85.825.360
Ethylenediaminetetraacetic acid disodium salt solution (EDTA)	Sigma-Aldrich, St. Louis, MO, USA	E7889
Fetal calf serum (FCS), Fetal bovine serum (FBS)	Gibco, Thermo Fisher Scientific™, Waltham, MA, USA	10500-056
L-Glutamine (200 mM)	Gibco, Thermo Fisher Scientific™, Waltham, MA, USA	25030081 13462629
Methanol	VWR International, Radnor, Pennsylvania, USA	1.06009.2511

Bovine Serum Albumin Fraction V (pH 7.0) (BSA)	AppliChem GmbH, Darmstadt, USA	A1391.0100
Sodium Hydroxide (NaOH)	Merck, Darmstadt, Germany	1.06498.1000
Triton X-100	Sigma-Aldrich, St. Louis, MO, USA	X100-500ML
Trypan blue	Sigma-Aldrich, St. Louis, MO, USA	T-8154
Trypsin	Serva Electrophoresis GmbH, Heidelberg, Germany	37289.02
Tween® 20 Biochemica	AppliChem GmbH, Darmstadt, Germany	A1389.1000
Celltiter-Glo 3D Luminescent cell viability assay	Promega, Madison, USA	G9682
Histofix (4% Formaldehyde solution)	Carl Roth, Karlsruhe, Germany	P087.3
Advanced Dulbecco's Modified Eagle Medium/F12 (DMEM/F12)	Gibco	12634-010
HEPES (1M)	Gibco	15630-080
GlutaMAX (100X)	Gibco	35050-061
Cell recovery solution	Corning	354253
TrypLE Express (1X)	Gibco	12605-010
Rock-Inhibitor (Y-27632 dihydrochloride)	Tocris Biocscience	1254
B27 supplement	Gibco	17504-044
N-2 supplement (100X)	Gibco	17502-001
Nicotinamide	Sigma	N0636-100G
N-acetyl-L-cysteine	Sigma-Aldrich	A9165-25G
Recombinant Mouse Noggin	Sino Biological Inc.	50688-M02H / LC15NO1002
A8301	Tocris	2939
SB 202190	Sigma-Aldrich	S7067
Gastrin I (human)	Tocris	3006
Human EGF	PeproTech	AF-100-15
Matrigel Matrix Basement Membrane, Growth factor reduced	Discovery Labware	356231
Stem-Cellbanker	Nippon Zenyaku Kogyo,	230418

	Zenoaq	

2.1.3 Media formulations

Table 3

	Stock concentration	Final concentration
Advanced DMEM/F12	1x	1x
HEPES	1 M	10 mM
Glutamax	200 mM	2 mM
Coating medium		
BSA	1%	1%
Basal medium	1x	1x
Trypsin for Organoids		
Cell recovery solution	1x	1x
TripLE	1x	1x
Y27632 Rock-inh	10 mM	10 µM
ENAS- media		
B27 supplement	50x	1x
N2 supplement	100x	1x
Nicotinamide	1 M	10 mM
N-acetyl-L-cystein	500 mM	1 mM
Noggin	100 µg/ml	100 ng/ml
A8301	500 µM	500 nM
SB202190	10 mM	10 µM
Gastrin	100 µM	10 nM
EGF	1 mg/ml	50 ng/ml
Basal media	1x	1x
ENAS+ media		
Rock- Inhibitor	10 mM	10 µM
ENAS – media	1x	1x
Omin		
Basal media with 2% FCS	1x	1x

2.1.4 Buffers and Supplements

Table 4

Name	Composition
Blocking buffer (ICW assay)	1x PBS 0.5% BSA
Collagen matrix	2mg/ml collagen type I

	1x DPBS DMEM + 5% FCS 1M NaOH
Dulbecco's Modified Eagle Medium (DMEM)	10% Fetal calf serum (FCS) 1% L-Glutamine
DMEM advanced F12	1% FCS
Trypsin-EDTA	245 ml 1x PBS 1g (2.2 U/mg) Trypsin 5 ml 1% Na_2EDTA (pH 7.4)
Tween washing solution (ICW)	1x PBS 0.1% Tween-20
PBST (IF OOTA)	PBS + 0.5% Tween20
TBST (IF OOTA)	Tris buffered saline + 0.5% Tween20
Blocking buffer (IF OOTA)	1x PBS 1.5% BSA

2.1.5 Antibodies, IgG and dies

Table 5

Antibody/Dye/IgG	**Company**	**Product#**	**Dilution**
Immunofluorescence staining			
Anti – rabbit secondary antibody AF 555 PLUS	Invitrogen	A32732	1:500
Anti-mouse secondary labelled antibody 594	Thermo Fisher	A11032	1.500
Anti-rabbit secondary labelled antibody 488	Thermo Fischer	A11034	1:500
CC3 (Cleaved caspase 3) primary antibody	Cell Signalling	9664	1:500
DAPI	Thermo Fischer	D1308	100µl of 2µg/ml
EpCAM primary labelled antibody 555	Cell signalling	5488	1:200
FAP primary Antibody	Cell signalling	66562	1:100
Ki67 primary antibody	Cell signalling	9449	1:500
Vimentin-647 primary labelled Antibody	Abcam	Ab195878	1:5000
α-SMA-488 primary labelled Antibody	Abcam	Ab184675	1:150

ICW			
CellTag 700	Li-COR Biosciences	962- 41090	1:500
FAP primary Antibody (rabbit, IgG)	Cell signalling	66562	1:100
Goat anti-mouse labelled Secondary Antibody, iRDye 800 CW	Li-COR Biosciences	926-32210	1:800
Goat anti-rabbit labelled Secondary Antibody, iRDye 800 CW	Li-COR Biosciences	926-32211	1:800
Goat anti-rat labelled Secondary Antibody, iRDye 800 CW	Li-COR Biosciences	926-32219	1:800
IL-1R-1 primary Antibody (rabbit, pAb)	Abcam	Ab106278	1:100
Mouse IgG2a	Thermo Fischer	02-6200	Concentration adjusted to α-SMA primary labelled Antibody, then 1:300
PD-L1 primary Antibody (rabbit, IgG)	Cell signalling	13684	1:200
PD-L2 primary Antibody (mouse, IgG2a)	R&D	MAB1224-SP	1:100
PDPLN (Podoplanin) primary Antibody (rat, IgG2a)	Biolegend	337002	1:100
Rabbit IgG	Santa Cruz	Sc-3888	1:100
Rabbit pAB	Abcam	Ab171870	1:200
Rat IgG2a	Santa Cruz	Sc-3883	1:10
α- SMA primary unlabelled Antibody (mouse, IgG2a)	Dako	M0851	1:300

2.1.6 Treatments

Table 6

Treatment	Company	Product#
IL-4	Biolegend	574004
TGF-β1	Pepro Tech	100-21
A 83-01	Tocris	2939
IL-13	PeproTech	200-13

2.1.7 Devices and software

Table 7

Device/software name	Company
BBD 6220 CO2 Incubator	Thermo Fisher ScientificTM, Waltham, MA, USA
Bead Bath M714	Lab Armor, LLC, Cornelius, OR, USA
Countess 3 FL automated cell counter	Invitrogen by Thermo Fisher ScientificTM, Waltham, MA, USA
Confocal Laser Scanning Microscope Leica TCS SP8	Leica Microsystems, Wetzlar, Germany
Eppendorf Centrifuge 5810 R	Eppendorf AG, Hamburg, Germany
Graphpad Prism	Dotmatics, Boston, Massachusetts
Image Studio software	LI-COR Biosciences, Lincoln, NE, USA
ImageJ	ImageJ.net
Laminar flow hood (MSC advantage class II biological safety cabinet)	Thermo Fisher ScientificTM, Waltham, MA, USA
Liquid nitrogen tank	Arpege 170, Air Liquide S.A., Paris, France
Odyssey CLX Scanner	LI-COR Biosciences, Lincoln, NE, USA
Biotek Synergy Photometer	Biotek Instruments, Winooski, VT, USA
Olympus IX51 Microscope with XC50 camera and TH4-200	Olympus Shinjuku, Tokio, Japan

2.2. Cell culture

All cell culture procedures were performed in a laminar flow hood under sterile conditions. Cells were incubated at 37°C, 5% CO_2, and 95% humidity in a BBD 6220 CO_2 Incubator. Primary cancer-associated fibroblasts (CAF 6388/19; CAF BGM2008) previously isolated from human colon carcinomas were cultured in 100-mm culture dishes with endothelial growth medium (EGM™-2MV). EGM supplemented with 5% fetal bovine serum (FBS), recombinant human epidermal growth factor (rhEGF), hydrocortisone, recombinant human

vascular endothelial growth factor (VEGF), recombinant human fibroblast growth factor-basic (rhFGF-B), human recombinant insulin-like growth factor (long R3 IGF) and ascorbic acid (Unterleuthner et al., 2020).
Patient-derived organoids (BGM2008) have been isolated previously from human colon carcinomas and cultured in 24-well plates as 40µl Matrigel domes in ENAS media.

2.2.1 Passaging of CAFs

CAFs were split when they were at full confluence. First, the culture medium in the dish was removed, and the cells were washed using phosphate-buffered saline (PBS). To detach the cells from the bottom of the dish, the cells were incubated in 1 ml Trypsin-EDTA (TE) for 4 min at 37°C. After inactivating Trypsin by pipetting 6 ml of DMEM into the dish, the cell solution was collected in a Falcon tube and centrifuged at 250 g for 3 minutes at room temperature (Centrifuge 5810 R, Eppendorf AG, Hamburg, Germany). The supernatant was discarded, and the pellet was resuspended in EGM medium. Cells were split 1:3 into new cell culture dishes. The passage number is indicated as p in brackets.

2.2.2 Passaging of organoids

Organoids were passaged every 5-7 days, based on confluence. First, the media was removed from the wells, followed by washing the Matrigel domes with cold PBS containing Rock Inhibitor, ensuring the domes were not damaged. Subsequently, the Matrigel domes were resuspended in 500 µl Organoid-Trypsin and incubated at 37°C with 5% CO_2 for 5 minutes until single cells were observed microscopically. Next, 1 ml of coating medium was added to the wells, and the organoids were transferred to a 15 ml tube and centrifuged at 300g for 3 minutes. The supernatant was removed, and the cells were resuspended in 40-50 µl of ice-cold Matrigel, which was then plated into a 24-well plate for continued culture. After 30 minutes at 37°C with 5% CO_2, 500 µl of ENAS media supplemented with Rock Inhibitor (ENAS+) was added. Media changes were conducted every 2-3 days.

2.2.3 Thawing and freezing of CAFs

The cryotubes thawed quickly at 37°C. Subsequently, the cell suspension was diluted in 5 ml of DMEM supplemented with 10% FCS and 1% L-glutamine in a 15 ml Falcon tube. The cells were centrifuged at 1000 rpm for three minutes at room temperature (RT). Subsequently, the supernatant was discarded, and the cell pellet was resuspended in the corresponding culture medium.
For freezing, cells were cultured to a confluence of around 70%. After discarding the culture medium and washing the cells with PBS, they were trypsinised, resuspended in DMEM supplemented with 10% FCS and 1% L-glutamine and transferred to a 15 ml tube. Then, the cell suspension was centrifuged at 250 g for 3 minutes at room temperature, and the

supernatant was removed. After resuspending the pellet in 1 ml freezing medium, the mixture was filled into a sterile cryotube containing 90% FCS and 10% dimethyl sulfoxide (DMSO). Next, the tubes were frozen overnight at -80°C in a freezing container, leading to an optimal temperature drop of 1°C/min to -80°C. The following day, the cryotubes were transferred to a liquid nitrogen tank (Arpege 170, Air Liquide S.A., Paris, France) at -196°C for long-term storage.

2.2.4 Thawing and freezing of organoids

Cells were stored in cryotubes at -195°C in liquid nitrogen tanks for long-term storage. The cryotubes thawed quickly at 37°C. Subsequently, the cell suspension was diluted in 1 ml of Coating Media in a 15 ml Falcon tube. The cells were centrifuged at 300 g for three minutes at room temperature (RT). Subsequently, the supernatant was discarded, and the cell pellet was resuspended in 2 ml of PBS plus 10 µM Rock-Inhibitor. The cells were centrifuged at 300 g for 3 minutes at RT, and the supernatant was carefully removed. The organoids were resuspended in 100-150 µl of Matrigel, and 40-50 µl were plated per well in a pre-warmed 24-well plate as domes. The Matrigel was allowed to set in the incubator for 15 minutes. ENAS media supplemented with 10 µM Rock-Inhibitor was added to cover the Matrigel domes for the first 3-5 days to recover from freezing. Subsequently, ENAS media was used for organoid maintenance.
For freezing, cells were cultured to a confluence of around 70%. After discarding the culture medium, the organoids were resuspended in PBS with 10 µM Rock-Inhibitor and transferred to a 15 ml tube. Then, the cell suspension was centrifuged at 300 g for 3 minutes at room temperature, and the supernatant was removed. After resuspending the pellet in 1 ml freezing medium, the mixture was filled into a sterile cryotube containing 1 ml of Cellbanker with 10 µM Rock-Inhibitor. Next, the tubes were frozen overnight at -80°C in a freezing container, leading to an optimal temperature drop of 1°C/min to -80°C. The following day, the cryotubes were transferred to a liquid nitrogen tank (Arpege 170, Air Liquide S.A., Paris, France) at -196°C for long-term storage.

2.2.5 Starvation

For some experiments, it was necessary to synchronise the cell cycle of all cells in the culture. For this purpose, cells were washed with 1x DPBS, and subsequently, a medium containing only a very small amount of serum (FCS) was added. DMEM +1% FCS +1% L-Glutamine was used for this purpose.

2.2.6 Seeding of cells

Cells were counted by mixing the cell suspension and Trypan blue solution (0,4%) 1:1. 10 µl were loaded on a cell counting chamber slide and counted with Countess 3FL Automated

cell counter.

2.3 In-Cell Western Assay

In each well of a flat-bottom 96-well plate, 15,000 CAFs were seeded in 200 µl of EGM media. After 24 hours, the CAFs were treated for 24-72 hours (as indicated). Treatments included: IL-4 at 2 or 10 ng/ml, TGFβ-1 at 2 and/or 10 ng/ml, IL-13 at 2 ng/ml, IFN-γ at 50 ng/ml, A8301 at 1 µM, IL-1β + TNF-α (2 ng/ml) and combinations thereof. Control wells (untreated) and IgG controls remained untreated. Next, cells were fixed with 100 µl of Histofix (4% Paraformaldehyde) for 15 minutes at room temperature (RT). Subsequently, residual Histofix was removed by washing the cells with 200 µl of PBS. 200 µl of ice-cold 90% methanol was added to permeabilise the cells, and the plates were stored at -20°C for at least 30 minutes.
After methanol removal, the cells were washed with 200 µl of PBS on a rocking platform to eliminate any remaining methanol. Then, cells were blocked with 150 µl of blocking buffer (PBS + 0,5% BSA) for 1 hour at RT with moderate shaking.
The primary antibody for the target was diluted to the appropriate concentration in the blocking buffer, and 50 µl of this antibody solution was added to each well except for the isotype control wells. Isotype controls were prepared by diluting the appropriate amount of IgG in a blocking buffer to match the concentrations of primary antibodies overnight at 4°C with gentle shaking. After incubation, three washing steps were followed with 200 µl of Tween washing solution (PBS + 0,1% Tween) for five minutes at RT on a rotator. Subsequent steps were performed under minimal light exposure. The secondary antibodies were diluted in blocking buffer at ratios of 1:800. CellTag-700 was diluted at 1:500. To reduce background fluorescence, Tween-20 was added to a final concentration of 0,2%. 50 µl of the secondary antibody solution and CellTag 700 were added to all wells for one hour at RT on a rotator. After incubation, the cells were washed five times with 200 µl of Tween washing solution.
The plates were scanned using the Odyssey® CLx scanning system and Image StudioTM Software. ICW settings were chosen, with a resolution of 169 µm and a focus offset of 3 mm. Image channels with wavelengths of 700 nm and 800 nm were used to detect targets and CellTag stain, respectively. The highest scan quality was selected to ensure optimal conditions for further analysis.
The mean fluorescence intensities (MFIs) of targets and CellTag stain were measured, and each channel was analysed separately. Isotype control means MFIs were subtracted from each result, and target MFIs were divided by CellTag stain to normalise the acquired data. Statistical analysis (Ordinary one-way ANOVA, GraphPad Prism 10) was performed to assess differences in target expression between treatment groups.

2.4 Immunofluorescence (IF) staining for confocal microscopy

In each 8-well tissue culture chamber well, 15.000 CAF cells were seeded in 0,5 ml of EGM. After 24 hours, CAFs were treated with IL-4 (2 ng/ml), IL-13 (2 ng/ml), TGF-β1 (2 ng/ml), A 83-01 (1 µM), and combinations thereof for 48 hours or as indicated. One well was left untreated as a control.
Subsequently, the cells were rinsed twice with 1x PBS and fixed in 0,5 ml of Histofix (4% Formaldehyde) for 15 minutes at room temperature. After fixation, wells were washed with 1x PBS and 0,5 ml of ice-cold 90% Methanol was added for a minimum of 30 minutes. After blocking with 0,5 ml of PBST + 1% BSA for 1 hour at room temperature, the cells were washed three times with 1x PBS.
For staining with FAP, cells were incubated with 150 µl / well of the primary antibody diluted 1:100 in 1x PBS + 0.5% Tween + 1% BSA for 3 hours at room temperature or overnight at 4°C. Then a washing step was performed thrice with PBST (0,5% Tween). After this, 150 µl / well secondary 1:500 was added to the blocking buffer for 3 hours at room temperature or overnight at 4°C. Wells were then washed thrice with PBST (0,5% Tween).
For staining for α-SMA, the cells were exposed to 120 µl of directly labelled antibody diluted (1:150 in PBST (0,5% Tween) for 3 hours at room temperature or overnight at 4°C in the dark. Subsequently, they were rinsed three times with 1x PBST (0,5% Tween). DAPI solution (100 µl of 2 µg/ml in 1x PBS) was then applied, and the cells were incubated in the dark for approximately 8 minutes at room temperature to stain the nuclei. Finally, the cells were washed with 1x PBS.
Images were taken with Confocal Laser scanning microscope Leica TCS SP8 (20x objective).

ImageJ analysis of α-SMA or FAP positive pixels
Images were analysed in an 8-bit format as a stack. For this, all pictures were opened in the ImageJ software. Next, all pictures were organised into a stack under the drop-down Image, stacks, image to stacks. For this, under the drop-down Image, adjust, threshold was applied. The same threshold value was chosen for all the pictures of one experiment. The area of α-SMA or FAP positive pixels was measured and normalised to the area of DAPI-positive pixels for each image (by dividing the positive pixel areas). Statistical analysis (Ordinary one-way ANOVA, GraphPad Prism 10) assessed differences in positive areas between treatment groups.

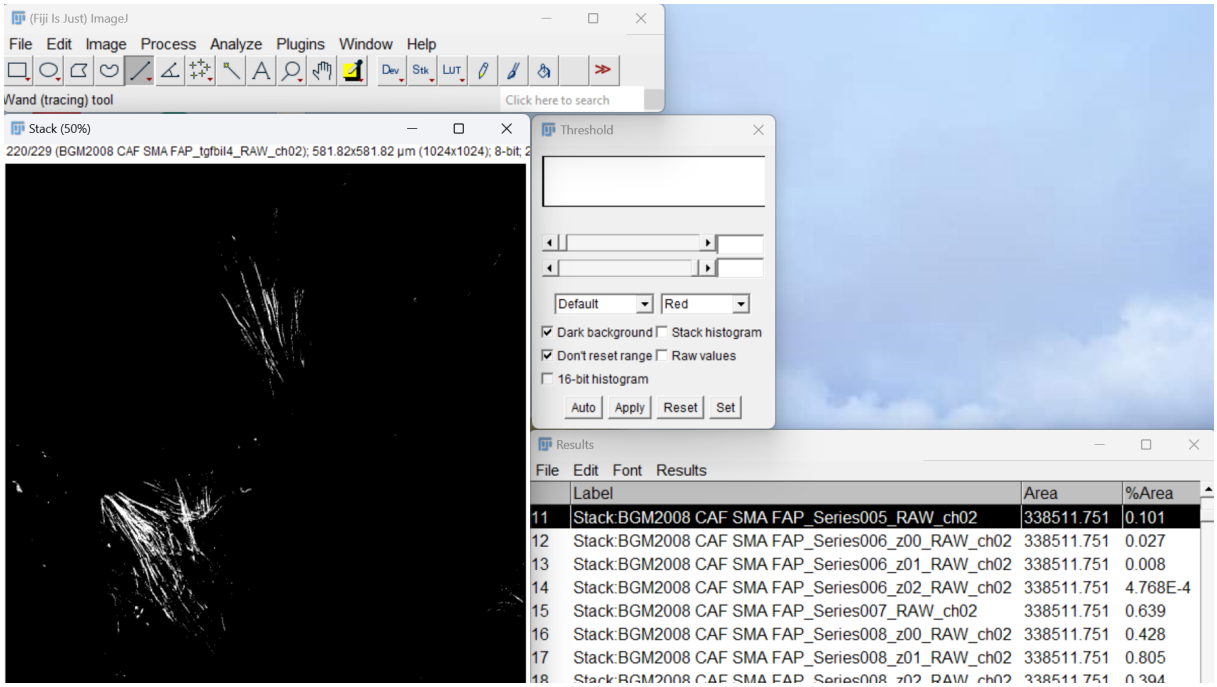


Figure 6: Visual representation of α-SMA positive area measurements using ImageJ software. White Area on the left depicts the α-SMA positive area with a set threshold of an image of BGM2008 CAF in a confocal microscopical image**.** The top right depicts threshold setting. The bottom left depicts measurements as % positive area from the total image area.

Statistical analysis (Ordinary one-way ANOVA, GraphPad Prism 10) was performed to assess differences in α-SMA-positive area between treatment groups.

2.5 CellTiter-Glo 3D Viability assay of organoids in CAF-conditioned media

Conditioned media was prepared by seeding CAFs in 6 cm dishes. When they grew confluent, they were treated with 2 ng/ml treatment for 2 days in 3 ml EGM, followed by media change and re-treatment for 2 days. Treatments included 2 ng/ml of IL-4, TGF-β, IL-1β + TNF-α, IL-4 + TGF-β, IL-4 + IL-1β + TNF-α, TGF-β + IL-1β + TNF-α, and IL-4 + TGF-β + IL-1β + TNF-α (as indicated in graphs).
After washing with PBS, 4 ml Omin was added, and conditioned media was collected and filtered after 2 days. This process was repeated to obtain additional conditioned media.
Organoids were trypsinised to single cells, and 2000 cells were seeded in a 96-well plate in 10 µl Matrigel. Conditioned media, diluted 1:1 with Omin, was added for the specified duration. Controls included ENAS, Omin, and conditioned media from untreated CAFs. Media changes were performed every 3 days. The media was reduced to 50 µl for viability measurement, and then 50 µl of CellTiter-Glo (CTG) was added. The organoid domes were disrupted, and after 20 minutes on a shaker, luminescence was measured using a Biotek plate reader (Biotek Synergy HT photometer). The number of viable cells can be determined by quantifying the luminescence, which is directly proportional to the ATP present.

2.6 Organoid Organotypic Transwell Assay (OOTA)

Pre-treatment of CAFs
CAFs were seeded in 6 cm dishes, and when fully confluent, they were treated at a 2 ng/ml treatment concentration in 2D culture for 48 hours. Treatments included 2ng/ml of IL-4, TGF-β, IL-1β + TNF-α, IL-4 + TGF-β, IL-4 + IL-1β + TNF-α, TGF-β + IL-1β + TNF-α, and IL-4 + TGF-β + IL-1β + TNF-α (as indicated in graphs).

Preparation of Collagen Gel
Silicon forms were securely attached to the inside surface of 6-well plates using sterile forceps. The CAFs were trypsinised, neutralised with DMEM supplemented with 10% FCS, and counted. A total of 300.000 cells were prepared for each gel. A 300 µl collagen I gel mixture was prepared to contain Collagen I at a final concentration of 2mg/ml, 30 µl of 10x PBS, and the remainder of the volume made up of medium. The mixture was neutralised to the correct pH using 1 M NaOH until the colour turned salmon pink, indicating the desired pH level of a weak acidic solution. The CAFs were then resuspended in the collagen gel, taking care to avoid forming bubbles. A nylon mesh was added to the collagen gel to prevent shrinking, which was then placed at 37°C for 30 minutes to harden. After hardening, the silicon forms were removed.

Preparation of Organoids
Organoids were dissociated into single cells and counted. The collagen gel was transferred onto the insert, and 40.000 organoid cells were resuspended in 25 µl Matrigel per sample. These organoid-Matrigel mixtures were then placed on top of the collagen gel. The setup was allowed to be set for 1 hour with 1 ml Omin medium placed on the side to maintain humidity. After setting, the medium was topped up until it touched the base of the Transwell, approximately 1.5-2 ml total, so the organoids were grown at the air-liquid interface.

Culture Conditions and Maintenance
Cultures were maintained for 5 days in Omin medium, consisting of Advanced DMEM/F12 supplemented with 1% GlutaMAX, 10 mM HEPES, and 2% FCS. Media changes were performed every 2 days, and the cultures were treated with 2ng/ml as indicated. Treatments included 2ng/ml of IL-4, TGF-β, IL-1β + TNF-α, IL-4 + TGF-β, IL-4 + IL-1β + TNF-α, TGF-β + IL-1β + TNF-α, and IL-4 + TGF-β + IL-1β + TNF-α (as indicated in graphs). Daily images were captured using a microscope (OLYMPUS IX51) to monitor the cultures, and their size was analysed in ImageJ.

ImageJ analysis of growth area
Pictures were taken on Olympus IX51 Microscope, including a 500 µM ruler bar at the bottom left. Day 2 and day 5 pictures were analysed for organoid size. The ruler bar was used to set scale in Image J (Analyse, set scale, distance in pixels 588 (measured with straight line over ruler), known distance 500, OK). Oval selection from the menu was used, and organoids were circled. Then, with the “Ctrl+t” key combination, each oval shape was added to the ROI manager. ROI manager pop-up allows measurement of oval shapes to measure the area of organoids. Both the total area (sum of oval shapes) and each individual organoid area was plotted using Graphpad Prism software. Day 5 was normalised on Day 2 by division of the total areas. Statistical analysis (Ordinary one-way ANOVA, GraphPad Prism 10) assessed differences in organoid area between treatment groups.

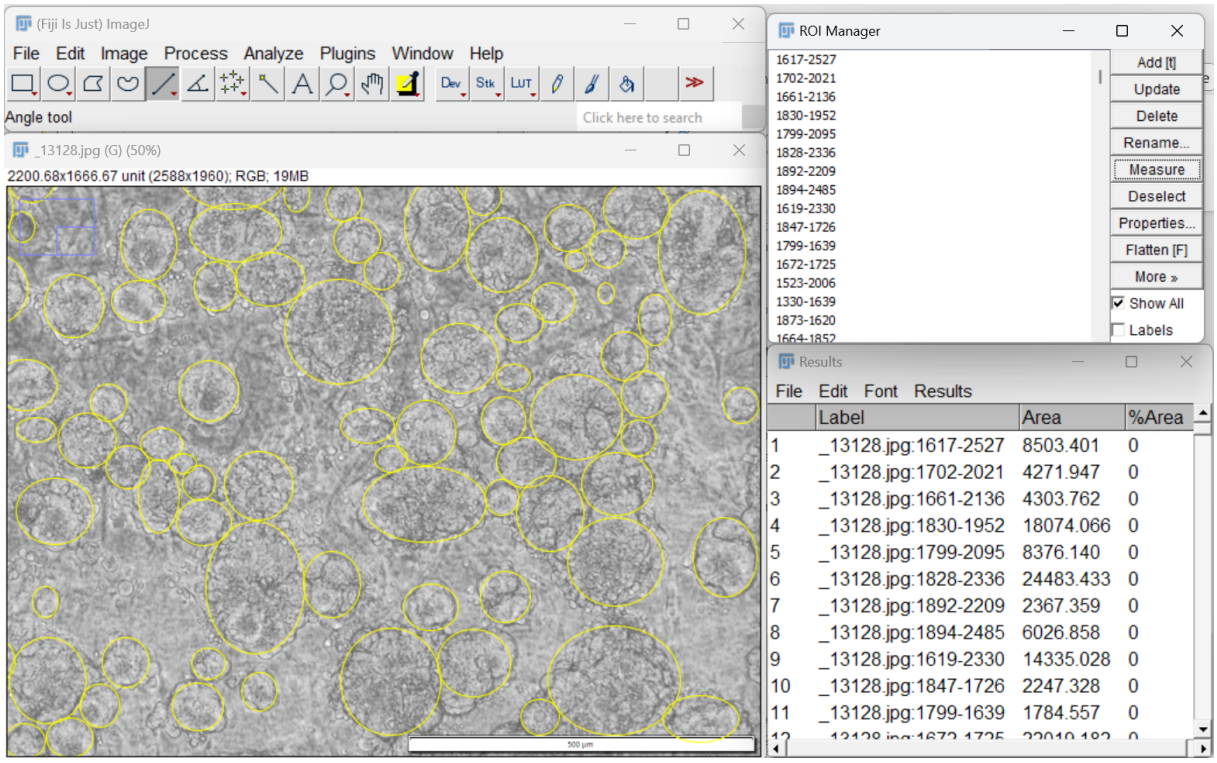


Figure 7: Visual representation of organoid size measurements using ImageJ software. Area on the bottom left depicts a picture taken of BGM2008 (zoomed in) with a 500 µM scale bar**.** The top right depicts the ROI Manager, and the bottom right represents the measurements of the oval-shaped area drawn over the organoids.

In situ Immunofluorescence of OOTAs

First, OOTAs were washed with PBS, then Histofix (4% Paraformaldehyde) was added for 40 minutes at RT. Next, gels were washed with TBST (0.5% Tween 20) thrice for 10 minutes at RT. After that, three washes with PBST (0.5% Tween 20) for 10 minutes at RT were done. OOTAs were cut with a scalpel to stain for several targets. We performed two sets of stains: the first set aimed to investigate different organoid targets, which comprised EPCAM, cleaved caspase 3 (CC3), Ki-67, Vimentin and DAPI. The second set was focused on CAF targets: α-SMA, FAP, Vimentin and DAPI. Next, the gel pieces were blocked with 1.5% BSA for 3 hours in PBST at RT or overnight at 4°C.

Organoid staining

In 250 µl blocking solution, primary non-labelled antibodies Ki-67 (1:500) and CC3 (1:500) were applied for 3 hours at RT or overnight at°C. Afterwards, gels were washed thrice with PBST for 20 minutes at RT and followed by another blocking step for 20 minutes. Afterwards, secondary labelled antibodies (Anti-mouse 594 for Ki-67, Anti-rabbit 488 for CC3) were

diluted 1:500 in 250 µl blocking solution and applied to gels for 3 hours at RT or overnight at 4°C. Three washes of PBST followed this. Next, the directly labelled primary antibodies were added EpCAM 555 (1:100) and Vimentin 647 (1:5000) was added overnight at 4°C. Then the DAPI stain followed (see below).
Immunofluorescence images were captured using a Leica TCS SP8 confocal microscope (Leica Microsystems, Wetzlar, Germany). The picture area was chosen in the DAPI channel only. Pictures were taken in 3 z-planes (roughly 10µm total z distance), and 6 images per condition were analysed (18 total datapoints per condition).

CAF staining
In 250 µl blocking solution, primary non-labelled antibody FAP (1:100) was applied for 3 hours at RT or overnight at 4°C. Afterwards, gels were washed thrice with PBST for 20 minutes at RT, and another blocking step was followed for 20 minutes. Afterwards, secondary labelled antibody (Anti-rabbit 555 for FAP) was diluted 1:500 in 250 µl blocking solution and applied to gels for 3 hours at RT or overnight at 4°C. Three washes of PBST followed this. Next, the directly labelled primary antibodies were added α-SMA (1:150) and Vimentin 647 (1:5000) were added overnight at 4°C.
The next day, gels were washed thrice in PBST for 20 minutes. Finally, DAPI was diluted to 1:2000 in PBS and added for 40 minutes at RT. After washing three times in PBST for 20 minutes, the gel was carefully removed from the dish and placed on a slide, using PBS to attach it to the coverslip.
Immunofluorescence images were captured using a Leica TCS SP8 confocal microscope (Leica Microsystems, Wetzlar, Germany). The picture area was chosen in the DAPI channel only to guarantee objectivity. Pictures were taken in 5 z-planes (roughly 10 µm total z distance), and 6 pictures per condition were analysed (30 total datapoints per condition).

ImageJ analysis
ImageJ analysis of Ki-67, Cleaved Caspase -3 (CC3), α-SMA or FAP positive pixels:
Images were analysed as described previously. However, for Ki-67 and CC3 staining, two different threshold setting methods were used as indicated in the graphs (Otsu and fixed threshold). The area of Ki-67 and Cleaved Caspase-3 (CC3) positive pixels was measured and normalised to the area of DAPI-positive pixels for each image (by dividing the positive pixel areas). The area of α-SMA and FAP positive pixels was measured and normalised to the area of vimentin-positive pixels for each image, as normalisation on DAPI was not possible, because the organoids showed positive DAPI area as well.

2.7 Statistics

All statistical analyses were performed with GraphPad Prism 10. Outliers were identified and removed when indicated. Furthermore, the normal distribution of the data was checked

(using Lognormality and Normality QQ plot). If the data passed the Normality test, One-way ANOVA (analysis of variance) was used. Statistical significance was finally determined with a p-value of less than 0.05. The following classification indicates the statistical significance of the p-values: ns * ** *** $p > 0.05$ $p \leq 0.05$ $p \leq 0.01$ $p \leq 0.001$ **** $p \leq 0.0001$. GraphPad Prism was used to represent the data graphically. Error bars, representing standard deviation (SD), have been added to all diagrams to indicate measurement errors.

3. Results

3.1 The effect of IL-4, TGF-β1 and IFN-γ treatment on α-SMA expression in CAF 6388/19

Alpha-smooth muscle actin (α-SMA) is the most widely used marker of an activated cancer-associated fibroblast subtype (Sahai et al., 2020). Transforming growth factor-beta (TGF-β) plays a crucial role in activating and trans-differentiating CAFs, mainly through the upregulation of α-SMA (Hawinkels et al., 2014; Carthy, 2018; Stylianou et al., 2018; Yang et al., 2023).

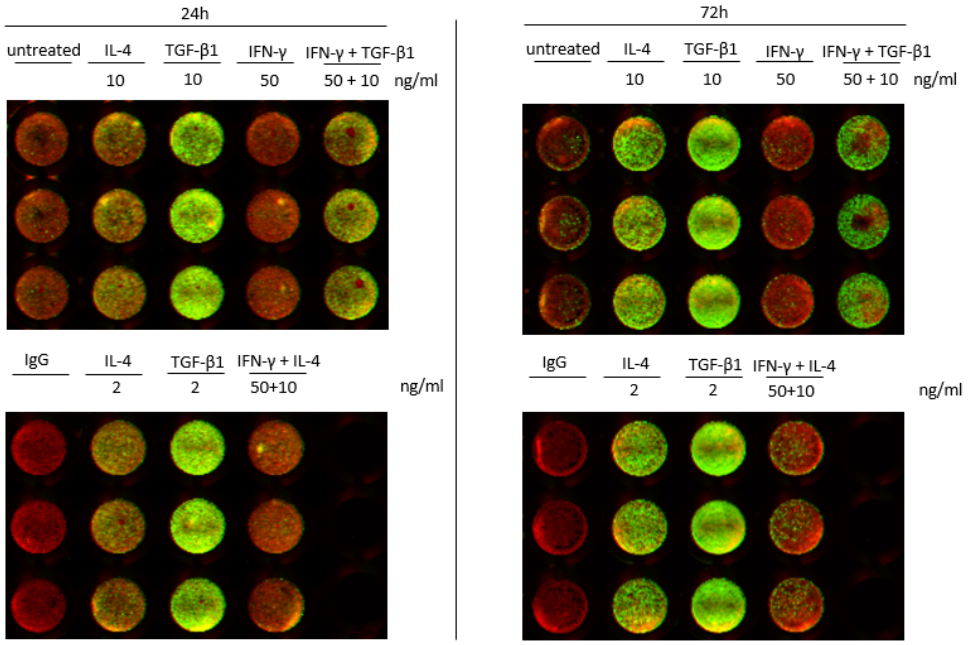
First, we wanted to test how other cytokines of the TME, which are connected to fibrosis and inflammation, affect α-SMA in CAF 6388/19. We investigated the effects of 2 ng/ml and 10 ng/ml IL-4, TGF-β1, and 50 ng/ml IFN-γ treatment on α-SMA in colorectal CAF 6388/19 (p11) using an In-Cell Western assay. We also investigated the concerted action of IL4 and IFN-γ in this setup to validate a potential antagonistic effect of these cytokines in the CAFs. For this, 15.000 CAF 6388/19 (p11) were seeded per well in 2D in a 96-well plate. The next day, CAFS were serum-starved for 24 hours to eliminate potential interference effects of serum factors on cytokine-induced α-SMA expression. Subsequently, CAFs were treated with different concentrations (2 ng/ml or 10 ng/ml) of IL-4, IL-13, TGF-β1, 50 ng/ml IFN-γ, and combinations thereof for 24 and 72 hours. Celltag (red) total protein stain was used to normalise the fluorescence data based on cell numbers. Furthermore, an IgG control was used as a control for antibody specificity. All treatments were compared to non-treated cells. Untreated CAFs exhibited basal levels of α-SMA expression as expected. Interestingly, α-SMA upregulation was not uniform but concentrated in small regions, suggesting a heterogeneous response in the CAFs (Figures 8A and 8B).

Both concentrations of IL-4 (2 ng/ml and 10 ng/ml) significantly increased α-SMA expression compared to untreated CAFs at both time points (Figures 8B and 8C). Interestingly, the difference in α-SMA expression between the two concentrations of IL-4 was minimal, with only slightly enhanced expression under high IL-4 concentration. This suggests that even lower concentrations of IL-4 are sufficient to trigger a maximal response in α-SMA upregulation (Figures 8B and 8C). Both treatment concentrations of IL-4 lead to a 2-fold increase in α-SMA levels at 24 hours. At 72 hours, levels of α-SMA were 3.5-fold higher compared to control (Figure 8C). However, the degree of α-SMA upregulation induced by IL-4 was lower than that caused by TGF-β1, a potent and well-established inducer of α-SMA expression.

At both time points, TGF-β1 treatment resulted in a pronounced upregulation of α-SMA expression, as indicated by the intense green fluorescence (Figure 8A). TGF-β1 upregulates α-SMA about 4-fold compared to untreated CAFs after 24 hours of treatment. As with IL-4, TGF-β1 induced α-SMA levels are higher at 72 hours, displaying a 4.5-fold increase

compared to no treatment (Figures 8A, 8B, 8C). However, the increase at 72 hours is not as much as for IL-4 (Figures 8A, 8B, 8C).
IFN-γ treatment alone did not downregulate the basal α-SMA levels in CAFs at 24 hours. However, at 72 hours of treatment, the α-SMA signal was reduced by 35% compared to untreated cells at this time point. However, this was not significant (Figures 8A and 8C). Interestingly, IFN-γ significantly attenuated the upregulation of α-SMA induced by IL-4 (Figures 8B and 8C). CAFs treated with IL-4 (10 ng/ml) and IFN-γ (at a surplus of 50 ng/ml) displayed the same α-SMA levels as untreated cells within 24 hours of treatment. The antagonistic effect of IFN-γ was sustained at 72 hours, indicating a prolonged inhibitory influence of IFN-γ on IL-4-induced α-SMA upregulation (Figure 8C). This supports the hypothesis that the signalling pathways activated by IFN-γ oppose those activated by IL-4, resulting in the reduction of α-SMA expression. Additionally, IFN-γ attenuated the upregulation of α-SMA induced by TGF-β1 at the 24-hour time point, resulting in a 2.5-fold increase in α-SMA levels (Figures 8A and 8B). This effect was only partially sustained at 72 hours, with α-SMA levels being 4 times as high as those of untreated CAF (Figures 8A and 8C). As for IL-4, IFN-γ was able to attenuate the levels of α-SMA induced by TGF-β1, but not to the basal levels of α-SMA seen in the untreated CAFs. Thus, the impact of IFN-γ on TGF-β1-related α-SMA upregulation is less compared to the effect IFN-γ has on IL-4-controlled increase of α-SMA (Figure 8).
Taken together, these results show that IL-4 significantly upregulates α-SMA in our CAFs, as measured by ICW. Additionally, the assay confirmed the role of TGF-β1 in promoting α-SMA expression. Furthermore, the ability of IFN-γ to act as a negative regulator of CAF activation by counteracting the effects of both IL-4 and, to a partial extent, TGF-β1. These findings provide valuable insight into the interplay between cytokine signalling pathways in regulating the pro-fibrotic phenotype of CAFs, with implications for understanding the tumour-promoting activities of CAFs within the tumour microenvironment.

A

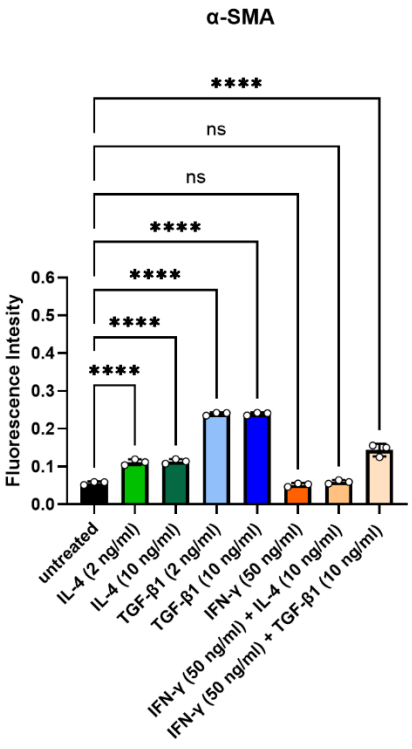

24h
untreated
IL-4
10
TGF-β1
10
IFN-γ
50
IFN-γ + TGF-β1
50 + 10
ng/ml
IgG
IL-4
2
TGF-β1
2
IFN-γ + IL-4
50+10
ng/ml
72h
untreated
IL-4
10
TGF-β1
10
IFN-γ
50
IFN-γ + TGF-β1
50 + 10
ng/ml
IgG
IL-4
2
TGF-β1
2
IFN-γ + IL-4
50+10
ng/ml

B

24h

C

72h


α-SMA
Fluorescence Intesity
0.0
0.1
0.2
0.3
0.4
0.5
0.6
****
ns
ns
****
****
****
untreated
IL-4 (2 ng/ml)
IL-4 (10 ng/ml)
TGF-β1 (2 ng/ml)
TGF-β1 (10 ng/ml)
IFN-γ (50 ng/ml)
IFN-γ (50 ng/ml) + IL-4 (10 ng/ml)
IFN-γ (50 ng/ml) + TGF-β1 (10 ng/ml)

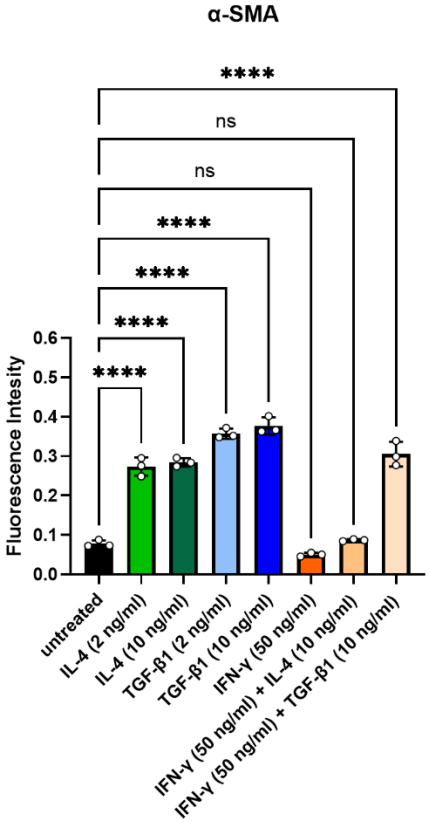

α-SMA
Fluorescence Intesity
0.0
0.1
0.2
0.3
0.4
0.5
0.6
****
ns
ns
****
****
****
****
untreated
IL-4 (2 ng/ml)
IL-4 (10 ng/ml)
TGF-β1 (2 ng/ml)
TGF-β1 (10 ng/ml)
IFN-γ (50 ng/ml)
IFN-γ (50 ng/ml) + IL-4 (10 ng/ml)
IFN-γ (50 ng/ml) + TGF-β1 (10 ng/ml)

Figure 8: **In-Cell Western (ICW) assay of CAF 6388/19 shows upregulation of α-SMA upon IL-4 and TGF-β1 treatment.** CAFs 6388/19 (p11) were treated in 96-well plates in 2D with IL-4, TGF-β1, IFN-γ, and combinations at the indicated concentrations for 24 or 72 hours. The levels of α-SMA were determined using the ICW method. (**A**) Images of α-SMA (green) and Celltag (total protein stain, red, used for normalisation) staining. (**B, C**) Analysis of ICW fluorescence intensity measurement data at 24 and 72 hours, respectively. Mean values are shown as bars, SD (error bars) of technical replicates (n=3) are depicted, **** indicates a P <0.0001 using ordinary one-way ANOVA.

3.2 The effect of IL-4, IL-13, TGF-β1 and TGF-β signalling inhibition (A 83-01) on α-SMA expression in CAF 6388/19

This set of experiments aimed to investigate whether IL-13 can upregulate α-SMA in CAF 6388/19. IL-13, a cytokine closely related to IL-4, is reported as a regulator of fibroblast-related collagen deposition and desmoplasia (Bailey et al., 2012;Gieseck et al., 2016; J. K. Nguyen et al., 2020). As with IL-4, the literature did not provide data on the effect of IL-13 in colonic CAFs. Moreover, we tested whether the combination of cytokines shown in the previous experiment to induce α-SMA elicited a synergistic effect. Furthermore, we aimed to test whether the upregulation of α-SMA by IL-4 and IL-13 is independent of TGF-β receptor signalling. A-83-01, a small-molecule TGF-β receptor type I (ALK 5/4/7) inhibitor diminishing Smad 2/3 phosphorylation, was used for this (Tojo et al., 2005). In addition, given the critical role of TGF-β signalling in CAF function, it is essential to determine how specific components of organoid growth media, such as A-83-01, may interfere with CAF activity in future organoid/CAF coculture experiments.

As seen in the previous assay, untreated CAFs show restricted α-SMA-positive areas, suggesting that certain cells express α-SMA without treatment (Figures 9A and 9B). In this experiment, α-SMA levels of untreated CAFs were higher than in the previous experiment (Figures 9A and 9B, 9A and 9B).

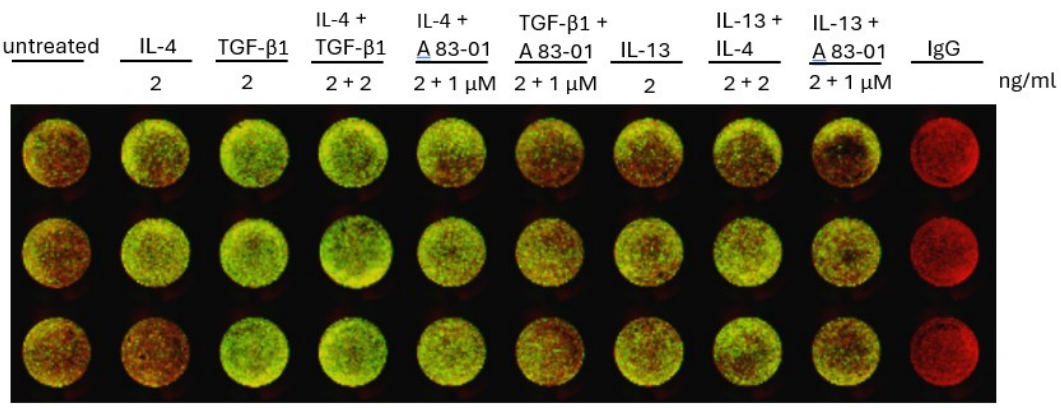
The normalised values for α-SMA expression induced by IL-4 (2 ng/ml) and IL-13 (2 ng/ml) are comparable. Both showed a 1.5-fold increase in α-SMA expression compared to untreated CAF 6388/19 (Figure 9B). TGF-β1 treatment led to a 2.2-fold increase in α-SMA levels compared to controls. However, all three individual cytokine treatments caused a significant upregulation of α-SMA (Figures 9A and 9B).

The combination treatment of IL-4 (2 ng/ml) with TGF-β1 (2 ng/ml) did not result in any further enhancement of α-SMA expression compared to TGF-β1 treatment alone (Figure 9B). Similarly, combining IL-13 with IL-4 did not lead to a substantially higher α-SMA expression than IL-4 or IL-13 alone, indicating that IL-4 and IL-13 might activate overlapping or converging signalling pathways in promoting CAF activation (Figure 9B).

To further investigate whether the TGF-β signalling is required for IL-4 and IL-13-induced α-SMA upregulation, A 83-01, a TGF-β1 receptor type I inhibitor which prevents downstream Smad 2/3 phosphorylation, was used. Treatment with A 83-01 (1 μM) did not significantly reduce the upregulation of α-SMA induced by both IL-4 and IL-13 (Figure 9B). This finding suggests that IL-4 and IL-13 can upregulate α-SMA expression largely independent of TGF-β receptor type I signalling, as the inhibition of TGF-β1 does not drastically reduce their effects (Figure 9B). Conversely, when A 83-01 was combined with TGF-β1, α-SMA expression was significantly reduced compared to TGF-β1 treatment alone (Figure 9B) and showed intensities comparable to the signal of untreated CAFs, confirming that the upregulation of α-SMA by TGF-β1 strongly depends on its receptor signalling.

These results further highlight that IL-4, IL-13, and TGF-β1 upregulate α-SMA expression in the CAFs. Interestingly, IL-4 and IL-13 do so via mechanisms primarily independent of TGF-β receptor type I signalling, whereas TGF-β1 relies on this pathway for its full effect. These results also shed light on the impact of A-83-01, often used in media for culturing organoids, on CAF. These findings underscore the importance of carefully selecting components for use in media during CAF and organoid co-culture experiments.

A


untreated
IL-4
2
TGF-β1
2
IL-4 + TGF-β1
2 + 2
IL-4 + A 83-01
2 + 1 μM
TGF-β1 + A 83-01
2 + 1 μM
IL-13
2
IL-13 + IL-4
2 + 2
IL-13 + A 83-01
2 + 1 μM
IgG
ng/ml

B

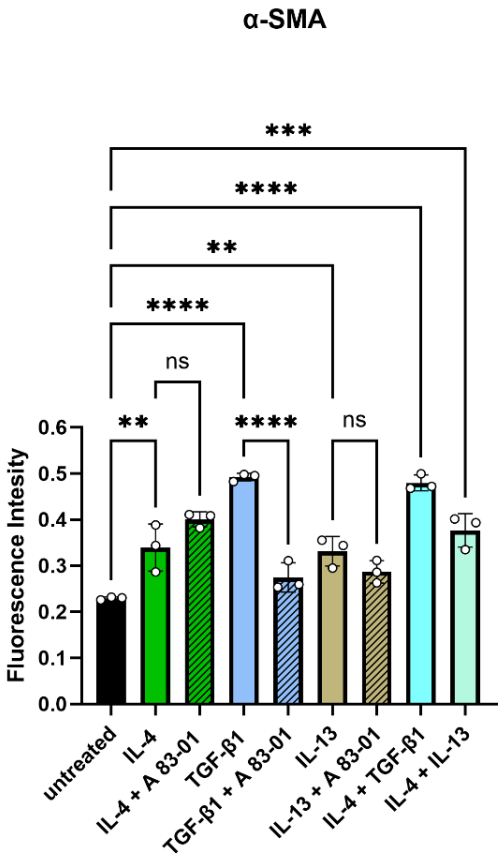

α-SMA
Fluorescence Intesity
0.0
0.1
0.2
0.3
0.4
0.5
0.6
***
****
**
****
ns
**
****
ns
untreated
IL-4
IL-4 + A 83-01
TGF-β1
TGF-β1 + A 83-01
IL-13
IL-13 + A 83-01
IL-4 + TGF-β1
IL-4 + IL-13

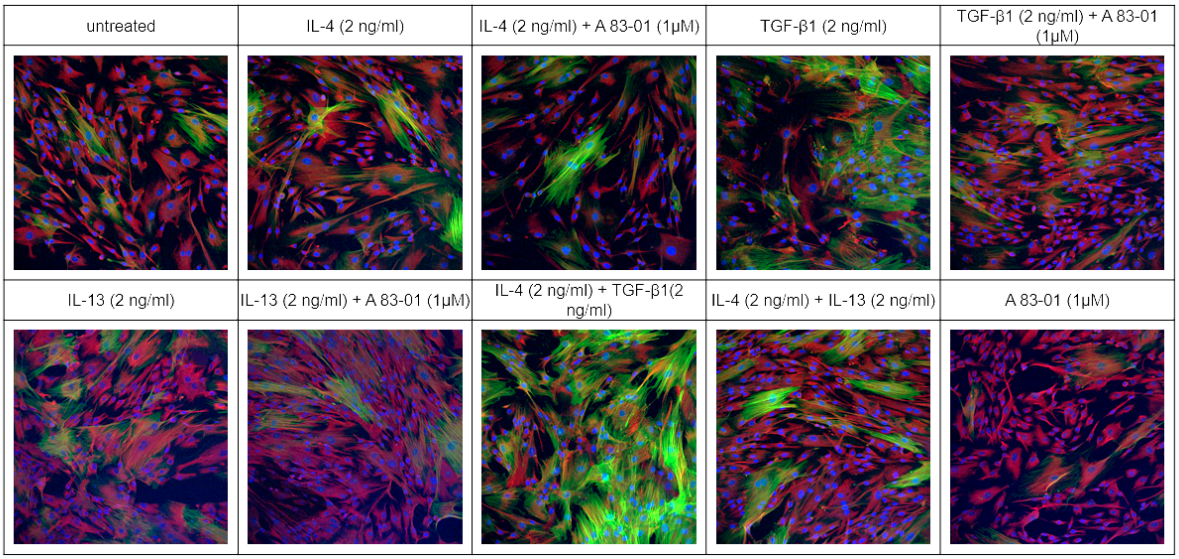
Figure 9: **In-Cell Western (ICW) assay shows the effect of IL-4, IL-13, TGF-β1 and A 83-01 (TGF-β1 signalling inhibition) on α-SMA expression in CAF 6388/19.** CAF 6388/19 (p15) were treated in 96-well plates in 2D with 2 ng/ml IL-4, IL-4/A 83-01 (1 μM), TGF-β1, TGF-β1/A 83-01, IL-13, IL-13/ A 83-01, IL-4/TGF-β1, IL-4/IL-13 at the indicated concentrations for 24 hours. The levels of α-SMA were determined using the ICW method. (A) Representative pictures of α-SMA (green) and Celltag (total protein stain, red, used for normalisation) staining. (B, C) Analysis of ICW fluorescence intensity measurement data at 24 and 72 hours, respectively. Mean values, SD (error bars) of technical replicates (n=3) are depicted, **** indicates a P <0.0001 using ordinary one-way ANOVA.

3.3 Determining the effect of IL-4, IL-13, TGF-β1 and TGF-β1 signalling inhibition (A 83-01) on α-SMA expression in CAF 6388/19 using immunofluorescence staining for confocal microscopy

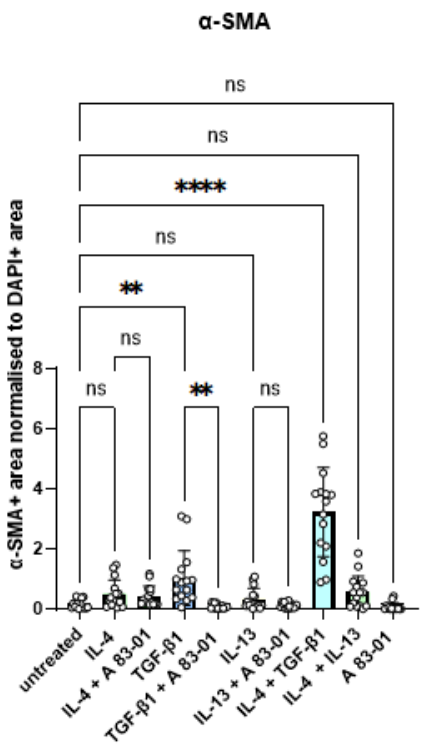
The previous In-Cell Western experiments showed that IL-4, IL-13 and TGF-β1 can upregulate α-SMA expression in CAFs. However, this assay is not instructive for the intracellular localisation of SMA. However, as pointed out in the introduction, the presence of α-SMA in stress fibres is essential for myofibroblast function (Hinz & Lagares, Myofibroblasts - Methods in Molecular Biology 2299, Springer 2021). Thus, using immunofluorescence staining for confocal microscopy, the following experiment assessed α-SMA upregulation and subcellular localisation after cytokine treatment.
For this, CAFs were seeded in an 8-well chamber slide as a 2D monolayer and treated the following day with either 2 ng/ml of IL-4, IL-13, TGF-β1, or 1 µM of A8301 (TGF-β1 receptor inhibitor) and combinations thereof for 48 hours, followed by immunofluorescence staining for Vimentin and α-SMA. The picture area was chosen objectively, as described in the methods. In brief, the areas were randomly selected in the DAPI channel to avoid investigator-based bias for SMA expression. Subsequently, quantitative analysis of SMA expression in the confocal images using ImageJ was performed.
Representative confocal images display α-SMA (green) expression alongside DAPI-stained nuclei and Vimentin (Figure 10A). These images were selected to represent the mean α-SMA positive pixel count for each condition, highlighting the visual differences in α-SMA expression levels across the various treatments (Figure 10A). All pictures analysed can be found in Appendix Figure 1. In the controls, only a minority of the cells exhibited an α-SMA-positive signal, indicating a heterogeneous cell population (see Figure 10A). As expected, SMA was induced upon TGF-β treatment or upon addition of TGFB/IL-4. Importantly, α-SMA expression was restricted to stress fibres, as clear fibre structures are detectable, rather than a diffuse uniform cytoplasm stain (Figure 10A; compare to Figure 5 in the Introduction).
First, we determined the α-SMA-positive pixel areas, normalised to the DAPI-positive nuclei area, in ImageJ. Since this type of analysis for SMA quantification had not been validated in the lab before, a manual count of SMA+ cells was performed in addition to ensure that the analysis using ImageJ produced reliable and comparable results. The graphs of both analysis methods show a similar pattern. The α-SMA-positive cell count generally yielded higher values than analysing α-SMA-positive pixels (compare Figures 10B and C). This is most likely due to measuring α-SMA-positive areas in the cells and normalising them to the number of cells present in the frame by the DAPI area (Figure 10B). These α-SMA-positive areas only account for a fraction of the individual cell bodies. In contrast, Figure 10C focuses on the number of cells positive for α-SMA based on a binary decision (yes/no for α-SMA positivity). However, both analysis methods yield meaningful results and reveal an identical pattern of SMA expression across all tested conditions. Considering the analysis time,

especially with many images, the analysis of α-SMA-positive area is an effective and objective method for this assessment.
In detail, a trend towards increasing α-SMA expression was observed with IL-4 treatment, as measured by the number of α-SMA-positive pixels (Figure 10B). Additionally, IL-4 significantly upregulated the number of α-SMA-positive cells (Figure 10C). Both analysis methods demonstrate that the effect of IL-4 is independent of TGF-β receptor inhibition, as no decrease was observed with the addition of A-83-01 (Figure 10B, C), thereby confirming the ICW data. IL-13 treatment did not significantly increase the number of α-SMA positive pixels or α-SMA positive cells (Figure 10B and C). However, there is a trend of upregulation of α-SMA-positive cells (Figure 10C). Both analysis methods indicate that the trend of upregulation with IL-13 treatment is independent of TGF-β1-inhibition (Figure 10B, C). The effect of TGF-β1 upregulating α-SMA was significant in both analysis methods. TGF-β1 upregulated α-SMA more potently than IL-4 and IL-13, individually or in combination (Figures 10B,C). Adding A-83-01 reduced α-SMA expression by approximately half, as indicated by the number of α-SMA-positive cells (Figure 10C). This effect was more pronounced when measuring α-SMA-positive pixels, where the expression of α-SMA was almost entirely blocked by adding A-83-01 (Figure 10B). IL-4, in combination with IL-13, upregulated α-SMA, but not more than IL-4 or IL-13 alone (see Figures 10B and 10C). This non-additive effect suggests that they activate the same downstream signalling cascades. Interestingly, IL-4 in combination with TGF-β1 showed the highest upregulation. The combination synergises when assessing α-SMA positive pixels (Figure 10B). The resulting α-SMA level of the combination is almost twice as much as the measurements of individual treatments added (Figure 10B).
Taken together, these results show that IL-4 alone at 2 ng/ml upregulates α-SMA in the stress fibres; however, there is a lack of significance in the SMA area quantification method, whereas when counting SMA+ cells, a significant increase is detectable. Moreover, this experiment confirms that TGF-β1 has the most robust effect on CAF activation via increased α-SMA in the stress fibres. Combining IL-4 and TGF-β may indicate a synergistic effect, upregulating α-SMA exceptionally highly. As previously shown, IL-4 and IL-13 impact α-SMA upregulation in CAF 6388/19 independently of TGF-β receptor signalling.

A


untreated
IL-4 (2 ng/ml)
IL-4 (2 ng/ml) + A 83-01 (1µM)
TGF-β1 (2 ng/ml)
TGF-β1 (2 ng/ml) + A 83-01 (1µM)
IL-13 (2 ng/ml)
IL-13 (2 ng/ml) + A 83-01 (1µM)
IL-4 (2 ng/ml) + TGF-β1(2 ng/ml)
IL-4 (2 ng/ml) + IL-13 (2 ng/ml)
A 83-01 (1µM)

B


α-SMA
α-SMA+ area normalised to DAPI+ area
ns
ns
****
ns
**
ns
ns
**
ns
0
2
4
6
8
untreated
IL-4
IL-4 + A 83-01
TGF-β1
TGF-β1 + A 83-01
IL-13
IL-13 + A 83-01
IL-4 + TGF-β1
IL-4 + IL-13
A 83-01

C

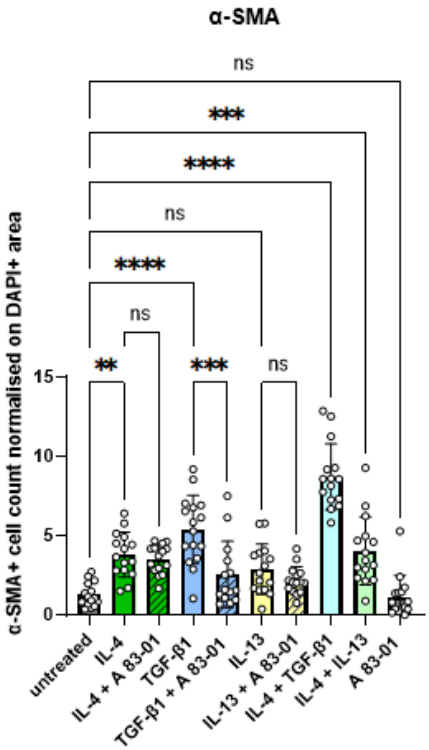

α-SMA
α-SMA+ cell count normalised on DAPI+ area
ns
***
****
ns
****
ns
**
***
ns
0
5
10
15
untreated
IL-4
IL-4 + A 83-01
TGF-β1
TGF-β1 + A 83-01
IL-13
IL-13 + A 83-01
IL-4 + TGF-β1
IL-4 + IL-13
A 83-01

Figure 10: **Confocal microscopy shows the effect of IL-4, IL-13, TGF-β1 and A 83-01 (TGF-β1 signalling inhibition) on α-SMA expression in CAF 6388/19.** 15.000 CAF 6388/19 (p11) were seeded in chamber slides and treated for 48 hours after 24 hours of preculturing. (**A**) Representative microscopic images are depicted. Nuclei were stained with DAPI (blue), Vimentin in red and α-SMA in green. (**B, C**) Analysis of confocal images using Image J (**B**) α-SMA positive pixels per area normalised on DAPI positive nuclei area (**C**) α-SMA positive cells manually counted and normalised to DAPI positive nuclei area. Mean values, SD (error bars) of technical replicates (pictures) (n=15) per condition are depicted, **** indicates a P <0.0001 using ordinary one-way ANOVA.

3.4 The influence of IL-4, TGF-β1, IL-1β+ TNF-α and treatment combinations on CAF BGM2008 expression of α-SMA, FAP, IL-1-R1, PDPLN and PD-L2.

We have demonstrated above that CAFs respond to various cytokines with different levels of SMA expression. Thus, it was tempting to speculate that these factors substantially impact the CAF phenotype and, hence, CAF marker expression. In this set of experiments, we aimed to characterise the response of BGM2008 CAFs to different cytokine stimulations based on α-SMA, FAP, IL-1R1, PDPLN, and PD-L2. These are all defined as bona fide markers for CAFs. The previously established treatments, including 2 ng/ml IL-4, IL-1β + TNF-α, TGF-β1, and their combinations, were used, and the change in expression of the markers as mentioned earlier was assessed.
Again, we used the In-Cell Western to assess changes in CAF marker expression. In short, we seeded 15,000 CAF-BGM2008 cells per well of a 96-well plate in 2D, starved them for 24 hours, and treated them for 48 hours with the cytokines as mentioned above. IgG controls were used for each antibody.

α-SMA
Basal expression of α-SMA was observed in untreated CAF-BGM2008 (p10), as previously seen with CAF-6388/19 (p11) (Figure 11A and B). Treatment with IL-4 led to a highly significant induction of α-SMA expression, with a 3.7-fold increase compared to the untreated control (Figures 11A and 11B). As expected, TGF-β1 treatment resulted in an even higher level of α-SMA, with a 5-fold increase (Figures 11A and 11B). Both results from the treatments with IL-4 and TGF-β1, thus compare well with the results of the 72-hour timepoint of CAF 6388/19 (Results section 3.1). In contrast, adding pro-inflammatory cytokines IL-1β and TNF-α did not significantly alter α-SMA levels (Figures 9A and 9B). Interestingly, combining IL-4 with TGF-β1 did not enhance α-SMA induction beyond the effect observed with TGF-β1 alone (Figures 11A and 11B). This is comparable to the In-Cell Western results using CAF 6388/19 (see Results 3.2). A slight increase in α-SMA expression was noted when IL-4 was combined with IL-1β and TNF-α compared to untreated levels (Figures 11A and 11B). Similarly, the combination of TGF-β1 with IL-1β and TNF-α resulted in a moderate upregulation in α-SMA, though the effect was less pronounced compared to TGF-β1 treatment alone (Figures 11A and 11B). The presence of all four cytokines (IL-4, TGF-β1, IL-1β, and TNF-α) resulted in α-SMA levels comparable to those observed with the combination of TGF-β1, IL-1β, and TNF-α (Figures 11A and 11B).

FAP
Very low basal expression of FAP was detected in BGM2008 (Figures 11A and 11B). IL-4 treatment did not induce any significant upregulation of FAP expression (Figures 11A and 11B). In contrast, TGF-β1 treatment led to a highly significant increase in FAP levels (Figure

11A and 11B). Treatment with IL-1β and TNF-α resulted in a minimal, non-significant increase in FAP expression (Figure 11A and 11B). The combination of IL-4 and TGF-β1 did not result in higher upregulation compared to TGF-β1 alone (Figures 11A and 11B). Interestingly, when IL-4 was combined with IL-1β and TNF-α, a FAP was highly significantly upregulated to approximately the same level as TGF-β1-treated cells (Figures 11A and 11B). Similarly, TGF-β1/IL-1β/TNF-α, elicited a highly significant 3,8-fold increase in FAP compared to TGF-β1 treatment alone (Figure 11A and 11B). Interestingly, the combination of all four cytokines showed a similar response with high upregulation of FAP (Figure 11A and 11B).

IL-1R1

Untreated CAFs exhibited high levels of IL-1R1 expression (Figures 11A and 11B). Upon treatment with IL-4, a notable downregulation of IL-1R1 was observed, with a 36% reduction (Figures 11A and 11B). TGF-β1 treatment reduced IL-1R1 to about half of the level of untreated CAFs (Figures 11A and 11B). The combination of IL-1β + TNF-α resulted in a similar decrease in IL-1R1 expression as TGF-β1 (Figures 11A and 11B). IL-4 and TGF-β1, in combination, reduced IL-1R1 expression by 60%, comparable to the effect of IL-4 and inflammatory treatment (IL-1β + TNF-α) (Figures 11A and 11B). TGF-β1 + IL-1β + TNF-α resulted in a reduction of IL-1R1 to the same extent (Figures 11A and 11B). The most significant reduction was observed with all four cytokines, resulting in a 71% decrease (Figures 11A and 11B).

PDPLN

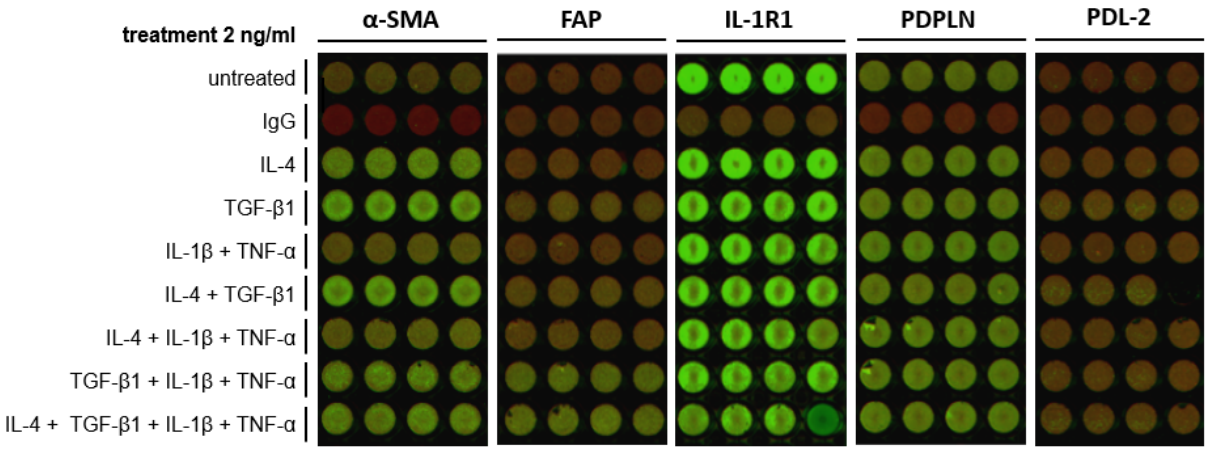
IL-4 treatment resulted in a moderate upregulation of podoplanin by 33% compared to untreated controls (Figures 11A and 11B). TGF-β1 did not significantly change PDPLN levels, but a trend towards an increase was detected (Figures 11A and 11B). The highest levels of PDPLN expression were observed in CAFs treated with IL-1β and TNF-α, showing a highly significant upregulation compared to untreated CAFs, with an absolute increase of 77% (Figures 11A and 11B). IL-4 and TGF-β1 did not enhance PDPLN expression beyond TGF-β1 alone (Figures 11A and 11B). Combining IL-4 with IL-1β + TNF-α significantly increased PDPLN expression at a moderate level to about the expression of IL-4 alone (Figures 11A and 11B). TGF-β1, in combination with IL-1β + TNF-α, led to a significant upregulation, with a 30% absolute increase (Figures 11A and 11B). The presence of all four cytokines increased PDPLN (Figures 11A and 11B), indistinguishable from the triple treatments. Overall, IL-4 and TGF-β1 appeared to attenuate the expression of PDPLN induced by IL-1β + TNF-α treatment (Figures 11A and 11B).

PD-L2

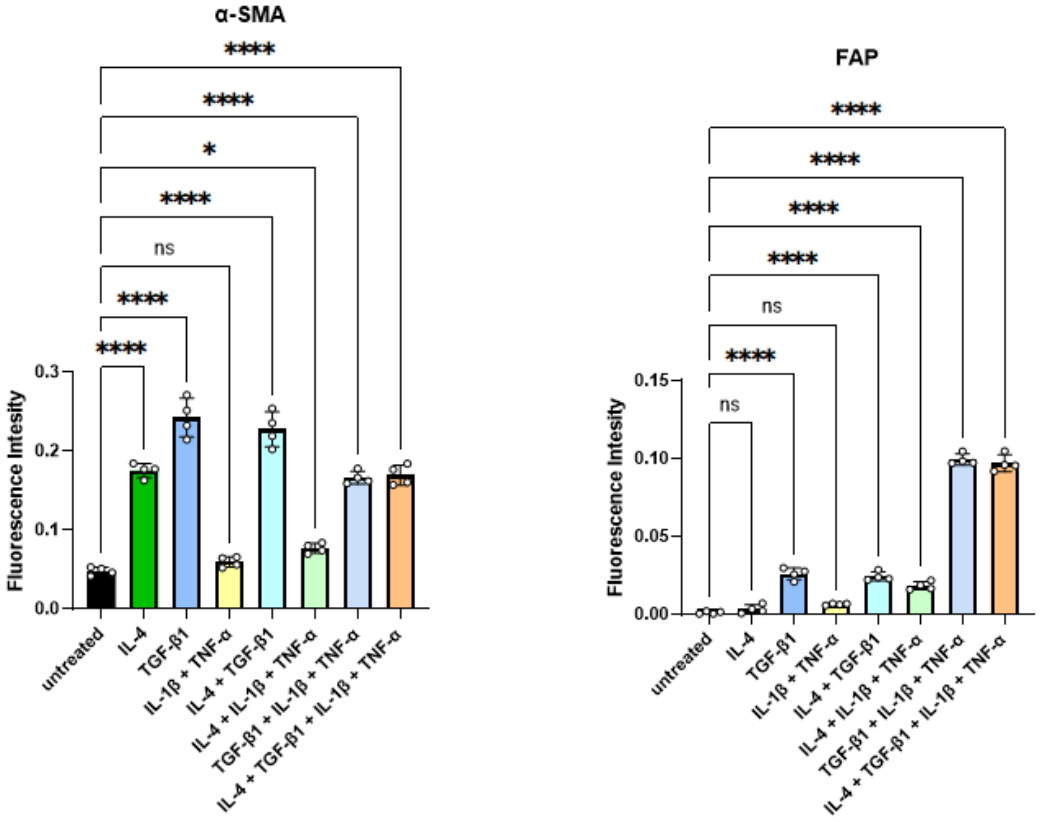
Untreated CAF-BGM2008 showed no PD-L2 expression. IL-4 treatment did not result in an upregulation (Figures 11A and 11B). However, TGF-β1 treatment induced a highly

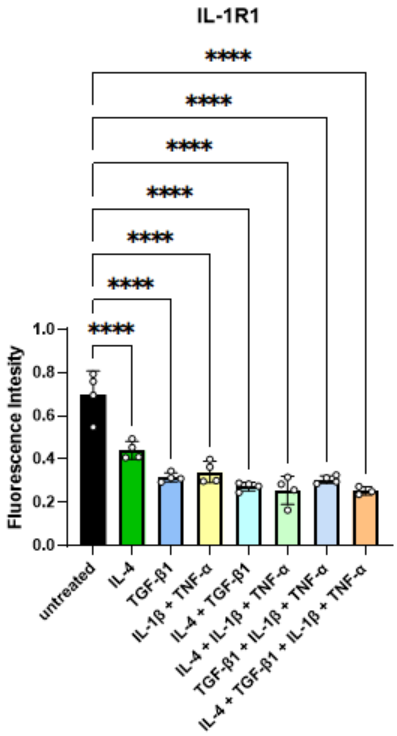
significant upregulation of PD-L2 but at a generally low signal (Figures 11A and 11B). The combination of IL-1β and TNF-α did not significantly alter PD-L2 expression, but a trend toward upregulation was observed (Figures 11A and 11B). When IL-4 was combined with TGF-β1, there was a substantial upregulation of PD-L2, higher than TGF-β1 alone, suggesting an additional contribution from IL-4 (Figures 11A and 11B). Combining IL-4 with IL-1β + TNF-α resulted in a modest, yet significant, increase in PD-L2, with levels higher than those observed with IL-1β + TNF-α alone (Figures 11A and 11B). TGF-β1, in combination with IL-1β and TNF-α, showed a significant upregulation; however, this was less pronounced than that of TGF-β1 alone. Finally, treating the CAFs with all four cytokines resulted in a highly significant upregulation of PD-L2, but to a lesser extent than with IL-4 and TGF-β alone (Figures 11A and 11B). Interestingly, PD-L2 upregulation approximately followed the pattern of α-SMA upregulation (Figures 11A and 11B).

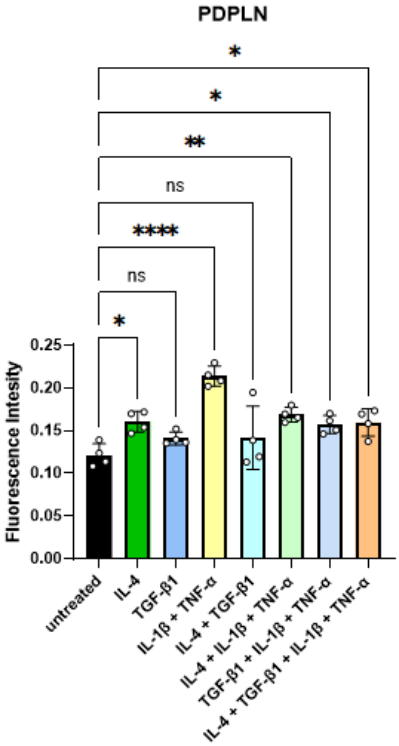
A


treatment 2 ng/ml
α-SMA
FAP
IL-1R1
PDPLN
PDL-2
untreated
IgG
IL-4
TGF-β1
IL-1β + TNF-α
IL-4 + TGF-β1
IL-4 + IL-1β + TNF-α
TGF-β1 + IL-1β + TNF-α
IL-4 + TGF-β1 + IL-1β + TNF-α

B


α-SMA
FAP
Fluorescence Intesity
****
*
ns
0.0
0.1
0.2
0.3
0.00
0.05
0.10
0.15
untreated
IL-4
TGF-β1
IL-1β + TNF-α
IL-4 + TGF-β1
IL-4 + IL-1β + TNF-α
TGF-β1 + IL-1β + TNF-α
IL-4 + TGF-β1 + IL-1β + TNF-α


IL-1R1
Fluorescence Intesity
1.0
0.8
0.6
0.4
0.2
0.0
****
****
****
****
****
****
****
untreated
IL-4
TGF-β1
IL-1β + TNF-α
IL-4 + TGF-β1
IL-4 + IL-1β + TNF-α
TGF-β1 + IL-1β + TNF-α
IL-4 + TGF-β1 + IL-1β + TNF-α


PDPLN
Fluorescence Intesity
0.25
0.20
0.15
0.10
0.05
0.00
*
*
**
ns
****
ns
*
untreated
IL-4
TGF-β1
IL-1β + TNF-α
IL-4 + TGF-β1
IL-4 + IL-1β + TNF-α
TGF-β1 + IL-1β + TNF-α
IL-4 + TGF-β1 + IL-1β + TNF-α

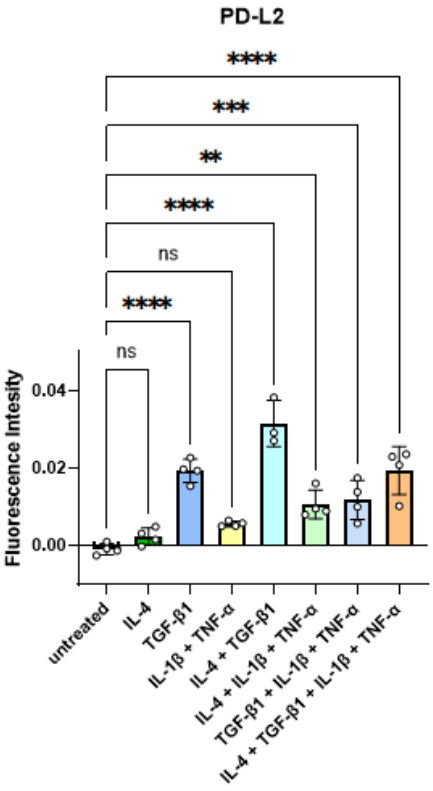

PD-L2
Fluorescence Intesity
0.04
0.02
0.00
****
***
**
****
ns
****
ns
untreated
IL-4
TGF-β1
IL-1β + TNF-α
IL-4 + TGF-β1
IL-4 + IL-1β + TNF-α
TGF-β1 + IL-1β + TNF-α
IL-4 + TGF-β1 + IL-1β + TNF-α

Figure 11: **In-Cell Western (ICW) assay measuring CAF BGM2008 marker regulation (α-SMA, FAP, IL-1R1, PDPLN and PD-L2) upon treatment of 2ng/ml of IL-4, TGFβ-1, IL-1β+ TNF-α and different combinations (as indicated).** CAFs BGM2008 (p10) were treated in 96-well plates in 2D with 2 ng/ml of IL-4, TGF-β1, IL-1β + TNF-α and combinations thereof as indicated for 48 hours. The levels of α-SMA were determined using the ICW method. (**A**) Representative pictures of α-SMA, FAP, IL-1R1, PDPLN and PD-L2 (green, as indicated) and Celltag (total protein stain, red, used for normalisation) staining. (**B, C**) Analysis of ICW fluorescence intensity measurement data. Mean values, SD (error bars) of technical replicates (n=3) are depicted, **** indicates a P <0.0001 using ordinary one-way ANOVA.

3.5 The influence of IL-4, TGF-β1, IL-1β+ TNF-α and treatment combinations on CAF BGM2008 expression of α-SMA and FAP using immunofluorescence staining for confocal microscopy

The following experiment assessed α-SMA and FAP expression after cytokine treatment using immunofluorescence staining for confocal microscopy. It was performed as described in the Results section 3.3, using CAF-BGM2008 (p8).
In brief, 15.000 CAF were seeded in an 8-well chamber slide as a 2D monolayer and treated the following day with 2ng/ml of IL-4, TGF-β1, IL-1β + TNF-α and combinations thereof for 48 hours. This was followed by immunofluorescence staining for FAP, vimentin, α-SMA, and nuclei (DAPI). The picture area was chosen objectively, as described in the methods, and pictures were acquired in three optical planes. Quantitative analysis of confocal images using ImageJ followed. Representative confocal images display α-SMA (green), FAP (yellow), DAPI-stained nuclei (blue) and Vimentin (red) (Figure 12A, B). These maximal projection images of the three planes were selected to represent the mean α-SMA (Figure 12A) and FAP (Figure 12B) positive pixel count for each condition, highlighting the visual differences in marker expression levels across the various treatments. All pictures analysed can be found in Appendix Figures 5 and 6.

α-SMA
As reported above, α-SMA was detected in stress fibres (Figure 12A; compare to Figure 4B of the Introduction). Untreated CAFs displayed low α-SMA signal, as measured by α-SMA positive pixels normalised to nuclei (DAPI stain) (Figures 12A, C). A slight trend toward upregulation of α-SMA was observed with IL-4 treatment (Figures 12A and 12B). A similar non-significant trend was observed with TGF-β1 treatment; potentially, the significance is limited due to high variability among individual pictures (Figures 12A and 12B). Treatment with IL-1β + TNF-α showed no detectable α-SMA expression (Figures 12A and 12B).
In contrast, IL-4 in combination with TGF-β1 resulted in a highly significant upregulation of α-SMA (Figures 12A and 12B). Combining IL-4 with IL-1β + TNF-α failed to substantially induce α-SMA expression (Figures 12A and 12B). The combination of TGF-β1 with IL-1β + TNF-α showed a trend towards α-SMA upregulation, but this effect did not reach statistical significance (Figures 12A and 12B). Higher levels, comparable to all four treatments, were seen in the In-Cell Western assay for this condition (Results 3.5). Notably, the highest levels of α-SMA-positive pixels were observed with high significance with the combination of all four cytokines (Figures 12A and 12B).

FAP
Only some cells showed FAP expression, which indicates a heterogeneous cell population (Figure 12B, Appendix Figure 6). Untreated and IL-4-treated CAFs show no FAP-positive

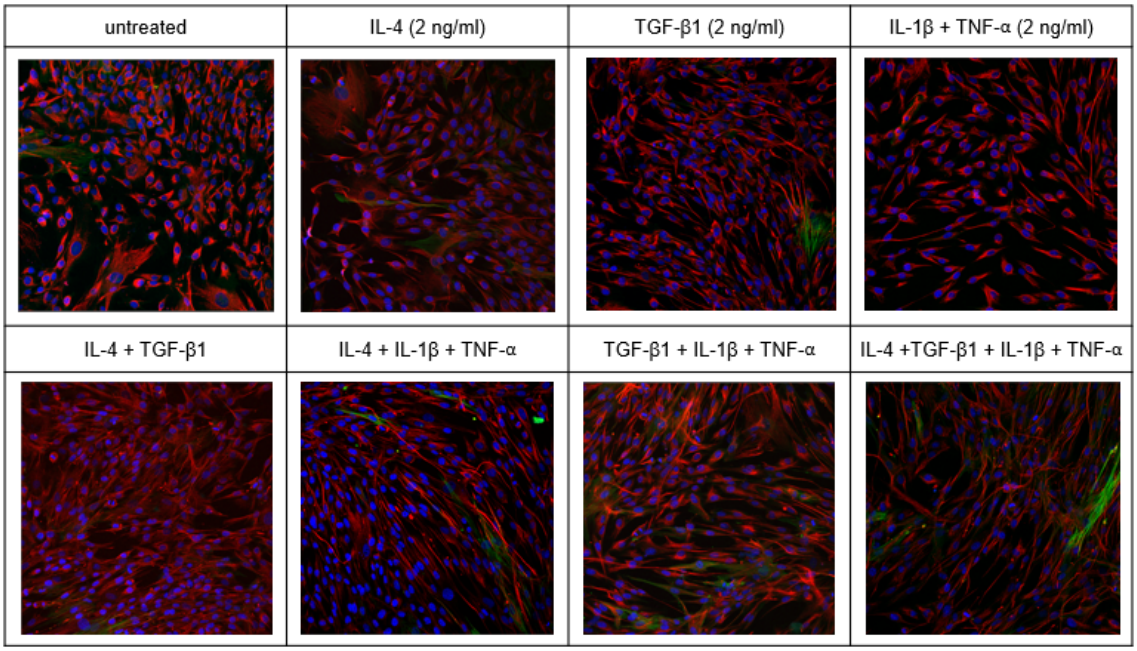
pixels normalised to nuclei at a set threshold (Figures 12B and 12C). This matches the results seen in the In-Cell Western (Results 3.5). TGF-β1 clearly shows increased FAP levels, with high significance (Figures 12B and 12C). In-Cell Western in Results 3.5 also showed an increase of FAP with TGF-β1 treatment (Figures 12B and 12C). Treatment with the inflammatory cytokines, IL-1β + TNF-α, showed some FAP upregulation, although this was not significant (Figures 12B and 12C). The upregulation of FAP with inflammatory cytokines was about half of the level compared to TGF-β1 treatment (Figures 12B and 12C). IL-4 and TGF-β1 in combination increased FAP highly significantly compared to untreated (12B and 12C). The signal is about two times the TGF-β1 signal (Figures 12B and 12C). This is interesting, as IL-4 alone showed no effect on FAP upregulation (Figures 12B and 12C). These results are in agreement with the In-Cell Western analysis, which also showed an increase in FAP upregulation upon Il-4+TGF-β1 treatment, with levels comparable to TGF-β1 single treatment (Results 3.5). IL-4 and IL-1β + TNF-α significantly upregulated FAP, comparable to levels of TGF-β1 upregulation Figures 12B and 12C).

Interestingly, TGF-β1 in combination with IL-1β + TNF-α showed less upregulation than TGF-β1 alone (Figures 12B and 12C). This is in contrast to the In-Cell Western detected levels, where the combination of TGF-β1 with IL-1β + TNF-α resulted in a significant increase (Results 3.5)

Treatment with all four cytokines upregulated FAP the most, resulting in levels that were 760-fold higher than untreated and about twice as strong compared to IL-4 + TGF-β1 (Figures 12B and 12C).

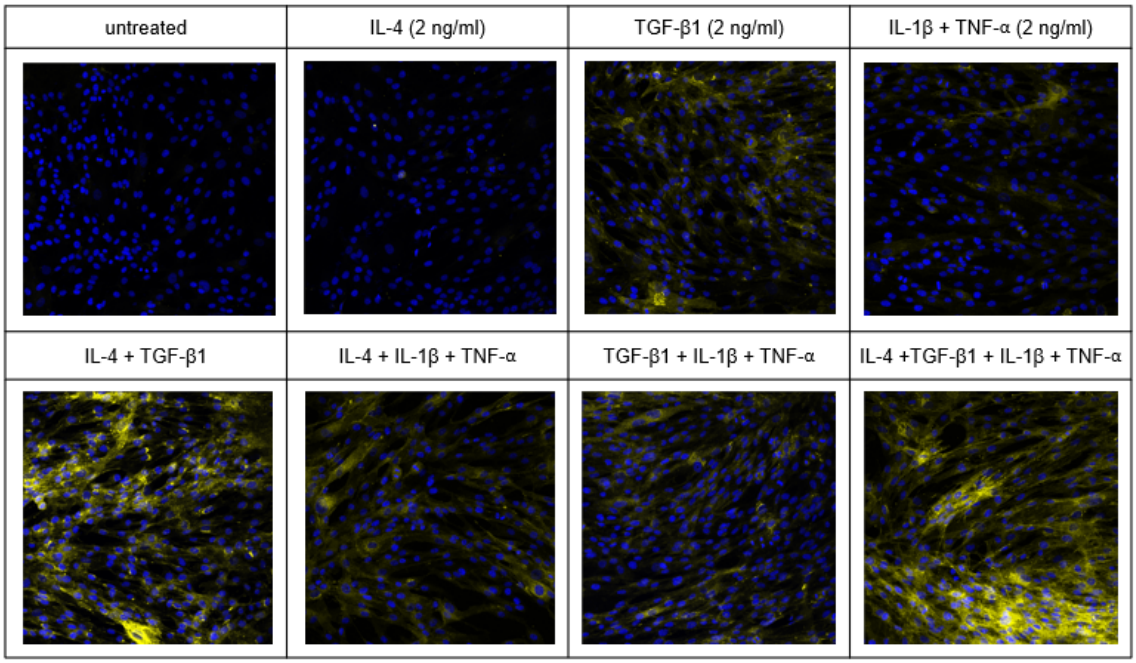
A

α-SMA


untreated
IL-4 (2 ng/ml)
TGF-β1 (2 ng/ml)
IL-1β + TNF-α (2 ng/ml)
IL-4 + TGF-β1
IL-4 + IL-1β + TNF-α
TGF-β1 + IL-1β + TNF-α
IL-4 +TGF-β1 + IL-1β + TNF-α

B

FAP


untreated
IL-4 (2 ng/ml)
TGF-β1 (2 ng/ml)
IL-1β + TNF-α (2 ng/ml)
IL-4 + TGF-β1
IL-4 + IL-1β + TNF-α
TGF-β1 + IL-1β + TNF-α
IL-4 +TGF-β1 + IL-1β + TNF-α

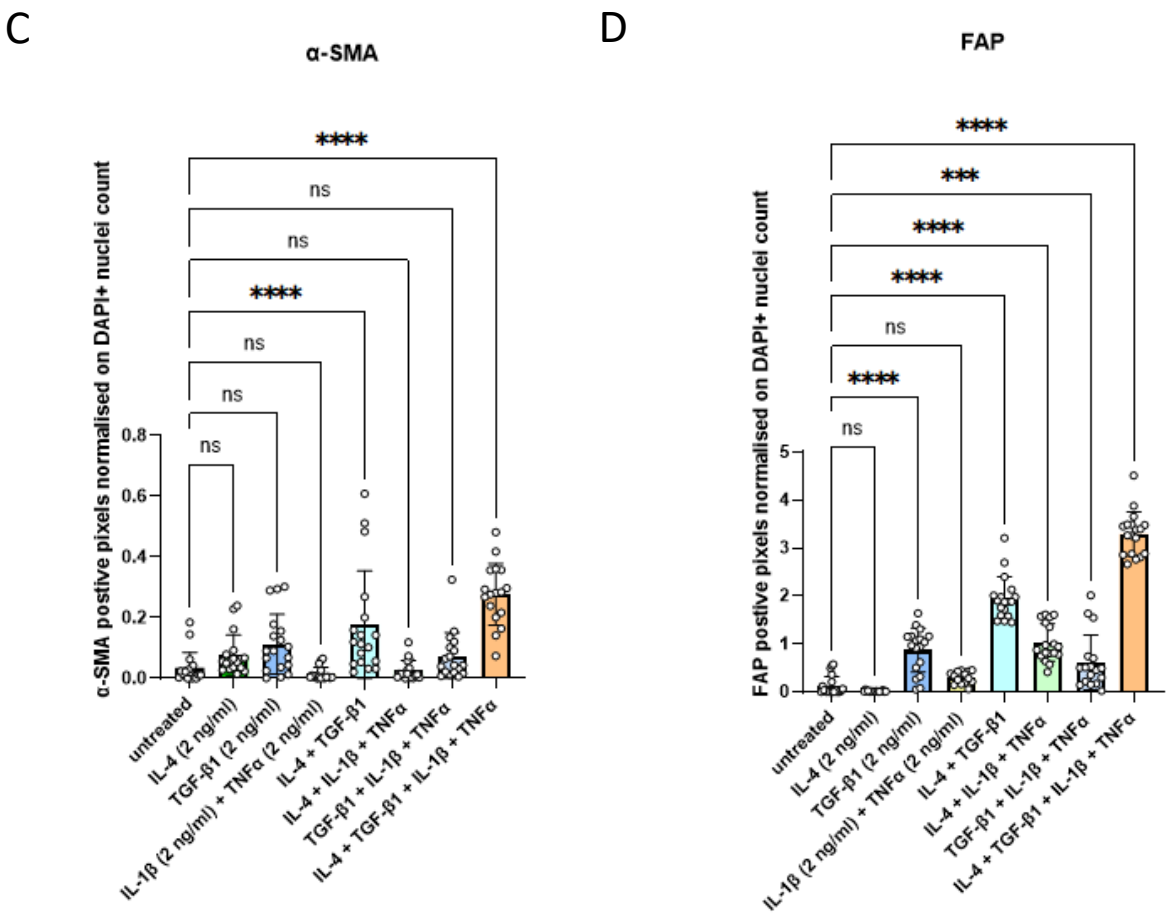


Figure 12: **Confocal microscopy shows the effect of IL-4, TGF-β1 and IL-1β +TNF-α treatment on α-SMA and FAP expression in CAF BGM2008.** 15.000 CAF BGM2008 (p8) were seeded in chamber slides and treated for 48 hrs following 24 hrs of preculturing. (**A, B**) Representative microscopic images are depicted. Nuclei were stained with DAPI (blue), Vimentin in red, α-SMA in green and FAP in yellow. (**C, D**) Analysis of confocal images using Image J (**B**) α-SMA positive pixels per area normalised on DAPI positive nuclei area (**C**) FAP positive pixels per area normalised on DAPI positive nuclei area. Mean values, SD (error bars) of technical replicates (pictures) (n=18) per condition depicted (3 planes per picture, 6 images per condition), **** indicates a P <0.0001 using ordinary one-way ANOVA.

3.6 The influence of IL-4, TGF-β1, IL-1β+ TNF-α treated CAF 6388/19 conditioned media and its effect on BGM2008 CRC organoid growth using CellTiter-Glo 3D assay

In the previous experiments, we concentrated on the CAF phenotype upon treatment with specific factors. In the following experiments, we focused on the effects of these different CAF states on cancer cell proliferation/survival. We were specifically interested in whether CAFs change their secretome at different states and how this would influence cancer cell growth.

We established above that 2 ng/ml of IL-4, TGFβ-1 and especially the combination of IL-4 and TGFβ-1 upregulate α-SMA in CAF 6388/19 and induce a robust myofibroblast phenotype (myCAF). IL-13 was also found to upregulate α-SMA, but combined with IL-4, it did not show a more pronounced upregulation than IL-4 alone. Hence, we decided to focus on the effects of IL-4 and TGF-β1 in the following experiments. To broaden the scope of the research, we decided to add inflammatory induction by adding the combination of IL-1β and TNF-α to our CAF treatments. IL-1β and TNF-α have been shown to induce an inflammatory (iCAF) phenotype in CAFs (Schauer et al., 2013; Dudás et al., 2011; Díaz-Maroto et al., 2021; Rubinstein-Achiasaf et al., 2021; Koncina et al., 2023). Thus, we aimed to measure the impact of two principal states of CAF- iCAF and myCAF (Kennel et al., 2023) – on patient derived CRC organoids.

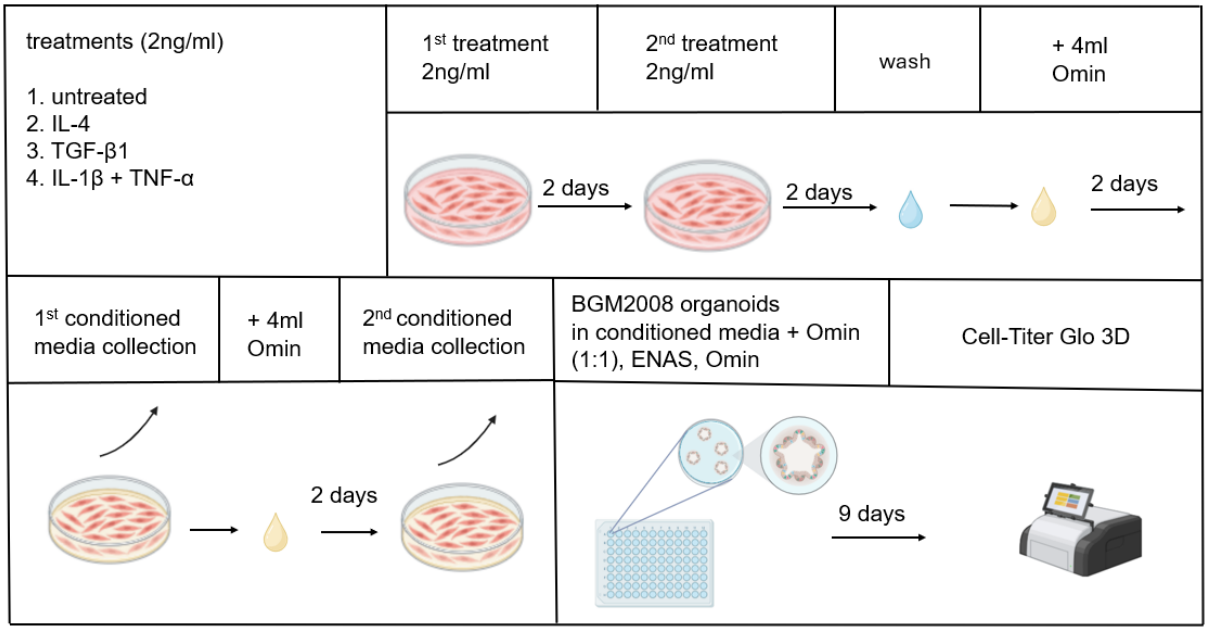
We treated CAF 6388/19 (p13) in 2D at full confluence with 2 ng/ml of IL-4, TGF-β, IL-1β and TNF-α for 48 hours, then treated them again for 48 hours (Figure 13A). Then, we washed the cells with PBS to remove any cytokine treatment residues and added Omin (minimal organoid medium) media. After 48 and 96 hours, the conditioned media were collected. The collected media were combined and mixed 1:1 with fresh Omin to replenish nutrients. This mixture was then used to treat BGM2008 organoids (p25 (B; D), p14 (C; D)) seeded as single cells in 10 µl Matrigel domes (2000 cells /per well/per 10 µl Matrigel). After 3 days, treatment was prolonged with fresh CM/Omin. On days 5 or 9 (as indicated in Figure 7), organoid growth/viability was assessed using the CellTiter-Glo 3D assay. As controls, organoids were also grown in untreated CAF-conditioned media, Omin and ENAS media.

At first, the luminescence of BGM2008 organoids on day 5 was measured to test the best endpoint for the newly established assay. No significant change in ATP levels of organoids cultured in cytokine-treated conditioned media was detectable (see Figure 13D). Furthermore, no increase in the number or size of organoids was visible with any conditioned media (Figure 13B). Organoids grown in Omin showed less luminescence than untreated conditioned Omin 1:1 mix media (-74% absolute decrease) (Figures 13B and 13D). ENAS media supported organoid growth better than Omin alone at day 5. Yet, untreated CAF-conditioned media better supported organoid growth, with ATP values twice as high as ENAS (Figures 13B and 13D).

The experiment was repeated as a trend was detectable. This time, organoids were grown longer until a visible difference was observable at day 9 (Figure 13C). The Cell Titer Glo assay at day 9 showed that organoids grown in IL-1β+ TNF-α pre-treated conditioned media had significantly higher ATP values (+26% abs. increase) (Figure 13E). There were no significant changes, but a trend towards increased organoid growth with pre-treatment of CAFs with IL-4 (+13% absolute increase) and TGF-β1 (+20% absolute increase) (Figures 13C and 13E). As per the previous experiment, organoids grown in Omin showed less luminescence than those grown in untreated conditioned Omin 1:1 mix media (-72% absolute decrease) (Figure 13B and 13D). Furthermore, ENAS media supported organoid growth better than Omin (+41% absolute increase), yet not as well as CAF-conditioned media (Figures 13C and 13E).

These results indicate that conditioned media from inflammatory CAFs, resulting from pre-treatment of CAF 6388/19 with inflammatory cytokines, led to a significant increase in ATP values of organoids grown in that media for 9 days. TGF-β1 and IL-4 pre-treatment showed a trend of increased luminescence; however, the effect was not significant. This data suggests that treating CAF with cytokines may alter their secretome profile, increasing cancer organoid growth. Further research is needed to determine the exact changes in proteins secreted by CAF in response to each cytokine treatment.

A



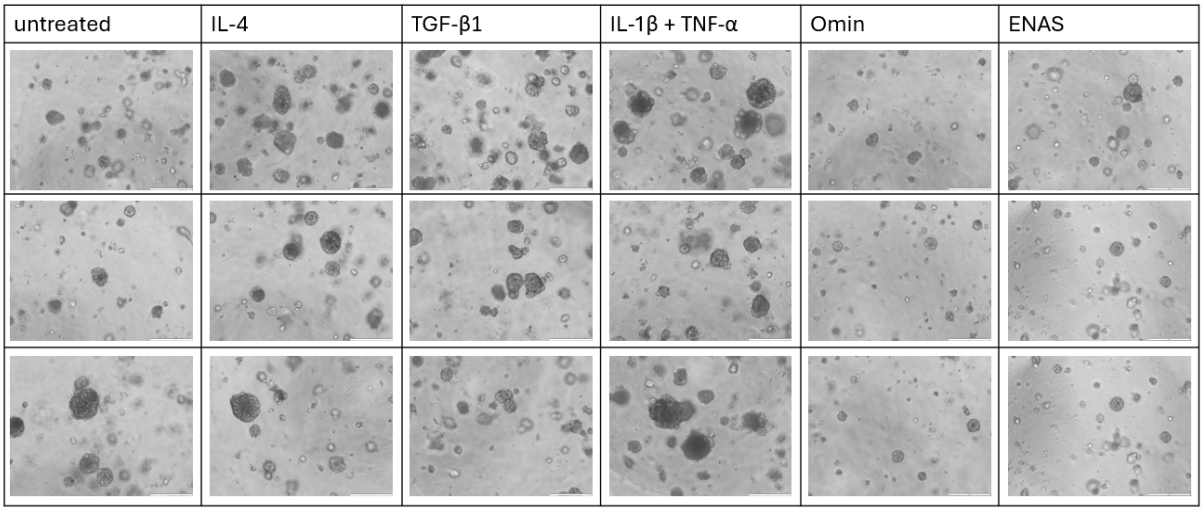
B

Day 5

untreated	IL-4	TGF-β1	IL-1β + TNF-α	Omin	ENAS

C

Day 9


untreated
IL-4
TGF-β1
IL-1β + TNF-α
Omin
ENAS

D

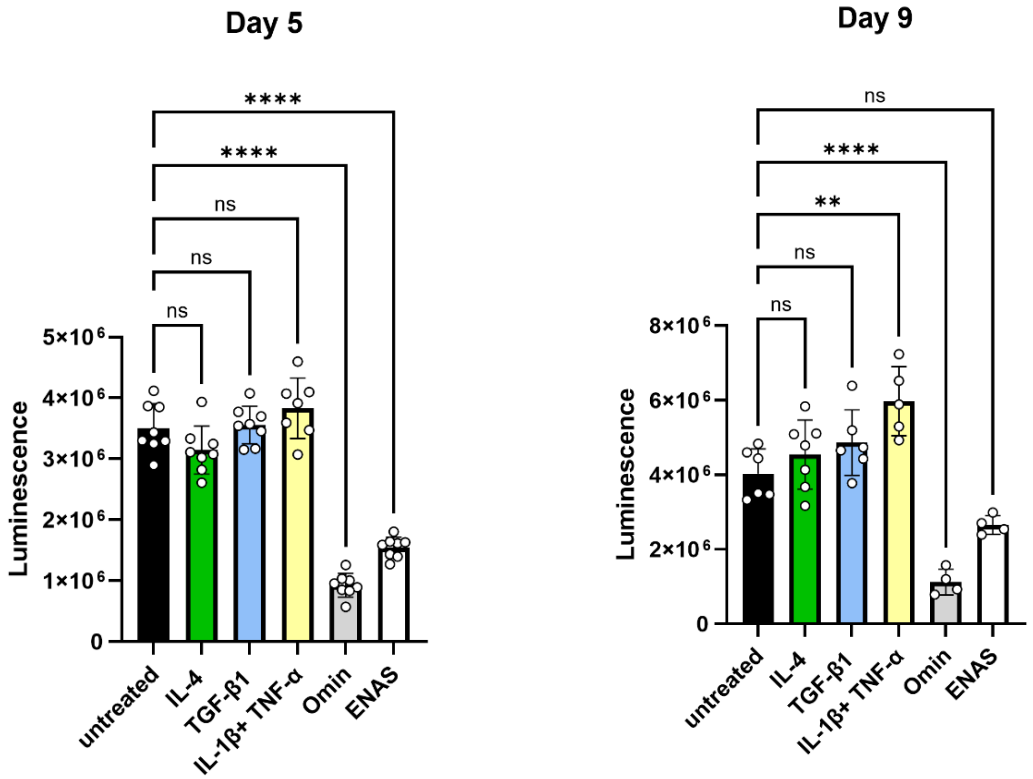

Day 5
Luminescence
5×10⁶
4×10⁶
3×10⁶
2×10⁶
1×10⁶
0
****
****
ns
ns
ns
untreated
IL-4
TGF-β1
IL-1β+ TNF-α
Omin
ENAS
Day 9
Luminescence
8×10⁶
6×10⁶
4×10⁶
2×10⁶
0
ns
****
**
ns
ns
untreated
IL-4
TGF-β1
IL-1β+ TNF-α
Omin
ENAS

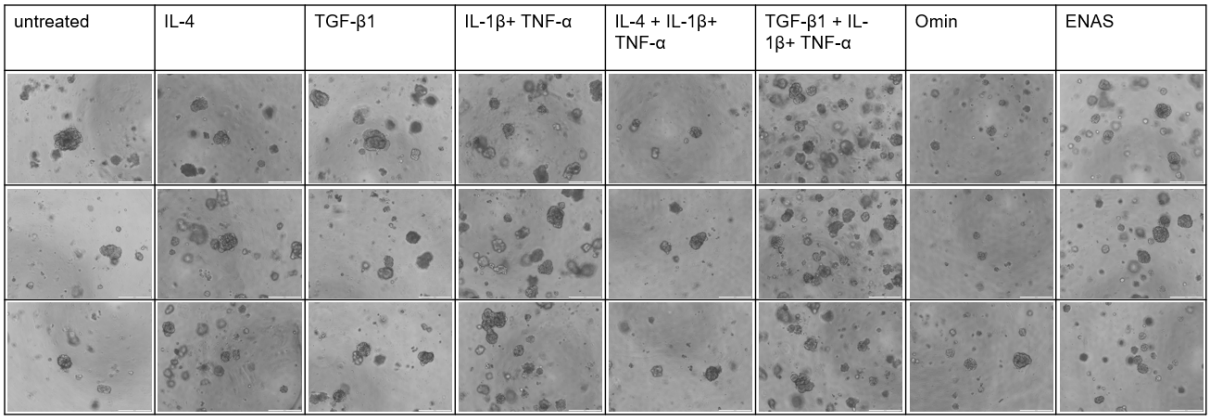
Figure 13: **The influence of cytokine pre-treated CAF 6388/19 conditioned media on BGM2008 CRC organoid viability using Cell Titer Glo 3D assay.** CAF 6388/19 (p13) were seeded in 6 cm dishes in 2D and at confluency they were treated with 2 ng/ml of IL-4, TGF-β1, IL-1β+TNF-α twice for 48 hours. After washing with PBS, 4 ml of Omin was added. Conditioned media (CM) were harvested after 48 hours, and the last step was repeated to obtain more CM. CM was mixed with Omin 1:1, ENAS and pure Omin were used as controls. Conditioned and control media were used to grow BGM2008 organoids (p25 (B; D), p14 (C; D)) in Matrigel domes (2000 cells/10 µL/well) for the indicated time. After that, Cell Titer Glo 3D assay was performed to assess viability (**A**) Schematic representation of the assay using biorender.com (**B, C**) Microscope pictures of organoids in Matrigel domes grown for (**B**) 5 days (**C**) and 9 days in cytokine pre-treated CAF 6388/19 conditioned media. (**D, E**) Analysis of Cell Titer Glo 3D luminescence (**D**) 5 days (**E**) and 9 days. Mean values, SD (error bars) of technical replicates are depicted: treatments (n≥6), Omin and ENAS (n≥4), **** indicates a P <0.0001 using ordinary one-way ANOVA.

3.7 The influence of IL-4, TGF-β1, IL-1β + TNF-α and combinations of these treatments on CAF BGM2008 conditioned media and its effect on patient-matched CRC organoid viability using Cell Titer Glo 3D assay.

After proof of principle that IL-1β + TNF-α treated CAF 6388/19 secrete factors that increase the growth of BGM2008 organoids, we asked whether the patient-matched CAFs from BGM2008 tumours would have the same effect on BGM2008 organoids. Furthermore, we investigated whether treating with combinations of cytokines leads to a combinatorial effect. The assay was performed as described in 3.4 and the methods.
The assay was performed twice with different treatment combinations (Figure 14A, B, C, D). CAF BGM2008 (p5) and BGM2008 organoids (p20 (Figure 14A and C; Day 5) and p31 (Figure 14B and D; Day 9) were used. A summary Figure 14E combining both experiments was created by normalising the treatments to the untreated in the respective assay. Treating CAFs with IL-4 or TGF-β1 alone did not significantly increase organoid luminescence (Figures 14A, B, C, D, E). However, a combination of the pro-inflammatory cytokines IL-1β and TNF-α led to a significant increase in the luminescence signal of the organoids, with an absolute increase of 211% compared to the untreated control (Figure 14A, C, E). The combination of IL-4 and TGF-β1 almost doubled (96% absolute increase) organoid viability (Figure 14B, D, E). No significant effects were seen with the IL-4 +IL-1β + TNF-α (Figure 14 A, B, C, D). IL-4 seems to oppose the effects of inflammatory treatment (Figure 14A, B, C, D). Interestingly, a mixture of TGF-β1, IL-1β, and TNF-α resulted in a marked increase in detected ATP (+90% absolute increase), comparable to IL-1β + TNF-α values (Figure 14A, C, E). This indicates that TGF-β does not increase growth further than treatment with IL-1β and TNF-α alone (Figure 14A, C, E). However, the most substantial response was observed when all cytokines were combined, resulting in a luminescence signal 3.8-fold greater than the signal of untreated conditioned media (Figure 14B, D, E).
Control experiments using organoids in Omin media (without conditioned media) exhibited a reduced signal relative to the Omin/conditioned media mixture (1:1). Additionally, organoids in ENAS media without conditioned media displayed higher ATP levels (+117% absolute increase) than untreated conditioned media (Figure 14A, C, E).
Importantly, the effect of different cytokine treatments of CAFs and their impact on cancer growth was additionally shown in a different biological replicate regarding the CAFs. Taken together, these results show that inflammatory treatment strongly affects the CAF secretome, significantly increasing the growth of cancer organoids. Furthermore, combined pre-treating CAFs with IL-4 and TGF-β1 increased organoid growth/viability comparable to values of TGF-β1 in combination with IL-1β and TNF-α. IL-4 counteracted the effect of inflammatory treatment. Astonishingly, the combination of all cytokines led to the most significant impact.

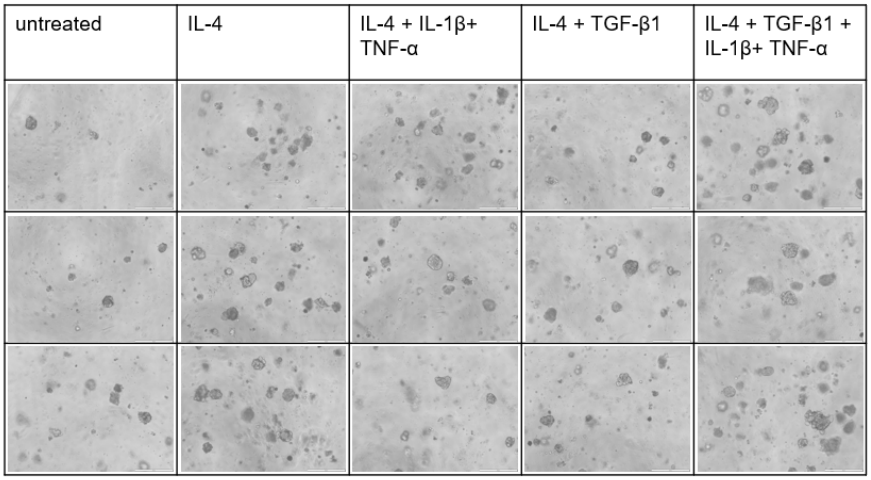
A

Day 9

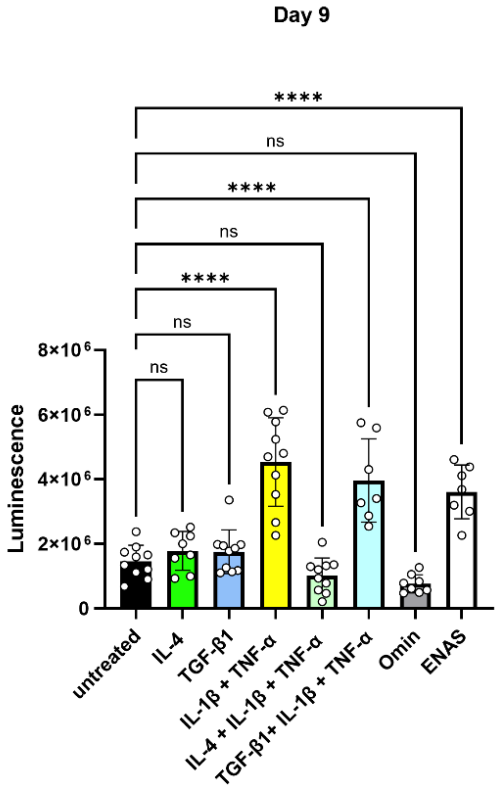

untreated
IL-4
TGF-β1
IL-1β+ TNF-α
IL-4 + IL-1β+ TNF-α
TGF-β1 + IL-1β+ TNF-α
Omin
ENAS

B

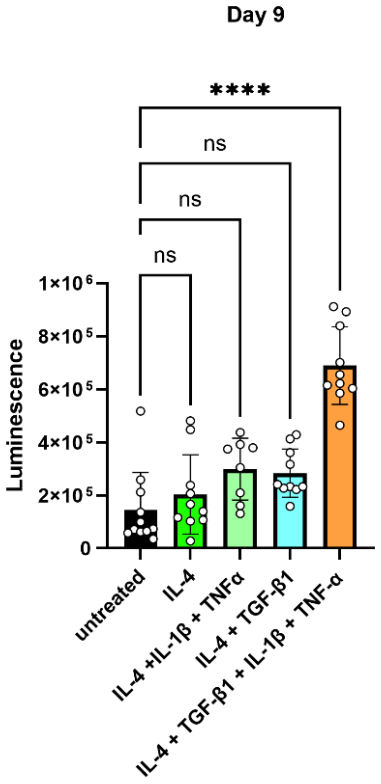
Day 9


untreated
IL-4
IL-4 + IL-1β+ TNF-α
IL-4 + TGF-β1
IL-4 + TGF-β1 + IL-1β+ TNF-α

C


Day 9
Luminescence
8×10⁶
6×10⁶
4×10⁶
2×10⁶
0
****
ns
****
ns
****
ns
ns
untreated
IL-4
TGF-β1
IL-1β + TNF-α
IL-4 + IL-1β + TNF-α
TGF-β1+ IL-1β + TNF-α
Omin
ENAS

D


Day 9
Luminescence
1×10⁶
8×10⁵
6×10⁵
4×10⁵
2×10⁵
0
****
ns
ns
ns
untreated
IL-4
IL-4 +IL-1β + TNFα
IL-4 + TGF-β1
IL-4 + TGF-β1 + IL-1β + TNF-α

E

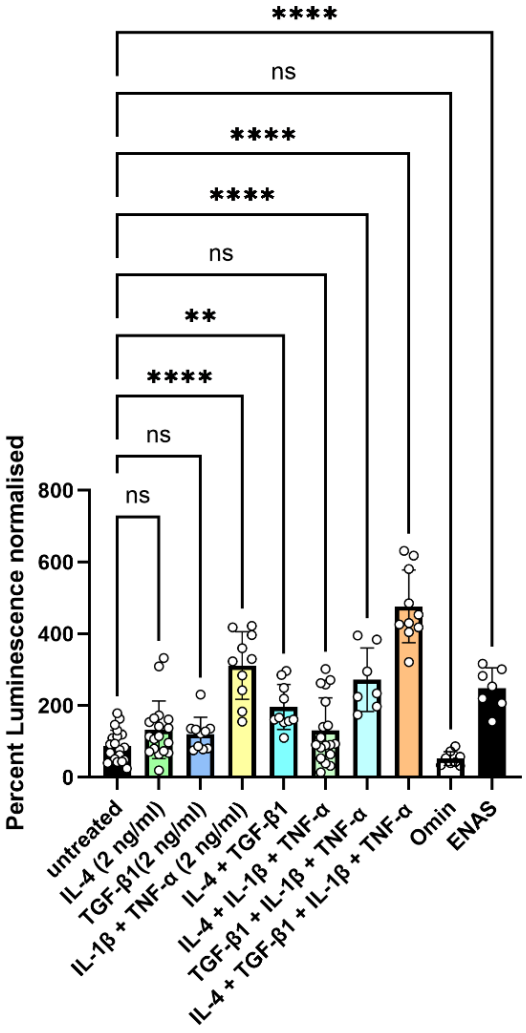

Day 9
****
ns
****
****
ns
**
****
ns
ns
Percent Luminescence normalised
800
600
400
200
0
untreated
IL-4 (2 ng/ml)
TGF-β1(2 ng/ml)
IL-1β + TNF-α (2 ng/ml)
IL-4 + TGF-β1
IL-4 + IL-1β + TNF-α
TGF-β1 + IL-1β + TNF-α
IL-4 + TGF-β1 + IL-1β + TNF-α
Omin
ENAS

Figure 14: **The influence of IL-4, TGF-β1, IL-1β+ TNF-α and combinations of these treatments on CAF BGM2008 conditioned media and their effect on patient-matched CRC organoid viability using Cell Titer Glo 3D assay.** CAFs BGM2008 (p5) were seeded in 6 cm dishes in 2D and at confluency they were treated with 2 ng/ml of IL-4, TGF-β1, IL-1β+TNF-α twice for 48 hours. After washing with PBS, 4 ml of Omin was added. Conditioned media (CM) were harvested after 48 hours, and the last step was repeated. CM was mixed with Omin 1:1, ENAS and pure Omin were used as controls. These media were used to grow BGM2008 organoids (p20 (A;C) and p31 (B; D)) in Matrigel domes (2000 cells/10 µL/well) for the indicated time. After that, the Cell Titer Glo 3d assay was performed to assess viability (A, B). Microscope pictures of organoids in Matrigel domes grown in conditioned media of cytokine-pretreated CAF BGM2008. (**B, C, D**) Analysis of Cell Titer Glo 3D luminescence. Mean values, SD (error bars) of technical replicates are depicted: treatments (n≥10), Omin and ENAS (n≥7), **** indicates a P <0.0001 using ordinary one-way ANOVA.

3.8 OOTA co-culture of pretreated BGM2008 CAF with patient-matched CRC-Organoids

To test the effect of the cytokines on CAF and organoids, we implemented a co-culture model termed “Organotypic organoid transwell assay” (OOTA). For this, CAFs are seeded in a collagen I gel, and organoids in Matrigel are seeded on top. The OOTA has not been used as a growth assay before in the lab, so the number of organoid cells seeded had to be estimated. CAF were pre-treated with cytokines: When CAF reached confluency in a 2D monolayer grown in a 6 cm dish, they were treated with 2 ng/ml cytokines for 48 hours. Then, a 3D collagen gel with 300.000 CAF was formed, and 40.000 organoid cells in Matrigel were seeded on top. Disappointingly, IL-4 pretreatment could not be done according to plan due to an infection. The decision was made to continue with untreated cells and treat them on day 2 and day 4 with 2ng/ml IL-4. Thus, the IL-4 condition is marked with a *(Figure 15A and following). Three pictures of the same area per condition were taken daily with the microscope and analysed as described in Methods for the growth area (Figures 15B and C). Treatment at 2ng/ml was added on days 2 and 4 for the media change for all the conditions. On day 5, the OOTA was fixed. The OOTAs were then cut into quarters. Using one-quarter of each OOTA, the organoids were stained for DAPI, Vimentin, cleaved Caspase-3, EpCAM, and Ki-67 (Figures 16B and C). Another quarter of the CAFs were stained using α-SMA and FAP (Figures 17A and B). Pictures were taken with the confocal microscope in 3 planes and analysed as described in the methods.

Over five days, all organoids of different conditions showed a healthy morphology with absent dark cores (Figure 15B and C). Untreated organoids retained a compact, dense, and spherical morphology (Figure 15B and C). In contrast, treatment with cytokines induced distinct structural alterations. IL-4-treated organoids displayed more irregular borders, with some peripheral cells appearing not integrated into organoids (Figure 15B and C). Organoids exposed to TGF-β1 or IL-1β + TNF-α as single treatments appeared smaller and more uniformly rounded (Figure 15B and C). The combination of IL-4 + TGF-β1 resulted in organoids with diffuse, less defined borders and a less spherical, possibly flattened morphology (Figure 15B and C). Treatment with IL-4 + IL-1β + TNF-α led to larger organoids accompanied by numerous individual cells at the periphery (Figure 15B and C). In contrast, TGF-β1 + IL-1β + TNF-α produced many small, rounded organoids (Figure 15B and C). The most pronounced morphological disruption was observed with the combination of all cytokines (IL-4 + TGF-β1 + IL-1β + TNF-α), which resulted in a low number of organoids with extensive spreading, diffuse borders and severely altered architecture (Figure 15B and C).

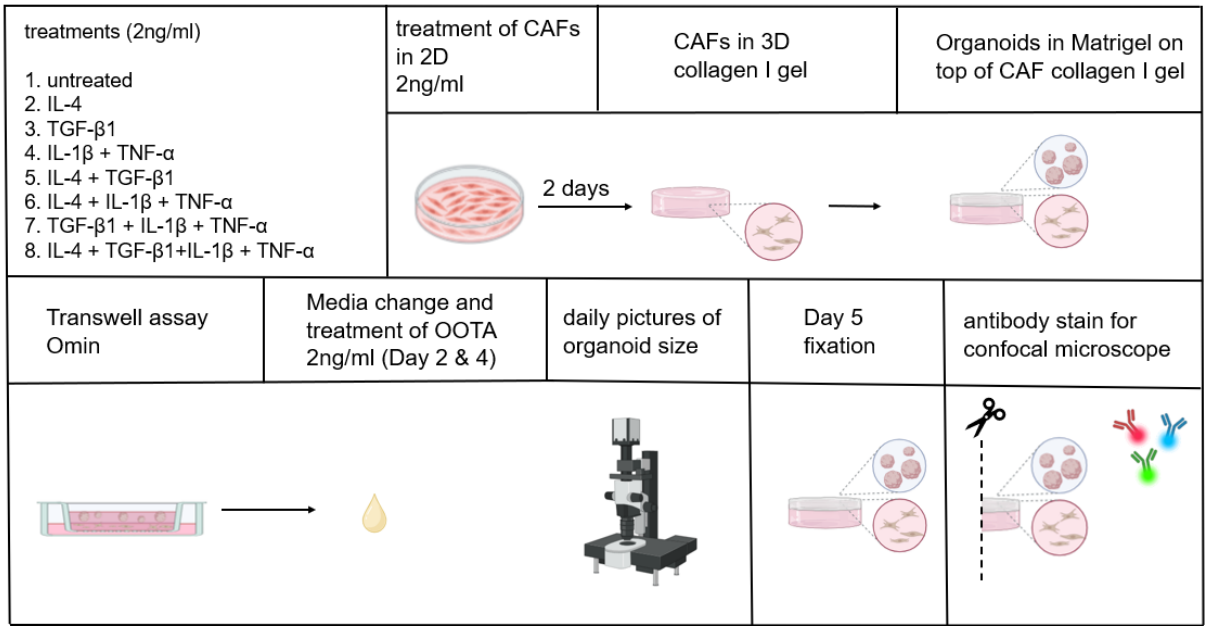
Quantitative analysis of total organoid area per picture reveals no statistically significant differences among treatments at Day 2 (Figure 15D) or Day 5 (Figure 15E) compared to untreated. IL-4 and TGF-β + IL-1β + TNF-α show a high deviation of values for the organoid

area on day 2 (Figure 15D). Whereas treatment with all cytokines shows fewer organoids on Day 2 (Figure 15D). On day 5, there is less growth with IL-4 + TGF-β1 treatment (Figure 15E). The most significant difference in growth for day 5 is the condition treated with all cytokines (Figure 15E).

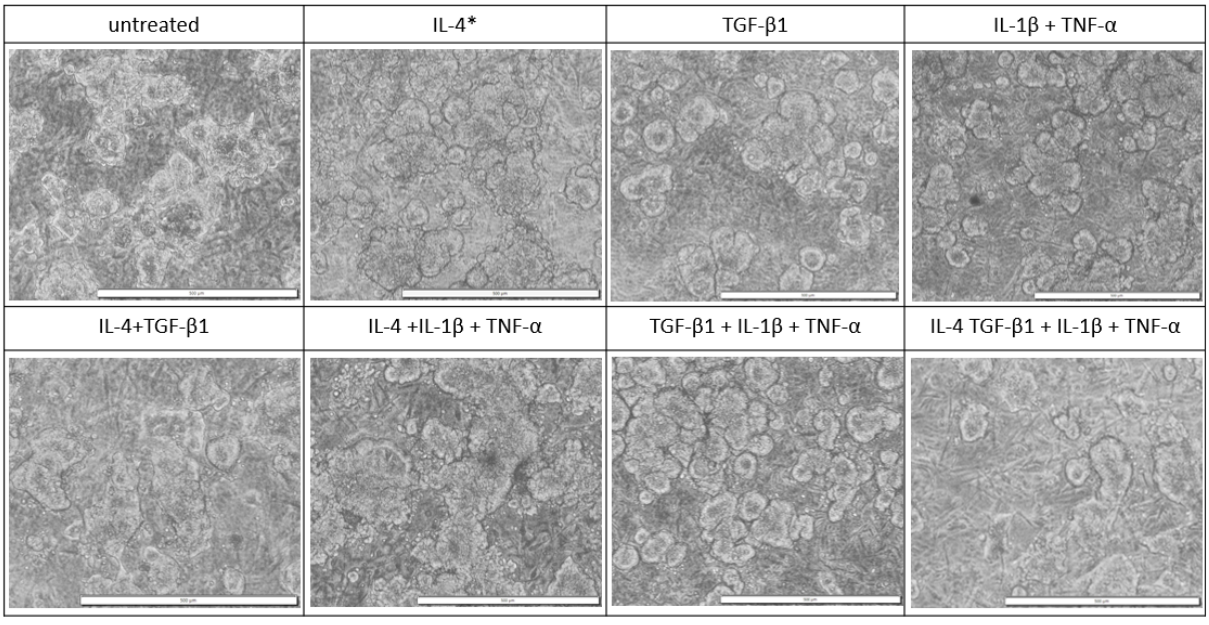
Normalising the total organoid area at Day 5 relative to Day 2 (fold growth) similarly does not show significant differences between conditions (Figure 15F). There is a trend of decreased growth with IL-4. Values for TGF-β1 and IL-1β + TNF-α single treatment are comparable to those of the untreated. There is less growth when IL-4 and TGF-β are combined (Figure 15F). IL-4 + IL-1β + TNF-α compared to the no-treatment control. There is less growth between Day 2 and Day 5 for TGF-β1 + IL-1β + TNF-α. All cytokines are comparable to untreated (Figure 15F). Growth trajectories plotted per condition showed a general increase in total organoid area over time across all treatment groups, reflecting the expected expansion of organoid cultures (Figure 15G).

Individual organoid size analysis revealed notable differences; for this, the individual organoid area (μm²) post-treatment on Day 2 (Figure 15H) and Day 5 (Figure 15I) was quantified. On Day 2, no significant differences in organoid area were observed between the untreated group and most treatment conditions. IL-4 + IL-1β + TNF-α showed modest but statistically significant increases in organoid size compared to untreated (Figure 15H). TGF-β1+ IL-1β + TNF-α showed a highly significant increase in organoid size, about double the mean size compared to untreated (Figure 15H). By Day 5, the organoid area increased substantially in the untreated group relative to several treatment conditions (Figure 15I). Single treatments of cytokines show about half the mean size of untreated. Interestingly, IL-4 + IL-1β + TNF-α and IL-4 +TGF-β1 + IL-1β + TNF-α show comparable results to untreated (Figure 15I).

A

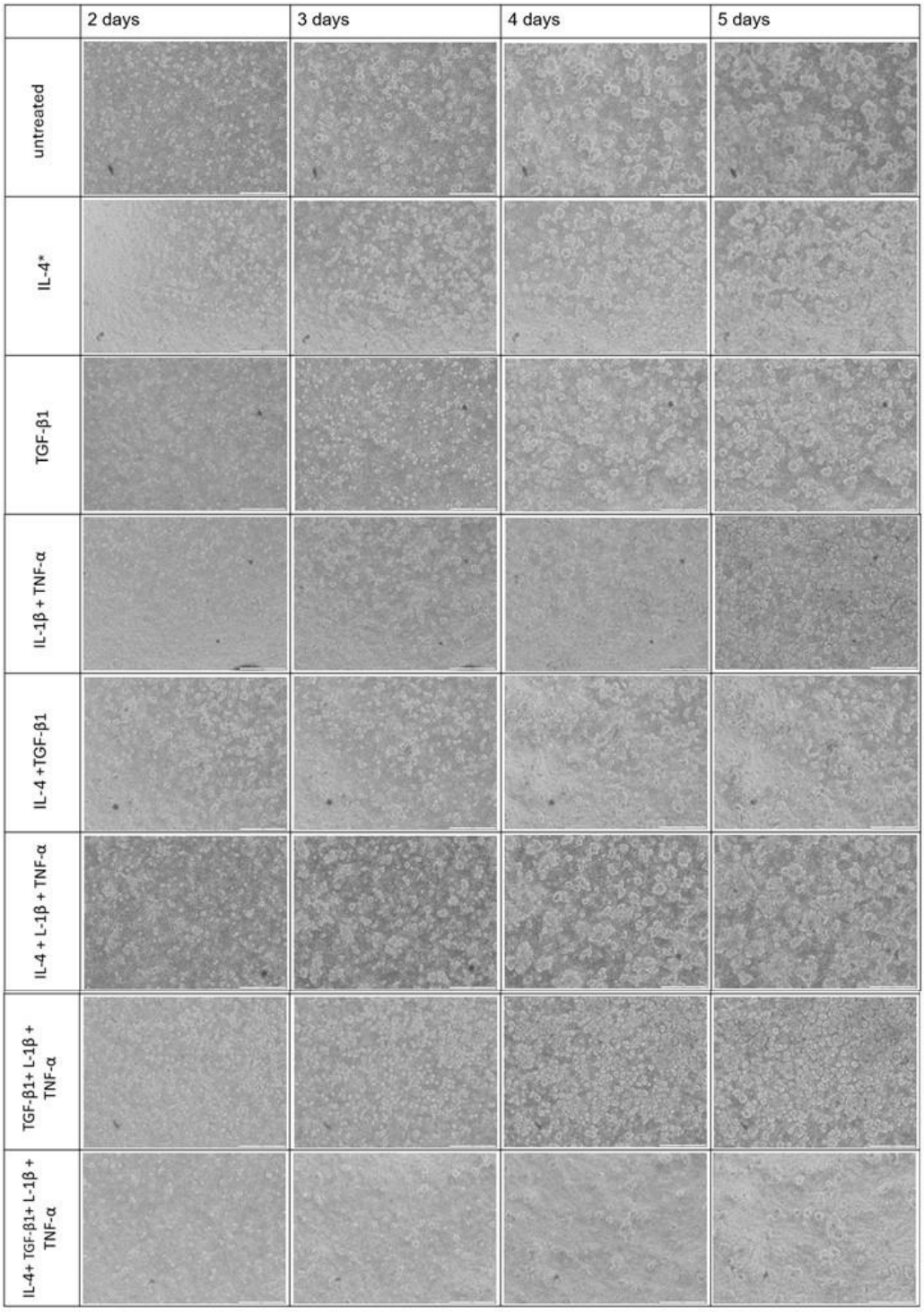

treatments (2ng/ml)
1. untreated
2. IL-4
3. TGF-β1
4. IL-1β + TNF-α
5. IL-4 + TGF-β1
6. IL-4 + IL-1β + TNF-α
7. TGF-β1 + IL-1β + TNF-α
8. IL-4 + TGF-β1+IL-1β + TNF-α
treatment of CAFs in 2D 2ng/ml
CAFs in 3D collagen I gel
Organoids in Matrigel on top of CAF collagen I gel
2 days
Transwell assay Omin
Media change and treatment of OOTA 2ng/ml (Day 2 & 4)
daily pictures of organoid size
Day 5 fixation
antibody stain for confocal microscope

B

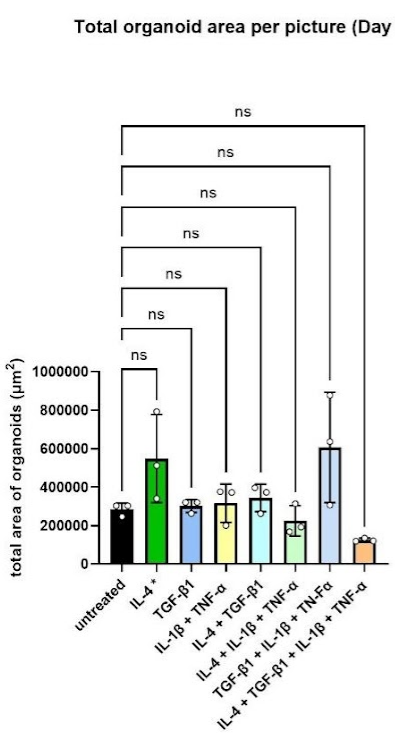

Day 5
untreated
IL-4*
TGF-β1
IL-1β + TNF-α
IL-4+TGF-β1
IL-4 +IL-1β + TNF-α
TGF-β1 + IL-1β + TNF-α
IL-4 TGF-β1 + IL-1β + TNF-α

C

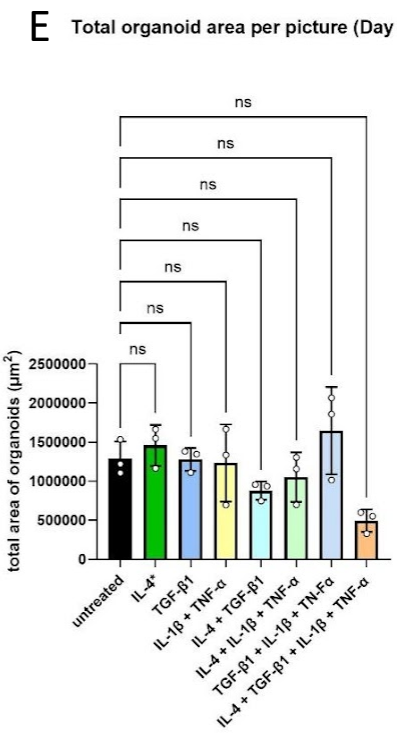
BGM2008 OOTA



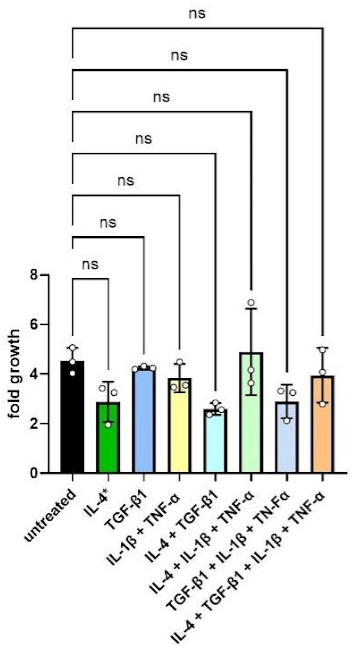
D


Total organoid area per picture (Day 2)
total area of organoids (µm²)
1000000
800000
600000
400000
200000
0
ns
untreated
IL-4*
TGF-β1
IL-1β + TNF-α
IL-4 + TGF-β1
IL-4 + IL-1β + TNF-α
TGF-β1 + IL-1β + TN-Fα
IL-4 + TGF-β1 + IL-1β + TNF-α

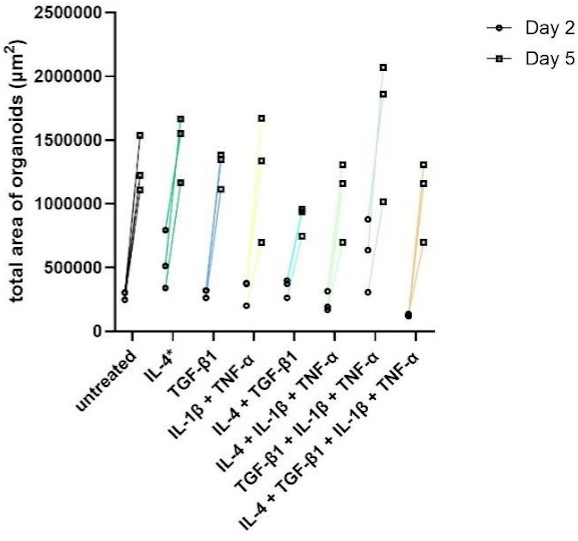
E


Total organoid area per picture (Day 5)
total area of organoids (µm²)
2500000
2000000
1500000
1000000
500000
0
ns
untreated
IL-4*
TGF-β1
IL-1β + TNF-α
IL-4 + TGF-β1
IL-4 + IL-1β + TNF-α
TGF-β1 + IL-1β + TN-Fα
IL-4 + TGF-β1 + IL-1β + TNF-α

F


Total organoid area normalised (Day 5/Day2)
fold growth
8
6
4
2
0
ns
untreated
IL-4*
TGF-β1
IL-1β + TNF-α
IL-4 + TGF-β1
IL-4 + IL-1β + TNF-α
TGF-β1 + IL-1β + TN-Fα
IL-4 + TGF-β1 + IL-1β + TNF-α

G


Growth per picture area
total area of organoids (µm²)
2500000
2000000
1500000
1000000
500000
0
Day 2
Day 5
untreated
IL-4*
TGF-β1
IL-1β + TNF-α
IL-4 + TGF-β1
IL-4 + IL-1β + TNF-α
TGF-β1 + IL-1β + TNF-α
IL-4 + TGF-β1 + IL-1β + TNF-α

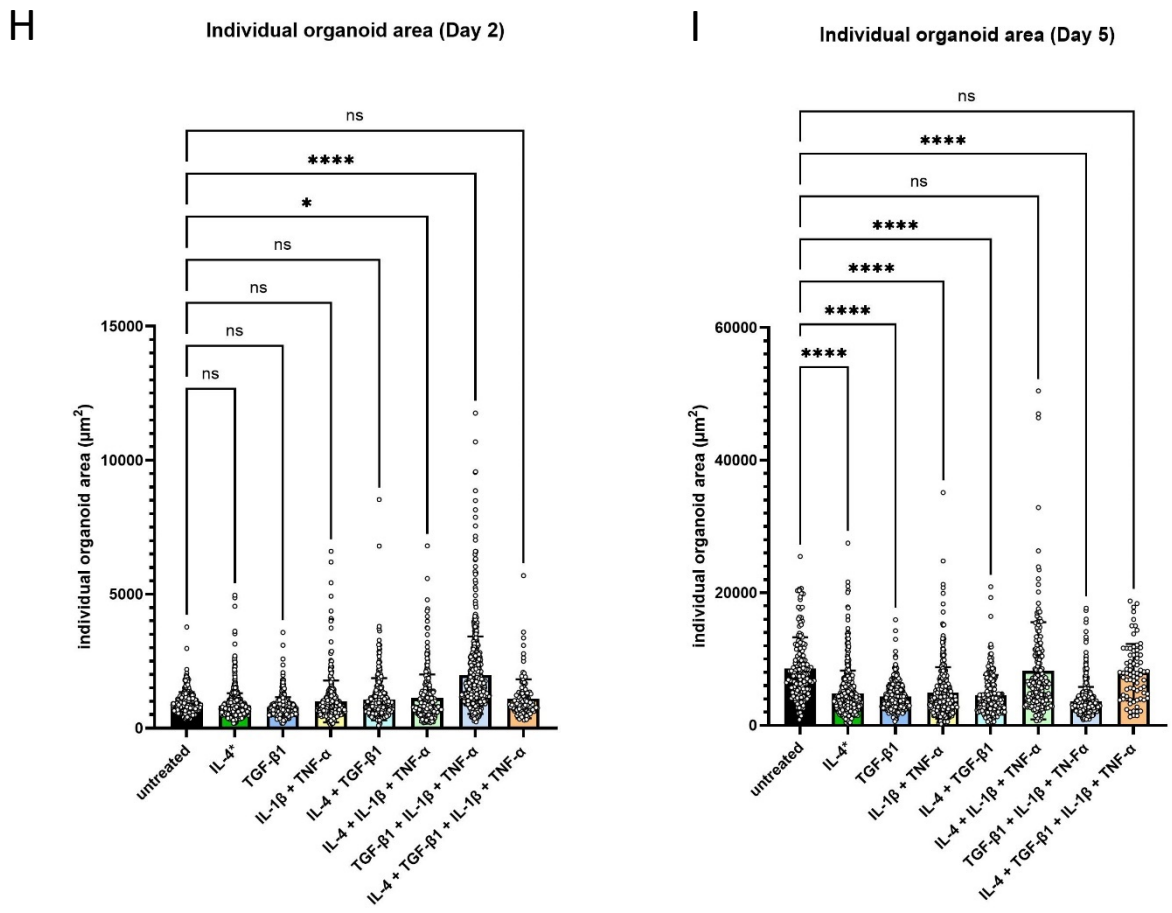


Figure 15: **CAF-BGM2008 (p12) and patient matched CRC organoid BGM2008 (p19) co-culture (OOTA) with different cytokine treatment conditions.** CAF BGM2008 (p12) were pretreated with 2 ng/ml of cytokines (as indicated) in 2D in 6cm dishes for 48 hours, then 300.000 CAF were distributed in a collagen I gel. 40.000 BGM2008 organoid cells (p19) were seeded on top in 20 µl Matrigel. Omin media was changed every 2 days and 2 ng/ml treatment was added. **(A)** Schematic representation of the assay using biorender.com **(B)** representative pictures of organoid morphology of different treatment conditions as indicated over 5 days (500 µM size bar at bottom right) **(C)** representative pictures of one frame per condition (as indicated) over 5 days **(D+E)** total organoid area measurements of growth (3 frames per condition) **(D)** day 2 **(E)** day 5 **(F)** total organoid area normalised day 5 divided by day 2 **(G)** Growth trajectories plotted per condition **(H+I)** individual organoid size measured **(H)** day 2 **(I)** day 5. Mean values, SD (error bars) per condition depicted, **** indicates a P <0.0001 using ordinary one-way ANOVA.

Next, the OOTA was stained for DAPI (white), Vimentin (green), cleaved Caspase-3 (yellow), EpCAM (turquoise) and Ki-67 (pink) (Figure 16A). Pictures were taken with the confocal microscope with the organoid side facing up. Quantitative analysis was performed for Ki-67 (Figures 16B and D) and cleaved Caspase-3 (Figures 16C and F) staining with ImageJ as described in Methods, with the percentage of positive pixels per staining depicted (Figures 16B, C, D and E). Two threshold methods were chosen for the analysis: Otsu (Figures 16B and C), an automated threshold based on an algorithm calculating pixel intensity variance, and a fixed threshold (Figures 16D and E). Cleaved caspase-3 serves as a marker of apoptosis, while Ki-67 staining is indicative of cellular proliferation. EpCAM is a cell adhesion molecule of epithelial cells.

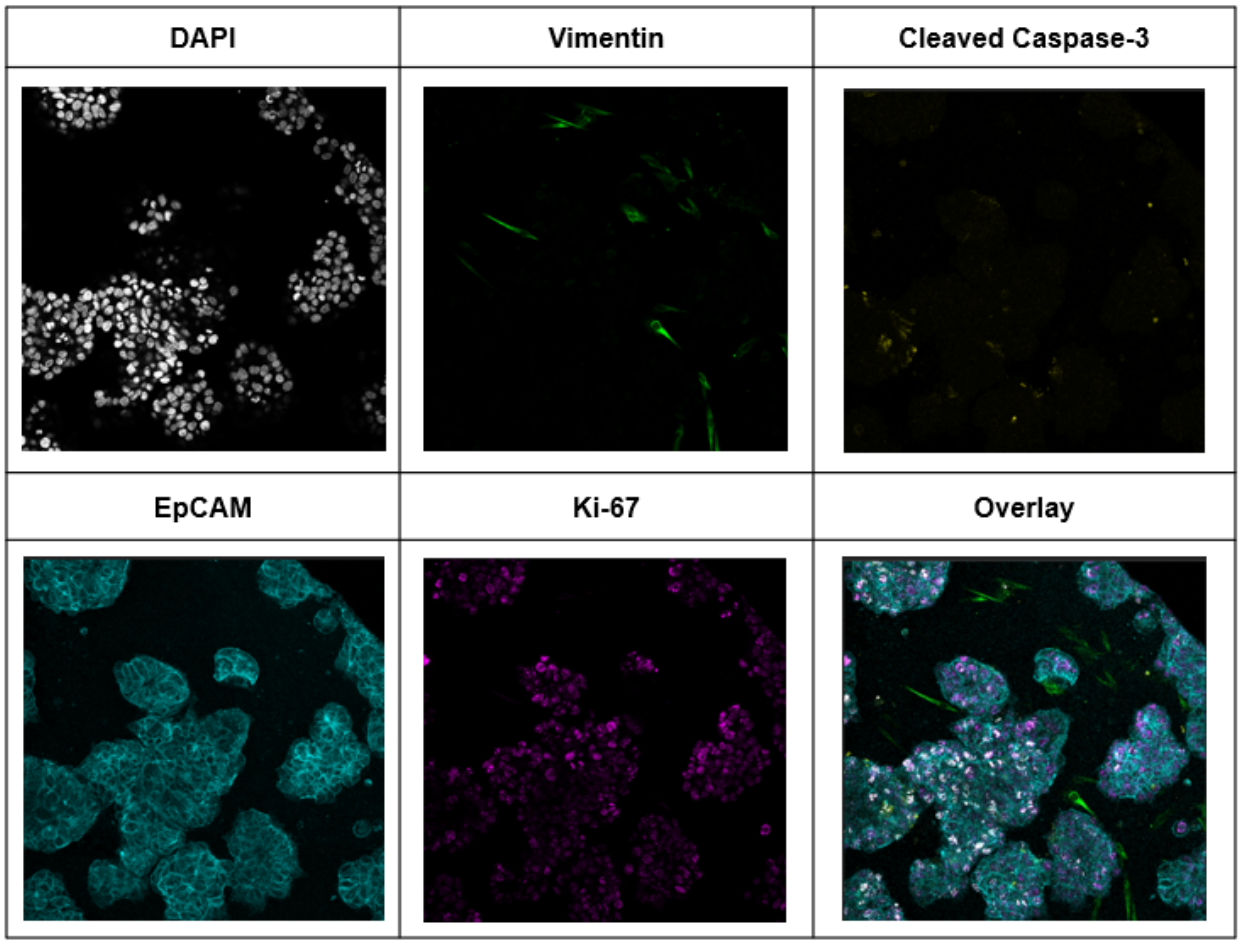
The Otsu method indicates significantly higher levels of Ki-67 for IL-1β + TNF-α than for the untreated (Figure 16B). Significantly lower proliferation was detected in the IL-4 + TGF-β1 condition. The other conditions show no significant change compared to untreated (Figure 16B).

The Otsu method shows significantly higher cleaved caspase-3 levels for IL-4-treated organoids (Figure 16C). Also, the single treatments with TGF-β1+ IL-1β + TNF-α show significantly higher apoptosis. Only TGF-β1 + IL-1β + TNF-α shows a significantly higher apoptosis level for the combination of treatments (Figure 16C).

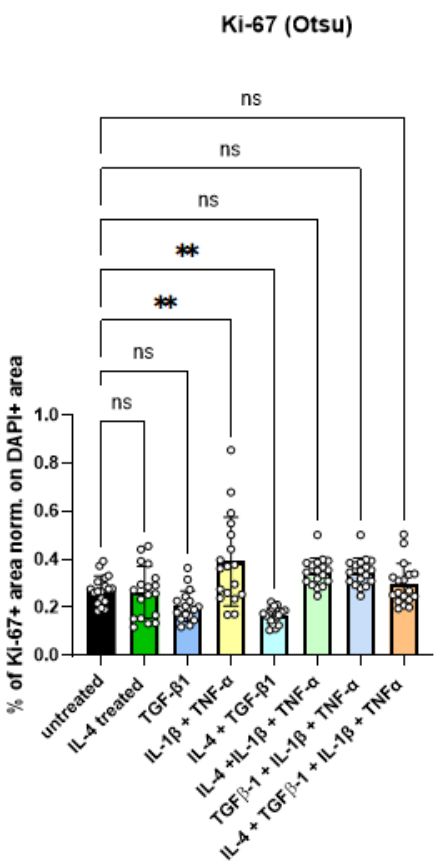
The fixed threshold method shows no significant change in Ki-67 levels in all the conditions (Figure 16D). For CC3 staining, IL-1β + TNF-α levels are significantly higher than those untreated (Figure 16E). The condition TGF-β1 + IL-1β + TNF-α shows the significantly highest level of apoptosis with the fixed threshold.

In summary, both analyses indicate higher proliferation for IL-1β + TNF-α and lower proliferation for IL-4 + TGF-β1. Additionally, increased apoptosis for IL-1β + TNF-α and TGF-β1 + IL-1β + TNF-α and a trend for TGF-β1 treatment alone.

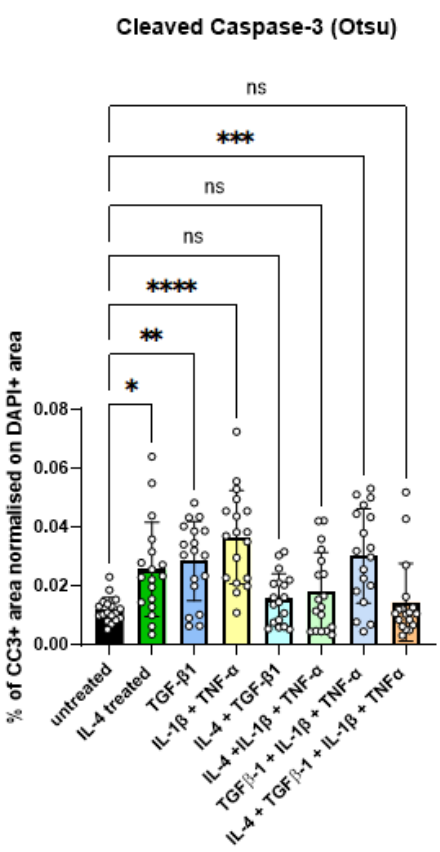
A BGM2008 OOTA



B


Ki-67 (Otsu)
% of KI-67+ area norm. on DAPI+ area
ns
ns
ns
**
**
ns
ns
1.0
0.8
0.6
0.4
0.2
0.0
untreated
IL-4 treated
TGF-β1
IL-1β + TNF-α
IL-4 + TGF-β1
IL-4 +IL-1β + TNF-α
TGFβ-1 + IL-1β + TNF-α
IL-4 + TGFβ-1 + IL-1β + TNFα

C


Cleaved Caspase-3 (Otsu)
% of CC3+ area normalised on DAPI+ area
ns
***
ns
ns
****
**
*
0.08
0.06
0.04
0.02
0.00
untreated
IL-4 treated
TGF-β1
IL-1β + TNF-α
IL-4 + TGF-β1
IL-4 +IL-1β + TNF-α
TGFβ-1 + IL-1β + TNF-α
IL-4 + TGFβ-1 + IL-1β + TNFα

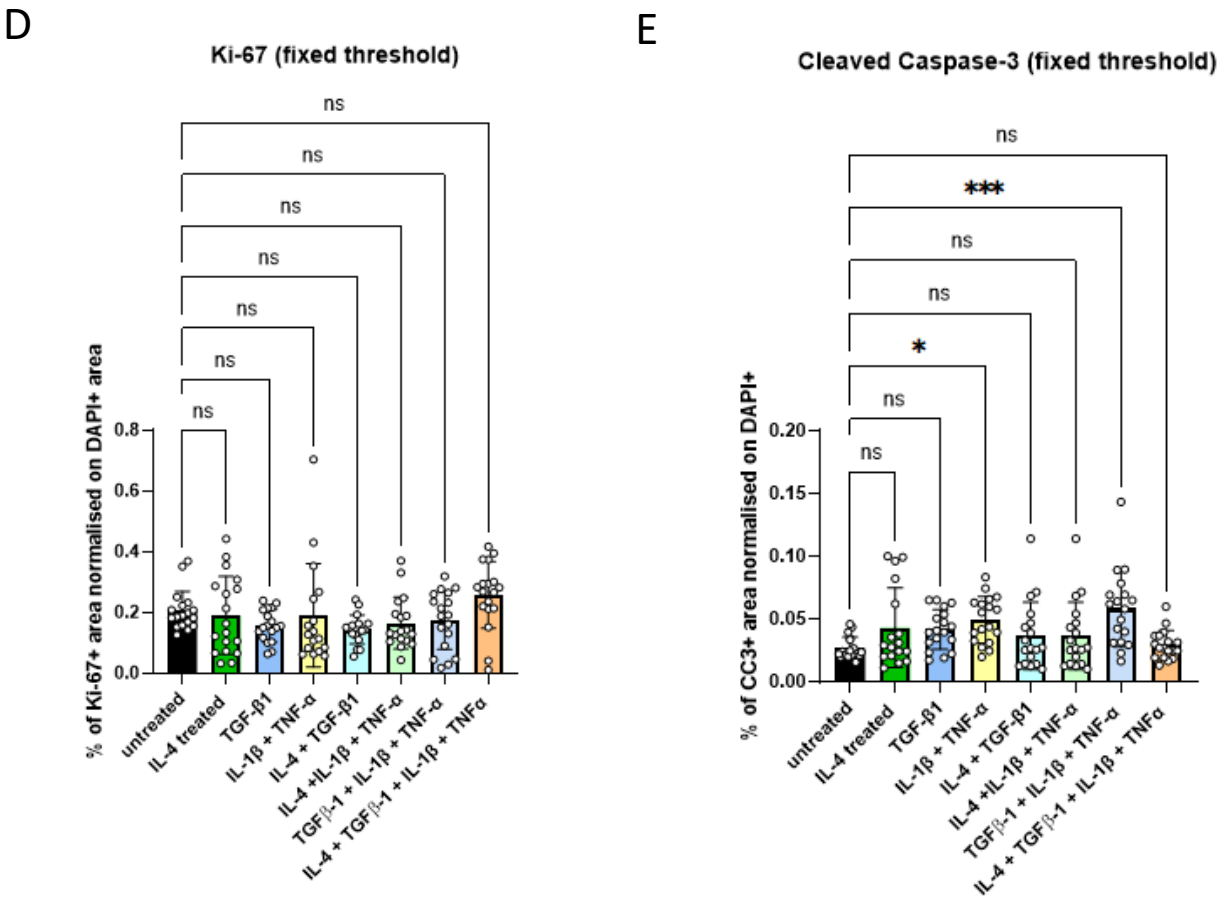


Figure 16: **Confocal images of CAF-BGM2008 (p12) and CRC organoid BGM2008 (p19) co-culture (OOTA) showing Ki-67 and Cleaved Caspase 3 (CC3) staining (A)** Representative confocal pictures showing DAPI (white), Vimentin (green), Cleaved Caspase-3 staining (CC3, yellow), EpCAM (turquoise), Ki-67 staining (pink) **(B, C, D, E)** analysis of staining depicted as percentage of positive area normalised on DAPI area of images with different treatment conditions of 2ng/ml of IL-4, TGF-β1, IL-1β and TNF-α in different combinations (as indicated) for 5 days **(B, C)** Analysis of confocal images using ImageJ using Otsu threshold **(B)** Ki-67 **(C)** CC3 **(D, E)** Analysis of confocal images using ImageJ using fixed threshold **(D)** Ki-67 **(C)** Cleaved Caspase 3 (CC3). Mean values, SD (error bars) and individual measurements (18 pictures per condition) depicted, no outliers removed, P <0.0001, Ordinary one-way ANOVA

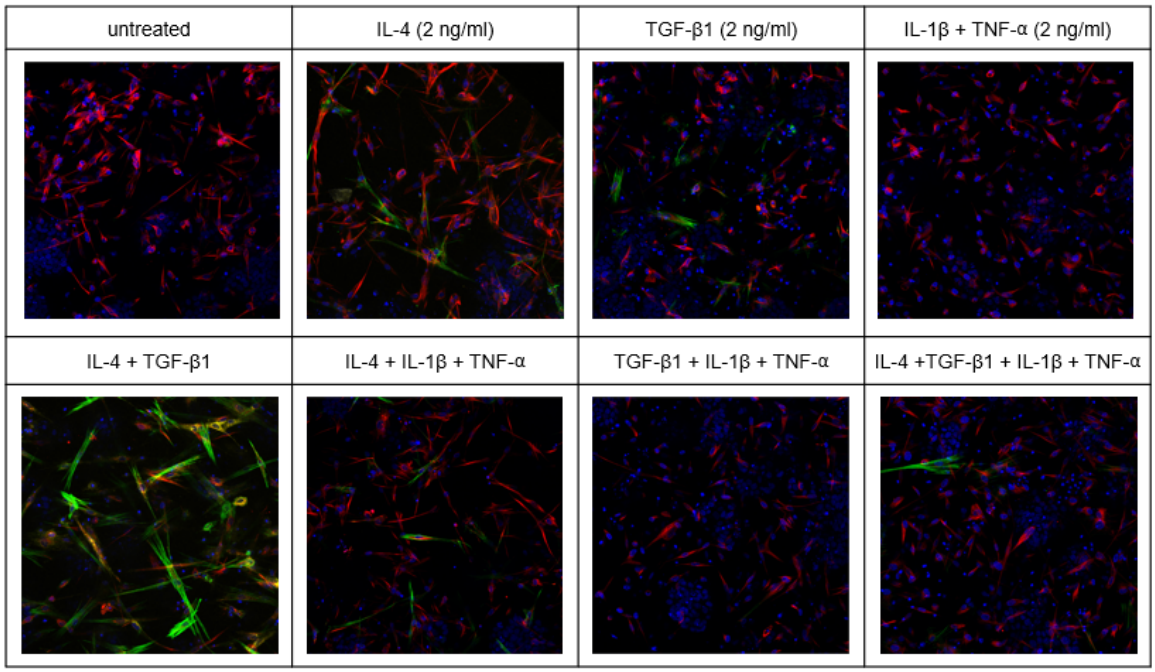
Next, the OOTA was stained for α-SMA (green), FAP (yellow) and Vimentin (red) and DAPI (blue). Pictures were taken with the confocal microscope with the CAF in collagen gel facing up. Quantitative analysis was performed as described in Methods, with the difference that the signal was normalised on vimentin this time, as the DAPI channel also showed nuclear staining of organoid cells, not just CAFs.

Assessment of α-SMA expression in BGM2008 CAFs revealed no detectable signal in untreated cells (Figure 17A and D). Treatment with IL-4 induced a slight increase in α-SMA expression, although this change was not statistically significant. Notably, contrary to expectations, TGF-β1 alone did not result in a substantial increase in α-SMA-positive cells (Figure 17A and D). Consistent with previous findings, IL-1β and TNF-α treatments did not induce α-SMA expression. In contrast, the combination of IL-4 and TGF-β1 led to a marked upregulation of α-SMA, yielding the highest signal among all conditions tested (Figure 17A and D). The signal of the combination IL-4 + TGF-β1 is about 8 times that of TGF-β1 alone. Other cytokine combinations, including IL-4 + IL-1β + TNF-α and TGF-β1 + IL-1β + TNF-α, did not promote α-SMA expression. Interestingly, simultaneous treatment with all four cytokines failed to induce α-SMA upregulation (Figure 17A and D).

Analysis of FAP expression in BGM2008 CAFs showed no upregulation in untreated cells or following IL-4 treatment (Figure 17B and E). TGF-β1 alone slightly increased FAP-positive cells, although this change did not reach statistical significance. Similarly, treatment with inflammatory cytokines IL-1β and TNF-α did not result in FAP upregulation. In contrast, combined treatment with IL-4 and TGF-β1 led to a highly significant increase in FAP expression (Figure 17B and E). Modest but comparable levels of FAP induction were observed with IL-4 + IL-1β + TNF-α and TGF-β1 + IL-1β + TNF-α combinations. The highest level of FAP upregulation was detected when all four cytokines were administered together, indicating a synergistic effect of the full cytokine combination on FAP expression (Figure 17B and E).

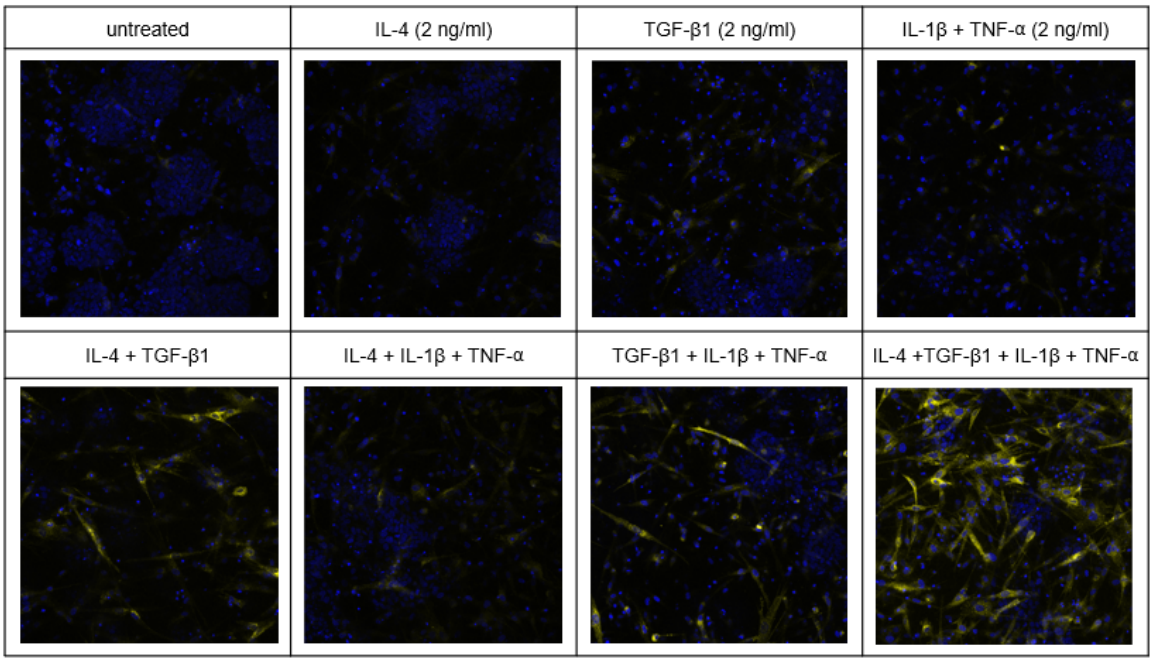
A

α-SMA


untreated
IL-4 (2 ng/ml)
TGF-β1 (2 ng/ml)
IL-1β + TNF-α (2 ng/ml)
IL-4 + TGF-β1
IL-4 + IL-1β + TNF-α
TGF-β1 + IL-1β + TNF-α
IL-4 +TGF-β1 + IL-1β + TNF-α

B

FAP


untreated
IL-4 (2 ng/ml)
TGF-β1 (2 ng/ml)
IL-1β + TNF-α (2 ng/ml)
IL-4 + TGF-β1
IL-4 + IL-1β + TNF-α
TGF-β1 + IL-1β + TNF-α
IL-4 +TGF-β1 + IL-1β + TNF-α

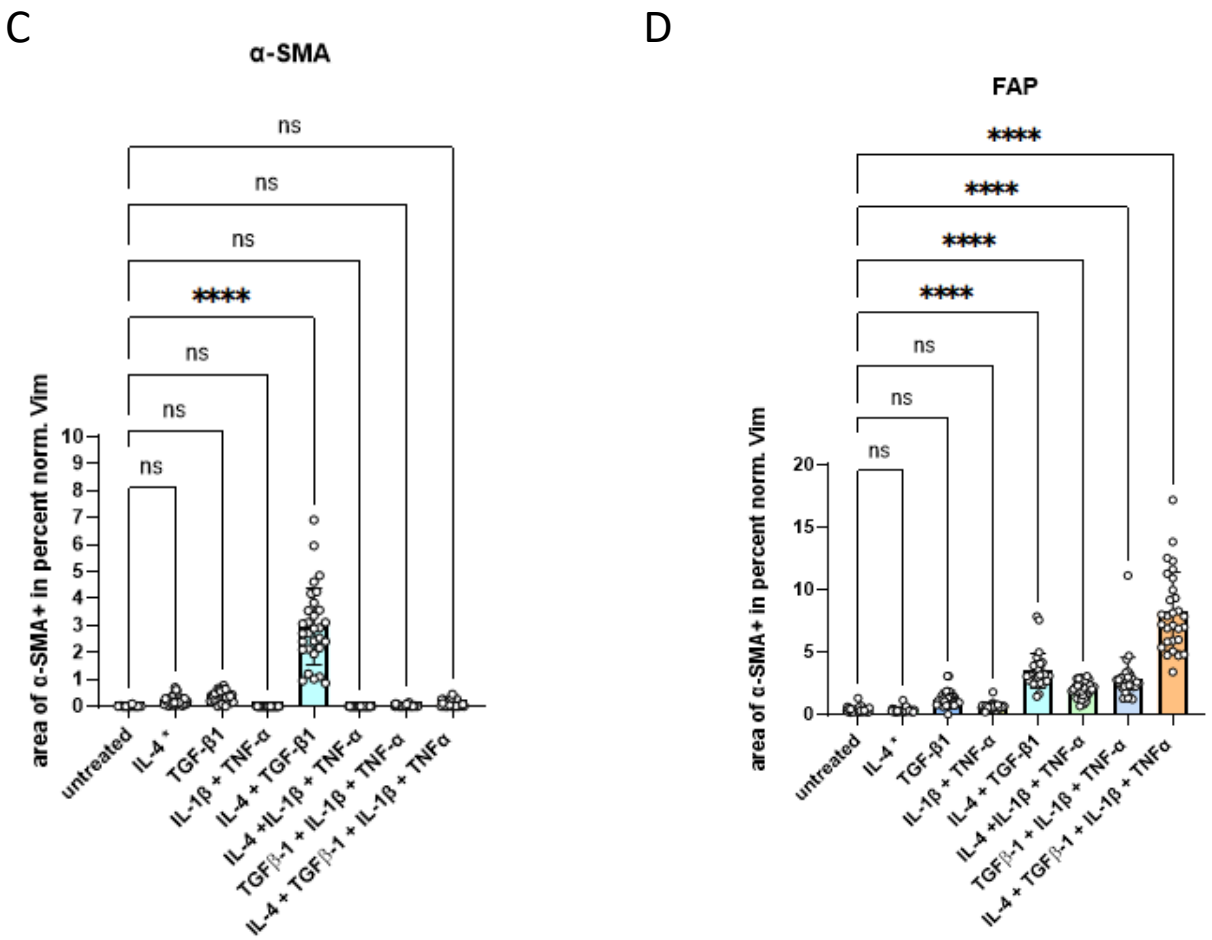


Figure 17: **Confocal images of CAF-BGM2008 (p12) and CRC organoid BGM2008 (p19) co-culture (OOTA) showing CAF upregulation of α-SMA and FAP** with treatment of 2ng/ml of IL-4, TGF-β1, IL-1β and TNF-α in different combinations (as indicated) for 5 days. **(A, B)** Representative pictures were chosen to match the mean α-SMA or FAP positive pixels per condition. Nuclei stained by DAPI (blue), Vimentin (red), α-SMA (green), and FAP (yellow). **(C)** Analysis of confocal images using ImageJ showing upregulation of **(C)** α-SMA **(D)** FAP with treatment in different combinations (as indicated) for 48 hours. The graphs depict an analysis of α-SMA/FAP positive pixels per area normalised on vimentin positive nuclei area using ImageJ. Mean values, SD (error bars) and individual measurements (pictures) (n=30 per condition) depicted, no outliers removed, P <0.0001, Ordinary one-way ANOVA

4.Discussion

Chronic inflammation plays a crucial role in the development and progression of colorectal cancer (CRC), consisting of a constant cycle of injury and repair (Percario et al., 2021; Zhao et al., 2021). In general, the inflammatory response can be categorised into Type 1 and Type 2, each with distinct members of cytokines. Type 1 cytokines primarily control intracellular pathogens through pro-inflammatory mechanisms, with IFN-γ being a key effector. In contrast, Type 2 cytokines, such as IL-4 and IL-13, play a crucial role in resolving the inflammation of the Type 1 response. Secondly, by remodelling the ECM, Type 2 mediates tissue repair following damage from Type 1 processes. Hence, Type 2 cytokines are essential factors that influence wound healing, activating pathways associated with fibrosis and the development of the tumour microenvironment. IL-4 and IL-13 are produced by immune cells, including eosinophils, Th2 cells, mast cells, and innate lymphoid cells. Additionally, cytokines such as TGF-β are part of the Type 2 response (Allen, 2024; Nguyen et al., 2020). Early in cancer development, both anti-tumour and pro-tumour immune and inflammatory responses are initially present; however, if the tumour is not eliminated, the pro-tumourigenic mechanisms ultimately prevail (Grivennikov et al., 2010).

The tumour microenvironment (TME) and the diverse functional states of cancer-associated fibroblasts (CAFs) play a pivotal role in modulating cancer progression, therapy response, and tissue remodelling (Tommelein et al., 2015; L. Deng et al., 2021; Hanahan, 2022;Glabman et al., 2022; Linares et al., 2021). CAFs play a crucial role in creating an immunosuppressive TME by secreting cytokines and chemokines that recruit and modulate immune cells (Monteran & Erez, 2019). CAF secrete a plethora of factors, and the TME consists of numerous cells contributing to this cytokine environment (Linares et al., 2021). CAFs are often described as a heterogeneous cell population, and their plasticity in response to external signals such as cytokines remains incompletely understood (Louault et al., 2020).

Recent research has identified IL-1 and TGF-β as key cytokines present in tumours that drive the heterogeneity of CAFs. TGF-β signalling suppresses IL-1 receptor 1 (IL-1R1) expression, inhibits IL-1 responses, and promotes the differentiation of fibroblasts into myofibroblast CAFs. In contrast, IL-1 signalling activates the JAK/STAT pathway, leading to the development of inflammatory CAFs (Yoshida, 2020). This dynamic has led to the concept of a "stromal switch," where “tumour-promoting” CAFs could potentially be reprogrammed into “tumour-suppressing” CAFs (D. Yang et al., 2023).

This thesis investigated how cytokine-mediated activation of CAFs alters their phenotypic marker expression and secretory profiles, and how these changes influence the growth and behaviour of patient-derived CRC organoids. The aim was to understand how specific cytokines, IL-4, IL-13, IFN-γ, TGF-β1, IL-1β, and TNF-α, either individually or in combination, modulate the phenotypic status of CAFs, exemplified by the expression of common CAF

markers (e.g. α-SMA, FAP, PD-L2, PDPN, and IL-1R1), and their tumour-supportive functions.
The first part focused on the marker expression of CRC CAFs and how CAF markers are regulated by cytokine treatment. Two CAF patient primary cultures, CAF 6388/19 and CAF BGM2008, were examined using two methods: In-Cell Western (ICW) and confocal microscopy, both of which applied immunofluorescence staining for CAF markers.
In the second part, the thesis further assessed whether these cytokine-induced alterations in CAFs enhance their ability to promote cancer organoid growth/viability using conditioned media from cytokine pre-treated CAFs. For this purpose, the CellTiter-Glo 3D assay, an ATP-based luminescence readout, was employed, serving as a measure of organoid viability.
Third, the work explored the impact of cytokine treatment on direct CAF–organoid interactions in a 3D patient-derived organoid co-culture (OOTA) model. Organoids were assessed regarding their size and morphology upon treatment with cytokines. Furthermore, confocal immunofluorescence was employed to detect apoptosis (cleaved Caspase-3) and proliferation levels (Ki-67) in organoids. Moreover, CAF markers, α-SMA and FAP, were quantified in CAFs.
Overall, these findings address the broader research question of how cytokine-driven stromal reprogramming shapes tumour-stroma dynamics, with implications for understanding CAF plasticity, tumour progression, and therapy resistance in colorectal cancer. A summary of all findings derived from one patient (BGM2008) is given in Table 8.

Table 8: Summary of combined 2D and 3D assessment of CAF phenotypes and organoid growth/viability (BGM 2008)

BGM2008-CAF

Treatments (2 ng/ml)	Marker expression (2D)					CM-organoid viability (CTG)	OOTA (3D co-culture)			
	α-SMA	FAP	IL-1R1	PDPLN	PD-L2		Ki-67*	CC3*	α-SMA	FAP
untreated	↑	-	↑↑↑↑↑	↑↑↑	-	↑	↑	↑	-	-
IL-4	↑↑	-	↑↑↑	↑↑↑↑	-	↑	↑	↑↑	↑	-
TGF-β1	↑↑↑	↑↑	↑↑	↑↑↑↑	↑↑↑↑	↑	-	↑↑	↑	↑
IL-1β + TNF-α	↑	↑	↑↑	↑↑↑↑↑	↑	↑↑↑	↑↑	↑↑↑	-	-
IL-4 +TGF-β1	↑↑↑	↑↑↑	↑↑	↑↑↑↑	↑↑↑↑↑	↑↑	↑	↑	↑↑↑↑↑	↑↑↑
IL-4 + IL-1β + TNF-α	↑	↑↑	↑↑	↑↑↑↑	↑↑	↑	↑	↑	-	↑↑
TGF-β1 + IL-1β + TNF-α	↑↑	↑	↑↑	↑↑↑↑	↑↑	↑↑↑	↑	↑↑	-	↑↑
IL-4 + TGF-β1 + IL-1β + TNF-α	↑↑↑↑↑	↑↑↑↑↑	↑↑	↑↑↑↑	↑↑↑	↑↑↑↑↑	↑	↑	-	↑↑↑↑↑

*Otsu threshold

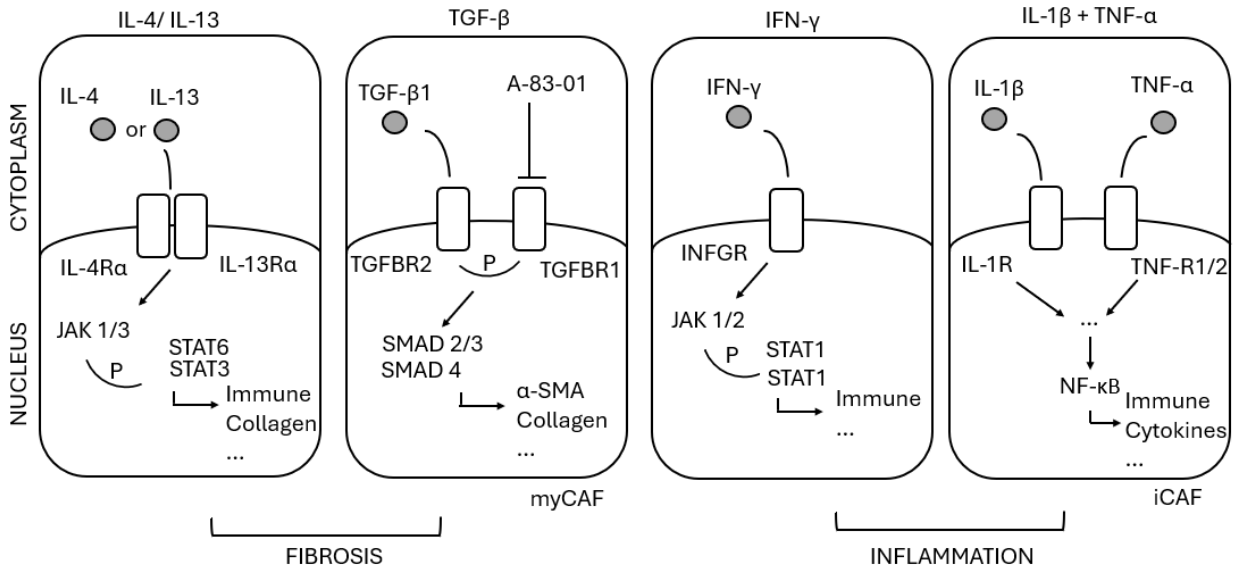


Figure 18: **Simplified overview of cytokine signalling (IL-4 and IL-13, TGF-β, IFN-γ and IL-1β + TNF-α) and its impact on CAF phenotypes.** TGF-β is associated with α-SMA expression and a myCAF phenotype, whereas treatment with IL-1β + TNF-α leads to an iCAF phenotype (by Elisa Ebner)

4.1 Cytokine regulation of colonic CAF marker expression

4.1.1 IL-4, IL-13, TGF-β1, IFN-γ, IL-1β and TNF-α differentially influence α-SMA expression

Untreated CAFs show clustered regions of cells with α-SMA expression

Untreated CAFs exhibit spatial heterogeneity in α-SMA expression, with clustered regions of α-SMA-positive cells visible as localised fluorescence spots in the ICW images (see Figures 8, 9 and 11). This was consistent across both patient-derived CAF models and confirmed by confocal microscopy (see Figures 10 and 12), which showed α-SMA in stress fibres in only a subset of cells, reflecting intra-population variability and a well-established hallmark of CAF biology (Louault et al., 2020; Chhabra & Weeraratna, 2023).

At both 24 and 72 hours, CAF 6388/19 showed stable basal α-SMA levels. Still, a twofold increase was observed at passage 14 compared to passage 11 (see Figures 8 and 9), suggesting that either passaging, stochastic fluctuations, or handling variations may elevate myofibroblastic activation. Comparable α-SMA levels in CAF 6388/19 (p11) and BGM2008 (p10) imply that passage number or handling may influence expression (see Figures 8 and 11). Mechanical stress from passaging might mimic injury, triggering α-SMA via wound-healing-like responses. Indeed, senescent fibroblasts can adopt myofibroblast features through TGF-β signalling (Mellone et al., 2016), and both senescence and stress-induced activation are linked to α-SMA upregulation (Mellone et al., 2016; Belle et al., 2024). These changes may parallel stromal ageing, where fibroblasts acquire contractile, ECM-rich phenotypes (H. Li et al., 2022).

In vitro passaging may thus skew CAF populations toward more activated states by selecting subpopulations with high α-SMA, particularly in the absence of in vivo niche signals. To preserve physiological relevance, early-passage, patient-matched CAFs are recommended. Finally, variation in α-SMA induction across CAF lines may reflect patient-specific traits, including prior exposure to TGF-β or epigenetic imprinting (Kehrberg et al., 2023).

TGF-β1 is a potent regulator of α-SMA expression

TGF-β1 binds to the type II TGF-β receptor (TGFBR2), leading to the phosphorylation and activation of the type I TGF-β receptor (TGFBR1/ALK-5). Activated TGFBR1 phosphorylates receptor-regulated SMADs (R-SMADs), including SMAD2 and SMAD3, which form complexes with SMAD4 and further regulate gene transcription. The small molecule A-83-01 inhibits TGFBR1/ALK-5 activation (together with type I nodal receptors ALK4 and ALK 7) (Tojo et al., 2005). Additionally, several non-canonical signalling pathways are activated by TGF-β1, including the PI3K/Akt, Rho/Rock, Ras/Raf, and TRAF/NF-κB/JNK pathways (Jung et al., 2017). TGF-β signalling is a key regulator of fibroblast activation in CRC and is marked

by increased expression of α-SMA, which drives CAFs toward a contractile and metastasis-promoting phenotype (Hawinkels et al., 2014; Calon et al., 2015; B. Deng et al., 2022). Thus, TGF-β is of good use as a control for studying CAF myofibroblast activation and α-SMA induction.

As expected, TGF-β1 robustly upregulated α-SMA expression in both patient-CAFs, in all assays and at different time points, confirming its dominant role in promoting the myofibroblastic CAF phenotype. Using ICW, TGF-β1 induced α-SMA expression with maximal effects observed at 72 hours, resulting in a 4- to 5-fold increase at low concentration (2 ng/ml) (CAF6388/19, p11; see Figure 8). CAF 6388/19 at a later passage number (p14) do not respond as much, with only a two-fold increase (see Figure 9), which might be due to the general higher levels of SMA expression at the start of treatment due to passaging effects. This requires further clarification. Intriguingly, α-SMA increase in BGM 2008 CAFs (p10, 24 hours) is comparable to CAF 6388/19 (p11) (see Figures 8 and 11). Confocal microscopy confirmed the incorporation of α-SMA into stress fibres, indicative of functional myofibroblast differentiation (see Figure 10). The TGF-β receptor I (TGFBRI) inhibitor A-83-01 entirely abolished this TGF-β1-mediated induction seen in ICW and confocal microscopy (see Figures 9 and 10). A-83-01 is commonly included in organoid culture media. This may suppress CAF activation by targeting TGF-β signalling, which should be carefully considered in co-culture systems. Organoid culture often relies on media with numerous exogenous growth factors, and small-molecule inhibitors may not fully recapitulate in vivo conditions, thus limiting physiological relevance (Wensink et al., 2021). In our OOTA setup, we completely avoid the addition of exogenous factors or inhibitors except for 1% FCS. We have previously shown that PDTO growth-supporting factors are entirely provided by the fibroblasts (Atanasova et al., 2023).

Although TGF-β is an extensively studied cytokine in cancer, much remains unknown about the connection between TGF-β and CAFs. The TGF-β pathway plays a central role in CRC development, and the TGF-β superfamily comprises many members, including bone morphogenetic proteins (BMPs), activins, and Nodal (Jung et al., 2017). Nodal has also been implicated in CAF activation via the TGF-β/SMAD/SNAIL pathway, correlating with increased α-SMA expression (Z. Li, Zhang, et al., 2019). Hence, it would be interesting to test the impact of Nodal and SNAIL on α-SMA expression using the methods established in this thesis.

Moreover, direct contact between CRC cells and bone marrow mesenchymal stromal cells (BMSCs) can transform BMSCs into CAFs through Notch-Jagged1 interaction, which activates the downstream TGF-β/SMAD signalling cascade (Y. Peng et al., 2014). These BMSCs-CAF could be compared to the patient-isolated CAFs. The origins of CAF are yet to be elucidated, and different cellular sources could add to the heterogeneity of this cell type (Kobayashi et al., 2022). Furthermore, activin A, another member of the TGF-β superfamily, promotes immunosuppression and progression in CRC (Wiley et al., 2025). Additionally, Kobayashi et al. found that BMP signalling balance in CAF predicts CRC progression.

GREM1 and ISLR (also known as Meflin) function as inhibitors and promoters of BMP signalling, respectively. In CRC patients, elevated GREM1 expression is linked to poorer survival, whereas high ISLR expression correlates with improved survival (Kobayashi et al., 2021).

IL-4 and IL-13 upregulate α-SMA independently of TGF-β-receptor

Interleukin-4 (IL-4) and Interleukin-13 (IL-13) signal through a common receptor complex composed of IL-4 receptor alpha (IL-4Rα) and IL-13 receptor alpha 1 (IL-13Rα1). These cytokines activate the Janus kinase (JAK) family members, JAK1 and JAK3, leading to the phosphorylation and activation of signal transducer and activator of transcription 6 (STAT6). Activated STAT6 translocates to the nucleus and regulates the transcription of genes involved in immune responses and fibrosis, such as type I collagen (Allen, 2024; Owen et al., 2019; J. K. Nguyen et al., 2020). Additional non-canonical downstream signalling of IL-4/IL-13 involves PI3K/Akt and ERK 1/2 (J. Shi et al., 2021). IL-4 is a multifunctional cytokine that plays a pivotal role in modulating immune responses, promoting cell growth, enhancing resistance to apoptosis, activating gene expression, and driving cellular differentiation in a diverse population of cells, including lymphocytes, macrophages, fibroblasts, and epithelial as well as endothelial cells (Luzina et al., 2012). IL-4 is involved in the promotion of asthma, allergic inflammation, and multiple types of cancer (Gour & Wills-Karp, 2015). Interleukin-13 acts through two receptor subtypes: IL-13Rα1 and IL-13Rα2. When paired with IL-4Rα via IL-13Rα1, or more prominently through IL-13Rα2, signalling via STAT6, focal adhesion kinase (FAK), and PI3K/Akt/mTOR is activated in CRC cells. High expression of IL-4Rα and IL-13Rα2 in CRC correlates with advanced disease and poorer prognosis (Bartolomé et al., 2015; H. Cao et al., 2016; H. Liu et al., 2017; Matsui et al., 2019). IL-4 and IL-13 are crucial regulators of fibroblast activation and fibrosis across various tissues, with STAT6 signalling primarily fulfilling these fibrosis-related functions (O'Reilly et al., 2016). IL-4 and IL-13 signalling have been extensively studied in fibrotic diseases, where they drive fibroblast-to-myofibroblast transition and ECM deposition (Aoudjehane et al., 2008; Arndt et al., 2023). However, their direct effects on CAFs have remained largely unexplored. The present findings thus provide novel insights into their profibrotic roles within the TME, especially in desmoplastic tumours such as CRC.

The ICW data show that IL-4 significantly increases α-SMA levels, reaching maximal induction observed at low concentrations (2 ng/ml) (see Figure 8). IL-13 induced α-SMA to a comparable level as IL-4 in the ICW (see Figure 9). Although IL-4 and IL-13 induced α-SMA upregulation, their potency was less than that seen using TGF-β1 (see Figure 9). Notably, these effects were not blocked by A-83-01, demonstrating that IL-4 and IL-13 act through TGF-β-receptor-I-independent pathways in our CAFs (see Figure 9). The combination of IL-4 and IL-13 did not produce additive or synergistic effects in the ICW, suggesting that their signalling pathways overlap (see Figure 9). Both IL-4 and IL-13 induced visible α-SMA stress fibres in confocal microscopy and showed a trend toward increased α-

SMA expression, particularly in cell counts; however, this was not statistically significant for the positive pixel method (see Figure 10) (for further details, see Methodological Considerations: ICW vs. Confocal Microscopy). The upregulation of α-SMA in both patient-derived CAF lines (CAF 6388/19 and CAF BGM2008) in response to IL-4 suggests that this response is not patient-specific but rather reflects a conserved feature of CAFs (see Figures 8,9,10,11,12). While IL-4 and IL-13 induced clear α-SMA-positive stress fibres in confocal microscopy, the quantitative increase in α-SMA signal was more pronounced in the ICW assay. This discrepancy may reflect a scenario in which IL-4/IL-13 increase total α-SMA protein levels without proportionately enhancing their incorporation into contractile fibres, a hallmark of fully activated myofibroblasts (for further details, see Methodological Considerations: ICW vs. Confocal Microscopy).

CRC tissue exhibits a distinct cytokine milieu (Braumüller et al., 2023; Maryam et al., 2023). Tosolini et al. reported that CRC tumour samples express IL-17A, IL-4, IL-5, IL-13, and the IL-12 receptor β2 (IL12Rb2) (Tosolini et al., 2011). Kim et al. reported that tumour samples contain IL-4, IL-6, IL-8, IL-10, IL-12, TNF-α, GMC-SF, IFN-γ, and VEGF (Kim et al., 2014). Both studies report spatial heterogeneity regarding cytokine expression and identify distinct profiles corresponding to T-cell subsets. For example, Th17-associated IL-17A indicates a poor prognosis, while Th2 cytokines (IL-4, IL-5, IL-13) do not predict outcome, and Th1-related IL-12Rb2 correlates with more favourable disease-free intervals (Tosolini et al., 2011; Kim et al., 2014). The cellular sources of IL-4 in the TME are diverse and include Th2 cells, regulatory T cells (Tregs), M2-polarised tumour-associated macrophages (TAMs), mast cells, eosinophils, and innate lymphoid cells (ILC2s) (Gámez-Belmonte et al., 2020).

Previous studies on lung cancer have shown that irradiated CAFs can secrete immunosuppressive molecules, including IL-4, reinforcing the idea that CAFs can both respond to and propagate type 2 cytokine signalling (Gorchs et al., 2015). Additionally, it is known that the CAF secretome is influenced by specific mutations in the tumour cells, as it was shown that KRAS mutant pancreatic ductal adenocarcinoma (PDAC) cancer cells activate CAFs, which is mediated by CXCR-2. This resulted in NF-κB-mediated secretion of IL-4, IL-10, and IL-13, while IL-6 was downregulated. Treatment with CXCL-1 increased IL-4, IL-13 and CXCL7, while downregulating α-SMA(Awaji et al., 2020; Linares et al., 2021). This is a curious result, as activation of NF-κB is believed to generate the iCAF phenotype (Biffi et al., 2019).

Thus, CAF responses to IL-4/IL-13 may be especially relevant in Th2-skewed or immune-suppressed TMEs, where these cytokines are abundant. While type 1 inflammatory cytokines are widely studied, there is a notable lack of research on type 2 cytokines.

The ability of IL-4 to upregulate α-SMA, even in the absence of TGF-β1 signalling, raises the question of whether IL-4 induces a distinct myCAF phenotype that may be functionally relevant in shaping the TME. This aligns with the emerging model of CAF heterogeneity, in which myCAFs and iCAFs represent the extremes of a plastic spectrum. A possible theory is that IL-4, as a known immune modulator, inhibits the inflammatory induction of CAFs,

thereby pushing them towards a myofibroblast fate. It is plausible that IL-4 suppresses iCAF-associated pathways (e.g., IL-1R1) while enhancing matrix-related gene expression, leading to a non-inflammatory, matrix-remodelling CAF state. However, IL-4's ability to increase α-SMA is evidence that it does not rely solely on iCAF inhibition, but also actively promotes a myofibroblast phenotype. This hypothesis aligns with observations in other fibrotic contexts but requires validation, especially in the context of the TME. Thus, additional experiments are needed to determine how exactly IL-4 and IL-13 cause α-SMA upregulation. Additionally, it should be investigated if or how the TGF-β1-induced myCAF phenotype differs from the IL-4 phenotype.

Although IL-4 and IL-13 had measurable effects on α-SMA, IL-13 was not further investigated due to its slightly weaker activity. However, it is essential to note that IL-13 can function independently of IL-4 in certain cancers, including CRC, where it contributes to epithelial proliferation, metastasis, and immune evasion (H. Cao et al., 2016). Thus, the non-redundant roles of IL-13 in CAF biology warrant further investigation, especially in tumours expressing IL-13Rα2. Further functional assays, such as collagen gel contraction, would be required to confirm whether the α-SMA induced by IL-4/IL-13 contributes to the generation of mechanical matrix force. Traction/atomic force microscopy can be used to measure the mechanical activity of the ECM (Otero et al., 2020). The effects of IL-4 and IL-13 on α-SMA could also intersect with other signalling pathways, such as the Rho/ROCK pathway. A study by Murray et al. demonstrated that the IL-6–JAK1–ROCK signalling pathway regulates actomyosin contractility in the tumour stroma, a mechanism potentially shared by IL-4 and IL-13. (Sanz-Moreno et al., 2011b). Elucidating these downstream events could reveal new therapeutic targets to selectively block profibrotic CAF activity. Moreover, the effects of IL-4 and IL-13 on ECM composition should be further explored.

The reliance on A-83-01 to assess TGF-β independence is informative but does not rule out non-canonical TGF-β signalling or convergence downstream, such as SMAD-independent pathways. Whether IL-4 and TGF-β-mediated α-SMA upregulation happens through distinct or shared signalling mechanisms needs to be determined. Synergy is seen in the confocal data of CAF 638819 when comparing α-SMA positive pixels, but not when looking at positive cell count (see Figure 10). CAF BGM2008 do not show any additive effect regarding α-SMA in the confocal (see Figure 12). The individual datapoints from the confocal analysis show high variability; thus, drawing a solid conclusion about synergy from just the means could be misleading. The crosstalk of TGF-β and JAK/STAT is vast, and interactions play critical roles in regulating transcriptional programs involved in pluripotency, differentiation, immune responses and tumour progression. SMADs and STATs are frequently co-assembled within the same transcriptional complexes (X. Hu et al., 2021). The TGF-β signalling pathway has been shown to modulate the JAK/STAT pathway in both stimulatory and inhibitory ways, depending on the specific cell type and the activation state of key signalling proteins (K. Luo, 2017). The TGF-β/STAT3 crosstalk has been explored in more detail (Tang et al., 2017; Hu et al., 2021). However, the TGF-β/STAT6 crosstalk needs further elucidation, especially

regarding CAFs. Both IL-4 and TGF-β share the commonality of upregulating the PI3K/AKT/mTOR signalling pathway; thus, it would be interesting to investigate whether this pathway is involved in α-SMA upregulation. Interestingly, the PI3K/AKT pathway was shown to promote the differentiation of various cells into CAFs, furthermore increasing their proliferation and survival (Wu et al., 2021). For future experiments, pharmacological inhibitors or CRISPRi/siRNA knockdown to block specific pathways during cytokine stimulation may help dissect the pathways regulating α-SMA expression.

Methodological Considerations: ICW vs. Confocal Microscopy

To confirm the ICW findings, confocal microscopy was employed to localise α-SMA expression and confirm its incorporation into actin stress fibres, a hallmark of myofibroblast differentiation (see Figures 10 and 12); (Hinz & Lagares, Myofibroblasts - Methods in Molecular Biology 2299, Springer 2021). Therefore, quantifying α-SMA protein levels using Western blotting or mRNA expression via qPCR is of limited value in this context. CAFs were stained for α-SMA, Vimentin, and DAPI, with α-SMA expression quantified via two different methods: pixel-based analysis using ImageJ and manual positive cell counting. Both analyses were normalised to the DAPI-positive area. Thus, it offers a sensitive measure of marker intensity. Manual cell counting, though more binary and time-consuming, captured discrete positive cells and tended to yield slightly higher values. However, both methods produced consistent trends, with pixel analysis being more objective and scalable. Confocal imaging, compared to ICW, provided enhanced spatial resolution. These results emphasise the utility of spatially resolved, image-based methods for high-throughput CAF phenotyping, offering deeper insight into marker localisation, heterogeneity, and myofibroblast activation. A limitation of this method is the higher variability observed in individual measurements compared to ICW. This may be due in part to the limited number of cells captured within each confocal frame. Additionally, α-SMA–positive cells tend to cluster in localised regions. The imaging frames were selected in the DAPI channel, thus stochastically probing the area and thus limiting the overall picture. The method could be advanced in the future by additional staining for actin or the splice variant ED-A of cellular fibronectin, as suggested by Hinz and Lagares (Hinz & Lagares, Myofibroblasts - Methods in Molecular Biology 2299, Springer 2021).

IFN-γ antagonises α-SMA Induction by IL-4 and TGF-β1

Interferon-γ (IFN-γ) is a type II interferon and a type 1 cytokine and thus opposes type 2 cytokine signalling. IFN-γ signals through the IFN-γ receptor (IFNGR), activating Janus kinase 1 (JAK1) and Janus kinase 2 (JAK2). JAKs phosphorylate STAT1, which forms homodimers and translocates to the nucleus, regulating the transcription of target genes involved in immune responses (Owen et al., 2019). IFN-γ signalling exerts diverse, context-dependent effects on CAFs. IFN-γ either suppresses tumour growth by limiting invasion and promoting immunity or supports cancer by increasing inflammation and stemness (Lu et al.,

2009;Bansal et al., 2012; X. Liu et al., 2019). In addition, IFN-γ prompts an immune-activating shift in CAFs (Grauel et al., 2020; Koppensteiner et al., 2025). Studies have documented that IFN-γ can also drive a pro-inflammatory CAF phenotype; these reports note effects such as increased TNF-α secretion (Z. Ma et al., 2022; Yamashita et al., 2024). In our experiments, IFN-γ alone did not significantly alter α-SMA levels, although a modest reduction was observed (see Figure 8). Strikingly, IFN-γ exerted strong antagonistic effects on both IL-4- and TGF-β1-induced α-SMA expression. It completely reversed IL-4-mediated α-SMA upregulation and partially suppressed the TGF-β1-induced response. Antagonising STAT signalling might explain the greater impact of IFN-γ on IL-4-mediated upregulation of α-SMA (Ohmori & Hamilton, 2000). Activated myofibroblasts may lose the capacity to induce growth-inhibitory STAT1 signalling (Kaler et al., 2014).
The opposing role of IFN-γ and IL-4 can also be seen in the context of TAM. In general, elevated levels of IFN-γ drive macrophages toward an M1 phenotype, whereas high levels of IL-4 and IL-13 promote polarisation into the M2 phenotype (Gunaydin, 2021). Further research is needed to elucidate the impact of IFN-γ signalling, the crosstalk with other cytokines, and the effect on the TME.

IL-1β and TNF-α do not upregulate α-SMA, but also do not diminish basal α-SMA expression

Interleukin (IL)-1β signals through the IL-1 receptor (IL-1R), activating interleukin-1 receptor-associated kinase (IRAK) family members and TNF receptor-associated factor 6 (TRAF6). This leads to the activation of mitogen-activated protein kinase (MAPK) and nuclear factor kappa B (NF-κB) signalling pathways (Weber et al., 2010). IL-1β-mediated activation of CAFs promotes the secretion of pro-inflammatory cytokines, chemokines, and matrix metalloproteinases. IL-1β secreted by tumour cells was shown to activate normal colonic fibroblasts, converting them into inflammatory CAFs (iCAFs) that further promote tumour progression (Bent et al., 2018; Díaz-Maroto et al., 2021; Koncina et al., 2023). The pro-inflammatory cytokine Tumour necrosis factor-alpha (TNF-α) binds to TNF receptors (TNFR1 and TNFR2). TNFR1 binding leads to the activation of NF-κB and MAPK signalling pathways (Holbrook et al., 2019). This way, TNF-α mediates the generation of inflammatory CAFs (Aoudjehane et al., 2008; Dash et al., 2021). Thus, IL-1β, in combination with TNF-α, robustly activates the canonical NF-κB pathway, leading to iCAF formation (Wu et al., 2021). IL-1β and TNF-α did not induce α-SMA expression in any of our assays (see Figures 11 and 12). This supports their association with inflammatory CAF (iCAF) phenotypes, which lack myofibroblastic features.
Papers describe that TNF-α suppresses the expression of α-SMA, even in combination with TGF-β (Goldberg et al., 2007). Another study stated that the addition of IL-1β diminished basal α-SMA expression in lung fibroblasts (Gabasa et al., 2013).
TNF-α and interleukin-6 (IL-6) are recognised as key contributors to inflammation in CRC. They drive the activation of critical oncogenic transcription factors, including nuclear factor-

κB (NF-κB) and signal transducer and activator of transcription 3 (STAT3), in intestinal epithelial cells, promoting cell proliferation and resistance to apoptosis. CAFs can secrete pro-inflammatory cytokines, such as TNF-α, IL-1, and IL-6, creating a chronic inflammatory environment that recruits immune cells, including myeloid cells. This inflammation facilitates tumour progression by promoting cell survival, proliferation, and angiogenesis (Kennel et al., 2023). Inflammatory CAFs (iCAFs) promote the induction and maintenance of an inflammatory environment by expressing inflammatory mediators, including IL-6, IL-11, COX-2, CXCL1 and CXCL2 (Erez et al., 2013; Monteran & Erez, 2019). Hence, it would be of interest to investigate the impact of additional inflammatory mediators, such as IL-6. In this context, a relatively new member of the IL-1 family, IL-33, was discovered, with increased expression in CAF. IL-33 also activates type 2 innate lymphoid cells (ILC), which in turn produce IL-13 (Yeoh et al., 2022; Ercolano et al., 2021).

Combination of inflammatory cytokines (IL-1β + TNF-α) counteracts α-SMA up-regulators (IL-4 and TGF-β1)

In the ICW and confocal experiments, inflammatory treatment counteracted IL-4-mediated SMA upregulation, bringing it to the level of the untreated group (see Figures 11 and 12). In contrast, IL-4 in combination with TGF-β1 reduced α-SMA levels compared to TGF-β1 alone; however, it still showed higher α-SMA levels than the untreated group in the confocal images (see Figure 12). However, the ICW only showed a slight reduction compared to TGF-β1 alone (see Figure 11). Unexpectedly, in both assays, treatment with inflammatory cytokines + IL-4 + TGF-β1 showed the highest upregulation of α-SMA.

Interestingly, IL-4–induced STAT6 activation plays a pivotal role in suppressing the inflammatory gene expression upregulated by TNF-α, in part by functioning as an antagonist of NF-κB through its interaction with the E-selectin gene promoter, thereby reducing leukocyte recruitment and inflammatory gene expression (X. Hu et al., 2021).

The crosstalk of TGF-β and IL-1 is dose-dependent in many cell types (T. Lu et al., 2007). IL-1β and TGF-β exhibit opposing effects on CAFs in preclinical models of PDAC.TGF-β was found to downregulate the interleukin-1 receptor (IL1R1) and inhibit JAK/STAT signalling, thereby preserving α-SMA expression and the myofibroblastic phenotype(Biffi et al., 2019). A study in CRC showed that, in combination, TGF-β offsets IL-1β's suppressive influence on α-SMA, supporting fibroblast survival and maintenance of the myofibroblastic state. Disruption of both IL-1β and TGF-β signalling, which was achieved by using a neutralising IL-1β antibody in combination with a TGFBR1 inhibitor, was counteracted by TAK1-mediated activation of the PI3K/Akt noncanonical TGF-β pathway. This activation alters the CAF cytokine and chemokine profile, resulting in sustained Akt signalling in CRC cells. However, dual inhibition of TAK1 and TGFBR1 effectively blocked IL-1β/TGF-β1–induced fibroblast activation, resulting in reduced secretion of proinflammatory cytokines (Díaz-Maroto et al., 2019b).

Literature on the combined action of TGF-β and TNF-α is minimal. In studies using human

dermal and gingival fibroblasts, TNF-α counteracted TGF-β action by inhibiting Smad phosphorylation via JNK activation (Goldberg et al., 2007).
Collectively, the literature describes independent roles for TGF-β and NF-κB pathway activation in establishing tumour-promoting fibroblast phenotypes (Biffi et al., 2019). However, the impact of their combined signalling in CAF remains relatively uncharacterized.

4.1.2 IL-4, TGF-β1, IL-1β and TNF-α differentially influence FAP expression

ICW and confocal imaging revealed low FAP expression in untreated CAFs and following IL-4 treatment. TGF-β1 significantly increased FAP expression in both assays (see Figures 11 and 12). Interestingly, the pro-inflammatory cytokines IL-1β and TNF-α induced only modest, non-significant increases in FAP levels, reaching approximately half the level caused by TGF-β1 alone, suggesting that inflammatory signalling by IL-1β and TNF-α alone is insufficient to substantially activate FAP expression. No synergistic effect was observed between IL-4 and TGF-β1 in ICW (see Figure 11). However, confocal imaging detected a clear synergistic response, with FAP expression roughly doubling compared to TGF-β1 treatment alone (see Figure 12). A similar pattern was previously noted with α-SMA, where confocal microscopy more effectively captured synergistic effects, suggesting that spatially resolved imaging may be more sensitive to subtle or localised activation patterns. Unexpectedly, the combination of IL-4, IL-1β and TNF-α resulted in a strong and significant upregulation of FAP. Similarly, the combination of TGF-β1 with IL-1β and TNF-α resulted in a marked increase in FAP expression, exceeding that observed with TGF-β1 alone in ICW. Interestingly, combined treatment with IL-1β + TNF-α and TGF-β1 in the confocal analysis unexpectedly resulted in lower FAP levels than TGF-β1 alone, diverging from ICW results. Further experiments are necessary to clarify this discrepancy and eliminate potential sources of error. Notably, the complete four-cytokine cocktail consistently produced the highest FAP expression.
FAP is widely considered a prominent CAF marker, and its expression is connected to tissue repair, fibrosis and ECM degradation (Nurmik et al., 2020b). However, FAP is also found to be upregulated during inflammation, but not in the context of cancer (Z. Wang et al., 2023). Thus, it is hard to associate FAP with either the myCAF or iCAF phenotype; however, most studies align FAP with the myCAF phenotype (Bueno-Urquiza et al., 2024). In breast cancer, FAP expression was found in both inflammatory and myofibroblastic subsets, but the myofibroblastic (FAP+/αSMA+, CD29+) cells were more strongly linked to immunosuppressive and ECM–related functions (Croizer et al., 2024). Intrahepatic cholangiocarcinoma studies describe FAP-positive CAFs with an inflammatory signature (for example, via STAT3-CCL2 signalling (X. Yang et al., 2016).
In colorectal cancer, a subset of CAFs characterised by high IL1R1 expression responds to tumour-derived IL-1β by upregulating FAP (alongside PDPN), acquiring an inflammatory iCAF phenotype that drives tumour growth in 3D co-culture assays and fosters

immunosuppression via macrophage polarisation and T-cell inhibition, effects reversed by IL-1 signalling blockade (Koncina et al., 2023). Our experiments can confirm these results. Additionally, it was shown that collagen induces FAP expression through the binding of α3β1 integrin (Fitzgerald & Weiner, 2020).
TGF-β1, acting via both canonical and noncanonical signalling, induces FAP expression in various other CAF populations (Kawase et al., 2015; Ping et al., 2023). Autophagy is reported to mediate this induction (M. Huang et al., 2021). Signalling pathways that activate STAT3 (through a uPAR–FAK–Src–JAK2 cascade) contribute to FAP upregulation (X. Yang et al., 2016).
FAP upregulation in colorectal CAFs is known to occur through a network of signalling cascades and microenvironmental cues, including TGF-β (Cho et al., 2020), WNT, FGF (Furuhashi et al., 2023), and PI3K/AKT/MAPK pathways (Henrich et al., 2024). Additionally, IFNAR1 downregulation is linked to increased levels of FAP in CRC (Cho et al., 2020). Furthermore, the cytokine IL-34 promotes FAP upregulation in CRC CAFs (Franzè et al., 2020). Radiation exposure and oxidative stress also elevate FAP expression in CRC CAFs (Hassametto et al., 2023; Garate et al., 2024). Thus, several other mechanisms behind FAP upregulation could be explored.

4.1.3 IL-4, TGF-β1, IL-1β and TNF-α Differentially Regulate CAF Markers: IL-1R1, PDPN, and PD-L2

Our experiments demonstrated that TGF-β1 functions as a central regulator of the CAF phenotype by upregulating PD-L2, while simultaneously repressing IL-1R1 expression (see Figure 12). IL-4 contributes to the upregulation of podoplanin (PDPN) and suppresses IL-1R1 levels. In contrast, the inflammatory cytokines IL-1β and TNF-α predominantly drive PDPN expression. Notably, synergistic regulation of PD-L2 is observed under specific cytokine combinations, particularly in the presence of both IL-4 and TGF-β1. These findings highlight the dynamic and context-dependent regulation of CAF phenotype by cytokine networks.

IL-1R1
Previous studies have shown that TGF-β signalling suppresses IL-1R1 expression in CAFs, contributing to a shift away from the iCAF phenotype (Biffi & Tuveson, 2021). Consistent with this, we observed IL-1R1 downregulation following TGF-β1 treatment (see Figure 12). IL-4 also led to a downregulation, however, to a lesser degree than TGF-β1 treatment. Interestingly, in our study, combined treatment with IL-1β and TNF-α also led to IL-1R1 downregulation, suggesting that pro-inflammatory cytokines themselves may initiate negative feedback or compensatory mechanisms that limit prolonged IL-1 signalling.

Notably, no further suppression of IL-1R1 expression was observed when combining any of the tested cytokines. IL-1R1 is critical for maintaining this iCAF phenotype, as genetic or pharmacological blockade of IL-1R1 significantly impairs organoid viability in co-culture models (Koncina et al., 2023). However, Koncina et al. focused on IL-1β alone, whereas our findings with IL-1β plus TNF-α suggest a more complex interplay, potentially involving feedback inhibition or signal crosstalk not evident in single-cytokine contexts.
Additional investigation is required to confirm and expand upon these findings, including assessments of feedback regulators (e.g., IRAK-M, IL-1RA), and functional assays targeting IL-1R1 in multi-cytokine environments (Zhukova et al., 2024).

Podoplanin
Ekwall et al. reported that podoplanin expression is induced by the pro-inflammatory cytokines IL-1β, TNF-α, and TGF-β1 in cultured primary synovial fibroblasts (Ekwall et al., 2011). This finding was partially confirmed by Croft et al., who observed induction by IL-1β and TNF-α, but not by TGF-β1 (Croft et al., 2016). Importantly, Koncina et al. (2023) also reported that IL-1β induces PDPN expression in colorectal CAFs (Koncina et al., 2023). In our study, IL-4 and IL-1β + TNF-α upregulated podoplanin, respectively (see Figure 12). In combination, no antagonistic effect of these cytokines was noticed.

PD-L2
In our study, PD-L2 upregulation matches FAP upregulation; thus, both markers are regulated by TGF-β (see Figure 12). Among the genes highly expressed by FAP^+ CAFs, PD-L2 and TNFSF4 (OX40L) have been identified as key mediators of sustained CAF–T cell interactions in breast cancer (Costa et al., 2018). Although most research has focused on the PD-L1/PD-1 axis, both PD-L1 and PD-L2 are capable of engaging PD-1, highlighting the potential role of PD-L2 in immunotherapy resistance (Mhaidly & Mechta-Grigoriou, 2021). Unfortunately, the IgG control for the PD-L1 antibody produced a strong background signal and hence could not be analysed. Since PD-L1 blockade may not inhibit PD-L2–PD-1 interactions, elevated PD-L2 expression in FAP^+ CAFs may represent an alternative mechanism of resistance to current immune checkpoint therapies (Topalian et al., 2016). In CRC, CAF-secreted factors, such as TGF-β, are linked to immune evasion and resistance to therapies like PD-1 blockade, highlighting the importance of targeting CAFs to improve immune control over tumours (Mariathasan et al., 2018; Linares et al., 2021).

Limitations and further directions
The study is based on 2D monoculture systems of established CAF patient primary cultures, which may not fully capture the cellular complexity and spatial organisation of the in vivo tumour microenvironment. For further assays, it would be helpful to investigate how long the markers remain upregulated. Additionally, it is necessary to validate marker expression and

function in a more physiologically relevant context, e.g. in a 3D collagen gel.
While marker expression was thoroughly evaluated, functional aspects such as matrix remodelling and contractility by CAFs in response to stimuli were not assessed. These cytokines likely alter not only α-SMA levels but also the quality and function of the ECM, including the deposition of fibronectin (ED-A splice variant), desmin, tenascin-C, CCN2 (also known as CTGF)(Karlsson & Nyström, 2022; Hinz & Lagares, Myofibroblasts - Methods in Molecular Biology 2299, Springer 2021). ECM alterations could be characterised through immunofluorescence staining, decellularised ECM analysis, or proteomic approaches such as mass spectrometry (Lee et al., 2025).
The observed divergence between ICW and spatially resolved readouts, such as confocal microscopy, particularly regarding stress fibre formation, underscores the need for multimodal quantification methods to assess CAF activation accurately. Single-cell analysis could resolve this problem. Many studies have implemented single-cell sequencing (scRNA-seq) with CAF (J. Ma et al., 2021; Lavie et al., 2022). A complementary method on the single-cell level could also be assessing the marker expression with flow cytometry after treatment with TGF-β1, IL-4, and combinations of inflammatory cytokines to identify distinct CAF subpopulations expressing specific markers. CAFs could also be sorted by marker expression, and their impact on organoid growth could be evaluated in a sorted culture to measure the effect of each marker.
Interestingly, it was found that tumour suppressors, such as p53, and oncogenes, like KRAS, influence the cytokine profile, and cells adapt to distinct cytokine signalling by regulating these proteins. TP53 deficiency, which occurs early in CRC development, is associated with increased levels of inflammation and the production of NF-κB-related cytokines and chemokines. RAS mutations directly influence several pro-inflammatory cytokines and chemokines, including IL-6, IL-8, IL-11, GM-CSF, and CXC-chemokine ligand 1 (CXCL1). KRAS or NRAS mutations in microsatellite-stable CRCs are associated with reduced expression of genes connected to Th1-type immunity, such as IFN-γ. KRAS also leads to a decrease in the tumour-suppressive effects of TGF-β (West et al., 2015). Thus, the impact of mutations on cytokine expression warrants further scientific exploration. Additional studies are required to clarify what signalling cascades are activated by cytokine signalling, especially of combined treatments.
The analysis focused on a small set of markers (α-SMA, FAP, PD-L2, PDPLN, IL-1R1). The inclusion of additional markers, such as Meflin (Takahashi et al., 2021), fibronectin (FN1) or platelet-derived growth factor- A/B (PDGF-A/B), would have provided a more comprehensive phenotypic profile. Marker expression is highly context- and method-dependent, underscoring the complexity of CAF responses. Apart from α-SMA and FAP, a plethora of other CAF markers can be found. Vimentin is found to be expressed in both CAFs and normal fibroblasts; thus, it is not CAF-specific (Z. H. Wang et al., 2012). Meflin is expressed by mesenchymal stem cells and exerts a suppressing effect, decreasing LOX activity. Matrix stiffness, TGF-β, hypoxia, and ageing inhibit Meflin in stromal cells, thereby

enhancing collagen production. Meflin expression in CAF is low compared to normal fibroblasts (Ishihara & Haga, 2022). Meflin-positive CAFs have been shown to suppress tumour progression by modulating collagen architecture and BMP signalling within the TME (Takahashi et al., 2021; Kobayashi et al., 2021). Additional CAF markers with modest specificity comprise fibroblast-specific protein 1 (FSP1), platelet-derived growth factor receptor (beta) (PDGFR(B)), collagen type I alpha 1 (COL1A1), fibronectin 1 (FN1), SPARC (Herrera et al., 2013; Zheng et al., 2021;Mele et al., 2022;Z. Zhao et al., 2022; Shah et al., 2024).
The selection of the time point was made according to the initial α-SMA experiments, thus might not reflect the best assessment of the other markers. While two independent CAF lines were tested, greater inter-patient variability in CAF responses may exist. Further validation across a broader panel of primary CAFs would strengthen the generalizability of findings. It would be of interest to assess the co-expression of markers, e.g. α-SMA and FAP, to see whether certain CAF express only one marker or both combined. Although informative, the findings remain unvalidated in animal models or patient-derived xenografts, which could confirm the in vivo relevance of IL-4/IL-13-driven CAF activation.

4.2 Impact of cytokine-pretreated CAF conditioned media on colorectal cancer organoid growth

To investigate whether different cytokine-activated colorectal CAFs influence tumour growth via secreted factors, we analysed the effects of conditioned media (CM) from pretreated CAFs on patient-derived CRC organoids (BGM2008) embedded in Matrigel using the CellTiter-Glo 3D assay (see Figures 13 and 14).

MyCAF-CM does not increase organoid viability

CM from CAFs treated with IL-4 or TGF-β1 alone, both of which are associated with myofibroblast-like (myCAF) phenotypes, did not significantly promote organoid growth (see Figure 14). While myCAFs are known for their ECM remodelling and contractile properties, they may not secrete factors that directly support tumour cell growth or survival, in line with the original subtype definition by Öhlund et al, in which myCAFs are characterised by strong ECM production and contractile features but do not contribute substantially to tumour progression through soluble factors. Instead, their primary roles involve ECM deposition, tissue stiffening, and mechanical modulation of the TME (Öhlund et al., 2017; Calon et al., 2015; Sahai et al., 2020). Indeed, single-cell RNA-seq data from lung cancer demonstrates that α-SMA-high CAFs (myCAFs) lack enrichment for inflammatory cytokines like IL-6 or CXCL12, which are instead expressed by iCAFs (Koppensteiner et al., 2025). Reviews of the CAF secretome further assert that key soluble tumour-supportive mediators (e.g., IL-6, IL-8, HGF) are predominantly produced by inflammatory CAF subsets, whereas myCAFs are ECM-focused (Vokurka et al., 2022; Wright et al., 2023).

The combination of IL-4 and TGF-β1 moderately increases organoid viability

Interestingly, the combination of IL-4 with TGF-β1 yielded a modest increase in patient-derived tumour organoids (PDTO) ATP luminescence, indicating a slight enhancement in organoid viability (see Figure 14). Thus, myCAF might have a more moderate impact on cancer growth compared to iCAF, which only shows a significant increase in viability when TGF-β and IL-4 are combined. MyCAF might not strongly impact cancer viability through paracrine secretion, but rather direct contact or ECM remodelling effect (Karagiannis et al., 2012; Erdogan & Webb, 2017). Matrix stiffness regulates pro-tumourigenic transcription factors, such as YAP/TAZ, β-catenin and Twist/Snail (Ishihara & Haga, 2022). This study describes patient-specific CAF heterogeneity in matrix stiffening after 21 days in culture, as measured by atomic force microscopy (AFM). Interestingly, the difference was lost when the cells were co-cultured with CRC cells (Micalet et al., 2024). This study suggests that the effects of CAFs on ECM stiffness develop gradually over time, and that crosstalk with cancer cells further influences this process. Future investigations should explore this further. For instance, proteomics data could elucidate ECM remodelling and desmoplastic proteins connected with it (Karagiannis, Petraki, et al., 2012).

iCAF-CM (IL-1β and TNF-α) significantly increases organoid viability

Notably, CM from CAFs stimulated with the pro-inflammatory cytokines IL-1β and TNF-α significantly enhanced organoid luminescence, indicating increased viability (see Figure 14). This suggests that inflammatory activation skews the CAF secretome toward a more pro-tumourigenic phenotype, likely through a reprogrammed secretome (Erez et al., 2010; LeBleu & Kalluri, 2018). Proteomic profiling of the conditioned media will be crucial in elucidating the specific soluble mediators responsible for these effects.

Inflammatory CAFs (iCAFs), which secrete IL-6 and other pro-inflammatory cytokines, are more often linked to paracrine stimulation of tumour growth. These results suggest that CAFs treated with inflammatory cytokines secrete tumour-supportive factors. Although the precise composition of the CAF secretome remains to be defined, it is likely to include known pro-tumourigenic mediators, such as IL-6, IL-8, VEGF, prostaglandins, IGF or HGF, which may promote tumour cell proliferation, survival, or the maintenance of cancer stem-like traits (Kalluri, 2016; Linares et al., 2021; Y. Chen et al., 2024). Konicna et al. showed that IL-1β–activated CAFs promote colorectal tumour growth through NF-κB signalling, enhance 3D tumour cell expansion, and polarise macrophages toward a pro-tumourigenic phenotype via CCL2 secretion. Blocking IL-1 signalling, either pharmacologically (by Anakinra) or genetically, reduced tumour growth, Th17 infiltration, and immunosuppression in the TME, leading to improved survival (Koncina et al., 2023). From a therapeutic perspective, our findings suggest that targeting inflammatory pathways in CAFs, such as IL-1R, TNFR, or downstream effectors like NF-κB, might reduce their tumour-promoting functions (Guo et al., 2024).

IL-4 counteracts IL-1β and TNF-α-mediated organoid viability
Interestingly, when IL-4 was combined with IL-1β and TNF-α, no significant enhancement in organoid growth was observed, with comparable levels to untreated (see Figure 14). This suggests that IL-4 attenuates the tumour-promoting effects of pro-inflammatory cytokines, pointing to antagonistic interactions between these signalling pathways. Notably, IL-4 appears capable of counteracting the dual effect induced by IL-1β and TNF-α. The anti-inflammatory role of IL-4 and IL-13 can be clearly seen in macrophages and other immune cells (Allen, 2024). IL-4 has been described as an anti-inflammatory agent in acute and chronic inflammatory conditions (Pan et al., 2025). More in-depth research is essential to better understand these opposing mechanisms.

TGF-β1 does not reduce the effect of IL-1β and TNF-α-mediated organoid viability
In contrast to IL-4, TGF-β1 pretreatment of CAFs, in combination with IL-1β and TNF-α, did not reduce the pro-tumourigenic effect observed with IL-1β and TNF-α alone, but also did not increase the organoid response. Only a slight reduction of luminescence compared to inflammatory treatment can be detected (see Figure 14). This might suggest a potentially antagonistic or regulatory interaction between TGF-β1 and the inflammatory cytokines in this context, like previously reported (Biffi et al., 2019;Koncina et al., 2023).

Combined Treatment with IL-4, TGF-β1, IL-1β, and TNF-α maximally enhances organoid viability
The most robust response was observed when all four cytokines (IL-4, TGF-β1, IL-1β, and TNF-α) were combined to pretreat CAFs, resulting in a 3.8-fold increase in luminescence compared to organoids cultured with untreated CAF-CM. Of note, the luminescent signal is more than the one with CAF CM produced by inflammatory cytokine treatment alone (see Figure 14).
These findings are particularly noteworthy as they suggest that iCAF and myCAF phenotypes may coexist and concurrently influence tumour progression, rather than being mutually exclusive. This challenges the prevailing model where cytokine signalling is thought to drive distinct and antagonistic CAF states, with TGF-β favouring myCAF differentiation and IL-1 promoting iCAF identity. Previous studies, including those by Biffi et al. and Koncina et al., have supported this dichotomy by demonstrating that TGF-β and IL-1 signalling pathways exert opposing effects on CAF fate (Biffi et al., 2019;Koncina et al., 2023). However, the observation that IL-4 can modulate this balance is a novel finding and introduces a new layer of complexity, suggesting that CAF heterogeneity may be more plastic and context-dependent than previously appreciated, potentially allowing for simultaneous activation of divergent CAF programs within the same microenvironment.

Conditioned media from CAFs support organoid growth more than standard media

Organoids cultured in Omin medium alone showed the lowest viability, whereas ENAS medium supported moderate growth, outperforming untreated CM but falling short of cytokine-activated CM (see Figure 14). In a previous study of our lab, we showed that colorectal cancer organoids and matched CAFs from the same patient can be cultured without exogenous niche factors. Co-cultures exhibited enhanced tumour cell heterogeneity, closely mirroring patient tumour morphology and transcriptional states (Atanasova et al., 2023).

Limitations and future perspectives

These experiments demonstrate that colorectal CAFs exhibit marked functional plasticity in response to diverse cytokine stimuli. The differential effects observed across inflammatory (iCAF) and myofibroblast-like (myCAF) conditions underscore that CAFs are not a uniform population but are highly dynamic entities shaped by their microenvironment. Specifically, the stimulation of pro-inflammatory cytokines (IL-1β + TNF-α) markedly enhanced the pro-tumourigenic activity of CAFs. This highlights the importance of cytokine context in driving CAF heterogeneity and plasticity, with implications for both tumour growth and therapeutic targeting strategies (Y. Chen et al., 2021)

There is a significant research gap in combined cytokine action, even involving prominent cytokines of the TME (e.g. TGF-β, IL-1β, and TNF-α), on CAF-mediated tumour growth. We have **a** limited understanding of how simultaneous or sequential exposure to multiple cytokines shapes CAF heterogeneity, function, and tumour-promoting capacity**.** Most studies to date have investigated TGF-β, IL-1β, or TNF-α in isolation**,** leading to a binary model of CAF polarisation**:** myCAF (TGF-β-driven) vs. iCAF (IL-1β- or TNF-α-driven)(Biffi & Tuveson, 2021). A more nuanced understanding is emerging regarding the different CAF subtypes. However**,** it is unclear how CAF-intrinsic signalling pathways integrate opposing inputs**.** The hierarchy or co-activation potential of these pathways in CAFs remains poorly defined. It's unknown whether CAF phenotypes switch in response to multiple cytokines or whether intermediate CAF states exist and how stable or functional they are.

Despite these insights, the study has several limitations. All experiments were conducted in vitro. Although primary CAFs and organoids provide improved physiological relevance compared to cell lines, they do not fully recapitulate the multicellular complexity and architecture of in vivo tumours. Cytokine treatments were administered over relatively short time frames (24–48 hours), which may not reflect chronic exposure scenarios relevant to disease. Furthermore, only two patient-isolated CAFs were analysed, limiting the generalizability of our findings across the broader spectrum of CRC-associated CAF phenotypes.

While organoid viability was modulated by CAF-CM, the specific secreted factors responsible for this modulation were not identified. Proteomic and transcriptomic profiling of cytokine-treated CAFs will be crucial in identifying these mediators (Mishra & Banerjee, 2023). Likewise, downstream effects on organoid signalling pathways, changing

morphology, invasion capacity, and stemness (CD44, CD133, CD24, EpCAM, LGR5 and ALDH) were not assessed but represent possibilities for follow-up experiments(Y. Zhou et al., 2018). To build on these findings, future studies should perform cytokine profiling (e.g., Luminex or ELISA) or MASSSPEC of the protein of CAF-CM to identify key tumour-supportive factors (De Boeck et al., 2013; S. X. Chen et al., 2014; Mishra & Banerjee, 2023; Linares et al., 2021). Additional studies should also investigate downstream signalling in organoids in response to CAF-CM. Furthermore, RNA-sequencing of cytokine-treated CAFs could be performed to map transcriptional reprogramming.

4.3 Cytokine effect in CAF-PDO co-culture (OOTA)

In this setup, an organotypic organotypical assay (OOTA) was employed to investigate the impact of cytokine-treated CRC-CAF (CAF BGM2008) on the morphology and growth of colorectal cancer organoids (BGM2008). CAFs were pretreated with IL-4, TGF-β1, IL-1β + TNF-α, or their combinations before embedding in collagen I. Then, organoids were seeded in Matrigel on top. Treatment followed on days 2 and 4 (see Figure 15).

Cytokines impact organoid morphology and growth

Over five days, organoid morphology varied significantly across different treatment conditions (see Figure 15B). Untreated organoids remained compact and spherical, whereas IL-4 and combination treatments disrupted their architecture, resulting in irregular borders and dispersed cells. The combination of all four cytokines resulted in the most severe disruption, characterised by diffuse and poorly structured organoids (see Figure 15B). Morphological changes, particularly under IL-4 and combined cytokine treatments, may reflect EMT-like behaviour, loss of polarity or perturbation of stemness/differentiation balance, key features of early invasion and metastasis. Staining for EMT markers like Snail, Twist, or ZEB, thus could be of interest. Additionally, E-cadherin (CDH1) downregulation and upregulation of N-cadherin (CDH2) of cancer cells could indicate EMT (Mele et al., 2014). Moreover, the expression of MMP is indicative of ECM remodelling, facilitating EMT (Yin et al., 2024).

Quantification of organoid growth (total area and fold change from day 2 to day 5) showed no statistically significant differences between conditions (see Figure 15D, E, F and G). However, the combination of IL-4 and TGF-β1, as well as the entire cytokine combination, displayed the least growth. Organoid size analysis revealed that TGF-β1 + IL-1β + TNF-α significantly increased individual organoid size on day 2, while single cytokine treatments resulted in smaller organoids by day 5 (see Figure 15H and I). This type of analysis might be expanded to an increased number of microscopy images to reach significance.

Immunofluorescence stain of Ki-67 (proliferation) and cleaved Caspase-3 (apoptosis)

Immunofluorescence confocal analysis of proliferation (Ki-67) and apoptosis (cleaved Caspase-3) of OOTAs fixed at the end of the experiment revealed that IL-1β + TNF-α increased proliferation, while IL-4 + TGF-β1 reduced it (Otsu's method is a way to automatically separate the foreground from the background in an image by finding the brightness threshold level that best divides the two) (see Figure 16B). Apoptosis was elevated in single treatments of IL-4, TGF-β, and IL-1β + TNF-α and in TGF-β1 + IL-1β + TNF-α conditions. (see Figure 16C).
The combination of IL-4 and TGF-β1, linked to myofibroblastic CAF phenotypes, resulted in reduced proliferation (Ki-67) and minimal growth, suggesting a potential tumour-restraining effect of myCAF-like conditions. This aligns with the results obtained previously with the conditioned media experiment. It is consistent with the hypothesis that myCAFs may play a less proliferative, more structural role in the TME. The effect of inflammatory cytokines, increased proliferation and apoptosis, suggests a tumour-promoting but unstable environment. IL-1β and TNF-α both can lead to increased apoptosis through distinct mechanisms (Borowczak et al., 2022). Excessive inflammatory signalling can lead to cellular stress; hence, this should be further investigated.

CAF activation markers showed that α-SMA was significantly induced only by IL-4 + TGF-β1, while FAP was upregulated most strongly by the combination of all cytokines
Interestingly, α-SMA expression in the 3D OOTA co-culture model showed the highest increase with combined IL-4 and TGF-β treatment, showing an approximately 8-fold increase compared to TGF-β alone (see Figure 17), in line with the ICW results. In contrast, single treatments with IL-4 or TGF-β resulted in only minimal, non-significant α-SMA activation, and no other cytokine combinations produced notable upregulation. This finding diverges from observations in 2D culture, where maximal α-SMA expression occurred with the combination of all four cytokines, including IL-1β and TNF-α. Notably, in the 3D OOTA setting, this four-cytokine combination did not result in significant upregulation, suggesting distinct regulatory mechanisms between 2D and 3D systems or the impact of the tumour cells in this setup, which were not present in the ICW analyses.
The underlying causes of this discrepancy are not yet clear. One explanation may be the presence of a fully embedded 3D collagen I matrix in the OOTA model, which differs from the monolayer fibroblast configuration used in 2D assays. Additionally, the direct crosstalk between CAFs and cancer organoids in the OOTA system may contribute significantly to α-SMA regulation. To delineate these two variables, the impact of 3D matrix context and the presence of tumour-derived signals, future experiments should independently assess α-SMA expression in 3D cultures of CAFs alone, and CAF cultures treated with cancer organoid–conditioned media in both 2D and 3D formats. This approach would help clarify whether matrix dimensionality, tumour-derived soluble factors, or their combination drives the observed expression patterns.
Even though the clear mechanism behind the different results in α-SMA upregulation of 2D

and 3D is missing, we can hypothesise that the underlying reason is an effect of the 3D collagen culture. 2D cultures are typically performed on rigid plastic surfaces, which are orders of magnitude stiffer than physiological tissue. This stiffness provides strong mechanical signals that promote stress fibre formation and α-SMA expression, as α-SMA is part of the contractile cytoskeleton associated with mechanotransduction. In 2D, fibroblasts spread out flat and generate large focal adhesions and actin stress fibres, structures that are linked to α-SMA incorporation into the cytoskeleton. 3D collagen gels, in contrast, are much softer; however, they resemble the mechanical properties of the in vivo ECM. In 3D, cells are embedded in all directions with different adhesion dynamics. This spatial arrangement alters actomyosin contractility and affects the integration of α-SMA into stress fibres. Cells in 3D matrices engage different sets of integrins and ECM receptors compared to 2D. This affects focal adhesion kinase (FAK) and Rho/ROCK pathway activity, both of which are important for regulating α-SMA expression.

In pancreatic CAFs and normal fibroblasts, stiffer collagen substrates induced higher α-SMA levels and stress fibre orientation, demonstrating that substrate rigidity in a 3D-like environment alters cytoskeletal activation (Stylianou et al., 2019). In microfluidic co-culture models embedding CAFs in a 3D collagen matrix, CAFs displayed markedly increased α-SMA, adopting contractile, spindle-shaped myofibroblast phenotypes, changes absent in simple 2D culture(Jeong et al., 2016). In breast cancer models, CAF encapsulated in higher-density collagen gels (e.g., 4 mg/ml) expressed significantly more α-SMA than in low-density gels (~1 mg/ml), showing that ECM density and 3D context promote CAF activation (Gao et al., 2021). CAFs embedded in collagen gels have been shown to exert contractile forces, retracting the matrix and remodelling fibre structure over time, a phenomenon closely linked to their α-SMA-positive, myofibroblast nature (Sapudom et al., 2020). However, this is not entirely applicable in our OOTA model, since this includes a nylon mesh to avoid contraction in the x-y axes and, thus, provides increased systemic stiffness in comparison to free-floating, unsupported collagen gels.

The FAP expression results of the OOTA more closely resemble those observed in the 2D model (see Figures 12 and 17). In both OOTA-CAF and 3D cultures, the combination of all four cytokines induced the strongest upregulation of FAP. While the qualitative pattern of cytokine-induced FAP expression was consistent across all culture conditions, with each cytokine treatment leading to an increase compared to the 2D model, the magnitude of this response differed. Notably, in the 3D culture setting, the combination of all four cytokines elicited a markedly greater upregulation of FAP expression compared to the other treatment conditions.

A single-cell sequencing study of CRC-CAF used reference component analysis, which sorted CAFs into two groups: CAF-A and CAF-B. CAF-A express matrix-metalloproteinase 2 (MMP2), decorin (DCN), collagen 1A2 (COL1A2), podoplanin (PDPN) and FAP. In contrast, CAF-B show marker expression of α-SMA (ACTA-2), transgelin (TGLN), Platelet-Derived Growth Factor A (PDGFA), lumican (LUM). CAF-A may depict an intermediate state

between normal fibroblasts and the CAF-B/myofibroblast state or an independent CAF subtype (H. Li et al., 2017). Thus, CAF-B cells expressed myCAF/cytoskeletal markers such as ACTA2, TALN and PDGFA. Whereas these markers were downregulated in CAF-A cells, which expressed matrix remodelling genes such as MMP2, DCN and COL1A2. However, TGFβ1 and SMAD3 activation in both CAF subtypes suggests a common regulation of these two CAF subsets (Lavie et al., 2022a). This suggests CAF either express α-SMA or FAP, which fits our results. This highlights the need to evaluate this CAF phenotype dichotomy using our confocal methodology or complementary single-cell methods. Additionally, assessment of the markers reported by Li et al. would be valuable.

Limitations and future perspectives

Several limitations should be considered when interpreting the results of this study. Firstly, due to contamination during IL-4 pretreatment, CAFs in the IL-4 condition were treated after embedding in collagen, deviating from the pre-treatment protocol used for other conditions. This variation may have influenced treatment outcomes and limits direct comparability. Additionally, there was high inter-sample variability, particularly in organoid growth measurements on day 2, with large standard deviations potentially obscuring statistically significant effects. This suggests that observed trends in growth and morphology should be interpreted with caution.

While organoid morphology was visibly altered under certain conditions, the quantification methods, primarily total area and individual size, may not fully capture complex three-dimensional changes or peripheral cell dissemination, highlighting a limitation in the resolution of the chosen analytical approach. Thus, changing the readout is advised. For a better readout Cell-Titer Glo assay could be used, this time in a 96-well format with transwells. A Nano-Luciferase (NLuc) -based assay developed in the lab could help investigate the relationship of CAF and organoids in a direct contact co-culture in Matrigel domes. NLuc serves as a luminescent reporter in organoid cells; thus, the viability of organoids can be measured after the addition of substrate. Moreover, the simultaneous application of cytokines to the co-culture system might have direct effects on organoids themselves, rather than exclusively via CAF modulation. This complicates the attribution of observed phenotypes solely to CAF-mediated interactions. Additionally, the study relied on a single CAF line and a single colorectal cancer organoid line (BGM2008), which limits the broader applicability of findings. More patient-oriented lines should be tested. Furthermore, the ratio of CAF to organoid cells has not been determined for this assay. The number of organoid cells might have been too high, as on Day 5, organoids in some conditions fully covered the area. Finally, the experimental duration of five days may be insufficient to capture longer-term stromal remodelling, CAF reprogramming, or sustained effects on tumour cell behaviour, warranting further investigation in extended culture systems.

The analysis regarding CAF-marker expression in the OOTA could be improved. In the 2D settings, we normalised the marker to DAPI (nuclei stain), but that can't be done in the OOTA

because the organoid nuclei are stained as well. Thus, the normalisation is based on vimentin. However, vimentin expression may also change with cytokine treatment; therefore, a different method should be employed. Vimentin expression in CAFs in CRC is linked to higher disease recurrence rates, shorter survival, and a higher risk of tumour invasion (Z. Zhao et al., 2023).

Further research should also investigate whether direct contact between CAFs and cancer cells is necessary for α-SMA induction, as CAF-cancer cell interactions are critical for tumour progression. This could be tested through co-culture experiments, where the role of direct cell-cell contact versus soluble factors could be discerned. Conditioned media of organoids and the effect on marker expression could be tested. However, the OOTA setup uses a mesh that might impact the contractility of CAF.

A comprehensive understanding of how myCAFs influence cancer progression is still lacking. Additional research is necessary to better understand the role of myCAFs in cancer development. Some studies suggest that physical interaction between CAFs and cancer cells is essential for modulating cancer cell behaviour, while others focus on the role of the ECM matrix. In early-stage (T1) CRC liver metastases, CAFs promote tumour invasion through direct cell–cell contact by enhancing extracellular matrix remodelling via cathepsin H secretion, which drives proteolytic activity and CD44-mediated cancer cell engagement, independently of paracrine signalling (Dang et al., 2023). In liver metastases from CRC, myCAFs derived from hepatic stellate cells secrete hyaluronan (HA) to promote tumour growth via CD44 signalling on cancer cells, whereas their concurrent production of type I collagen forms a dense extracellular matrix that mechanically restrains tumour expansion (Bhattacharjee et al., 2021).

Using patient-derived CRC organoids as a functional readout represents a significant strength of the study, offering a personalised and translationally relevant model (Z. Zhou et al., 2021; Xu et al., 2021). However, organoids lack immune and vascular compartments, and future co-culture systems that incorporate additional TME components, such as immune cells or endothelial cells, could yield a more holistic understanding of CAF-driven tumour progression (Naderi-Meshkin et al., 2023; J. Wang et al., 2025). The absence of immune components limits the relevance of our findings for understanding the immunoregulatory role of CAFs. CAFs orchestrate a complex immune landscape that facilitates tumour progression by creating a pro-inflammatory TME in the beginning and later an immunosuppressive microenvironment. Their interactions with immune cells, including Tregs, MDSCs, and macrophages, inhibit effective anti-tumour immunity and contribute to resistance to immune therapies (Sahai et al., 2020; Monteran & Erez, 2019). As key cytokines like IL-4, IFN-γ, and TNF-α are important regulators of the immune system, future studies should incorporate immune–CAF–tumour interactions to more faithfully model in vivo conditions. To further test the immune cell impact, a triple culture with macrophages developed with the help of our laboratory could be used, thus forming a more concise model of CRC (Kabiljo et al., 2024). Notably, CAF markers are correlated with the function of immune cells. For example, α-SMA

expression is negatively correlated with tumour-infiltrating lymphocytes (TILs), whereas fibronectin shows positive co-expression (Zadka et al., 2021). FAP expression also correlates with functional roles beyond matrix remodelling. Studies have shown that FAP+ CAFs can suppress anti-tumour immunity through the production of CCL2, CXCL12, and the regulation of T cell infiltration (Mhaidly & Mechta-Grigoriou, 2021).

The differential effects of cytokine-primed CAFs underscore the need to distinguish between tumour-promoting and restraining CAF subsets for targeted therapies. Anti-CAF strategies may need to avoid broadly targeting CAFs and instead consider selectively targeting CAF subsets, such as FAP-positive CAFs. Furthermore, inflammatory signalling could be modulated (e.g., IL-1β or TNF-α inhibitors) to suppress tumour-promoting aspects while preserving structural or homeostatic CAF functions. Furthermore, targeting fibrotic ECM can enhance drug delivery and aid immunotherapy (Mai et al., 2024).

5. Conclusion

The thesis investigates the impact of cytokines IL-4, IL-13, IFN-γ, TGF-β1, IL-1β, and TNF-α on CAF markers (α-SMA, FAP, PD-L2, PDPN, IL-1R1) and CRC tumour-supportive functions. Patient-derived CRC-CAFs were analysed using In-Cell Western and confocal microscopy. TGF-β1 strongly upregulated α-SMA, while IL-4 and IL-13 induced moderate increases independent of TGF-β receptor signalling. IFN-γ antagonised IL-4 and TGF-β1–mediated α-SMA induction, whereas IL-1β and TNF-α counteracted IL-4-driven upregulation. FAP was absent in untreated CAFs and after IL-4 treatment but was strongly induced by TGF-β1, with synergistic enhancement when IL-4 was combined. IL-1β + TNF-α upregulated podoplanin, and PD-L2 regulation mirrored FAP, with TGF-β1 as a central driver. Conditioned media from IL-1β + TNF-α-treated CAFs significantly enhanced organoid growth, demonstrating iCAF-mediated paracrine support, while IL-4 counteracted this effect. Combined treatment with all four cytokines induced a highly secretory CAF phenotype, maximally promoting organoid viability. In 3D co-cultures (OOTA), α-SMA was induced only by IL-4 + TGF-β1, while FAP was most strongly upregulated by the full cytokine combination. This thesis demonstrated for the first time that IL-4 affects CAF by upregulating α-SMA, independently of TGF-β1. Further, it confirmed the strong impact of TGF-β1 on CAF markers α-SMA, FAP, IL-1R1 and PD-L2. This sheds light on the complex regulation of FAP expression, which is widely regarded as a general marker of CAFs. The results challenge the view that iCAFs and myCAFs are mutually exclusive and both simultaneously impact the viability of CRC cancer organoids. Some markers, like α-SMA, are majorly impacted by 3D organoid culture, whereas others, like FAP, show the same regulation pattern as in 2D.
Future experiments need to analyse the differential CAF-secretome induced by cytokine treatments. Single-cell RNA sequencing would help to unravel CAF subpopulations in vitro and compare them to their counterparts found in vivo in CRC. This would also enable us to validate our complex in vitro culture models as physiologically highly relevant systems that accurately reflect CAF heterogeneity. Additionally, a direct contact co-culture of CAF and organoids should be implemented, further investigating the role of myCAF phenotype and its impact on ECM remodelling and cancer growth over a longer period. Moreover, the impact of CAF cytokines and markers on immune cells needs to be assessed.

6. Literature

Abudukelimu, S., de Miranda, N. F. C. C., & Hawinkels, L. J. A. C. (2024). Fibroblasts in Orchestrating Colorectal Tumourigenesis and Progression. In *CMGH* (Vol. 17, Issue 5, pp. 821–826). Elsevier Inc. https://doi.org/10.1016/j.jcmgh.2024.01.013

Akimoto, N., Ugai, T., Zhong, R., Hamada, T., Fujiyoshi, K., Giannakis, M., Wu, K., Cao, Y., Ng, K., & Ogino, S. (2021). Rising incidence of early-onset colorectal cancer — a call to action. *Nature Reviews Clinical Oncology*, *18*(4), 230–243. https://doi.org/10.1038/s41571-020-00445-1

Alaryani, F. S., & Alrdahe, S. S. (2022). A REVIEW OF TREATMENT, RISK FACTORS, AND INCIDENCE OF COLORECTAL CANCER. In *International Journal of Applied Pharmaceutics* (Vol. 14, Issue 1, pp. 1–6). Innovare Academics Sciences Pvt. Ltd. https://doi.org/10.22159/ijap.2022v14i1.42820

Albrengues, J., Bertero, T., Grasset, E., Bonan, S., Maiel, M., Bourget, I., Philippe, C., Herraiz Serrano, C., Benamar, S., Croce, O., Sanz-Moreno, V., Meneguzzi, G., Feral, C. C., Cristofari, G., & Gaggioli, C. (2015). Epigenetic switch drives the conversion of fibroblasts into proinvasive cancer-associated fibroblasts. *Nature Communications*, *6*. https://doi.org/10.1038/ncomms10204

Allen, J. E. (2024a). IL-4 and IL-13: Regulators and Effectors of Wound Repair. *Annual Review of Immunology*. https://doi.org/10.1146/annurev-immunol-101921

Aoudjehane, L., Pissaia, A., Scatton, O., Podevin, P., Massault, P. P., Chouzenoux, S., Soubrane, O., Calmus, Y., & Conti, F. (2008). Interleukin-4 induces the activation and collagen production of cultured human intrahepatic fibroblasts via the STAT-6 pathway. *Laboratory Investigation*, *88*(9), 973–985. https://doi.org/10.1038/labinvest.2008.61

Arena, E. A., & Bilchik, A. J. (n.d.). *What is the Optimal Means of Staging Colon Cancer?*

Arnold, M., Sierra, M. S., Laversanne, M., Soerjomataram, I., Jemal, A., & Bray, F. (2017). Global patterns and trends in colorectal cancer incidence and mortality. *Gut*, *66*(4), 683–691. https://doi.org/10.1136/gutjnl-2015-310912

Asif, P. J., Longobardi, C., Hahne, M., & Medema, J. P. (2021). The role of cancer-associated fibroblasts in cancer invasion and metastasis. In *Cancers* (Vol. 13, Issue 18). MDPI. https://doi.org/10.3390/cancers13184720

Atanasova, V. S., de Jesus Cardona, C., Hejret, V., Tiefenbacher, A., Mair, T., Tran, L., Pfneissl, J., Draganić, K., Binder, C., Kabiljo, J., Clement, J., Woeran, K., Neudert, B., Wohlhaupter, S., Haase, A., Domazet, S., Hengstschläger, M., Mitterhauser, M., Müllauer, L., … Egger, G. (2023). Mimicking Tumour Cell Heterogeneity of Colorectal Cancer in a Patient-derived Organoid-Fibroblast Model. *CMGH*, *15*(6), 1391–1419. https://doi.org/10.1016/j.jcmgh.2023.02.014

Avagliano, A., Granato, G., Ruocco, M. R., Romano, V., Belviso, I., Carfora, A., Montagnani, S., & Arcucci, A. (2018). Metabolic Reprogramming of Cancer Associated Fibroblasts:

The Slavery of Stromal Fibroblasts. In *BioMed Research International* (Vol. 2018). Hindawi Limited. https://doi.org/10.1155/2018/6075403

Avery, D., Govindaraju, P., Jacob, M., Todd, L., Monslow, J., & Puré, E. (2018). Extracellular matrix directs phenotypic heterogeneity of activated fibroblasts. *Matrix Biology*, *67*, 90–106. https://doi.org/10.1016/j.matbio.2017.12.003

Awaji, M., Saxena, S., Wu, L., Prajapati, D. R., Purohit, A., Varney, M. L., Kumar, S., Rachagani, S., Ly, Q. P., Jain, M., Batra, S. K., & Singh, R. K. (2020). CXCR2 signaling promotes secretory cancer-associated fibroblasts in pancreatic ductal adenocarcinoma. *FASEB Journal*, *34*(7), 9405–9418. https://doi.org/10.1096/fj.201902990R

Bailey, J. R., Bland, P. W., Tarlton, J. F., Peters, I., Moorghen, M., Sylvester, P. A., Probert, C. S. J., & Whiting, C. V. (2012). IL-13 Promotes Collagen Accumulation in Crohn's Disease Fibrosis by Down-Regulation of Fibroblast MMP Synthesis: A Role for Innate Lymphoid Cells? *PLoS ONE*, *7*(12). https://doi.org/10.1371/journal.pone.0052332

Bansal, R., Tomar, T., Oštman, A., Poelstra, K., & Prakash, J. (2012). Selective targeting of interferon γ to stromal fibroblasts and pericytes as a novel therapeutic approach to inhibit angiogenesis and tumour growth. *Molecular Cancer Therapeutics*, *11*(11), 2419–2428. https://doi.org/10.1158/1535-7163.MCT-11-0758

Barrett, R., & Puré, E. (2020). Cancer-associated fibroblasts: key determinants of tumour immunity and immunotherapy. In *Current Opinion in Immunology* (Vol. 64, pp. 80–87). Elsevier Ltd. https://doi.org/10.1016/j.coi.2020.03.004

Bartolomé, R. A., García-Palmero, I., Torres, S., López-Lucendo, M., Balyasnikova, I. V., & Casal, J. I. (2015). IL13 receptor α2 signaling requires a scaffold protein, FAM120A, to activate the FAK and PI3K pathways in colon cancer metastasis. *Cancer Research*, *75*(12), 2434–2444. https://doi.org/10.1158/0008-5472.CAN-14-3650

Bartoschek, M., Oskolkov, N., Bocci, M., Lövrot, J., Larsson, C., Sommarin, M., Madsen, C. D., Lindgren, D., Pekar, G., Karlsson, G., Ringnér, M., Bergh, J., Björklund, Å., & Pietras, K. (2018). Spatially and functionally distinct subclasses of breast cancer-associated fibroblasts revealed by single cell RNA sequencing. *Nature Communications*, *9*(1). https://doi.org/10.1038/s41467-018-07582-3

Belhabib, I., Zaghdoudi, S., Lac, C., Bousquet, C., & Jean, C. (2021). Extracellular matrices and cancer-associated fibroblasts: Targets for cancer diagnosis and therapy? In *Cancers* (Vol. 13, Issue 14). MDPI AG. https://doi.org/10.3390/cancers13143466

Bent, R., Moll, L., Grabbe, S., & Bros, M. (2018). Interleukin-1 beta—A friend or foe in malignancies? In *International Journal of Molecular Sciences* (Vol. 19, Issue 8). MDPI AG. https://doi.org/10.3390/ijms19082155

Bhattacharjee, S., Hamberger, F., Ravichandra, A., Miller, M., Nair, A., Affo, S., Filliol, A., Chin, L. K., Savage, T. M., Yin, D., Wirsik, N. M., Mehal, A., Arpaia, N., Seki, E., Mack, M., Zhu, D., Sims, P. A., Kalluri, R., Stanger, B. Z., … Schwabe, R. F. (2021). Tumour restriction by type I collagen opposes tumour-promoting effects of cancer-associated fibroblasts. *Journal of Clinical Investigation*, *131*(11). https://doi.org/10.1172/JCI146987

Biffi, G., Oni, T. E., Spielman, B., Hao, Y., Elyada, E., Park, Y., Preall, J., & Tuveson, D. A. (2019). Il1-induced Jak/STAT signaling is antagonized by TGFβ to shape CAF heterogeneity in pancreatic ductal adenocarcinoma. *Cancer Discovery*, *9*(2), 282–301. https://doi.org/10.1158/2159-8290.CD-18-0710

Biffi, G., & Tuveson, D. A. (2021). Diversity and biology of cancerassociated fibroblasts. *Physiological Reviews*, *101*(1), 147–176. https://doi.org/10.1152/physrev.00048.2019

Boland, P. M., & Ma, W. W. (2017). Immunotherapy for colorectal cancer. In *Cancers* (Vol. 9, Issue 5). MDPI AG. https://doi.org/10.3390/cancers9050050

Boraldi, F., Lofaro, F. D., Bonacorsi, S., Mazzilli, A., Garcia-Fernandez, M., & Quaglino, D. (2024). The Role of Fibroblasts in Skin Homeostasis and Repair. In *Biomedicines* (Vol. 12, Issue 7). Multidisciplinary Digital Publishing Institute (MDPI). https://doi.org/10.3390/biomedicines12071586

Borowczak, J., Szczerbowski, K., Maniewski, M., Kowalewski, A., Janiczek-Polewska, M., Szylberg, A., Marszałek, A., & Szylberg, Ł. (2022). The Role of Inflammatory Cytokines in the Pathogenesis of Colorectal Carcinoma—Recent Findings and Review. In *Biomedicines* (Vol. 10, Issue 7). MDPI. https://doi.org/10.3390/biomedicines10071670

Braumüller, H., Mauerer, B., Andris, J., Berlin, C., Wieder, T., & Kesselring, R. (2023). The Cytokine Network in Colorectal Cancer: Implications for New Treatment Strategies. In *Cells* (Vol. 12, Issue 1). MDPI. https://doi.org/10.3390/cells12010138

Brown, M. A., & Ried, T. (2022). Shifting the Focus of Signaling Abnormalities in Colon Cancer. In *Cancers* (Vol. 14, Issue 3). MDPI. https://doi.org/10.3390/cancers14030784

Bueno-Urquiza, L. J., Godínez-Rubí, M., Villegas-Pineda, J. C., Vega-Magaña, A. N., Jave-Suárez, L. F., Puebla-Mora, A. G., Aguirre-Sandoval, G. E., Martínez-Silva, M. G., Ramírez-de-Arellano, A., & Pereira-Suárez, A. L. (2024). Phenotypic Heterogeneity of Cancer Associated Fibroblasts in Cervical Cancer Progression: FAP as a Central Activation Marker. *Cells*, *13*(7). https://doi.org/10.3390/cells13070560

Burgos-Molina, A. M., Téllez Santana, T., Redondo, M., & Bravo Romero, M. J. (2024). The Crucial Role of Inflammation and the Immune System in Colorectal Cancer Carcinogenesis: A Comprehensive Perspective. In *International Journal of Molecular Sciences* (Vol. 25, Issue 11). Multidisciplinary Digital Publishing Institute (MDPI). https://doi.org/10.3390/ijms25116188

Busek, P., Mateu, R., Zubal, M., Kotackova, L., & Sedo, A. (2018). Targeting fibroblast activation protein in cancer-Prospects and caveats. In *Frontiers In Bioscience* (Vol. 23).

Calon, A., Lonardo, E., Berenguer-Llergo, A., Espinet, E., Hernando-Momblona, X., Iglesias, M., Sevillano, M., Palomo-Ponce, S., Tauriello, D. V. F., Byrom, D., Cortina, C., Morral, C., Barceló, C., Tosi, S., Riera, A., Attolini, C. S. O., Rossell, D., Sancho, E., & Batlle, E. (2015). Stromal gene expression defines poor-prognosis subtypes in colorectal cancer. *Nature Genetics*, *47*(4), 320–329. https://doi.org/10.1038/ng.3225

Calvo, F., Ege, N., Grande-Garcia, A., Hooper, S., Jenkins, R. P., Chaudhry, S. I., Harrington, K., Williamson, P., Moeendarbary, E., Charras, G., & Sahai, E. (2013).

Mechanotransduction and YAP-dependent matrix remodelling is required for the generation and maintenance of cancer-associated fibroblasts. *Nature Cell Biology*, *15*(6), 637–646. https://doi.org/10.1038/ncb2756

Cao, H., Zhang, J., Liu, H., Wan, L., Zhang, H., Huang, Q., Xu, E., & Lai, M. (2016). *IL-13/STAT6 signaling plays a critical role in the epithelial-mesenchymal transition of colorectal cancer cells*. www.impactjournals.com/oncotarget

Cao, Z., Quazi, S., Arora, S., Osellame, L. D., Burvenich, I. J., Janes, P. W., & Scott, A. M. (2025). Cancer-associated fibroblasts as therapeutic targets for cancer: advances, challenges, and future prospects. In *Journal of biomedical science* (Vol. 32, Issue 1, p. 7). https://doi.org/10.1186/s12929-024-01099-2

Carthy, J. M. (2018). TGFβ signaling and the control of myofibroblast differentiation: Implications for chronic inflammatory disorders. In *Journal of Cellular Physiology* (Vol. 233, Issue 1, pp. 98–106). Wiley-Liss Inc. https://doi.org/10.1002/jcp.25879

Cernat, L., Blaj, C., Jackstadt, R., Brandl, L., Engel, J., Hermeking, H., Jung, A., Kirchner, T., & Horst, D. (2014). Colorectal cancers mimic structural organization of normal colonic crypts. *PLoS ONE*, *9*(8). https://doi.org/10.1371/journal.pone.0104284

Chaffer, C. L., & Weinberg, R. A. (n.d.). *A Perspective on Cancer Cell Metastasis*. https://www.science.org

Chandra Jena, B., Sarkar, S., Rout, L., & Mandal, M. (2021). The transformation of cancer-associated fibroblasts: Current perspectives on the role of TGF-β in CAF mediated tumour progression and therapeutic resistance. In *Cancer Letters* (Vol. 520, pp. 222–232). Elsevier Ireland Ltd. https://doi.org/10.1016/j.canlet.2021.08.002

Chen, B., Chan, W. N., Xie, F., Mui, C. W., Liu, X., Cheung, A. H. K., Lung, R. W. M., Chow, C., Zhang, Z., Fang, C., Yu, P., Shi, S., Zhou, S., Chen, G., Wang, Z., Wang, S., Ding, X., Huang, B., Liang, L., … To, K. F. (2023). The molecular classification of cancer-associated fibroblasts on a pan-cancer single-cell transcriptional atlas. *Clinical and Translational Medicine*, *13*(12). https://doi.org/10.1002/ctm2.1516

Chen, B., Scurrah, C. R., McKinley, E. T., Simmons, A. J., Ramirez-Solano, M. A., Zhu, X., Markham, N. O., Heiser, C. N., Vega, P. N., Rolong, A., Kim, H., Sheng, Q., Drewes, J. L., Zhou, Y., Southard-Smith, A. N., Xu, Y., Ro, J., Jones, A. L., Revetta, F., … Lau, K. S. (2021). Differential pre-malignant programs and microenvironment chart distinct paths to malignancy in human colorectal polyps. *Cell*, *184*(26), 6262-6280.e26. https://doi.org/10.1016/j.cell.2021.11.031

Chen, S. X., Xu, X. E., Wang, X. Q., Cui, S. J., Xu, L. L., Jiang, Y. H., Zhang, Y., Yan, H. B., Zhang, Q., Qiao, J., Yang, P. Y., & Liu, F. (2014). Data from a proteomic analysis of colonic fibroblasts secretomes. *Data in Brief*, *1*, 19–24. https://doi.org/10.1016/j.dib.2014.08.003

Chen, Y., Liang, Z., & Lai, M. (2024). Targeting the devil: Strategies against cancer-associated fibroblasts in colorectal cancer. In *Translational Research* (Vol. 270, pp. 81–93). Elsevier Inc. https://doi.org/10.1016/j.trsl.2024.04.003

Chen, Y., McAndrews, K. M., & Kalluri, R. (2021). Clinical and therapeutic relevance of cancer-associated fibroblasts. In *Nature Reviews Clinical Oncology* (Vol. 18, Issue 12, pp. 792–804). Nature Research. https://doi.org/10.1038/s41571-021-00546-5

Chhabra, Y., & Weeraratna, A. T. (2023). Fibroblasts in cancer: Unity in heterogeneity. In *Cell* (Vol. 186, Issue 8, pp. 1580–1609). Elsevier B.V. https://doi.org/10.1016/j.cell.2023.03.016

Cho, C., Mukherjee, R., Peck, A. R., Sun, Y., McBrearty, N., Katlinski, K. V., Gui, J., Govindaraju, P. K., Puré, E., Rui, H., & Fuchs, S. Y. (2020). Cancer-associated fibroblasts downregulate type I interferon receptor to stimulate intratumoural stromagenesis. *Oncogene*, *39*(38), 6129–6137. https://doi.org/10.1038/s41388-020-01424-7

Choi, S. Y., Sung, R., Lee, S. J., Lee, T. G., Kim, N., Yoon, S. M., Lee, E. J., Chae, H. B., Youn, S. J., & Park, S. M. (2013). Podoplanin, α-smooth muscle actin or S100A4 expressing cancer-associated fibroblasts are associated with different prognosis in colorectal cancers. *Journal of Korean Medical Science*, *28*(9), 1293–1301. https://doi.org/10.3346/jkms.2013.28.9.1293

Comito, G., Giannoni, E., Segura, C. P., Barcellos-De-Souza, P., Raspollini, M. R., Baroni, G., Lanciotti, M., Serni, S., & Chiarugi, P. (2014). Cancer-associated fibroblasts and M2-polarized macrophages synergize during prostate carcinoma progression. *Oncogene*, *33*(19), 2423–2431. https://doi.org/10.1038/onc.2013.191

Cornista, A. M., Giolito, M. V., Baker, K., Hazime, H., Dufait, I., Datta, J., Khumukcham, S. S., De Ridder, M., Roper, J., Abreu, M. T., Breckpot, K., & Van der Jeught, K. (2023). Colorectal Cancer Immunotherapy: State of the Art and Future Directions. In *Gastro Hep Advances* (Vol. 2, Issue 8, pp. 1103–1119). American Gastroenterological Association. https://doi.org/10.1016/j.gastha.2023.09.007

Costa, A., Kieffer, Y., Scholer-Dahirel, A., Pelon, F., Bourachot, B., Cardon, M., Sirven, P., Magagna, I., Fuhrmann, L., Bernard, C., Bonneau, C., Kondratova, M., Kuperstein, I., Zinovyev, A., Givel, A. M., Parrini, M. C., Soumelis, V., Vincent-Salomon, A., & Mechta-Grigoriou, F. (2018). Fibroblast Heterogeneity and Immunosuppressive Environment in Human Breast Cancer. *Cancer Cell*, *33*(3), 463-479.e10. https://doi.org/10.1016/j.ccell.2018.01.011

Costa, A., Scholer-Dahirel, A., & Mechta-Grigoriou, F. (2014). The role of reactive oxygen species and metabolism on cancer cells and their microenvironment. In *Seminars in Cancer Biology* (Vol. 25, pp. 23–32). Academic Press. https://doi.org/10.1016/j.semcancer.2013.12.007

Coto-Llerena, M., Ercan, C., Kancherla, V., Taha-Mehlitz, S., Eppenberger-Castori, S., Soysal, S. D., Ng, C. K. Y., Bolli, M., von Flüe, M., Nicolas, G. P., Terracciano, L. M., Fani, M., & Piscuoglio, S. (2020). High Expression of FAP in Colorectal Cancer Is Associated With Angiogenesis and Immunoregulation Processes. *Frontiers in Oncology*, *10*. https://doi.org/10.3389/fonc.2020.00979

Croft, A. P., Naylor, A. J., Marshall, J. L., Hardie, D. L., Zimmermann, B., Turner, J., Desanti, G., Adams, H., Yemm, A. I., Müller-Ladner, U., Dayer, J. M., Neumann, E., Filer, A., & Buckley, C. D. (2016). Rheumatoid synovial fibroblasts differentiate into distinct subsets in the presence of cytokines and cartilage. *Arthritis Research and Therapy*, *18*(1). https://doi.org/10.1186/s13075-016-1156-1

Croizer, H., Mhaidly, R., Kieffer, Y., Gentric, G., Djerroudi, L., Leclere, R., Pelon, F., Robley, C., Bohec, M., Meng, A., Meseure, D., Romano, E., Baulande, S., Peltier, A., Vincent-Salomon, A., & Mechta-Grigoriou, F. (2024). Deciphering the spatial landscape and plasticity of immunosuppressive fibroblasts in breast cancer. *Nature Communications*, *15*(1). https://doi.org/10.1038/s41467-024-47068-z

Czekay, R. P., Cheon, D. J., Samarakoon, R., Kutz, S. M., & Higgins, P. J. (2022a). Cancer-Associated Fibroblasts: Mechanisms of Tumour Progression and Novel Therapeutic Targets. In *Cancers* (Vol. 14, Issue 5). MDPI. https://doi.org/10.3390/cancers14051231

Czekay, R. P., Cheon, D. J., Samarakoon, R., Kutz, S. M., & Higgins, P. J. (2022b). Cancer-Associated Fibroblasts: Mechanisms of Tumour Progression and Novel Therapeutic Targets. In *Cancers* (Vol. 14, Issue 5). MDPI. https://doi.org/10.3390/cancers14051231

Dang, H., Harryvan, T. J., Liao, C. Y., Danen, E. H. J., Spalburg, V. N. L. N., Kielbasa, S. M., Mei, H., Goeman, J. J., de Jonge-Muller, E. S., Janson, S. G. T., van der Reijden, J. J., Crobach, S., Hardwick, J. C. H., Boonstra, J. J., de Miranda, N. F. C. C., & Hawinkels, L. J. A. C. (2023). Cancer-Associated Fibroblasts Are Key Determinants of Cancer Cell Invasion in the Earliest Stage of Colorectal Cancer. *CMGH*, *16*(1), 107–131. https://doi.org/10.1016/j.jcmgh.2023.04.004

D'Arcangelo, E., Wu, N. C., Cadavid, J. L., & McGuigan, A. P. (2020a). The life cycle of cancer-associated fibroblasts within the tumour stroma and its importance in disease outcome. In *British Journal of Cancer* (Vol. 122, Issue 7, pp. 931–942). Springer Nature. https://doi.org/10.1038/s41416-019-0705-1

D'Arcangelo, E., Wu, N. C., Cadavid, J. L., & McGuigan, A. P. (2020b). The life cycle of cancer-associated fibroblasts within the tumour stroma and its importance in disease outcome. In *British Journal of Cancer* (Vol. 122, Issue 7, pp. 931–942). Springer Nature. https://doi.org/10.1038/s41416-019-0705-1

Das, S., Feng, Q., Balasubramanian, I., Lin, X., Liu, H., Pellón-Cardenas, O., Yu, S., Zhang, X., Liu, Y., Wei, Z., Bonder, E. M., Verzi, M. P., Hsu, W., Zhang, L., Wang, T. C., & Gao, N. (2022). Colonic healing requires Wnt produced by epithelium as well as Tagln+and Acta2+stromal cells. *Development (Cambridge)*, *149*(1). https://doi.org/10.1242/dev.199587

Dash, S., Sahu, A. K., Srivastava, A., Chowdhury, R., & Mukherjee, S. (2021). Exploring the extensive crosstalk between the antagonistic cytokines- TGF-β and TNF-α in regulating cancer pathogenesis. In *Cytokine* (Vol. 138). Academic Press. https://doi.org/10.1016/j.cyto.2020.155348

De Boeck, A., Hendrix, A., Maynard, D., Van Bockstal, M., Daniëls, A., Pauwels, P.,

Gespach, C., Bracke, M., & De Wever, O. (2013). Differential secretome analysis of cancer-associated fibroblasts and bone marrow-derived precursors to identify microenvironmental regulators of colon cancer progression. *Proteomics*, *13*(2), 379–388. https://doi.org/10.1002/pmic.201200179

de Visser, K. E., & Joyce, J. A. (2023). The evolving tumour microenvironment: From cancer initiation to metastatic outgrowth. In *Cancer Cell* (Vol. 41, Issue 3, pp. 374–403). Cell Press. https://doi.org/10.1016/j.ccell.2023.02.016

Deng, L., Jiang, N., Zeng, J., Wang, Y., & Cui, H. (2021). The Versatile Roles of Cancer-Associated Fibroblasts in Colorectal Cancer and Therapeutic Implications. In *Frontiers in Cell and Developmental Biology* (Vol. 9). Frontiers Media S.A. https://doi.org/10.3389/fcell.2021.733270

Dhungel, N., & Dragoi, A. M. (2024). Exploring the multifaceted role of direct interaction between cancer cells and fibroblasts in cancer progression. In *Frontiers in Molecular Biosciences* (Vol. 11). Frontiers Media SA. https://doi.org/10.3389/fmolb.2024.1379971

Di Maggio, F., & El-Shakankery, K. H. (2020). Desmoplasia and Biophysics in Pancreatic Ductal Adenocarcinoma: Can We Learn from Breast Cancer? In *Pancreas* (Vol. 49, Issue 3, pp. 313–325). Lippincott Williams and Wilkins. https://doi.org/10.1097/MPA.0000000000001504

Díaz-Maroto, N. G., Garcia-Vicién, G., Polcaro, G., Bañuls, M., Albert, N., Villanueva, A., & Molleví, D. G. (2021a). The blockade of tumoural il1β-mediated signaling in normal colonic fibroblasts sensitizes tumour cells to chemotherapy and prevents inflammatory caf activation. *International Journal of Molecular Sciences*, *22*(9). https://doi.org/10.3390/ijms22094960

Díaz-Maroto, N. G., Garcia-Vicién, G., Polcaro, G., Bañuls, M., Albert, N., Villanueva, A., & Molleví, D. G. (2021b). The blockade of tumoural il1β-mediated signaling in normal colonic fibroblasts sensitizes tumour cells to chemotherapy and prevents inflammatory caf activation. *International Journal of Molecular Sciences*, *22*(9). https://doi.org/10.3390/ijms22094960

Díaz-Maroto, N. G., Sanz-Pamplona, R., Berdiel-Acer, M., Cimas, F. J., García, E., Gonçalves-Ribeiro, S., Albert, N., Garcia-Vicien, G., Capella, G., Moreno, V., Salazar, R., Villanueva, A., & Molleví, D. G. (2019a). Noncanonical TGFb pathway relieves the blockade of IL1B/TGFb-mediated crosstalk between tumour and stroma: TGFBR1 and TAK1 inhibition in colorectal cancer. *Clinical Cancer Research*, *25*(14), 4466–4479. https://doi.org/10.1158/1078-0432.CCR-18-3957

Díaz-Maroto, N. G., Sanz-Pamplona, R., Berdiel-Acer, M., Cimas, F. J., García, E., Gonçalves-Ribeiro, S., Albert, N., Garcia-Vicien, G., Capella, G., Moreno, V., Salazar, R., Villanueva, A., & Molleví, D. G. (2019b). Noncanonical TGFb pathway relieves the blockade of IL1B/TGFb-mediated crosstalk between tumour and stroma: TGFBR1 and TAK1 inhibition in colorectal cancer. *Clinical Cancer Research*, *25*(14), 4466–4479. https://doi.org/10.1158/1078-0432.CCR-18-3957

Dobre, M., Salvi, A., Pelisenco, I. A., Vasilescu, F., De Petro, G., Herlea, V., & Milanesi, E. (2021). Crosstalk Between DNA Methylation and Gene Mutations in Colorectal Cancer. *Frontiers in Oncology*, *11*. https://doi.org/10.3389/fonc.2021.697409

Drost, J., Van Jaarsveld, R. H., Ponsioen, B., Zimberlin, C., Van Boxtel, R., Buijs, A., Sachs, N., Overmeer, R. M., Offerhaus, G. J., Begthel, H., Korving, J., Van De Wetering, M., Schwank, G., Logtenberg, M., Cuppen, E., Snippert, H. J., Medema, J. P., Kops, G. J. P. L., & Clevers, H. (2015). Sequential cancer mutations in cultured human intestinal stem cells. *Nature*, *521*(7550), 43–47. https://doi.org/10.1038/nature14415

Dunn, G. P., Old, L. J., & Schreiber, R. D. (2004). The three Es of cancer immunoediting. In *Annual Review of Immunology* (Vol. 22, pp. 329–360). https://doi.org/10.1146/annurev.immunol.22.012703.104803

Dunne, P. D., & Arends, M. J. (2024). Molecular pathological classification of colorectal cancer—an update. In *Virchows Archiv* (Vol. 484, Issue 2, pp. 273–285). Springer Science and Business Media Deutschland GmbH. https://doi.org/10.1007/s00428-024-03746-3

Ekwall, A. K. H., Eisler, T., Anderberg, C., Jin, C., Karlsson, N., Brisslert, M., & Bokarewa, M. I. (2011). The tumour-associated glycoprotein podoplanin is expressed in fibroblast-like synoviocytes of the hyperplastic synovial lining layer in rheumatoid arthritis. *Arthritis Research and Therapy*, *13*(2). https://doi.org/10.1186/ar3274

Elyada, E., Bolisetty, M., Laise, P., Flynn, W. F., Courtois, E. T., Burkhart, R. A., Teinor, J. A., Belleau, P., Biffi, G., Lucito, M. S., Sivajothi, S., Armstrong, T. D., Engle, D. D., Yu, K. H., Hao, Y., Wolfgang, C. L., Park, Y., Preall, J., Jaffee, E. M., … Tuveson, D. A. (2019). Cross-species single-cell analysis of pancreatic ductal adenocarcinoma reveals antigen-presenting cancer-associated fibroblasts. In *Cancer Discovery* (Vol. 9, Issue 8, pp. 1102–1123). American Association for Cancer Research Inc. https://doi.org/10.1158/2159-8290.CD-19-0094

Ercolano, G., Gomez-Cadena, A., Dumauthioz, N., Vanoni, G., Kreutzfeldt, M., Wyss, T., Michalik, L., Loyon, R., Ianaro, A., Ho, P. C., Borg, C., Kopf, M., Merkler, D., Krebs, P., Romero, P., Trabanelli, S., & Jandus, C. (2021). PPARγ drives IL-33-dependent ILC2 pro-tumoural functions. *Nature Communications*, *12*(1). https://doi.org/10.1038/s41467-021-22764-2

Erdogan, B., & Webb, D. J. (2017). Cancer-associated fibroblasts modulate growth factor signaling and extracellular matrix remodeling to regulate tumour metastasis. In *Biochemical Society Transactions* (Vol. 45, Issue 1, pp. 229–236). Portland Press Ltd. https://doi.org/10.1042/BST20160387

Erez, N., Truitt, M., Olson, P., & Hanahan, D. (2010). Cancer-Associated Fibroblasts Are Activated in Incipient Neoplasia to Orchestrate Tumour-Promoting Inflammation in an NF-κB-Dependent Manner. *Cancer Cell*, *17*(2), 135–147. https://doi.org/10.1016/j.ccr.2009.12.041

Fan, A., Wang, B., Wang, X., Nie, Y., Fan, D., Zhao, X., & Lu, Y. (2021). Immunotherapy in

colorectal cancer: Current achievements and future perspective. In *International Journal of Biological Sciences* (Vol. 17, Issue 14, pp. 3837–3849). Ivyspring International Publisher. https://doi.org/10.7150/IJBS.64077

Fang, Z., Meng, Q., Xu, J., Wang, W., Zhang, B., Liu, J., Liang, C., Hua, J., Zhao, Y., Yu, X., & Shi, S. (2023). Signaling pathways in cancer-associated fibroblasts: recent advances and future perspectives. In *Cancer Communications* (Vol. 43, Issue 1, pp. 3–41). John Wiley and Sons Inc. https://doi.org/10.1002/cac2.12392

Fares, J., Fares, M. Y., Khachfe, H. H., Salhab, H. A., & Fares, Y. (2020). Molecular principles of metastasis: a hallmark of cancer revisited. In *Signal Transduction and Targeted Therapy* (Vol. 5, Issue 1). Springer Nature. https://doi.org/10.1038/s41392-020-0134-x

Fearon, D. T. (2014). The carcinoma-associated fibroblast expressing fibroblast activation protein and escape from immune surveillance. *Cancer Immunology Research*, *2*(3), 187–193. https://doi.org/10.1158/2326-6066.CIR-14-0002

Fearon, E. F., & Vogelstein, B. (1990). A Genetic Model for Colorectal Tumourigenesis. In *Cell* (Vol. 61).

Feig, C., Jones, J. O., Kraman, M., Wells, R. J. B., Deonarine, A., Chan, D. S., Connell, C. M., Roberts, E. W., Zhao, Q., Caballero, O. L., Teichmann, S. A., Janowitz, T., Jodrell, D. I., Tuveson, D. A., & Fearon, D. T. (2013). Targeting CXCL12 from FAP-expressing carcinoma-associated fibroblasts synergizes with anti-PD-L1 immunotherapy in pancreatic cancer. *Proceedings of the National Academy of Sciences of the United States of America*, *110*(50), 20212–20217. https://doi.org/10.1073/pnas.1320318110

Fiorini, E., Veghini, L., & Corbo, V. (2020). Modeling Cell Communication in Cancer With Organoids: Making the Complex Simple. In *Frontiers in Cell and Developmental Biology* (Vol. 8). Frontiers Media S.A. https://doi.org/10.3389/fcell.2020.00166

Fitzgerald, A. A., & Weiner, L. M. (2020). The role of fibroblast activation protein in health and malignancy. In *Cancer and Metastasis Reviews* (Vol. 39, Issue 3, pp. 783–803). Springer. https://doi.org/10.1007/s10555-020-09909-3

Formica, V., Cereda, V., Nardecchia, A., Tesauro, M., & Roselli, M. (2014). Immune reaction and colorectal cancer: Friends or foes? In *World Journal of Gastroenterology* (Vol. 20, Issue 35, pp. 12407–12419). WJG Press. https://doi.org/10.3748/wjg.v20.i35.12407

Foster, D. S., Jones, R. E., Ransom, R. C., Longaker, M. T., & Norton, J. A. (2018). The evolving relationship of wound healing and tumour stroma. In *JCI insight* (Vol. 3, Issue 18). NLM (Medline). https://doi.org/10.1172/jci.insight.99911

Fotsitzoudis, C., Koulouridi, A., Messaritakis, I., Konstantinidis, T., Gouvas, N., Tsiaoussis, J., & Souglakos, J. (2022). Cancer-Associated Fibroblasts: The Origin, Biological Characteristics and Role in Cancer—A Glance on Colorectal Cancer. In *Cancers* (Vol. 14, Issue 18). MDPI. https://doi.org/10.3390/cancers14184394

Franzè, E., Di Grazia, A., Sica, G. S., Biancone, L., Laudisi, F., & Monteleone, G. (2020). Interleukin-34 enhances the tumour promoting function of colorectal cancer-associated

fibroblasts. *Cancers*, *12*(12), 1–15. https://doi.org/10.3390/cancers12123537
Friedenreich, C. M., Ryder-Burbidge, C., & McNeil, J. (2021). Physical activity, obesity and sedentary behavior in cancer etiology: epidemiologic evidence and biologic mechanisms. In *Molecular Oncology* (Vol. 15, Issue 3, pp. 790–800). John Wiley and Sons Ltd. https://doi.org/10.1002/1878-0261.12772
Furuhashi, S., Bustos, M. A., Mizuno, S., Ryu, S., Naeini, Y., Bilchik, A. J., & Hoon, D. S. B. (2023). Spatial profiling of cancer-associated fibroblasts of sporadic early onset colon cancer microenvironment. *Npj Precision Oncology*, *7*(1). https://doi.org/10.1038/s41698-023-00474-w
Gabasa, M., Royo, D., Molina-Molina, M., Roca-Ferrer, J., Pujols, L., Picado, C., Xaubet, A., & Pereda, J. (2013). Lung Myofibroblasts Are Characterized by Down-Regulated Cyclooxygenase-2 and Its Main Metabolite, Prostaglandin E2. *PLoS ONE*, *8*(6). https://doi.org/10.1371/journal.pone.0065445
Gallicchio, L., Devasia, T. P., Tonorezos, E., Mollica, M. A., & Mariotto, A. (2022). Estimation of the Number of Individuals Living with Metastatic Cancer in the United States. *Journal of the National Cancer Institute*, *114*(11), 1476–1483. https://doi.org/10.1093/jnci/djac158
Gallo, G., Vescio, G., De Paola, G., & Sammarco, G. (2021). Therapeutic targets and tumour microenvironment in colorectal cancer. In *Journal of Clinical Medicine* (Vol. 10, Issue 11). MDPI. https://doi.org/10.3390/jcm10112295
Ganesh, K. (2022). Optimizing immunotherapy for colorectal cancer. In *Nature Reviews Gastroenterology and Hepatology* (Vol. 19, Issue 2, pp. 93–94). Nature Research. https://doi.org/10.1038/s41575-021-00569-4
Ganguly, D., Chandra, R., Karalis, J., Teke, M., Aguilera, T., Maddipati, R., Wachsmann, M. B., Ghersi, D., Siravegna, G., Zeh, H. J., Brekken, R., Ting, D. T., & Ligorio, M. (2020). Cancer-associated fibroblasts: Versatile players in the tumour microenvironment. In *Cancers* (Vol. 12, Issue 9, pp. 1–35). MDPI AG. https://doi.org/10.3390/cancers12092652
Gao, H., Tian, Q., Zhu, L., Feng, J., Zhou, Y., & Yang, J. (2021). 3D Extracellular Matrix Regulates the Activity of T Cells and Cancer Associated Fibroblasts in Breast Cancer. *Frontiers in Oncology*, *11*. https://doi.org/10.3389/fonc.2021.764204
Garate, E., Serrano-Mendioroz, I., Fernandez, L., Andrea, C. Ed., Barrio-Alonso, C., Herrero, C., Luri-Rey, C., Teijeira, A., Claus, C., Tanos, T., Klein, C., Umaña, P., Rullan, A., Simon, J. A., Collantes, M., Sanchez-Mateos, P., Melero, I., & Rodriguez-Ruiz, M. E. (2024). *781 4–1BB agonist targeted to fibroblast activation protein α synergizes with radiotherapy to treat murine breast tumour models*. A886–A886. https://doi.org/10.1136/jitc-2024-sitc2024.0781
Gelfo, V., Mazzeschi, M., Grilli, G., Lindzen, M., Santi, S., D'uva, G., Győrffy, B., Ardizzoni, A., Yarden, Y., & Lauriola, M. (2018). A novel role for the interleukin-1 receptor axis in resistance to anti-EGFR therapy. *Cancers*, *10*(10).

https://doi.org/10.3390/cancers10100355
Geng, X., Chen, H., Zhao, L., Hu, J., Yang, W., Li, G., Cheng, C., Zhao, Z., Zhang, T., Li, L., & Sun, B. (2021). Cancer-Associated Fibroblast (CAF) Heterogeneity and Targeting Therapy of CAFs in Pancreatic Cancer. In *Frontiers in Cell and Developmental Biology* (Vol. 9). Frontiers Media S.A. https://doi.org/10.3389/fcell.2021.655152
Gieseck, R. L., Ramalingam, T. R., Hart, K. M., Vannella, K. M., Cantu, D. A., Lu, W. Y., Ferreira-González, S., Forbes, S. J., Vallier, L., & Wynn, T. A. (2016). Interleukin-13 Activates Distinct Cellular Pathways Leading to Ductular Reaction, Steatosis, and Fibrosis. *Immunity*, *45*(1), 145–158. https://doi.org/10.1016/j.immuni.2016.06.009
Glabman, R. A., Choyke, P. L., & Sato, N. (2022). Cancer-Associated Fibroblasts: Tumourigenicity and Targeting for Cancer Therapy. In *Cancers* (Vol. 14, Issue 16). MDPI. https://doi.org/10.3390/cancers14163906
Goldberg, M. T., Han, Y. P., Yan, C., Shaw, M. C., & Garner, W. L. (2007). TNF-α suppresses α-smooth muscle actin expression in human dermal fibroblasts: An implication for abnormal wound healing. *Journal of Investigative Dermatology*, *127*(11), 2645–2655. https://doi.org/10.1038/sj.jid.5700890
Goldberg, M. T., Han, Y.-P., Yan, C., Shaw, M. C., & Garner, W. L. (n.d.). *TNF-α Suppresses α-Smooth Muscle Actin Expression in Human Dermal Fibroblasts: An Implication for Abnormal Wound Healing*.
Golshani, G., & Zhang, Y. (2020). Advances in immunotherapy for colorectal cancer: a review. In *Therapeutic Advances in Gastroenterology* (Vol. 13). SAGE Publications Ltd. https://doi.org/10.1177/1756284820917527
Gorchs, L., Hellevik, T., Bruun, J. A., Camilio, K. A., Al-Saad, S., Stuge, T. B., & Martinez-Zubiaurre, I. (2015). Cancer-associated fibroblasts from lung tumours maintain their immunosuppressive abilities after high-dose irradiation. *Frontiers in Oncology*, *5*(MAY). https://doi.org/10.3389/fonc.2015.00087
Gorchs, L., Moro, C. F., Bankhead, P., Kern, K. P., Sadeak, I., Meng, Q., Rangelova, E., & Kaipe, H. (2019). Human pancreatic carcinoma-associated fibroblasts promote expression of co-inhibitory markers on CD4+ and CD8+ T-cells. *Frontiers in Immunology*, *10*(APR). https://doi.org/10.3389/fimmu.2019.00847
Gour, N., & Wills-Karp, M. (2015). IL-4 and IL-13 signaling in allergic airway disease. In *Cytokine* (Vol. 75, Issue 1, pp. 68–78). Academic Press. https://doi.org/10.1016/j.cyto.2015.05.014
Grauel, A. L., Nguyen, B., Ruddy, D., Laszewski, T., Schwartz, S., Chang, J., Chen, J., Piquet, M., Pelletier, M., Yan, Z., Kirkpatrick, N. D., Wu, J., deWeck, A., Riester, M., Hims, M., Geyer, F. C., Wagner, J., MacIsaac, K., Deeds, J., … Cremasco, V. (2020). TGFβ-blockade uncovers stromal plasticity in tumours by revealing the existence of a subset of interferon-licensed fibroblasts. *Nature Communications*, *11*(1). https://doi.org/10.1038/s41467-020-19920-5
Grivennikov, S. I., Wang, K., Mucida, D., Stewart, C. A., Schnabl, B., Jauch, D., Taniguchi,

K., Yu, G. Y., Österreicher, C. H., Hung, K. E., Datz, C., Feng, Y., Fearon, E. R., Oukka, M., Tessarollo, L., Coppola, V., Yarovinsky, F., Cheroutre, H., Eckmann, L., … Karin, M. (2012). Adenoma-linked barrier defects and microbial products drive IL-23/IL-17-mediated tumour growth. *Nature*, *491*(7423), 254–258. https://doi.org/10.1038/nature11465

Groenendijk, F. H., & Bernards, R. (2014). Drug resistance to targeted therapies: Déjà vu all over again. In *Molecular Oncology* (Vol. 8, Issue 6, pp. 1067–1083). Elsevier B.V. https://doi.org/10.1016/j.molonc.2014.05.004

Guinney, J., Dienstmann, R., Wang, X., De Reyniès, A., Schlicker, A., Soneson, C., Marisa, L., Roepman, P., Nyamundanda, G., Angelino, P., Bot, B. M., Morris, J. S., Simon, I. M., Gerster, S., Fessler, E., De Sousa E Melo, F., Missiaglia, E., Ramay, H., Barras, D., … Tejpar, S. (2015). *The Consensus Molecular Subtypes of Colorectal Cancer*. https://doi.org/10.7303/syn2623706

Guo, L., Wang, C., Qiu, X., Pu, X., & Chang, P. (2020). Colorectal Cancer Immune Infiltrates: Significance in Patient Prognosis and Immunotherapeutic Efficacy. In *Frontiers in Immunology* (Vol. 11). Frontiers Media S.A. https://doi.org/10.3389/fimmu.2020.01052

Guo, Q., Jin, Y., Chen, X., Ye, X., Shen, X., Lin, M., Zeng, C., Zhou, T., & Zhang, J. (2024). NF-κB in biology and targeted therapy: new insights and translational implications. In *Signal Transduction and Targeted Therapy* (Vol. 9, Issue 1). Springer Nature. https://doi.org/10.1038/s41392-024-01757-9

Han, C., Liu, T., & Yin, R. (2020). Biomarkers for cancer-associated fibroblasts. In *Biomarker Research* (Vol. 8, Issue 1). BioMed Central Ltd. https://doi.org/10.1186/s40364-020-00245-w

Hanahan, D. (2022). Hallmarks of Cancer: New Dimensions. In *Cancer Discovery* (Vol. 12, Issue 1, pp. 31–46). American Association for Cancer Research Inc. https://doi.org/10.1158/2159-8290.CD-21-1059

Hanahan, D., & Weinberg, R. A. (2011). Hallmarks of cancer: The next generation. In *Cell* (Vol. 144, Issue 5, pp. 646–674). https://doi.org/10.1016/j.cell.2011.02.013

Hanley, C. J., Noble, F., Ward, M., Bullock, M., Drifka, C., Mellone, M., Manousopoulou, A., Johnston, H. E., Hayden, A., Thirdborough, S., Liu, Y., Smith, D. M., Mellows, T., Kao, W. J., Garbis, S. D., Mirnezami, A., Underwood, T. J., Eliceiri, K. W., & Thomas, G. J. (n.d.). *A subset of myofibroblastic cancer-associated fibroblasts regulate collagen fiber elongation, which is prognostic in multiple cancers* (Vol. 7, Issue 5). www.impactjournals.com/oncotarget

Hassametto, A., Tanomrat, R., Muangthong, T., Worawichawong, S., & Suwannalert, P. (2023). Role of Oxidative Stress-Dependent C/EBPβ Expression on CAF Transformation Inducing HCT116 Colorectal Cancer Cell Progression; Migration and Invasion. *Asian Pacific Journal of Cancer Prevention*, *24*(11), 3825–3835. https://doi.org/10.31557/APJCP.2023.24.11.3825

Hawinkels, L. J. A. C., Paauwe, M., Verspaget, H. W., Wiercinska, E., Van Der Zon, J. M.,

Van Der Ploeg, K., Koelink, P. J., Lindeman, J. H. N., Mesker, W., Ten Dijke, P., & Sier, C. F. M. (2014). Interaction with colon cancer cells hyperactivates TGF-β signaling in cancer-associated fibroblasts. *Oncogene*, *33*(1), 97–107. https://doi.org/10.1038/onc.2012.536

Henrich, L. M., Greimelmaier, K., Wessolly, M., Klopp, N. A., Mairinger, E., Krause, Y., Berger, S., Wohlschlaeger, J., Schildhaus, H. U., Baba, H. A., Mairinger, F. D., & Borchert, S. (2024). The Impact of Cancer-Associated Fibroblasts on the Biology and Progression of Colorectal Carcinomas. *Genes*, *15*(2). https://doi.org/10.3390/genes15020209

Henriksson, M. L., Edin, S., Dahlin, A. M., Oldenborg, P. A., Öberg, Å., Van Guelpen, B., Rutegård, J., Stenling, R., & Palmqvist, R. (2011). Colorectal cancer cells activate adjacent fibroblasts resulting in FGF1/FGFR3 signaling and increased invasion. *American Journal of Pathology*, *178*(3), 1387–1394. https://doi.org/10.1016/j.ajpath.2010.12.008

Henry, L. R., Lee, H. O., Lee, J. S., Klein-Szanto, A., Watts, P., Ross, E. A., Chen, W. T., & Cheng, J. D. (2007). Clinical implications of fibroblast activation protein in patients with colon cancer. *Clinical Cancer Research*, *13*(6), 1736–1741. https://doi.org/10.1158/1078-0432.CCR-06-1746

Herrera, M., Herrera, A., Domínguez, G., Silva, J., García, V., García, J. M., Gómez, I., Soldevilla, B., Muñoz, C., Provencio, M., Campos-Martin, Y., García de Herreros, A., Casal, I., Bonilla, F., & Peña, C. (2013). Cancer-associated fibroblast and M2 macrophage markers together predict outcome in colorectal cancer patients. *Cancer Science*, *104*(4), 437–444. https://doi.org/10.1111/cas.12096

Hinz, B. (2016). The role of myofibroblasts in wound healing. *Current Research in Translational Medicine*, *64*(4), 171–177. https://doi.org/10.1016/j.retram.2016.09.003

Hinz, B., & Lagares, D. (n.d.-a). *Myoo broblasts Methods and Protocols Methods in Molecular Biology 2299*. http://www.springer.com/series/7651

Hinz, B., & Lagares, D. (n.d.-b). *Myoo broblasts Methods and Protocols Methods in Molecular Biology 2299*. http://www.springer.com/series/7651

Hinz, B., & Lagares, D. (n.d.-c). *Myoo broblasts Methods and Protocols Methods in Molecular Biology 2299*. http://www.springer.com/series/7651

Hirano, H., Takashima, A., Hamaguchi, T., Shida, D., & Kanemitsu, Y. (2021). Current status and perspectives of immune checkpoint inhibitors for colorectal cancer. In *Japanese Journal of Clinical Oncology* (Vol. 51, Issue 1, pp. 10–19). Oxford University Press. https://doi.org/10.1093/jjco/hyaa200

Holbrook, J., Lara-Reyna, S., Jarosz-Griffiths, H., & McDermott, M. (2019). Tumour necrosis factor signalling in health and disease. In *F1000Research* (Vol. 8). F1000 Research Ltd. https://doi.org/10.12688/f1000research.17023.1

Hossain, M. S., Karuniawati, H., Jairoun, A. A., Urbi, Z., Ooi, D. J., John, A., Lim, Y. C., Kaderi Kibria, K. M., Mohiuddin, A. K. M., Ming, L. C., Goh, K. W., & Hadi, M. A. (2022).

Colorectal Cancer: A Review of Carcinogenesis, Global Epidemiology, Current Challenges, Risk Factors, Preventive and Treatment Strategies. In *Cancers* (Vol. 14, Issue 7). MDPI. https://doi.org/10.3390/cancers14071732

Hou, W., Yi, C., & Zhu, H. (2022). Predictive biomarkers of colon cancer immunotherapy: Present and future. In *Frontiers in Immunology* (Vol. 13). Frontiers Media S.A. https://doi.org/10.3389/fimmu.2022.1032314

Hu, G., Zhong, K., Chen, W., Wang, S., & Huang, L. (2018). Podoplanin-positive cancer-associated fibroblasts predict poor prognosis in lung cancer patients. *OncoTargets and Therapy*, *11*, 5607–5619. https://doi.org/10.2147/OTT.S175566

Hu, X., li, J., Fu, M., Zhao, X., & Wang, W. (2021). The JAK/STAT signaling pathway: from bench to clinic. In *Signal Transduction and Targeted Therapy* (Vol. 6, Issue 1). Springer Nature. https://doi.org/10.1038/s41392-021-00791-1

Huang, K. C. Y., Chiang, S. F., Chen, T. W., Chen, W. T. L., Yang, P. C., Ke, T. W., & Chao, K. S. C. (2020a). Prognostic relevance of programmed cell death 1 ligand 2 (PDCD1LG2/PD-L2) in patients with advanced stage colon carcinoma treated with chemotherapy. *Scientific Reports*, *10*(1). https://doi.org/10.1038/s41598-020-79419-3

Huang, K. C. Y., Chiang, S. F., Chen, T. W., Chen, W. T. L., Yang, P. C., Ke, T. W., & Chao, K. S. C. (2020b). Prognostic relevance of programmed cell death 1 ligand 2 (PDCD1LG2/PD-L2) in patients with advanced stage colon carcinoma treated with chemotherapy. *Scientific Reports*, *10*(1). https://doi.org/10.1038/s41598-020-79419-3

Huang, M., Fu, M., Wang, J., Xia, C., Zhang, H., Xiong, Y., He, J., Liu, J., Liu, B., Pan, S., & Liu, F. (2021). TGF-β1-activated cancer-associated fibroblasts promote breast cancer invasion, metastasis and epithelial-mesenchymal transition by autophagy or overexpression of FAP-α. *Biochemical Pharmacology*, *188*. https://doi.org/10.1016/j.bcp.2021.114527

IJsselsteijn, M. E., Sanz-Pamplona, R., Hermitte, F., & de Miranda, N. F. C. C. (2019). Colorectal cancer: A paradigmatic model for cancer immunology and immunotherapy. In *Molecular Aspects of Medicine* (Vol. 69, pp. 123–129). Elsevier Ltd. https://doi.org/10.1016/j.mam.2019.05.003

Ikuta, D., Miyake, T., Shimizu, T., Sonoda, H., Mukaisho, K.-I., Tokuda, A., Ueki, T., Sugihara, H., & Tani, M. (n.d.). *Fibrosis in metastatic lymph nodes is clinically correlated to poor prognosis in colorectal cancer*. www.oncotarget.com

Irvine, A. F., Waise, S., Green, E. W., Stuart, B., & Thomas, G. J. (2021). Characterising cancer-associated fibroblast heterogeneity in non-small cell lung cancer: a systematic review and meta-analysis. *Scientific Reports*, *11*(1). https://doi.org/10.1038/s41598-021-81796-2

Isella, C., Brundu, F., Bellomo, S. E., Galimi, F., Zanella, E., Porporato, R., Petti, C., Fiori, A., Orzan, F., Senetta, R., Boccaccio, C., Ficarra, E., Marchionni, L., Trusolino, L., Medico, E., & Bertotti, A. (2017). Selective analysis of cancer-cell intrinsic transcriptional traits defines novel clinically relevant subtypes of colorectal cancer.

Nature Communications, *8*. https://doi.org/10.1038/ncomms15107
Ishihara, S., & Haga, H. (2022). Matrix Stiffness Contributes to Cancer Progression by Regulating Transcription Factors. In *Cancers* (Vol. 14, Issue 4). MDPI. https://doi.org/10.3390/cancers14041049
Ismail, H., & Shatat, A.-A. (2024). Colorectal Cancer Risk Factors: Insights into the Significance of Modifiable Environmental and Nutritional Lifestyle Factors. *ERU Research Journal*, *0*(0), 0–0. https://doi.org/10.21608/erurj.2024.254115.1101
Janakiram, N. B., & Rao, C. V. (2014). *The Role of Inflammation in Colon Cancer* (pp. 25–52). https://doi.org/10.1007/978-3-0348-0837-8_2
Jeong, S. Y., Lee, J. H., Shin, Y., Chung, S., & Kuh, H. J. (2016). Co-culture of tumour spheroids and fibroblasts in a collagen matrix-incorporated microfluidic chip mimics reciprocal activation in solid tumour microenvironment. *PLoS ONE*, *11*(7). https://doi.org/10.1371/journal.pone.0159013
Jia, D., Liu, Z., Deng, N., Tan, T. Z., Huang, R. Y. J., Taylor-Harding, B., Cheon, D. J., Lawrenson, K., Wiedemeyer, W. R., Walts, A. E., Karlan, B. Y., & Orsulic, S. (2016). A COL11A1-correlated pan-cancer gene signature of activated fibroblasts for the prioritization of therapeutic targets. *Cancer Letters*, *382*(2), 203–214. https://doi.org/10.1016/j.canlet.2016.09.001
Joanito, I., Wirapati, P., Zhao, N., Nawaz, Z., Yeo, G., Lee, F., Eng, C. L. P., Macalinao, D. C., Kahraman, M., Srinivasan, H., Lakshmanan, V., Verbandt, S., Tsantoulis, P., Gunn, N., Venkatesh, P. N., Poh, Z. W., Nahar, R., Oh, H. L. J., Loo, J. M., … Tan, I. B. (2022). Single-cell and bulk transcriptome sequencing identifies two epithelial tumour cell states and refines the consensus molecular classification of colorectal cancer. *Nature Genetics*, *54*(7), 963–975. https://doi.org/10.1038/s41588-022-01100-4
Jung, B., Staudacher, J. J., & Beauchamp, D. (2017). Transforming Growth Factor β Superfamily Signaling in Development of Colorectal Cancer. In *Gastroenterology* (Vol. 152, Issue 1, pp. 36–52). W.B. Saunders. https://doi.org/10.1053/j.gastro.2016.10.015
Kabiljo, J., Theophil, A., Homola, J., Renner, A. F., Stürzenbecher, N., Ammon, D., Zirnbauer, R., Stang, S., Tran, L., Laengle, J., Kulu, A., Chen, A., Fabits, M., Atanasova, V. S., Pusch, O., Weninger, W., Walczak, H., Herndler Brandstetter, D., Egger, G., … Bergmann, M. (2024). Cancer-associated fibroblasts shape early myeloid cell response to chemotherapy-induced immunogenic signals in next generation tumour organoid cultures. *Journal for Immunotherapy of Cancer*, *12*(11). https://doi.org/10.1136/jitc-2024-009494
Kalaei, Z., Manafi-Farid, R., Rashidi, B., Kiani, F. K., Zarei, A., Fathi, M., & Jadidi-Niaragh, F. (2023). The Prognostic and therapeutic value and clinical implications of fibroblast activation protein-α as a novel biomarker in colorectal cancer. In *Cell Communication and Signaling* (Vol. 21, Issue 1). BioMed Central Ltd. https://doi.org/10.1186/s12964-023-01151-y
Kaler, P., Owusu, B. Y., Augenlicht, L., & Klampfer, L. (2014). The role of STAT1 for

crosstalk between fibroblasts and colon cancer cells. *Frontiers in Oncology*, *4 APR*. https://doi.org/10.3389/fonc.2014.00088

Kalluri, R. (2016). The biology and function of fibroblasts in cancer. In *Nature Reviews Cancer* (Vol. 16, Issue 9, pp. 582–598). Nature Publishing Group. https://doi.org/10.1038/nrc.2016.73

Karagiannis, G. S., Petraki, C., Prassas, I., Saraon, P., Musrap, N., Dimitromanolakis, A., & Diamandis, E. P. (2012). Proteomic Signatures of the Desmoplastic Invasion Front Reveal Collagen Type XII as a Marker of Myofibroblastic Differentiation During Colorectal Cancer Metastasis. In *Oncotarget* (Vol. 3). www.impactjournals.com/oncotarget

Karagiannis, G. S., Poutahidis, T., Erdman, S. E., Kirsch, R., Riddell, R. H., & Diamandis, E. P. (2012). Cancer-associated fibroblasts drive the progression of metastasis through both paracrine and mechanical pressure on cancer tissue. In *Molecular Cancer Research* (Vol. 10, Issue 11, pp. 1403–1418). https://doi.org/10.1158/1541-7786.MCR-12-0307

Karlsson, S., & Nyström, H. (2022). The extracellular matrix in colorectal cancer and its metastatic settling – Alterations and biological implications. In *Critical Reviews in Oncology/Hematology* (Vol. 175). Elsevier Ireland Ltd. https://doi.org/10.1016/j.critrevonc.2022.103712

Kasi, P. M., Shahjehan, F., Cochuyt, J. J., Li, Z., Colibaseanu, D. T., & Merchea, A. (2019). Rising Proportion of Young Individuals With Rectal and Colon Cancer. *Clinical Colorectal Cancer*, *18*(1), e87–e95. https://doi.org/10.1016/j.clcc.2018.10.002

Kather, J. N., & Halama, N. (2019). Harnessing the innate immune system and local immunological microenvironment to treat colorectal cancer. In *British Journal of Cancer* (Vol. 120, Issue 9, pp. 871–882). Nature Publishing Group. https://doi.org/10.1038/s41416-019-0441-6

Kawase, T., Yasui, Y., Nishina, S., Hara, Y., Yanatori, I., Tomiyama, Y., Nakashima, Y., Yoshida, K., Kishi, F., Nakamura, M., & Hino, K. (2015). Fibroblast activation protein-aα-expressing fibroblasts promote the progression of pancreatic ductal adenocarcinoma. *BMC Gastroenterology*, *15*(1). https://doi.org/10.1186/s12876-015-0340-0

Kazakova, A. N., Lukina, M. M., Anufrieva, K. S., Bekbaeva, I. V., Ivanova, O. M., Shnaider, P. V., Slonov, A., Arapidi, G. P., & Shender, V. O. (2024). Exploring the diversity of cancer-associated fibroblasts: insights into mechanisms of drug resistance. In *Frontiers in Cell and Developmental Biology* (Vol. 12). Frontiers Media SA. https://doi.org/10.3389/fcell.2024.1403122

Kendall, R. T., & Feghali-Bostwick, C. A. (2014). Fibroblasts in fibrosis: Novel roles and mediators. In *Frontiers in Pharmacology: Vol. 5 MAY*. Frontiers Research Foundation. https://doi.org/10.3389/fphar.2014.00123

Kennel, K. B., Bozlar, M., De Valk, A. F., & Greten, F. R. (2023a). Cancer-Associated

Fibroblasts in Inflammation and Antitumour Immunity. In *Clinical Cancer Research* (Vol. 29, Issue 6, pp. 1009–1016). American Association for Cancer Research Inc. https://doi.org/10.1158/1078-0432.CCR-22-1031

Kennel, K. B., Bozlar, M., De Valk, A. F., & Greten, F. R. (2023b). Cancer-Associated Fibroblasts in Inflammation and Antitumour Immunity. In *Clinical Cancer Research* (Vol. 29, Issue 6, pp. 1009–1016). American Association for Cancer Research Inc. https://doi.org/10.1158/1078-0432.CCR-22-1031

Kim, S. K., Kim, S. Y., Kim, J. H., Roh, S. A., Cho, D. H., Kim, Y. S., & Kim, J. C. (2014). A nineteen gene-based risk score classifier predicts prognosis of colorectal cancer patients. *Molecular Oncology*, *8*(8), 1653–1666. https://doi.org/10.1016/j.molonc.2014.06.016

Kobayashi, H., Gieniec, K. A., Lannagan, T. R. M., Wang, T., Asai, N., Mizutani, Y., Iida, T., Ando, R., Thomas, E. M., Sakai, A., Suzuki, N., Ichinose, M., Wright, J. A., Vrbanac, L., Ng, J. Q., Goyne, J., Radford, G., Lawrence, M. J., Sammour, T., … Worthley, D. L. (2022). The Origin and Contribution of Cancer-Associated Fibroblasts in Colorectal Carcinogenesis. *Gastroenterology*, *162*(3), 890–906. https://doi.org/10.1053/j.gastro.2021.11.037

Kobayashi, H., Gieniec, K. A., Wright, J. A., Wang, T., Asai, N., Mizutani, Y., Lida, T., Ando, R., Suzuki, N., Lannagan, T. R. M., Ng, J. Q., Hara, A., Shiraki, Y., Mii, S., Ichinose, M., Vrbanac, L., Lawrence, M. J., Sammour, T., Uehara, K., … Woods, S. L. (2021). The Balance of Stromal BMP Signaling Mediated by GREM1 and ISLR Drives Colorectal Carcinogenesis. *Gastroenterology*, *160*(4), 1224-1239.e30. https://doi.org/10.1053/j.gastro.2020.11.011

Koncina, E., Nurmik, M., Pozdeev, V. I., Gilson, C., Tsenkova, M., Begaj, R., Stang, S., Gaigneaux, A., Weindorfer, C., Rodriguez, F., Schmoetten, M., Klein, E., Karta, J., Atanasova, V. S., Grzyb, K., Ullmann, P., Halder, R., Hengstschläger, M., Graas, J., … Letellier, E. (2023). IL1R1+ cancer-associated fibroblasts drive tumour development and immunosuppression in colorectal cancer. *Nature Communications*, *14*(1). https://doi.org/10.1038/s41467-023-39953-w

Koppensteiner, L., Mathieson, L., Neilson, L., O'Connor, R. A., & Akram, A. R. (2025a). IFNγ and TNFα drive an inflammatory secretion profile in cancer-associated fibroblasts from human non-small cell lung cancer. *FEBS Letters*. https://doi.org/10.1002/1873-3468.15083

Koppensteiner, L., Mathieson, L., Neilson, L., O'Connor, R. A., & Akram, A. R. (2025b). IFNγ and TNFα drive an inflammatory secretion profile in cancer-associated fibroblasts from human non-small cell lung cancer. *FEBS Letters*, *599*(5), 713–723. https://doi.org/10.1002/1873-3468.15083

Kraman, M., Bambrough, P. J., Arnold, J. N., Roberts, E. W., Magiera, L., Jones, J. O., Gopinathan, A., Tuveson, D. A., & Fearon, D. T. (2010). Suppression of antitumour immunity by stromal cells expressing fibroblast activation protein-α. *Science*,

330(6005), 827–830. https://doi.org/10.1126/science.1195300
Kumar, A., Gautam, V., Sandhu, A., Rawat, K., Sharma, A., & Saha, L. (2023). Current and emerging therapeutic approaches for colorectal cancer: A comprehensive review. *World Journal of Gastrointestinal Surgery*, *15*(4), 495–519. https://doi.org/10.4240/wjgs.v15.i4.495
Labernadie, A., Kato, T., Brugués, A., Serra-Picamal, X., Derzsi, S., Arwert, E., Weston, A., González-Tarragó, V., Elosegui-Artola, A., Albertazzi, L., Alcaraz, J., Roca-Cusachs, P., Sahai, E., & Trepat, X. (2017). A mechanically active heterotypic E-cadherin/N-cadherin adhesion enables fibroblasts to drive cancer cell invasion. *Nature Cell Biology*, *19*(3), 224–237. https://doi.org/10.1038/ncb3478
Lai Mun Wang, M. A. S. Z. D. R. B. Z. S. S. L. E. O. S. M. W. G. M. R. M. E. F. (2015). The prognostic role of desmoplastic stroma in pancreatic ductal adenocarcinoma. *Oncotarget*, *Vol.5 No.4*.
Lavie, D., Ben-Shmuel, A., Erez, N., & Scherz-Shouval, R. (2022a). Cancer-associated fibroblasts in the single-cell era. In *Nature Cancer* (Vol. 3, Issue 7, pp. 793–807). Nature Research. https://doi.org/10.1038/s43018-022-00411-z
Lavie, D., Ben-Shmuel, A., Erez, N., & Scherz-Shouval, R. (2022b). Cancer-associated fibroblasts in the single-cell era. In *Nature Cancer* (Vol. 3, Issue 7, pp. 793–807). Nature Research. https://doi.org/10.1038/s43018-022-00411-z
LeBleu, V. S., & Kalluri, R. (2018). A peek into cancer-associated fibroblasts: Origins, functions and translational impact. *DMM Disease Models and Mechanisms*, *11*(4). https://doi.org/10.1242/dmm.029447
Lee, H. J., Park, S. W., Lee, J. H., Chang, S. Y., Oh, S. M., Mun, S., Kang, J., Park, J. E., Choi, J. K., Kim, T. Il, Kim, J. Y., & Kim, P. (2025). Differential cellular origins of the extracellular matrix of tumour and normal tissues according to colorectal cancer subtypes: Cellular and Molecular Biology. *British Journal of Cancer*, *132*(9), 770–782. https://doi.org/10.1038/s41416-025-02964-z
Li, H., Courtois, E. T., Sengupta, D., Tan, Y., Chen, K. H., Goh, J. J. L., Kong, S. L., Chua, C., Hon, L. K., Tan, W. S., Wong, M., Choi, P. J., Wee, L. J. K., Hillmer, A. M., Tan, I. B., Robson, P., & Prabhakar, S. (2017). Reference component analysis of single-cell transcriptomes elucidates cellular heterogeneity in human colorectal tumours. *Nature Genetics*, *49*(5), 708–718. https://doi.org/10.1038/ng.3818
Li, J., Chen, D., & Shen, M. (2022). Tumour Microenvironment Shapes Colorectal Cancer Progression, Metastasis, and Treatment Responses. In *Frontiers in Medicine* (Vol. 9). Frontiers Media S.A. https://doi.org/10.3389/fmed.2022.869010
Li, J., Ma, X., Chakravarti, D., Shalapour, S., & Depinho, R. A. (2021a). *Genetic and biological hallmarks of colorectal cancer*. https://doi.org/10.1101/gad.348226
Li, J., Ma, X., Chakravarti, D., Shalapour, S., & Depinho, R. A. (2021b). *Genetic and biological hallmarks of colorectal cancer*. https://doi.org/10.1101/gad.348226
Li, Z., Sun, C., & Qin, Z. (2021). Metabolic reprogramming of cancer-associated fibroblasts

and its effect on cancer cell reprogramming. In *Theranostics* (Vol. 11, Issue 17, pp. 8322–8336). Ivyspring International Publisher. https://doi.org/10.7150/THNO.62378

Li, Z., Zhang, J., Zhou, J., Lu, L., Wang, H., Zhang, G., Wan, G., Cai, S., & Du, J. (2019). Nodal facilitates differentiation of fibroblasts to cancer-associated fibroblasts that support tumour growth in melanoma and colorectal cancer. *Cells*, *8*(6). https://doi.org/10.3390/cells8060538

Liao, Z., Tan, Z. W., Zhu, P., & Tan, N. S. (2019). Cancer-associated fibroblasts in tumour microenvironment – Accomplices in tumour malignancy. In *Cellular Immunology* (Vol. 343). Academic Press Inc. https://doi.org/10.1016/j.cellimm.2017.12.003

Linares, J., Marín-Jiménez, J. A., Badia-Ramentol, J., & Calon, A. (2021). Determinants and Functions of CAFs Secretome During Cancer Progression and Therapy. In *Frontiers in Cell and Developmental Biology* (Vol. 8). Frontiers Media S.A. https://doi.org/10.3389/fcell.2020.621070

Liu, H., Antony, S., Roy, K., Juhasz, A., Wu, Y., Lu, J., Meitzler, J. L., Jiang, G., Polley, E., & Doroshow, J. H. (2017). Oncotarget 38113 www.impactjournals.com/oncotarget Interleukin-4 and interleukin-13 increase NADPH oxidase 1-related proliferation of human colon cancer cells. In *Oncotarget* (Vol. 8, Issue 24). www.impactjournals.com/oncotarget/

Liu, X., Zhu, L., Wang, R., Lou, X., Yao, X., Ni, C., & Qin, Z. (2019). IFNγ inhibits fibroblast-leading tumour cell invasion through downregulating N-cadherin. *Biochemical and Biophysical Research Communications*, *512*(3), 544–551. https://doi.org/10.1016/j.bbrc.2019.03.136

Long, A. G., Lundsmith, E. T., & Hamilton, K. E. (2017). Inflammation and Colorectal Cancer. In *Current Colorectal Cancer Reports* (Vol. 13, Issue 4, pp. 341–351). Current Medicine Group LLC 1. https://doi.org/10.1007/s11888-017-0373-6

Louault, K., Li, R. R., & Declerck, Y. A. (2020a). Cancer-associated fibroblasts: Understanding their heterogeneity. In *Cancers* (Vol. 12, Issue 11, pp. 1–28). MDPI AG. https://doi.org/10.3390/cancers12113108

Louault, K., Li, R. R., & Declerck, Y. A. (2020b). Cancer-associated fibroblasts: Understanding their heterogeneity. In *Cancers* (Vol. 12, Issue 11, pp. 1–28). MDPI AG. https://doi.org/10.3390/cancers12113108

Lu, T., Tian, L., Han, Y., Vogelbaum, M., & Stark, G. R. (2007). Dose-dependent cross-talk between the transforming growth factor-and interleukin-1 signaling pathways CELL BIOLOGY. In *PNAS March* (Vol. 13, Issue 11).

Lu, Y., Yang, W., Qin, C., Zhang, L., Deng, J., Liu, S., & Qin, Z. (2009). Responsiveness of Stromal Fibroblasts to IFN-γ Blocks Tumour Growth via Angiostasis. *The Journal of Immunology*, *183*(10), 6413–6421. https://doi.org/10.4049/jimmunol.0901073

Lunardi, S., Muschel, R. J., & Brunner, T. B. (2014). The stromal compartments in pancreatic cancer: Are there any therapeutic targets? In *Cancer Letters* (Vol. 343, Issue 2, pp. 147–155). Elsevier Ireland Ltd. https://doi.org/10.1016/j.canlet.2013.09.039

Luo, H., Xia, X., Huang, L. Bin, An, H., Cao, M., Kim, G. D., Chen, H. N., Zhang, W. H., Shu, Y., Kong, X., Ren, Z., Li, P. H., Liu, Y., Tang, H., Sun, R., Li, C., Bai, B., Jia, W., Liu, Y., … Xu, H. (2022). Pan-cancer single-cell analysis reveals the heterogeneity and plasticity of cancer-associated fibroblasts in the tumour microenvironment. *Nature Communications*, *13*(1). https://doi.org/10.1038/s41467-022-34395-2

Luo, K. (2017). Signaling cross talk between TGF-β/Smad and other signaling pathways. In *Cold Spring Harbor Perspectives in Biology* (Vol. 9, Issue 1). Cold Spring Harbor Laboratory Press. https://doi.org/10.1101/cshperspect.a022137

Luo, M., Luo, Y., Mao, N., Huang, G., Teng, C., Wang, H., Wu, J., Liao, X., & Yang, J. (2018). Cancer-associated fibroblasts accelerate malignant progression of non-small cell lung cancer via connexin 43-formed unidirectional gap junctional intercellular communication. *Cellular Physiology and Biochemistry*, *51*(1), 315–336. https://doi.org/10.1159/000495232

Luzina, I. G., Keegan, A. D., Heller, N. M., Rook, G. A. W., Shea-Donohue, T., & Atamas, S. P. (2012). Regulation of inflammation by interleukin-4: a review of “alternatives.” *Journal of Leukocyte Biology*, *92*(4), 753–764. https://doi.org/10.1189/jlb.0412214

Lv, J., Jiang, Z., Yuan, J., Zhuang, M., Guan, X., Liu, H., Yin, Y., Ma, Y., Liu, Z., Wang, H., & Wang, X. (2023). Pan-cancer analysis identifies PD-L2 as a tumour promotor in the tumour microenvironment. *Frontiers in Immunology*, *14*. https://doi.org/10.3389/fimmu.2023.1093716

Ma, C., Yang, C., Peng, A., Sun, T., Ji, X., Mi, J., Wei, L., Shen, S., & Feng, Q. (2023). Pan-cancer spatially resolved single-cell analysis reveals the crosstalk between cancer-associated fibroblasts and tumour microenvironment. *Molecular Cancer*, *22*(1). https://doi.org/10.1186/s12943-023-01876-x

Ma, J., Liang, W., Qiang, Y., Li, L., Du, J., Pan, C., Chen, B., Zhang, C., Chen, Y., & Wang, Q. (2021). Interleukin-1 receptor antagonist inhibits matastatic potential by down-regulating CXCL12/CXCR4 signaling axis in colorectal cancer. *Cell Communication and Signaling*, *19*(1). https://doi.org/10.1186/s12964-021-00804-0

Ma, Z., Li, X., Mao, Y., Wei, C., Huang, Z., Li, G., Yin, J., Liang, X., & Liu, Z. (2022). Interferon-dependent SLC14A1+ cancer-associated fibroblasts promote cancer stemness via WNT5A in bladder cancer. *Cancer Cell*, *40*(12), 1550-1565.e7. https://doi.org/10.1016/j.ccell.2022.11.005

Mace, T. A., Ameen, Z., Collins, A., Wojcik, S., Mair, M., Young, G. S., Fuchs, J. R., Eubank, T. D., Frankel, W. L., Bekaii-Saab, T., Bloomston, M., & Lesinski, G. B. (2013). Pancreatic cancer-associated stellate cells promote differentiation of myeloid-derived suppressor cells in a StAT3-dependent manner. *Cancer Research*, *73*(10), 3007–3018. https://doi.org/10.1158/0008-5472.CAN-12-4601

Madar, S., Goldstein, I., & Rotter, V. (2013). “Cancer associated fibroblasts” - more than meets the eye. In *Trends in Molecular Medicine* (Vol. 19, Issue 8, pp. 447–453). https://doi.org/10.1016/j.molmed.2013.05.004

Mai, Z., Lin, Y., Lin, P., Zhao, X., & Cui, L. (2024). Modulating extracellular matrix stiffness: a strategic approach to boost cancer immunotherapy. In *Cell Death and Disease* (Vol. 15, Issue 5). Springer Nature. https://doi.org/10.1038/s41419-024-06697-4

Malik, R., Luong, T., Cao, X., Han, B., Shah, N., Franco-Barraza, J., Han, L., Shenoy, V. B., Lelkes, P. I., & Cukierman, E. (2019). Rigidity controls human desmoplastic matrix anisotropy to enable pancreatic cancer cell spread via extracellular signal-regulated kinase 2. *Matrix Biology*, *81*, 50–69. https://doi.org/10.1016/j.matbio.2018.11.001

Malla, S. B., Byrne, R. M., Lafarge, M. W., Corry, S. M., Fisher, N. C., Tsantoulis, P. K., Mills, M. L., Ridgway, R. A., Lannagan, T. R. M., Najumudeen, A. K., Gilroy, K. L., Amirkhah, R., Maguire, S. L., Mulholland, E. J., Belnoue-Davis, H. L., Grassi, E., Viviani, M., Rogan, E., Redmond, K. L., … Dunne, P. D. (2024). Pathway level subtyping identifies a slow-cycling biological phenotype associated with poor clinical outcomes in colorectal cancer. *Nature Genetics*, *56*(3), 458–472. https://doi.org/10.1038/s41588-024-01654-5

Manetti, M. (2021). Molecular morphology and function of stromal cells. In *International Journal of Molecular Sciences* (Vol. 22, Issue 24). MDPI. https://doi.org/10.3390/ijms222413422

Marcellinaro, R., Spoletini, D., Grieco, M., Avella, P., Cappuccio, M., Troiano, R., Lisi, G., Garbarino, G. M., & Carlini, M. (2024). Colorectal Cancer: Current Updates and Future Perspectives. In *Journal of Clinical Medicine* (Vol. 13, Issue 1). Multidisciplinary Digital Publishing Institute (MDPI). https://doi.org/10.3390/jcm13010040

Mariathasan, S., Turley, S. J., Nickles, D., Castiglioni, A., Yuen, K., Wang, Y., Kadel, E. E., Koeppen, H., Astarita, J. L., Cubas, R., Jhunjhunwala, S., Banchereau, R., Yang, Y., Guan, Y., Chalouni, C., Ziai, J., Şenbabaoğlu, Y., Santoro, S., Sheinson, D., … Powles, T. (2018). TGFβ attenuates tumour response to PD-L1 blockade by contributing to exclusion of T cells. *Nature*, *554*(7693), 544–548. https://doi.org/10.1038/nature25501

Maryam, S., Krukiewicz, K., Haq, I. U., Khan, A. A., Yahya, G., & Cavalu, S. (2023). Interleukins (Cytokines) as Biomarkers in Colorectal Cancer: Progression, Detection, and Monitoring. In *Journal of Clinical Medicine* (Vol. 12, Issue 9). Multidisciplinary Digital Publishing Institute (MDPI). https://doi.org/10.3390/jcm12093127

Matsui, S., Okabayashi, K., Tsuruta, M., Shigeta, K., Seishima, R., Ishida, T., Kondo, T., Suzuki, Y., Hasegawa, H., Shimoda, M., Sugimoto, S., Sato, T., & Kitagawa, Y. (2019). Interleukin-13 and its signaling pathway is associated with obesity-related colorectal tumourigenesis. *Cancer Science*, *110*(7), 2156–2165. https://doi.org/10.1111/cas.14066

McAndrews, K. M., Chen, Y., Darpolor, J. K., Zheng, X., Yang, S., Carstens, J. L., Li, B., Wang, H., Miyake, T., De Sampaio, P. C., Kirtley, M. L., Natale, M., Wu, C. C., Sugimoto, H., Lebleu, V. S., & Kalluri, R. (2022). Identification of Functional Heterogeneity of Carcinoma-Associated Fibroblasts with Distinct IL6-Mediated Therapy Resistance in Pancreatic Cancer. *Cancer Discovery*, *12*(6), 1580–1597.

https://doi.org/10.1158/2159-8290.CD-20-1484
McAndrews, K. M., Vázquez-Arreguín, K., Kwak, C., Sugimoto, H., Zheng, X., Li, B., Kirtley, M. L., LeBleu, V. S., & Kalluri, R. (2021). αSMA+ fibroblasts suppress Lgr5+ cancer stem cells and restrain colorectal cancer progression. *Oncogene*, *40*(26), 4440–4452. https://doi.org/10.1038/s41388-021-01866-7
Mele, V., Basso, C., Governa, V., Glaus Garzon, J. F., Muraro, M. G., Däster, S., Nebiker, C. A., Mechera, R., Bolli, M., Schmidt, A., Geiger, R., Spagnoli, G. C., Christoforidis, D., Majno, P. E., Borsig, L., & Iezzi, G. (2022). Identification of TPM2 and CNN1 as Novel Prognostic Markers in Functionally Characterized Human Colon Cancer-Associated Stromal Cells. *Cancers*, *14*(8). https://doi.org/10.3390/cancers14082024
Mele, V., Muraro, M. G., Calabrese, D., Pfaff, D., Amatruda, N., Amicarella, F., Kvinlaug, B., Bocelli-Tyndall, C., Martin, I., Resink, T. J., Heberer, M., Oertli, D., Terracciano, L., Spagnoli, G. C., & Iezzi, G. (2014). Mesenchymal stromal cells induce epithelial-to-mesenchymal transition in human colorectal cancer cells through the expression of surface-bound TGF-β. *International Journal of Cancer*, *134*(11), 2583–2594. https://doi.org/10.1002/ijc.28598
Mellone, M., Hanley, C. J., Thirdborough, S., Mellows, T., Garcia, E., Woo, J., Tod, J., Frampton, S., Jenei, V., Moutasim, K. A., Kabir, T. D., Brennan, P. A., Venturi, G., Ford, K., Herranz, N., Lim, K. P., Clarke, J., Lambert, D. W., Prime, S. S., … Thomas, G. J. (2016). Induction of fibroblast senescence generates a non-fibrogenic myofibroblast phenotype that differentially impacts on cancer prognosis. In *AGING* (Vol. 8). www.aging-us.com
Mhaidly, R., & Mechta-Grigoriou, F. (2021). Role of cancer-associated fibroblast subpopulations in immune infiltration, as a new means of treatment in cancer. In *Immunological Reviews* (Vol. 302, Issue 1, pp. 259–272). John Wiley and Sons Inc. https://doi.org/10.1111/imr.12978
Micalet, A., Upadhyay, A., Javanmardi, Y., de Brito, C. G., Moeendarbary, E., & Cheema, U. (2024). Patient-specific colorectal-cancer-associated fibroblasts modulate tumour microenvironment mechanics. *IScience*, *27*(6). https://doi.org/10.1016/j.isci.2024.110060
Mishra, D., & Banerjee, D. (2023). Secretome of Stromal Cancer-Associated Fibroblasts (CAFs): Relevance in Cancer. In *Cells* (Vol. 12, Issue 4). MDPI. https://doi.org/10.3390/cells12040628
Monteran, L., & Erez, N. (2019). The dark side of fibroblasts: Cancer-associated fibroblasts as mediators of immunosuppression in the tumour microenvironment. In *Frontiers in Immunology* (Vol. 10, Issue AUG). Frontiers Media S.A. https://doi.org/10.3389/fimmu.2019.01835
Mroz, E. A., & Rocco, J. W. (2017). The challenges of tumour genetic diversity. In *Cancer* (Vol. 123, Issue 6, pp. 917–927). John Wiley and Sons Inc. https://doi.org/10.1002/cncr.30430

Muchlińska, A., Nagel, A., Popęda, M., Szade, J., Niemira, M., Zieliński, J., Skokowski, J., Bednarz-Knoll, N., & Żaczek, A. J. (2022). Alpha-smooth muscle actin-positive cancer-associated fibroblasts secreting osteopontin promote growth of luminal breast cancer. In *Cellular and Molecular Biology Letters* (Vol. 27, Issue 1). BioMed Central Ltd. https://doi.org/10.1186/s11658-022-00351-7

Müller, M. F., Ibrahim, A. E. K., & Arends, M. J. (2016). Molecular pathological classification of colorectal cancer. In *Virchows Archiv* (Vol. 469, Issue 2, pp. 125–134). Springer Verlag. https://doi.org/10.1007/s00428-016-1956-3

Muzny, D. M., Bainbridge, M. N., Chang, K., Dinh, H. H., Drummond, J. A., Fowler, G., Kovar, C. L., Lewis, L. R., Morgan, M. B., Newsham, I. F., Reid, J. G., Santibanez, J., Shinbrot, E., Trevino, L. R., Wu, Y. Q., Wang, M., Gunaratne, P., Donehower, L. A., Creighton, C. J., … Thomson., E. (2012a). Comprehensive molecular characterization of human colon and rectal cancer. *Nature*, *487*(7407), 330–337. https://doi.org/10.1038/nature11252

Muzny, D. M., Bainbridge, M. N., Chang, K., Dinh, H. H., Drummond, J. A., Fowler, G., Kovar, C. L., Lewis, L. R., Morgan, M. B., Newsham, I. F., Reid, J. G., Santibanez, J., Shinbrot, E., Trevino, L. R., Wu, Y. Q., Wang, M., Gunaratne, P., Donehower, L. A., Creighton, C. J., … Thomson., E. (2012b). Comprehensive molecular characterization of human colon and rectal cancer. *Nature*, *487*(7407), 330–337. https://doi.org/10.1038/nature11252

Naderi-Meshkin, H., Cornelius, V. A., Eleftheriadou, M., Potel, K. N., Setyaningsih, W. A. W., & Margariti, A. (2023). Vascular organoids: unveiling advantages, applications, challenges, and disease modelling strategies. In *Stem Cell Research and Therapy* (Vol. 14, Issue 1). BioMed Central Ltd. https://doi.org/10.1186/s13287-023-03521-2

Nagarsheth, N., Wicha, M. S., & Zou, W. (2017). Chemokines in the cancer microenvironment and their relevance in cancer immunotherapy. In *Nature Reviews Immunology* (Vol. 17, Issue 9, pp. 559–572). Nature Publishing Group. https://doi.org/10.1038/nri.2017.49

Nair, N., Calle, A. S., Zahra, M. H., Prieto-Vila, M., Oo, A. K. K., Hurley, L., Vaidyanath, A., Seno, A., Masuda, J., Iwasaki, Y., Tanaka, H., Kasai, T., & Seno, M. (2017). A cancer stem cell model as the point of origin of cancer-associated fibroblasts in tumour microenvironment. *Scientific Reports*, *7*(1). https://doi.org/10.1038/s41598-017-07144-5

Nguyen, J. K., Austin, E., Huang, A., Mamalis, A., & Jagdeo, J. (2020a). The IL-4/IL-13 axis in skin fibrosis and scarring: mechanistic concepts and therapeutic targets. In *Archives of Dermatological Research* (Vol. 312, Issue 2, pp. 81–92). Springer. https://doi.org/10.1007/s00403-019-01972-3

Nguyen, J. K., Austin, E., Huang, A., Mamalis, A., & Jagdeo, J. (2020b). The IL-4/IL-13 axis in skin fibrosis and scarring: mechanistic concepts and therapeutic targets. In *Archives of Dermatological Research* (Vol. 312, Issue 2, pp. 81–92). Springer.

https://doi.org/10.1007/s00403-019-01972-3
Nguyen, L. H., Goel, A., & Chung, D. C. (2020). Pathways of Colorectal Carcinogenesis. *Gastroenterology*, *158*(2), 291–302. https://doi.org/10.1053/j.gastro.2019.08.059
Nicolas, A. M., Pesic, M., Engel, E., Ziegler, P. K., Diefenhardt, M., Kennel, K. B., Buettner, F., Conche, C., Petrocelli, V., Elwakeel, E., Weigert, A., Zinoveva, A., Fleischmann, M., Häupl, B., Karakütük, C., Bohnenberger, H., Mosa, M. H., Kaderali, L., Gaedcke, J., … Greten, F. R. (2022). Inflammatory fibroblasts mediate resistance to neoadjuvant therapy in rectal cancer. *Cancer Cell*, *40*(2), 168-184.e13. https://doi.org/10.1016/j.ccell.2022.01.004
Nikiteas, N. I., Weber, M., Antoniou, A., & Dimitroulis, D. (2016). Advances in Colorectal Cancer. In *BioMed Research International* (Vol. 2016). Hindawi Publishing Corporation. https://doi.org/10.1155/2016/7347648
Nurmik, M., Ullmann, P., Rodriguez, F., Haan, S., & Letellier, E. (2020a). In search of definitions: Cancer-associated fibroblasts and their markers. In *International Journal of Cancer* (Vol. 146, Issue 4, pp. 895–905). Wiley-Liss Inc. https://doi.org/10.1002/ijc.32193
Nurmik, M., Ullmann, P., Rodriguez, F., Haan, S., & Letellier, E. (2020b). In search of definitions: Cancer-associated fibroblasts and their markers. In *International Journal of Cancer* (Vol. 146, Issue 4, pp. 895–905). Wiley-Liss Inc. https://doi.org/10.1002/ijc.32193
Obenauf, A. C., & Massagué, J. (2015). Surviving at a Distance: Organ-Specific Metastasis. In *Trends in Cancer* (Vol. 1, Issue 1, pp. 76–91). Cell Press. https://doi.org/10.1016/j.trecan.2015.07.009
Öhlund, D., Handly-Santana, A., Biffi, G., Elyada, E., Almeida, A. S., Ponz-Sarvise, M., Corbo, V., Oni, T. E., Hearn, S. A., Lee, E. J., Chio, I. I. C., Hwang, C. Il, Tiriac, H., Baker, L. A., Engle, D. D., Feig, C., Kultti, A., Egeblad, M., Fearon, D. T., … Tuveson, D. A. (2017). Distinct populations of inflammatory fibroblasts and myofibroblasts in pancreatic cancer. *The Journal of Experimental Medicine*, *214*(3), 579–596. https://doi.org/10.1084/jem.20162024
Ohmori, Y., & Hamilton, T. A. (2000). Interleukin-4/STAT6 represses STAT1 and NF-κB-dependent transcription through distinct mechanisms. *Journal of Biological Chemistry*, *275*(48), 38095–38103. https://doi.org/10.1074/jbc.M006227200
Oleynikova, N. A., Mikhailov, I. A., Kharlova, O. A., Zavidnyi, T. Y., Danilova, N. V., & Mal`kov, P. G. (2023). Detection, Role and Prognostic Value of Cancer-associated Fibroblasts in Colorectal Cancer. *Indian Journal of Surgical Oncology*, *14*(1), 186–193. https://doi.org/10.1007/s13193-022-01653-0
O'Reilly, S., Ciechomska, M., Fullard, N., Przyborski, S., & Van Laar, J. M. (2016). IL-13 mediates collagen deposition via STAT6 and microRNA-135b: A role for epigenetics. *Scientific Reports*, *6*. https://doi.org/10.1038/srep25066
Otero, J., Navajas, D., & Alcaraz, J. (2020). Characterization of the elastic properties of

extracellular matrix models by atomic force microscopy. In *Methods in Cell Biology* (Vol. 156, pp. 59–83). Academic Press Inc. https://doi.org/10.1016/bs.mcb.2019.11.016

Owen, K. L., Brockwell, N. K., & Parker, B. S. (2019). Jak-stat signaling: A double-edged sword of immune regulation and cancer progression. In *Cancers* (Vol. 11, Issue 12). MDPI AG. https://doi.org/10.3390/cancers11122002

Özdemir, B. C., Pentcheva-Hoang, T., Carstens, J. L., Zheng, X., Wu, C. C., Simpson, T. R., Laklai, H., Sugimoto, H., Kahlert, C., Novitskiy, S. V., DeJesus-Acosta, A., Sharma, P., Heidari, P., Mahmood, U., Chin, L., Moses, H. L., Weaver, V. M., Maitra, A., Allison, J. P., … Kalluri, R. (2014). Depletion of carcinoma-associated fibroblasts and fibrosis induces immunosuppression and accelerates pancreas cancer with reduced survival. *Cancer Cell*, *25*(6), 719–734. https://doi.org/10.1016/j.ccr.2014.04.005

Pan, K., Li, Q., Guo, Z., & Li, Z. (2025). Healing action of Interleukin-4 (IL-4) in acute and chronic inflammatory conditions: Mechanisms and therapeutic strategies. In *Pharmacology and Therapeutics* (Vol. 265). Elsevier Inc. https://doi.org/10.1016/j.pharmthera.2024.108760

Pandurangan, A. kumar, Divya, T., Kumar, K., Dineshbabu, V., Velavan, B., & Sudhandiran, G. (2018). Colorectal carcinogenesis: Insights into the cell death and signal transduction pathways: A review. In *World Journal of Gastrointestinal Oncology* (Vol. 10, Issue 9, pp. 244–259). Baishideng Publishing Group Co. https://doi.org/10.4251/wjgo.v10.i9.244

Papait, A., Romoli, J., Stefani, F. R., Chiodelli, P., Montresor, M. C., Agoni, L., Silini, A. R., & Parolini, O. (2022). Fight the Cancer, Hit the CAF! In *Cancers* (Vol. 14, Issue 15). MDPI. https://doi.org/10.3390/cancers14153570

Passardi, A., Canale, M., Valgiusti, M., & Ulivi, P. (2017). Immune checkpoints as a target for colorectal cancer treatment. In *International Journal of Molecular Sciences* (Vol. 18, Issue 6). MDPI AG. https://doi.org/10.3390/ijms18061324

Peng, Y., Lei, Z., Yang, P., Newton, I. P., Ren, H., Zhang, L., Wu, H., & Li, Z. (2014). Direct contacts with colon cancer cells regulate the differentiation of bone marrow mesenchymal stem cells into tumour associated fibroblasts. *Biochemical and Biophysical Research Communications*, *451*(1), 68–73. https://doi.org/10.1016/j.bbrc.2014.07.074

Percario, R., Panaccio, P., Di Mola, F. F., Grottola, T., & Di Sebastiano, P. (2021). The complex network between inflammation and colorectal cancer: A systematic review of the literature. In *Cancers* (Vol. 13, Issue 24). MDPI. https://doi.org/10.3390/cancers13246237

Ping, Q., Wang, C., Cheng, X., Zhong, Y., Yan, R., Yang, M., Shi, Y., Li, X., Li, X., Huang, W., Wang, L., Bi, X., Hu, L., Yang, Y., Wang, Y., Gong, R., Tan, J., Li, R., Li, H., … Li, R. (2023). TGF-β1 dominates stromal fibroblast-mediated EMT via the FAP/VCAN axis in bladder cancer cells. *Journal of Translational Medicine*, *21*(1). https://doi.org/10.1186/s12967-023-04303-3

Plikus, M. V., Wang, X., Sinha, S., Forte, E., Thompson, S. M., Herzog, E. L., Driskell, R.

R., Rosenthal, N., Biernaskie, J., & Horsley, V. (2021). Fibroblasts: Origins, definitions, and functions in health and disease. In *Cell* (Vol. 184, Issue 15, pp. 3852–3872). Elsevier B.V. https://doi.org/10.1016/j.cell.2021.06.024

Pula, B., Witkiewicz, W., Dziegiel, P., & Podhorska-Okolow, M. (2013). Significance of podoplanin expression in cancer-associated fibroblasts: A comprehensive review. In *International Journal of Oncology* (Vol. 42, Issue 6, pp. 1849–1857). https://doi.org/10.3892/ijo.2013.1887

Puré, E., & Blomberg, R. (2018). Pro-tumourigenic roles of fibroblast activation protein in cancer: back to the basics. In *Oncogene* (Vol. 37, Issue 32, pp. 4343–4357). Nature Publishing Group. https://doi.org/10.1038/s41388-018-0275-3

Pyo, J. S., Shin, Y. M., & Kang, D. W. (2019). Prognostic implication of metastatic lymph node ratio in colorectal cancers: Comparison depending on tumour location. *Journal of Clinical Medicine*, *8*(11). https://doi.org/10.3390/jcm8111812

Qi, M., Fan, S., Huang, M., Pan, J., Li, Y., Miao, Q., Lyu, W., Li, X., Deng, L., Qiu, S., Liu, T., Deng, W., Chu, X., Jiang, C., He, W., Xia, L., Yang, Y., Hong, J., Qi, Q., … Zhang, D. (2022). Targeting FAPα-expressing hepatic stellate cells overcomes resistance to antiangiogenics in colorectal cancer liver metastasis models. *Journal of Clinical Investigation*, *132*(19). https://doi.org/10.1172/JCI157399

Quante, M., Tu, S. P., Tomita, H., Gonda, T., Wang, S. S. W., Takashi, S., Baik, G. H., Shibata, W., DiPrete, B., Betz, K. S., Friedman, R., Varro, A., Tycko, B., & Wang, T. C. (2011). Bone Marrow-Derived Myofibroblasts Contribute to the Mesenchymal Stem Cell Niche and Promote Tumour Growth. *Cancer Cell*, *19*(2), 257–272. https://doi.org/10.1016/j.ccr.2011.01.020

Quintanilla, M., Montero, L. M., Renart, J., & Villar, E. M. (2019). Podoplanin in inflammation and cancer. In *International Journal of Molecular Sciences* (Vol. 20, Issue 3). MDPI AG. https://doi.org/10.3390/ijms20030707

Raskov, H., Søby, J. H., Troelsen, J., Bojesen, R. D., & Gögenur, I. (2020). Driver Gene Mutations and Epigenetics in Colorectal Cancer. In *Annals of Surgery* (Vol. 271, Issue 1, pp. 75–85). Lippincott Williams and Wilkins. https://doi.org/10.1097/SLA.0000000000003393

Reynolds, A., Wharton, N., Parris, A., Mitchell, E., Sobolewski, A., Kam, C., Bigwood, L., El Hadi, A., Münsterberg, A., Lewis, M., Speakman, C., Stebbings, W., Wharton, R., Sargen, K., Tighe, R., Jamieson, C., Hernon, J., Kapur, S., Oue, N., … Williams, M. R. (2014). Canonical Wnt signals combined with suppressed TGFβ/BMP pathways promote renewal of the native human colonic epithelium. *Gut*, *63*(4), 610–621. https://doi.org/10.1136/gutjnl-2012-304067

Rizzo, A., Pallone, F., Monteleone, G., & Fantini, M. C. (2011). Intestinal inflammation and colorectal cancer: A doubleedged sword? In *World Journal of Gastroenterology* (Vol. 17, Issue 26, pp. 3092–3100). Baishideng Publishing Group Co. https://doi.org/10.3748/wjg.v17.i26.3092

Rodrigues, M., Kosaric, N., Bonham, C. A., & Gurtner, G. C. (2019). Wound Healing: A Cellular Perspective. *Physiol Rev*, *99*, 665–706. https://doi.org/10.1152/physrev.00067.2017.-Wound

Rozali, E. N., Hato, S. V., Robinson, B. W., Lake, R. A., & Lesterhuis, W. J. (2012). Programmed death ligand 2 in cancer-induced immune suppression. In *Clinical and Developmental Immunology* (Vol. 2012). https://doi.org/10.1155/2012/656340

Rubinstein-Achiasaf, L., Morein, D., Ben-Yaakov, H., Liubomirski, Y., Meshel, T., Elbaz, E., Dorot, O., Pichinuk, E., Gershovits, M., Weil, M., & Ben-Baruch, A. (2021). Persistent inflammatory stimulation drives the conversion of mscs to inflammatory cafs that promote pro-metastatic characteristics in breast cancer cells. *Cancers*, *13*(6). https://doi.org/10.3390/cancers13061472

Russo, A. G., Andreano, A., Sartore-Bianchi, A., Mauri, G., Decarli, A., & Siena, S. (2019). Increased incidence of colon cancer among individuals younger than 50 years: A 17 years analysis from the cancer registry of the municipality of Milan, Italy. *Cancer Epidemiology*, *60*, 134–140. https://doi.org/10.1016/j.canep.2019.03.015

Rybinski, B., Franco-Barraza, J., & Cukierman, E. (2014). The wound healing, chronic fibrosis, and cancer progression triad. *Physiol Genomics*, *46*, 223–244. https://doi.org/10.1152/physiolgenomics.00158.2013.-For

Sahai, E., Astsaturov, I., Cukierman, E., DeNardo, D. G., Egeblad, M., Evans, R. M., Fearon, D., Greten, F. R., Hingorani, S. R., Hunter, T., Hynes, R. O., Jain, R. K., Janowitz, T., Jorgensen, C., Kimmelman, A. C., Kolonin, M. G., Maki, R. G., Powers, R. S., Puré, E., … Werb, Z. (2020). A framework for advancing our understanding of cancer-associated fibroblasts. In *Nature Reviews Cancer* (Vol. 20, Issue 3, pp. 174–186). Nature Research. https://doi.org/10.1038/s41568-019-0238-1

Sakai, E., Nakayama, M., Oshima, H., Kouyama, Y., Niida, A., Fujii, S., Ochiai, A., Nakayama, K. I., Mimori, K., Suzuki, Y., Hong, C. P., Ock, C. Y., Kim, S. J., & Oshima, M. (2018). Combined mutation of Apc, Kras, and Tgfbr2 effectively drives metastasis of intestinal cancer. *Cancer Research*, *78*(5), 1334–1346. https://doi.org/10.1158/0008-5472.CAN-17-3303

Santos, A. M., Jung, J., Aziz, N., Kissil, J. L., & Puré, E. (2009). Targeting fibroblast activation protein inhibits tumour stromagenesis and growth in mice. *Journal of Clinical Investigation*, *119*(12), 3613–3625. https://doi.org/10.1172/JCI38988

Sanz-Moreno, V., Gaggioli, C., Yeo, M., Albrengues, J., Wallberg, F., Viros, A., Hooper, S., Mitter, R., Féral, C. C., Cook, M., Larkin, J., Marais, R., Meneguzzi, G., Sahai, E., & Marshall, C. J. (2011a). ROCK and JAK1 Signaling Cooperate to Control Actomyosin Contractility in Tumour Cells and Stroma. *Cancer Cell*, *20*(2), 229–245. https://doi.org/10.1016/j.ccr.2011.06.018

Sanz-Moreno, V., Gaggioli, C., Yeo, M., Albrengues, J., Wallberg, F., Viros, A., Hooper, S., Mitter, R., Féral, C. C., Cook, M., Larkin, J., Marais, R., Meneguzzi, G., Sahai, E., & Marshall, C. J. (2011b). ROCK and JAK1 Signaling Cooperate to Control Actomyosin

Contractility in Tumour Cells and Stroma. *Cancer Cell*, *20*(2), 229–245. https://doi.org/10.1016/j.ccr.2011.06.018

Sapudom, J., Müller, C. D., Nguyen, K. T., Martin, S., Anderegg, U., & Pompe, T. (2020). Matrix remodeling and hyaluronan production by myofibroblasts and cancer-associated fibroblasts in 3d collagen matrices. *Gels*, *6*(4), 1–17. https://doi.org/10.3390/gels6040033

Sarrazy, V., Billet, F., Micallef, L., Coulomb, B., & Desmoulière, A. (2011). Mechanisms of pathological scarring: Role of myofibroblasts and current developments. *Wound Repair and Regeneration*, *19*(SUPPL. 1), s10–s15. https://doi.org/10.1111/j.1524-475X.2011.00708.x

Sato, H., Hara, T., Meng, S., Tsuji, Y., Arao, Y., Saito, Y., Sasaki, K., Kobayashi, S., Doki, Y., Eguchi, H., & Ishii, H. (2023). Multifaced roles of desmoplastic reaction and fibrosis in pancreatic cancer progression: Current understanding and future directions. In *Cancer Science* (Vol. 114, Issue 9, pp. 3487–3495). John Wiley and Sons Inc. https://doi.org/10.1111/cas.15890

Schmitt, M., & Greten, F. R. (2021). The inflammatory pathogenesis of colorectal cancer. In *Nature Reviews Immunology* (Vol. 21, Issue 10, pp. 653–667). Nature Research. https://doi.org/10.1038/s41577-021-00534-x

Sculthorpe, D. J., Denton, A., Fadhil, W., Rusnita, D., Ilyas, M., & Mukherjee, A. (2024). High α-SMA expression in the tumour stroma is associated with adverse clinical parameters in mismatch repair-proficient colorectal cancers only. *American Journal of Clinical Pathology*. https://doi.org/10.1093/ajcp/aqae145

Sebastian, A., Hum, N. R., Martin, K. A., Gilmore, S. F., Peran, I., Byers, S. W., Wheeler, E. K., Coleman, M. A., & Loots, G. G. (2020). Single-cell transcriptomic analysis of tumour-derived fibroblasts and normal tissue-resident fibroblasts reveals fibroblast heterogeneity in breast cancer. *Cancers*, *12*(5). https://doi.org/10.3390/cancers12051307

Shah, R., Johnson, K. A., Lippert, A. E. L., Kraus, S. G., Emmerich, P. B., Pasch, C. A., Zhang, W., Matkowskyj, K. A., LeBeau, A. M., & Deming, D. A. (2024). Cancer-Associated Fibroblast Proteins as Potential Targets against Colorectal Cancers. *Cancers*, *16*(18). https://doi.org/10.3390/cancers16183158

Shaw, T. J., & Rognoni, E. (2020). Dissecting Fibroblast Heterogeneity in Health and Fibrotic Disease. In *Current Rheumatology Reports* (Vol. 22, Issue 8). Springer. https://doi.org/10.1007/s11926-020-00903-w

Shi, J., Song, X., Traub, B., Luxenhofer, M., & Kornmann, M. (2021). Involvement of IL-4, IL-13 and their receptors in pancreatic cancer. In *International Journal of Molecular Sciences* (Vol. 22, Issue 6, pp. 1–16). MDPI AG. https://doi.org/10.3390/ijms22062998

Shi, X., Young, C. D., Zhou, H., & Wang, X. (2020). Transforming growth factor-β signaling in fibrotic diseases and cancer-associated fibroblasts. In *Biomolecules* (Vol. 10, Issue 12, pp. 1–22). MDPI AG. https://doi.org/10.3390/biom10121666

Sinn, M., Denkert, C., Striefler, J. K., Pelzer, U., Stieler, J. M., Bahra, M., Lohneis, P., Dörken, B., Oettle, H., Riess, H., & Sinn, B. V. (2014). α-Smooth muscle actin expression and desmoplastic stromal reaction in pancreatic cancer: Results from the CONKO-001 study. *British Journal of Cancer*, *111*(10), 1917–1923. https://doi.org/10.1038/bjc.2014.495

Sirica, A. E., & Gores, G. J. (2014). Desmoplastic stroma and cholangiocarcinoma: Clinical implications and therapeutic targeting. In *Hepatology* (Vol. 59, Issue 6, pp. 2397–2402). John Wiley and Sons Inc. https://doi.org/10.1002/hep.26762

Song, M., Chan, A. T., & Sun, J. (2020). Influence of the Gut Microbiome, Diet, and Environment on Risk of Colorectal Cancer. *Gastroenterology*, *158*(2), 322–340. https://doi.org/10.1053/j.gastro.2019.06.048

Steeg, P. S. (2016). Targeting metastasis. In *Nature Reviews Cancer* (Vol. 16, Issue 4, pp. 201–218). Nature Publishing Group. https://doi.org/10.1038/nrc.2016.25

Strell, C., Paulsson, J., Jin, S. B., Tobin, N. P., Mezheyeuski, A., Roswall, P., Mutgan, C., Mitsios, N., Johansson, H., Wickberg, S. M., Svedlund, J., Nilsson, M., Hall, P., Mulder, J., Radisky, D. C., Pietras, K., Bergh, J., Lendahl, U., Warnberg, F., & Ostman, A. (2019). Impact of Epithelial–Stromal Interactions on Peritumoural Fibroblasts in Ductal Carcinoma in Situ. *Journal of the National Cancer Institute*, *111*(9), 983–995. https://doi.org/10.1093/JNCI/DJY234

Stylianou, A., Gkretsi, V., Louca, M., Zacharia, L. C., & Stylianopoulos, T. (2019). Collagen content and extracellular matrix cause cytoskeletal remodelling in pancreatic fibroblasts. *Journal of the Royal Society Interface*, *16*(154). https://doi.org/10.1098/rsif.2019.0226

Stylianou, A., Gkretsi, V., & Stylianopoulos, T. (2018). Transforming growth factor-β modulates pancreatic cancer associated fibroblasts cell shape, stiffness and invasion. *Biochimica et Biophysica Acta - General Subjects*, *1862*(7), 1537–1546. https://doi.org/10.1016/j.bbagen.2018.02.009

Suchanski, J., Tejchman, A., Zacharski, M., Piotrowska, A., Grzegrzolka, J., Chodaczek, G., Nowinska, K., Rys, J., Dziegiel, P., Kieda, C., & Ugorski, M. (2017). Podoplanin increases the migration of human fibroblasts and affects the endothelial cell network formation: A possible role for cancer-associated fibroblasts in breast cancer progression. *PLoS ONE*, *12*(9). https://doi.org/10.1371/journal.pone.0184970

Sun, G., Dong, X., Tang, X., Qu, H., Zhang, H., & Zhao, E. (2019). The prognostic value of immunoscore in patients with colorectal cancer: A systematic review and meta-analysis. *Cancer Medicine*, *8*(1), 182–189. https://doi.org/10.1002/cam4.1921

Sun, K.-H., Chang, Y., Reed, N. I., & Sheppard, D. (2016). Smooth muscle actin is an inconsistent marker of fibroblasts responsible for force-dependent TGF activation or collagen production across multiple models of organ fibrosis. *Am J Physiol Lung Cell Mol Physiol*, *310*, 824–836. https://doi.org/10.1152/ajplung.00350.2015.-Fibrosis

Sun, Y., Campisi, J., Higano, C., Beer, T. M., Porter, P., Coleman, I., True, L., & Nelson, P.

S. (2012). Treatment-induced damage to the tumour microenvironment promotes prostate cancer therapy resistance through WNT16B. *Nature Medicine*, *18*(9), 1359–1368. https://doi.org/10.1038/nm.2890

Sung, H., Ferlay, J., Siegel, R. L., Laversanne, M., Soerjomataram, I., Jemal, A., & Bray, F. (2021). Global Cancer Statistics 2020: GLOBOCAN Estimates of Incidence and Mortality Worldwide for 36 Cancers in 185 Countries. *CA: A Cancer Journal for Clinicians*, *71*(3), 209–249. https://doi.org/10.3322/caac.21660

Suzuki, H., Kaneko, M. K., & Kato, Y. (2022). Roles of Podoplanin in Malignant Progression of Tumour. In *Cells* (Vol. 11, Issue 3). MDPI. https://doi.org/10.3390/cells11030575

Takahashi, M., Kobayashi, H., Mizutani, Y., Hara, A., Iida, T., Miyai, Y., Asai, N., & Enomoto, A. (2021). Roles of the Mesenchymal Stromal/Stem Cell Marker Meflin/Islr in Cancer Fibrosis. In *Frontiers in Cell and Developmental Biology* (Vol. 9). Frontiers Media S.A. https://doi.org/10.3389/fcell.2021.749924

Takasugi, M., Yoshida, Y., & Ohtani, N. (2022). Cellular senescence and the tumour microenvironment. In *Molecular Oncology* (Vol. 16, Issue 18, pp. 3333–3351). John Wiley and Sons Ltd. https://doi.org/10.1002/1878-0261.13268

Tang, L. Y., Heller, M., Meng, Z., Yu, L. R., Tang, Y., Zhou, M., & Zhang, Y. E. (2017). Transforming growth factor-β (TGF-β) directly activates the JAK1-STAT3 axis to induce hepatic fibrosis in coordination with the SMAD pathway. *Journal of Biological Chemistry*, *292*(10), 4302–4312. https://doi.org/10.1074/jbc.M116.773085

Tape, C. J., Ling, S., Dimitriadi, M., McMahon, K. M., Worboys, J. D., Leong, H. S., Norrie, I. C., Miller, C. J., Poulogiannis, G., Lauffenburger, D. A., & Jørgensen, C. (2016). Oncogenic KRAS Regulates Tumour Cell Signaling via Stromal Reciprocation. *Cell*, *165*(4), 910–920. https://doi.org/10.1016/j.cell.2016.03.029

-Tavirani, M., Rezaei-Tavirani, M., Safaei, A., & Zali, M. R. (2013). The Association between Polymorphismsin Insulin and Obesity Related Genesand Risk of Colorectal Cancer. In *Colorectal Cancer. Iran J Cancer Prev* (Vol. 4, Issue 4).

Theocharis, A. D., Skandalis, S. S., Gialeli, C., & Karamanos, N. K. (2016). Extracellular matrix structure. In *Advanced Drug Delivery Reviews* (Vol. 97, pp. 4–27). Elsevier B.V. https://doi.org/10.1016/j.addr.2015.11.001

Tojo, M., Hamashima, Y., Hanyu, A., Kajimoto, T., Saitoh, M., Miyazono, K., Node, M., & Imamura, T. (2005). The ALK-5 inhibitor A-83-01 inhibits Smad signaling and epithelial-to-mesenchymal transition by transforming growth factor-β. *Cancer Science*, *96*(11), 791–800. https://doi.org/10.1111/j.1349-7006.2005.00103.x

Tommelein, J., Verset, L., Boterberg, T., Demetter, P., Bracke, M., & De Wever, O. (2015). Cancer-associated fibroblasts connect metastasispromoting communication in colorectal cancer. In *Frontiers in Oncology* (Vol. 5). Frontiers Media S.A. https://doi.org/10.3389/fonc.2015.00063

Topalian, S. L., Taube, J. M., Anders, R. A., & Pardoll, D. M. (2016). Mechanism-driven biomarkers to guide immune checkpoint blockade in cancer therapy. In *Nature Reviews*

Cancer (Vol. 16, Issue 5, pp. 275–287). Nature Publishing Group. https://doi.org/10.1038/nrc.2016.36

Tosolini, M., Kirilovsky, A., Mlecnik, B., Fredriksen, T., Mauger, S., Bindea, G., Berger, A., Bruneval, P., Fridman, W. H., Pagès, F., & Galon, J. (2011). Clinical impact of different classes of infiltrating T cytotoxic and helper cells (Th1, Th2, Treg, Th17) in patients with colorectal cancer. *Cancer Research*, *71*(4), 1263–1271. https://doi.org/10.1158/0008-5472.CAN-10-2907

Tsujino, T., Seshimo, I., Yamamoto, H., Chew, Y. N., Ezumi, K., Takemasa, I., Ikeda, M., Sekimoto, M., Matsuura, N., & Monden, M. (2007). Stromal myofibroblasts predict disease recurrence for colorectal cancer. *Clinical Cancer Research*, *13*(7), 2082–2090. https://doi.org/10.1158/1078-0432.CCR-06-2191

Tuan, J., & Chen, Y.-X. (2016). Dietary and Lifestyle Factors Associated with Colorectal Cancer Risk and Interactions with Microbiota: Fiber, Red or Processed Meat and Alcoholic Drinks. *Gastrointestinal Tumours*, *3*(1), 17–24. https://doi.org/10.1159/000442831

Ueno, H., Ishiguro, M., Nakatani, E., Ishikawa, T., Uetake, H., Murotani, K., Matsui, S., Teramukai, S., Sugai, T., Ajioka, Y., Maruo, H., Kotaka, M., Tsujie, M., Munemoto, Y., Yamaguchi, T., Kuroda, H., Fukunaga, M., Tomita, N., & Sugihara, K. (2021). Prognostic value of desmoplastic reaction characterisation in stage II colon cancer: prospective validation in a Phase 3 study (SACURA Trial). *British Journal of Cancer*, *124*(6), 1088–1097. https://doi.org/10.1038/s41416-020-01222-8

Unterleuthner, D., Neuhold, P., Schwarz, K., Janker, L., Neuditschko, B., Nivarthi, H., Crncec, I., Kramer, N., Unger, C., Hengstschläger, M., Eferl, R., Moriggl, R., Sommergruber, W., Gerner, C., & Dolznig, H. (2020). Cancer-associated fibroblast-derived WNT2 increases tumour angiogenesis in colon cancer. *Angiogenesis*, *23*(2), 159–177. https://doi.org/10.1007/s10456-019-09688-8

Valastyan, S., & Weinberg, R. A. (2011). Tumour metastasis: Molecular insights and evolving paradigms. In *Cell* (Vol. 147, Issue 2, pp. 275–292). Elsevier B.V. https://doi.org/10.1016/j.cell.2011.09.024

Varveri, A., Papadopoulou, M., Papadovasilakis, Z., Compeer, E. B., Legaki, A. I., Delis, A., Damaskou, V., Boon, L., Papadogiorgaki, S., Samiotaki, M., Foukas, P. G., Eliopoulos, A. G., Hatzioannou, A., Alissafi, T., Dustin, M. L., & Verginis, P. (2024). Immunological synapse formation between T regulatory cells and cancer-associated fibroblasts promotes tumour development. *Nature Communications*, *15*(1). https://doi.org/10.1038/s41467-024-49282-1

Vennin, C., Mélénec, P., Rouet, R., Nobis, M., Cazet, A. S., Murphy, K. J., Herrmann, D., Reed, D. A., Lucas, M. C., Warren, S. C., Elgundi, Z., Pinese, M., Kalna, G., Roden, D., Samuel, M., Zaratzian, A., Grey, S. T., Da Silva, A., Leung, W., … Timpson, P. (2019). CAF hierarchy driven by pancreatic cancer cell p53-status creates a pro-metastatic and chemoresistant environment via perlecan. *Nature Communications*, *10*(1).

https://doi.org/10.1038/s41467-019-10968-6
Verset, L., Tommelein, J., Moles Lopez, X., Decaestecker, C., Boterberg, T., De Vlieghere, E., Salmon, I., Mareel, M., Bracke, M., De Wever, O., & Demetter, P. (2015). Impact of neoadjuvant therapy on cancer-associated fibroblasts in rectal cancer. *Radiotherapy and Oncology*, *116*(3), 449–454. https://doi.org/10.1016/j.radonc.2015.05.007
Vokurka, M., Lacina, L., Brábek, J., Kolář, M., Ng, Y. Z., & Smetana, K. (2022). Cancer-Associated Fibroblasts Influence the Biological Properties of Malignant Tumours via Paracrine Secretion and Exosome Production. *J. Mol. Sci*, *2022*, 23. https://doi.org/10.3390/ijms
Wang, J., Tao, X., Zhu, J., Dai, Z., Du, Y., Xie, Y., Chu, X., Fu, G., & Lei, Z. (2025). Tumour organoid-immune co-culture models: exploring a new perspective of tumour immunity. In *Cell Death Discovery* (Vol. 11, Issue 1). Springer Nature. https://doi.org/10.1038/s41420-025-02407-x
Wang, Y., Du, J., Gao, Z., Sun, H., Mei, M., Wang, Y., Ren, Y., & Zhou, X. (2023). Evolving landscape of PD-L2: bring new light to checkpoint immunotherapy. In *British Journal of Cancer* (Vol. 128, Issue 7, pp. 1196–1207). Springer Nature. https://doi.org/10.1038/s41416-022-02084-y
Wang, Z. H., Ding, K. F., Yu, J. K., Zhai, X. H., Ruan, S. Q., Wang, S. W., Zhu, Y. L., Zheng, S., & Zhang, S. Z. (2012). Proteomic analysis of primary colon cancer-associated fibroblasts using the SELDI-ProteinChip platform. *Journal of Zhejiang University: Science B*, *13*(3), 159–167. https://doi.org/10.1631/jzus.B1100266
Wang, Z., Wang, J., Lan, T., Zhang, L., Yan, Z., Zhang, N., Xu, Y., & Tao, Q. (2023). Role and mechanism of fibroblast-activated protein-α expression on the surface of fibroblast-like synoviocytes in rheumatoid arthritis. In *Frontiers in Immunology* (Vol. 14). Frontiers Media S.A. https://doi.org/10.3389/fimmu.2023.1135384
Weber, A., Wasiliew, P., & Kracht, M. (2010). Interleukin-1 (IL-1) pathway. In *Science Signaling* (Vol. 3, Issue 105). https://doi.org/10.1126/scisignal.3105cm1
Welch, D. R., & Hurst, D. R. (2019). Defining the Hallmarks of Metastasis. In *Cancer Research* (Vol. 79, Issue 12, pp. 3011–3027). American Association for Cancer Research Inc. https://doi.org/10.1158/0008-5472.CAN-19-0458
Wensink, G. E., Elias, S. G., Mullenders, J., Koopman, M., Boj, S. F., Kranenburg, O. W., & Roodhart, J. M. L. (2021). Patient-derived organoids as a predictive biomarker for treatment response in cancer patients. In *npj Precision Oncology* (Vol. 5, Issue 1). Nature Research. https://doi.org/10.1038/s41698-021-00168-1
West, N. R., Mccuaig, S., Franchini, F., & Powrie, F. (2015). Emerging cytokine networks in colorectal cancer. In *Nature Reviews Immunology* (Vol. 15, Issue 10, pp. 615–629). Nature Publishing Group. https://doi.org/10.1038/nri3896
Wiley, M. B., Bauer, J., Alvarez, V., Kolics, Z., Cheng, W., Church, D. N., Kerr, D. J., Kerr, R. S., & Jung, B. (2025). Activin A affects colorectal cancer progression and immunomodulation in a stage dependent manner. *Scientific Reports*, *15*(1).

https://doi.org/10.1038/s41598-025-91853-9
Winkler, J., Abisoye-Ogunniyan, A., Metcalf, K. J., & Werb, Z. (2020). Concepts of extracellular matrix remodelling in tumour progression and metastasis. In *Nature Communications* (Vol. 11, Issue 1). Nature Research. https://doi.org/10.1038/s41467-020-18794-x
Wozniakova, M., Skarda, J., & Raska, M. (2022). The Role of Tumour Microenvironment and Immune Response in Colorectal Cancer Development and Prognosis. In *Pathology and Oncology Research* (Vol. 28). Frontiers Media S.A. https://doi.org/10.3389/pore.2022.1610502
Wright, K., Ly, T., Kriet, M., Czirok, A., & Thomas, S. M. (2023a). Cancer-Associated Fibroblasts: Master Tumour Microenvironment Modifiers. In *Cancers* (Vol. 15, Issue 6). Multidisciplinary Digital Publishing Institute (MDPI). https://doi.org/10.3390/cancers15061899
Wright, K., Ly, T., Kriet, M., Czirok, A., & Thomas, S. M. (2023b). Cancer-Associated Fibroblasts: Master Tumour Microenvironment Modifiers. In *Cancers* (Vol. 15, Issue 6). Multidisciplinary Digital Publishing Institute (MDPI). https://doi.org/10.3390/cancers15061899
Wright, K., Ly, T., Kriet, M., Czirok, A., & Thomas, S. M. (2023c). Cancer-Associated Fibroblasts: Master Tumour Microenvironment Modifiers. In *Cancers* (Vol. 15, Issue 6). Multidisciplinary Digital Publishing Institute (MDPI). https://doi.org/10.3390/cancers15061899
Wu, F., Yang, J., Liu, J., Wang, Y., Mu, J., Zeng, Q., Deng, S., & Zhou, H. (2021). Signaling pathways in cancer-associated fibroblasts and targeted therapy for cancer. In *Signal Transduction and Targeted Therapy* (Vol. 6, Issue 1). Springer Nature. https://doi.org/10.1038/s41392-021-00641-0
Xie, Y. H., Chen, Y. X., & Fang, J. Y. (2020). Comprehensive review of targeted therapy for colorectal cancer. In *Signal Transduction and Targeted Therapy* (Vol. 5, Issue 1). Springer Nature. https://doi.org/10.1038/s41392-020-0116-z
Xin, L., Gao, J., Zheng, Z., Chen, Y., Lv, S., Zhao, Z., Yu, C., Yang, X., & Zhang, R. (2021). Fibroblast Activation Protein-α as a Target in the Bench-to-Bedside Diagnosis and Treatment of Tumours: A Narrative Review. In *Frontiers in Oncology* (Vol. 11). Frontiers Media S.A. https://doi.org/10.3389/fonc.2021.648187
Xu, R., Zhou, X., Wang, S., & Trinkle, C. (2021). Tumour organoid models in precision medicine and investigating cancer-stromal interactions. In *Pharmacology and Therapeutics* (Vol. 218). Elsevier Inc. https://doi.org/10.1016/j.pharmthera.2020.107668
Yamaguchi, H., & Sakai, R. (2015). Direct interaction between carcinoma cells and cancer associated fibroblasts for the regulation of cancer invasion. In *Cancers* (Vol. 7, Issue 4, pp. 2054–2062). MDPI AG. https://doi.org/10.3390/cancers7040876
Yamashita, T., Horiguchi, H., Kadomatsu, T., Sato, M., Moroishi, T., & Oike, Y. (2024).

Immunotherapy-induced reprogramming of cancer-associated fibroblasts can promote tumour progression. *Genes to Cells*. https://doi.org/10.1111/gtc.13177

Yan, Y., Lin, H. W., Zhuang, Z. N., Li, M., & Guo, S. (2020). Interleukin-1 receptor antagonist enhances chemosensitivity to fluorouracil in treatment of Kras mutant colon cancer. *World Journal of Gastrointestinal Oncology*, *12*(8), 877–892. https://doi.org/10.4251/wjgo.v12.i8.877

Yang, D., Liu, J., Qian, H., & Zhuang, Q. (2023a). Cancer-associated fibroblasts: from basic science to anticancer therapy. In *Experimental and Molecular Medicine* (Vol. 55, Issue 7, pp. 1322–1332). Springer Nature. https://doi.org/10.1038/s12276-023-01013-0

Yang, D., Liu, J., Qian, H., & Zhuang, Q. (2023b). Cancer-associated fibroblasts: from basic science to anticancer therapy. In *Experimental and Molecular Medicine* (Vol. 55, Issue 7, pp. 1322–1332). Springer Nature. https://doi.org/10.1038/s12276-023-01013-0

Yang, D., Liu, J., Qian, H., & Zhuang, Q. (2023c). Cancer-associated fibroblasts: from basic science to anticancer therapy. In *Experimental and Molecular Medicine* (Vol. 55, Issue 7, pp. 1322–1332). Springer Nature. https://doi.org/10.1038/s12276-023-01013-0

Yang, D., Liu, J., Qian, H., & Zhuang, Q. (2023d). Cancer-associated fibroblasts: from basic science to anticancer therapy. In *Experimental and Molecular Medicine* (Vol. 55, Issue 7, pp. 1322–1332). Springer Nature. https://doi.org/10.1038/s12276-023-01013-0

Yang, H., Zhou, X., Sun, L., & Mao, Y. (2019). Correlation between PD-L2 expression and clinical outcome in solid cancer patients: A meta-analysis. *Frontiers in Oncology*, *9*(FEB). https://doi.org/10.3389/fonc.2019.00047

Yang, X., Lin, Y., Shi, Y., Li, B., Liu, W., Yin, W., Dang, Y., Chu, Y., Fan, J., & He, R. (2016a). FAP Promotes immunosuppression by cancer-associated fibroblasts in the tumour microenvironment via STAT3-CCL2 Signaling. *Cancer Research*, *76*(14), 4124–4135. https://doi.org/10.1158/0008-5472.CAN-15-2973

Yang, X., Lin, Y., Shi, Y., Li, B., Liu, W., Yin, W., Dang, Y., Chu, Y., Fan, J., & He, R. (2016b). FAP Promotes immunosuppression by cancer-associated fibroblasts in the tumour microenvironment via STAT3-CCL2 Signaling. *Cancer Research*, *76*(14), 4124–4135. https://doi.org/10.1158/0008-5472.CAN-15-2973

Yantiss, R. K. (2017). Persistent Problems in Colorectal Cancer Reporting. In *Surgical Pathology Clinics* (Vol. 10, Issue 4, pp. 961–976). W.B. Saunders. https://doi.org/10.1016/j.path.2017.07.010

Yin, J., Zhu, W., Feng, S., Yan, P., & Qin, S. (2024). The role of cancer-associated fibroblasts in the invasion and metastasis of colorectal cancer. In *Frontiers in Cell and Developmental Biology* (Vol. 12). Frontiers Media SA. https://doi.org/10.3389/fcell.2024.1375543

Yoshida, G. J. (2020). Regulation of heterogeneous cancer-associated fibroblasts: The molecular pathology of activated signaling pathways. In *Journal of Experimental and Clinical Cancer Research* (Vol. 39, Issue 1). BioMed Central. https://doi.org/10.1186/s13046-020-01611-0

Younesi, F. S., Miller, A. E., Barker, T. H., Rossi, F. M. V., & Hinz, B. (2024). Fibroblast and myofibroblast activation in normal tissue repair and fibrosis. In *Nature Reviews Molecular Cell Biology* (Vol. 25, Issue 8, pp. 617–638). Nature Research. https://doi.org/10.1038/s41580-024-00716-0

Yue, B. (2014). Biology of the extracellular matrix: An overview. In *Journal of Glaucoma* (Vol. 23, Issue 8, pp. S20–S23). Lippincott Williams and Wilkins. https://doi.org/10.1097/IJG.0000000000000108

Zadka, Ł., Chabowski, M., Grybowski, D., Piotrowska, A., & Dzięgiel, P. (2021). Interplay of stromal tumour-infiltrating lymphocytes, normal colonic mucosa, cancer-associated fibroblasts, clinicopathological data and the immunoregulatory molecules of patients diagnosed with colorectal cancer. *Cancer Immunology, Immunotherapy*, *70*(9), 2681–2700. https://doi.org/10.1007/s00262-021-02863-1

Zafari, N., Khosravi, F., Rezaee, Z., Esfandyari, S., Bahiraei, M., Bahramy, A., Ferns, G. A., & Avan, A. (2022). The role of the tumour microenvironment in colorectal cancer and the potential therapeutic approaches. *Journal of Clinical Laboratory Analysis*, *36*(8). https://doi.org/10.1002/jcla.24585

Zhang, J., Huang, D., Saw, P. E., & Song, E. (2022). Turning cold tumours hot: from molecular mechanisms to clinical applications. In *Trends in Immunology* (Vol. 43, Issue 7, pp. 523–545). Elsevier Ltd. https://doi.org/10.1016/j.it.2022.04.010

Zhang, L., Li, Z., Skrzypczynska, K. M., Fang, Q., Zhang, W., O'Brien, S. A., He, Y., Wang, L., Zhang, Q., Kim, A., Gao, R., Orf, J., Wang, T., Sawant, D., Kang, J., Bhatt, D., Lu, D., Li, C. M., Rapaport, A. S., … Yu, X. (2020). Single-Cell Analyses Inform Mechanisms of Myeloid-Targeted Therapies in Colon Cancer. *Cell*, *181*(2), 442-459.e29. https://doi.org/10.1016/j.cell.2020.03.048

Zhang, Q., Wang, Y., & Liu, F. (2023). Cancer-associated fibroblasts: Versatile mediators in remodeling the tumour microenvironment. *Cellular Signalling*, *103*. https://doi.org/10.1016/j.cellsig.2022.110567

Zhang, Y., Rajput, A., Jin, N., & Wang, J. (2020). Mechanisms of immunosuppression in colorectal cancer. In *Cancers* (Vol. 12, Issue 12, pp. 1–24). MDPI AG. https://doi.org/10.3390/cancers12123850

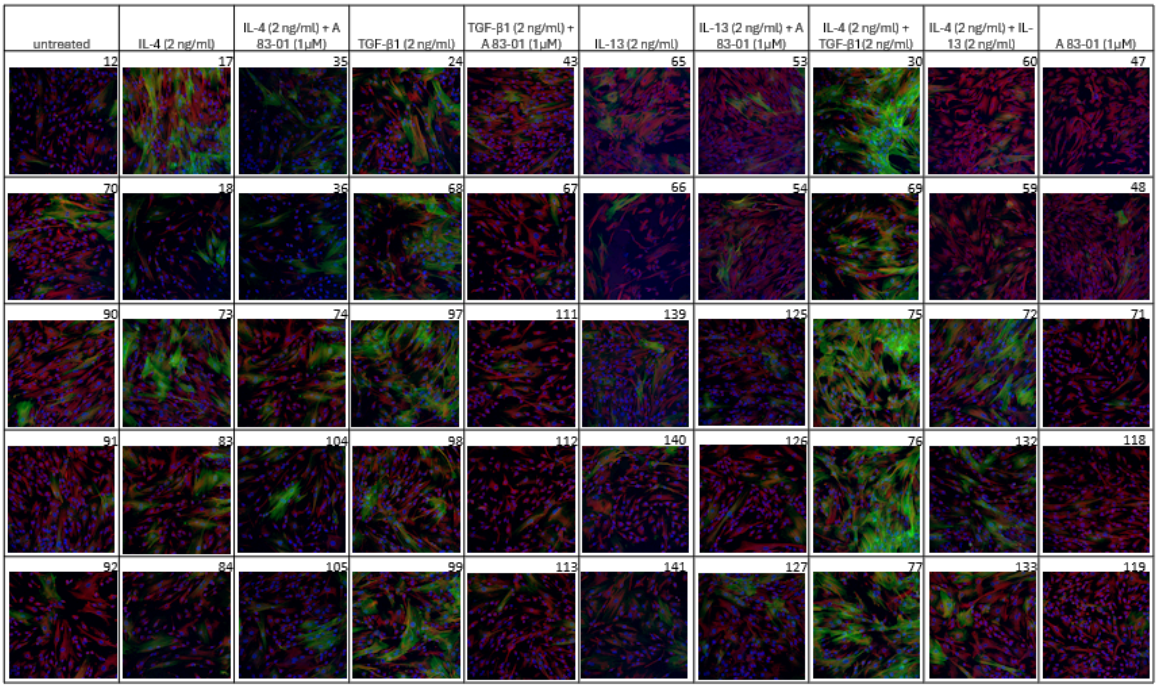
Zhang, Z., Zhang, Q., & Wang, Y. (2025). CAF-mediated tumour vascularization: From mechanistic insights to targeted therapies. In *Cellular Signalling* (Vol. 132). Elsevier Inc. https://doi.org/10.1016/j.cellsig.2025.111827

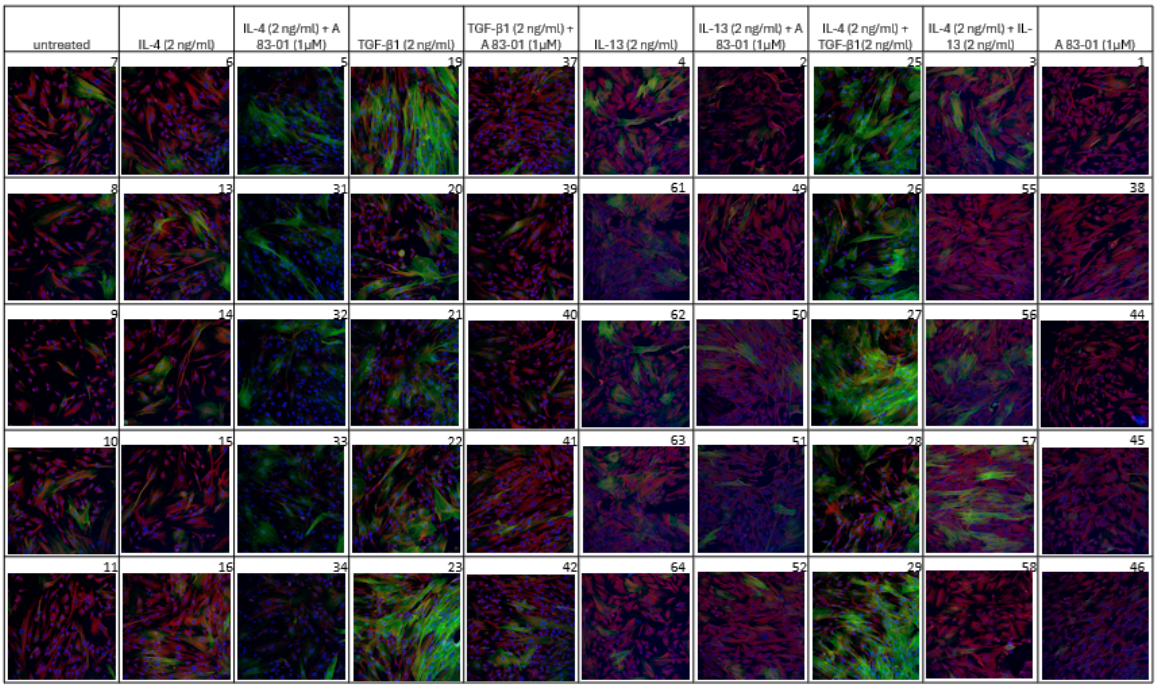
Zhao, H., Wu, L., Yan, G., Chen, Y., Zhou, M., Wu, Y., & Li, Y. (2021). Inflammation and tumour progression: signaling pathways and targeted intervention. In *Signal Transduction and Targeted Therapy* (Vol. 6, Issue 1). Springer Nature. https://doi.org/10.1038/s41392-021-00658-5

Zhao, J., & Chen, Y. (2022). Systematic identification of cancer-associated-fibroblast-derived genes in patients with colorectal cancer based on single-cell sequencing and transcriptomics. *Frontiers in Immunology*, *13*.

https://doi.org/10.3389/fimmu.2022.988246
Zhao, Z., Li, T., Yuan, Y., & Zhu, Y. (2023). What is new in cancer-associated fibroblast biomarkers? In *Cell Communication and Signaling* (Vol. 21, Issue 1). BioMed Central Ltd. https://doi.org/10.1186/s12964-023-01125-0
Zhou, Y., Xia, L., Wang, H., Oyang, L., Su, M., Liu, Q., Lin, J., Tan, S., Tian, Y., Liao, Q., & Cao, D. (2018). Oncotarget 33403 www.oncotarget.com Cancer stem cells in progression of colorectal cancer. In *Oncotarget* (Vol. 9, Issue 70). www.oncotarget.com
Zhou, Z., Van der Jeught, K., Fang, Y., Yu, T., Li, Y., Ao, Z., Liu, S., Zhang, L., Yang, Y., Eyvani, H., Cox, M. L., Wang, X., He, X., Ji, G., Schneider, B. P., Guo, F., Wan, J., Zhang, X., & Lu, X. (2021). An organoid-based screen for epigenetic inhibitors that stimulate antigen presentation and potentiate T-cell-mediated cytotoxicity. *Nature Biomedical Engineering*, *5*(11), 1320–1335. https://doi.org/10.1038/s41551-021-00805-x
Zhu, L., Qu, Y., Yang, J., Shao, T., Kuang, J., Liu, C., Qi, Y., Li, M., Li, Y., Zhang, S., Wang, J., Liu, Y., Liu, J., Hu, Y., Zhu, L., & Hou, T. (2024). PD-L2 act as an independent immune checkpoint in colorectal cancer beyond PD-L1. *Frontiers in Immunology*, *15*. https://doi.org/10.3389/fimmu.2024.1486888
Zhu, Y., Yin, W. Le, Ba, Y. F., Tian, L., Gu, Z. Q., Zhang, M. S., & Zhong, C. N. (2012). Transforming growth factor-1 promotes the transcriptional activation of plasminogen activator inhibitor type 1 in carcinoma-associated fibroblasts. *Molecular Medicine Reports*, *6*(5), 1001–1005. https://doi.org/10.3892/mmr.2012.1020
Zhukova, J. V., Lopatnikova, J. A., Alshevskaya, A. A., & Sennikov, S. V. (2024). Molecular mechanisms of regulation of IL-1 and its receptors. In *Cytokine and Growth Factor Reviews* (Vol. 80, pp. 59–71). Elsevier Ltd. https://doi.org/10.1016/j.cytogfr.2024.09.004

6. Appendix


untreated
IL-4 (2 ng/ml)
IL-4 (2 ng/ml) + A 83-01 (1µM)
TGF-β1 (2 ng/ml)
TGF-β1 (2 ng/ml) + A 83-01 (1µM)
IL-13 (2 ng/ml)
IL-13 (2 ng/ml) + A 83-01 (1µM)
IL-4 (2 ng/ml) + TGF-β1(2 ng/ml)
IL-4 (2 ng/ml) + IL-13 (2 ng/ml)
A 83-01 (1µM)
12 17 35 24 43 65 53 30 60 47
70 18 36 68 67 66 54 69 59 48
90 73 74 97 111 139 125 75 72 71
91 83 104 98 112 140 126 76 132 118
92 84 105 99 113 141 127 77 133 119


untreated
IL-4 (2 ng/ml)
IL-4 (2 ng/ml) + A 83-01 (1µM)
TGF-β1 (2 ng/ml)
TGF-β1 (2 ng/ml) + A 83-01 (1µM)
IL-13 (2 ng/ml)
IL-13 (2 ng/ml) + A 83-01 (1µM)
IL-4 (2 ng/ml) + TGF-β1(2 ng/ml)
IL-4 (2 ng/ml) + IL-13 (2 ng/ml)
A 83-01 (1µM)
7 6 5 19 37 4 2 25 3 1
8 13 31 20 39 61 49 26 55 38
9 14 32 21 40 62 50 27 56 44
10 15 33 22 41 63 51 28 57 45
11 16 34 23 42 64 52 29 58 46

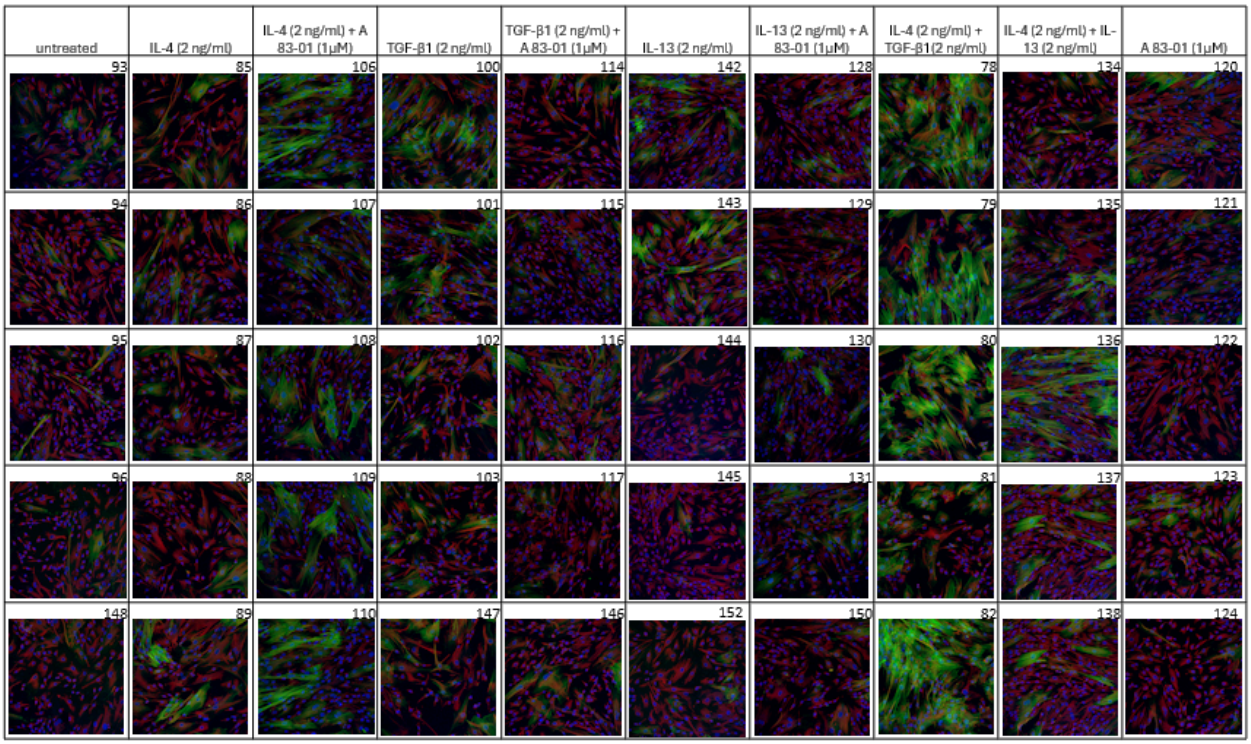


Figure 19: **Confocal images of CAF 6388/19 (p11) showing upregulation of α-SMA with treatment of 2ng/ml of IL-4, TGFβ-1, IL-13 and 1μM A 83-01 in different combinations (as indicated) for 48 hours**. (n=15) Nuclei stained by DAPI (blue), Vimentin (red), α-SMA (green).

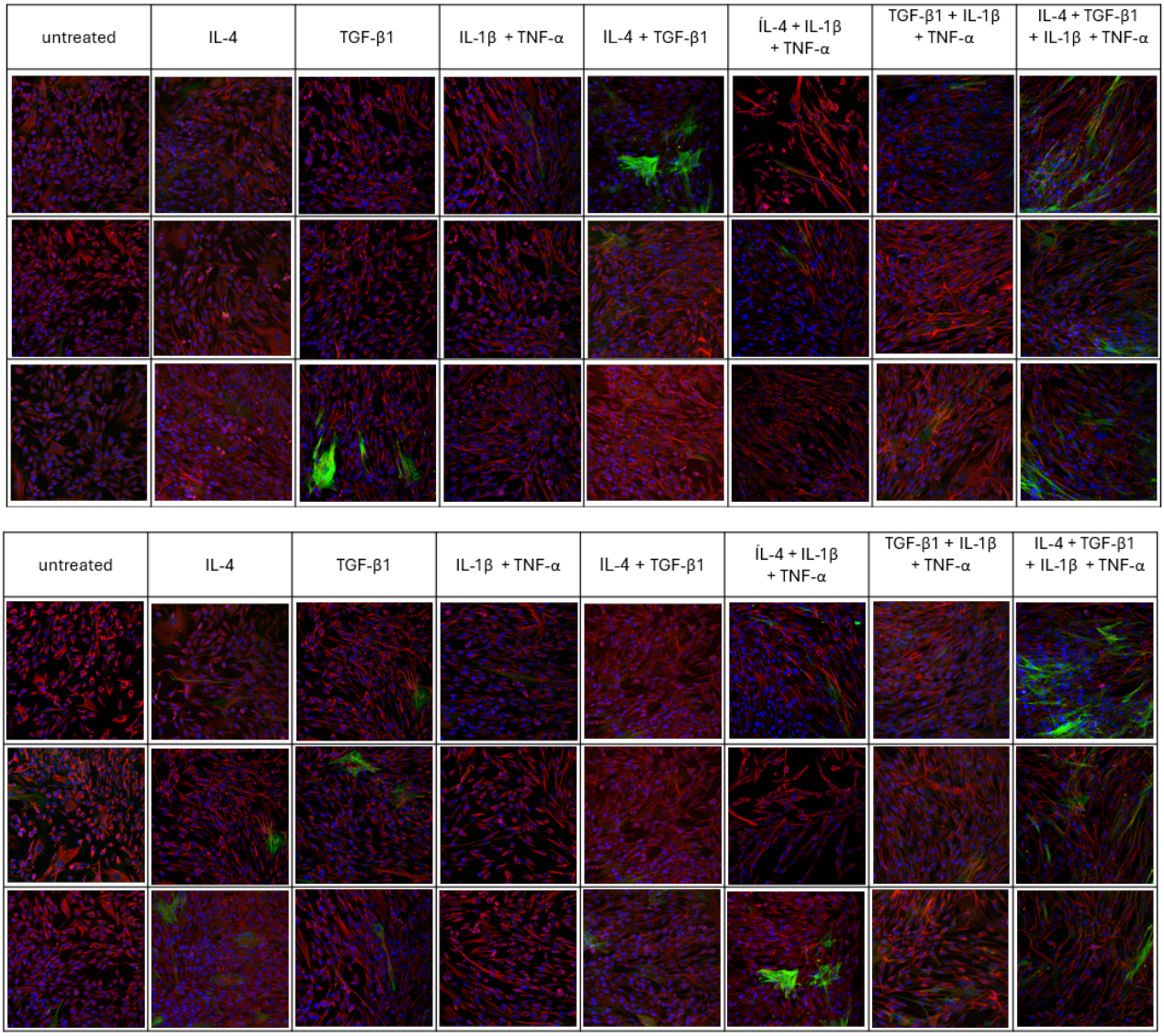
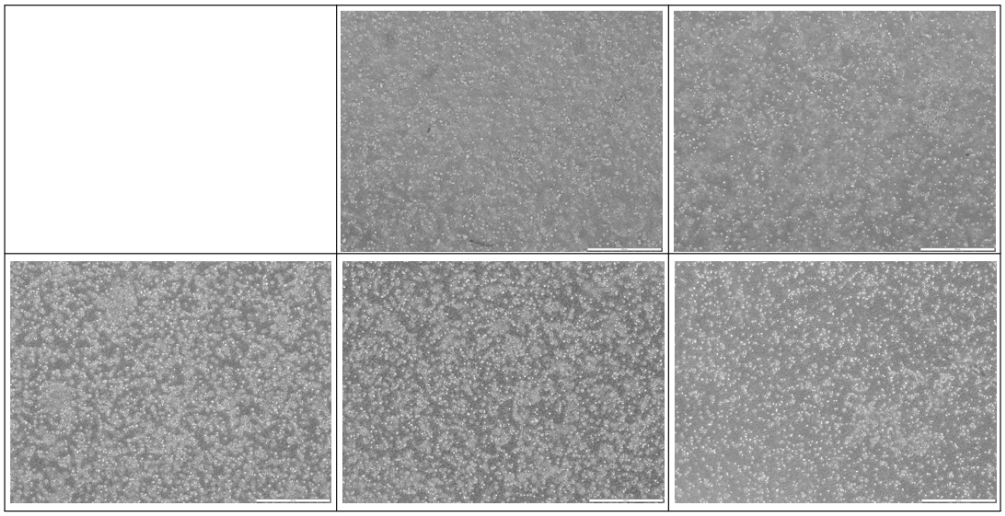
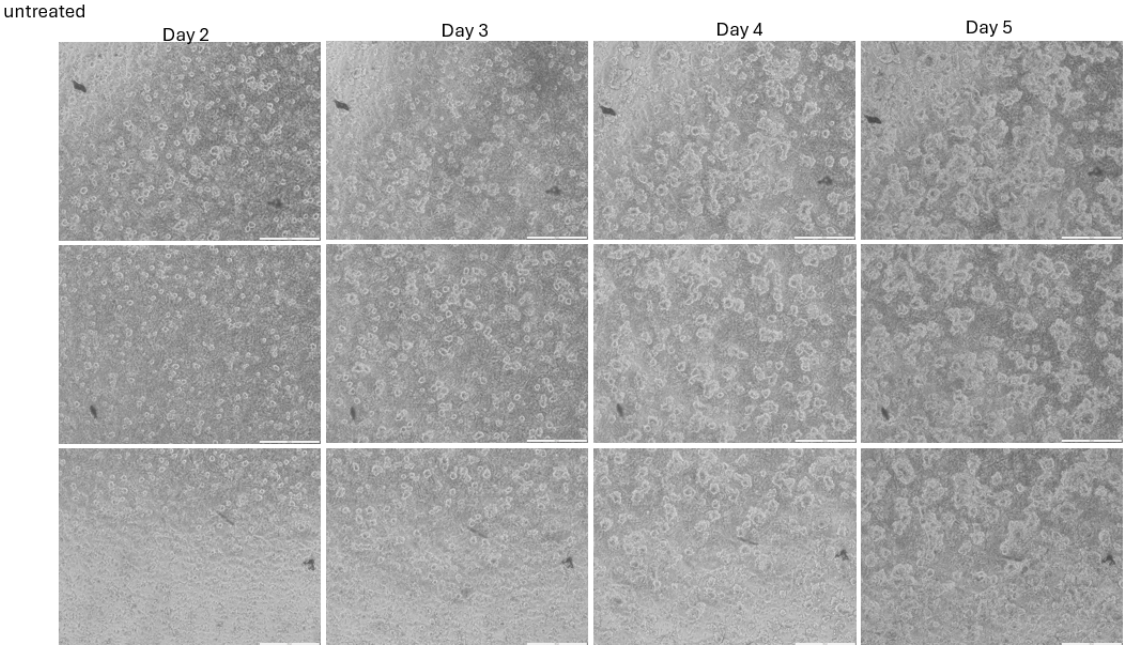


Figure 20: Confocal images of CAF BGM2008 (p7) showing upregulation of α-SMA with treatment of 2ng/ml of IL-4, TGFβ-1, IL-1β + TNF-α different combinations (as indicated) for 48 hours*. (n=6) Nuclei stained by DAPI (blue), Vimentin (red), α-SMA (green).*

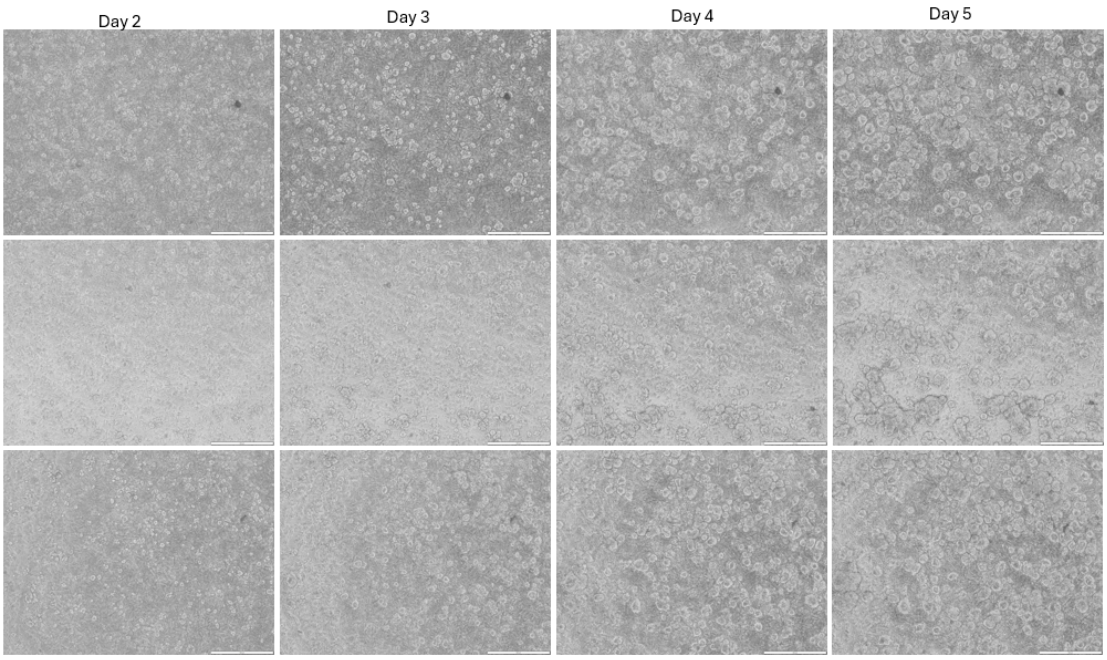
A



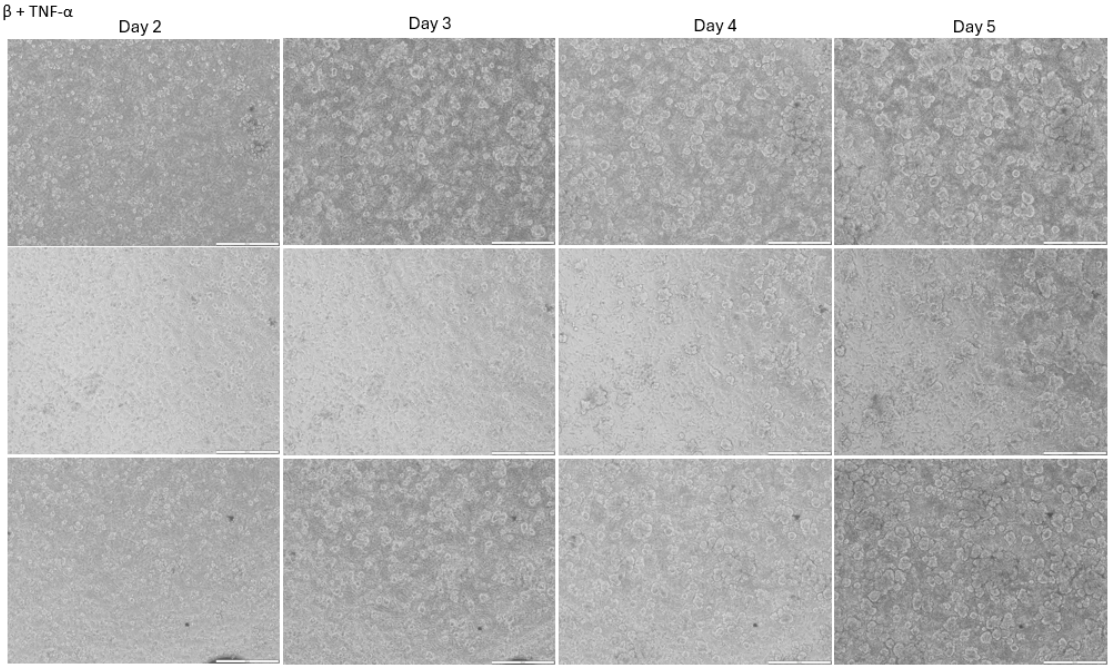
B



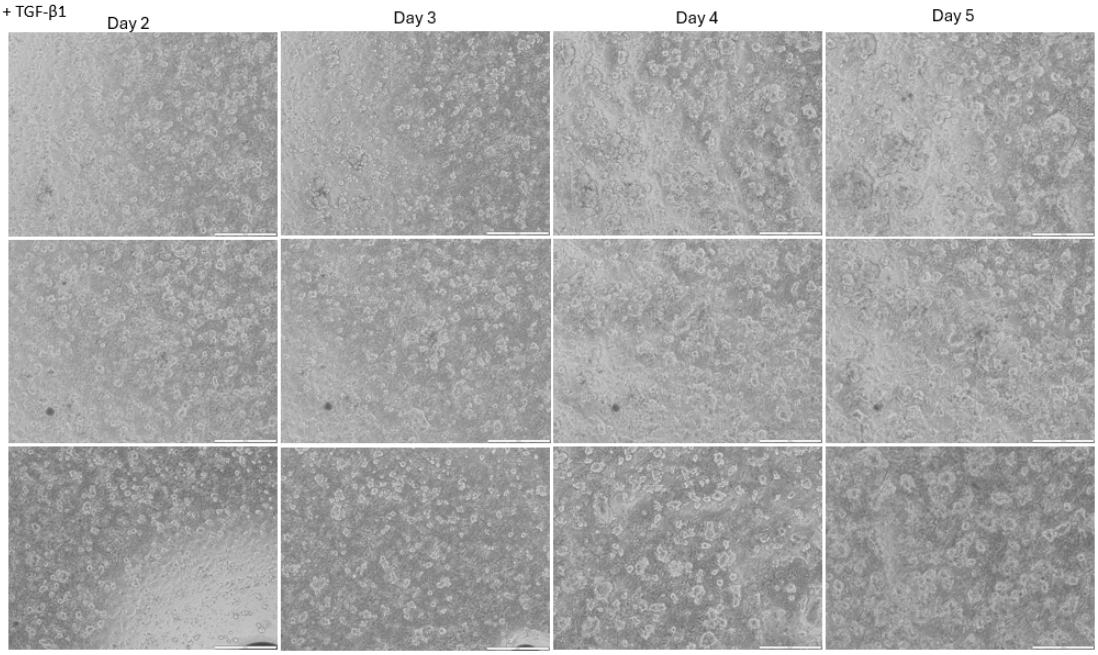
TGF-β1



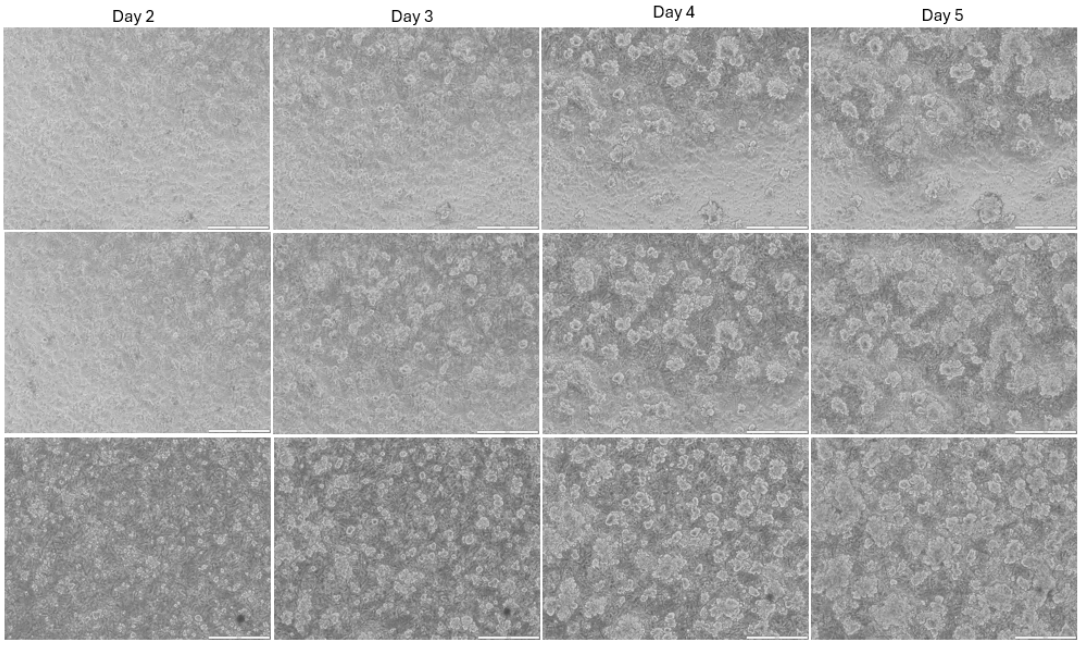
IL-1β + TNF-α



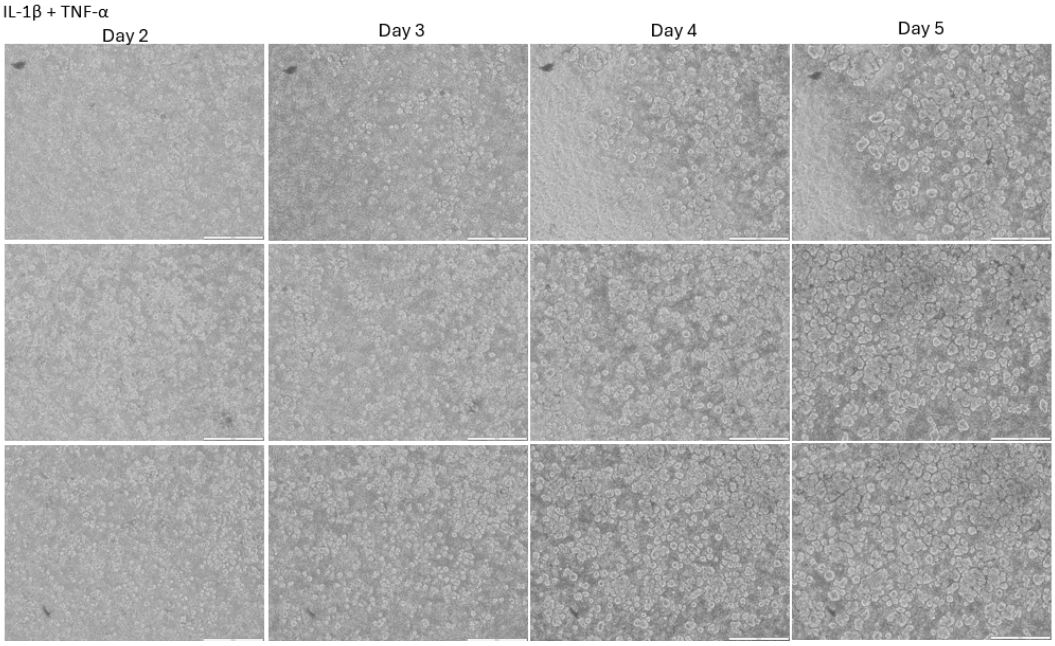
IL-4 + TGF-β1



IL-4 + IL-1β + TNF-α



TGF-β1 + IL-1β + TNF-α



IL-4 + TGF-β1 + IL-1β + TNF-α

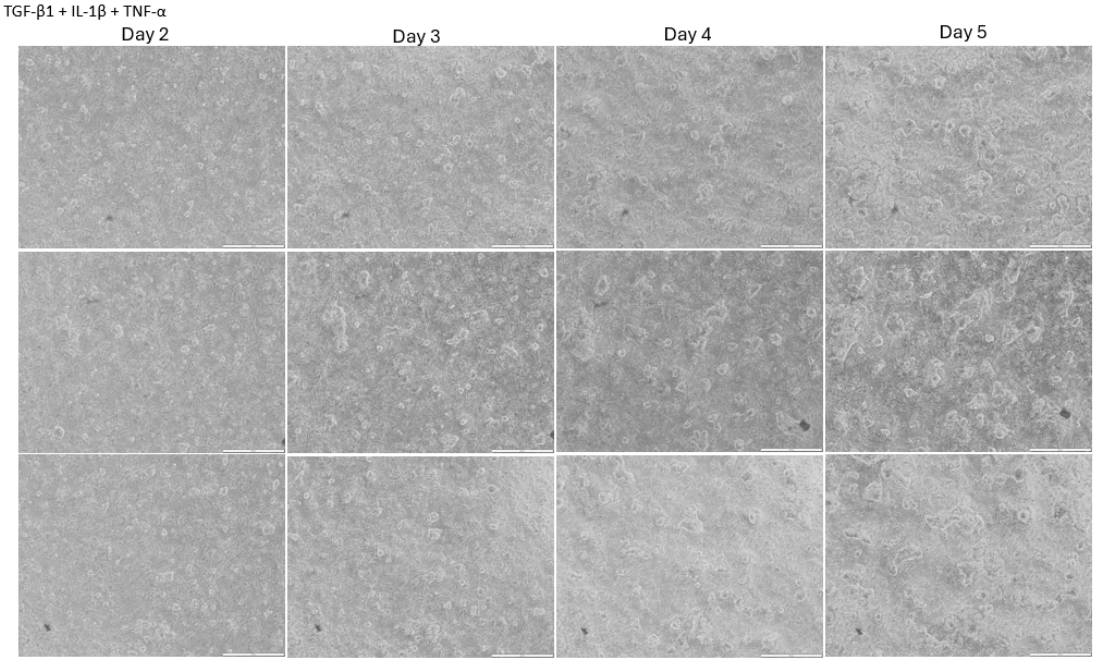


Figure 21: **Microscope images of OOTA (CAF-BGM2008 (p12) and CRC organoid co-culture) showing organoids with treatment of 2ng/ml of IL-4, TGFβ-1, IL-1β + TNF-α different combinations (as indicated) for 5 days. (A)** seeding of 5 randomly chosen OOTA **(B)** n=3 pictures per condition analysed **(C**) area analysed with ImageJ, n=3 pictures per condition

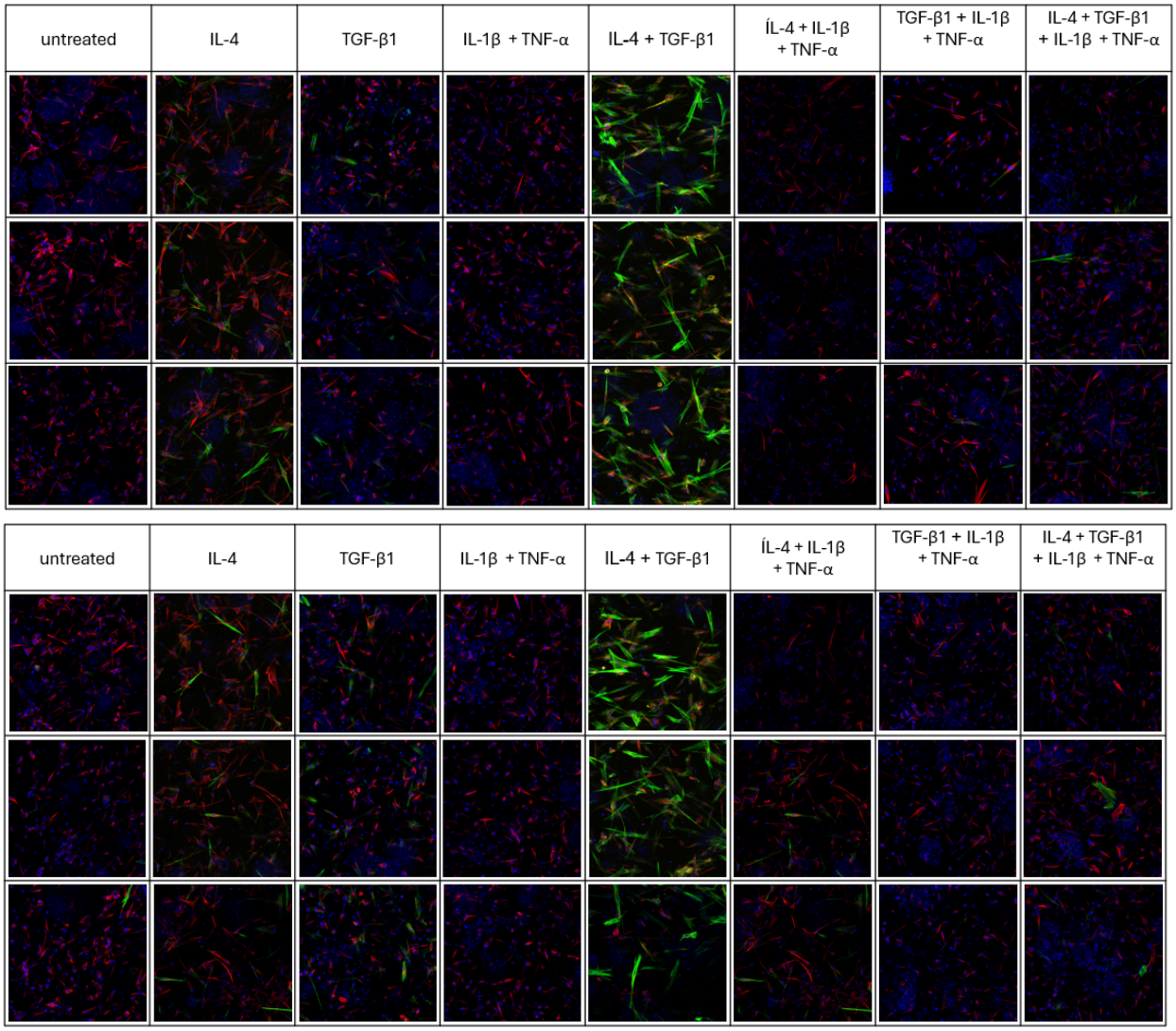


Figure 22: **Confocal images of OOTA (CAF-BGM2008 (p12) and CRC organoid (not visible) co-culture) showing upregulation of α-SMA with treatment of 2ng/ml of IL-4, TGFβ-1, IL-1β + TNF-α different combinations (as indicated) for 48 hours.** (n=6) Nuclei stained by DAPI (blue), Vimentin (red), α-SMA (green).

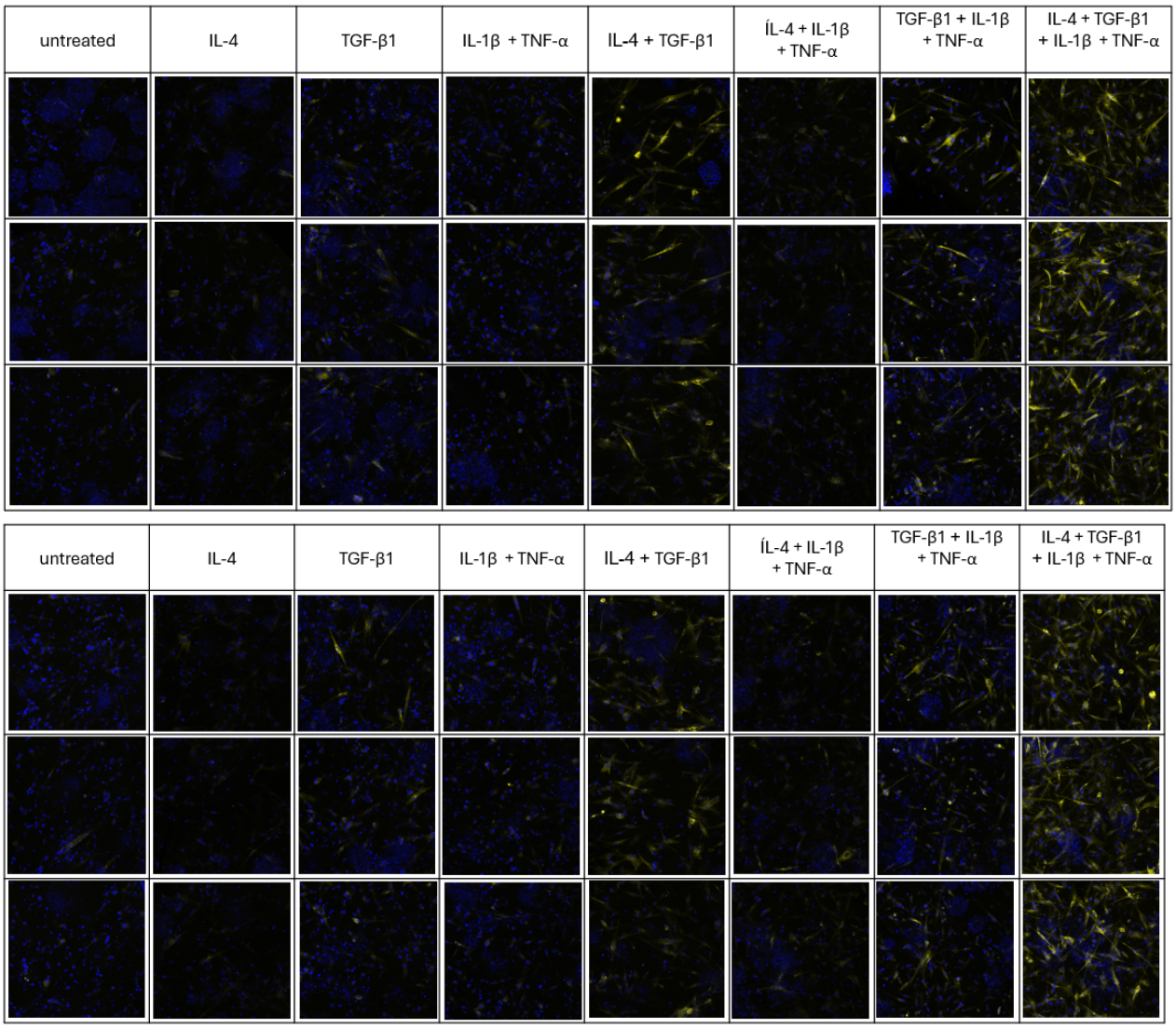


Figure 23: **Confocal images of OOTA (CAF-BGM2008 (p12) and CRC organoid co-culture) showing upregulation of FAP with treatment of 2ng/ml of IL-4, TGFβ-1, IL-1β + TNF-α different combinations (as indicated) for 48 hours.** (n=6) Nuclei stained by DAPI (blue), FAP (yellow). Vimentin not depicted for clarity.